Monodisperse macromolecules *via* the Passerini reaction

Zur Erlangung des akademischen Grades einer

DOKTORIN DER NATURWISSENSCHAFTEN

(Dr. rer. nat.)

von der KIT-Fakultät für Chemie und Biowissenschaften

des Karlsruher Instituts für Technologie (KIT)

genehmigte

DISSERTATION

von

M. Sc. Jiangling Liu

aus China

1. Referent: Prof. Dr. Michael A. R. Meier

2. Referent: Prof. Dr. Patrick Théato

Tag der mündlichen Prüfung: 09.12.2024

Yesterday is history, tomorrow is a mystery, but today is a gift. That is why it is called the present.

-Master Oogway 《(Kung Fu Panda》

Declaration of Authorship

Die vorliegende Arbeit wurde von Januar 2021 bis Dezember 2024 unter Anleitung von Prof. Dr. Michael A. R. Meier am Institut für Organische Chemie (IOC) des Karlsruher Instituts für Technologie (KIT) angefertigt.

Erklärung

Hiermit versichere ich, dass ich die Arbeit selbstständig angefertigt, nur die angegebenen Quellen und Hilfsmittel benutzt und mich keiner unzulässigen Hilfe Dritter bedient habe. Insbesondere habe ich wörtlich oder sinngemäß aus anderen Werken übernommene Inhalte als solche kenntlich gemacht. Die Satzung des Karlsruher Instituts für Technologie (KIT) zur Sicherung wissenschaftlicher Praxis habe ich beachtet. Des Weiteren erkläre ich, dass ich mich derzeit in keinem laufenden Promotionsverfahren befinde, und auch keine vorausgegangenen Promotionsversuche unternommen habe. Die elektronische Version der Arbeit stimmt mit der schriftlichen Version überein und die Primärdaten sind gemäß Abs. A (6) der Regeln zur Sicherung guter wissenschaftlicher Praxis des KIT beim Institut abgegeben und archiviert.

Karlsruhe, 26.10.2024

Jiangling Liu

Acknowledgements

Time flies. Looking back on this challenging and rewarding research journey, I am filled with deep emotion and gratitude. With a heart full of appreciation, I would like to express my sincerest thanks to all the professors, colleagues, friends, family, and loved ones who have supported, helped, and encouraged me along the way.

First, I would like to extend my heartfelt thanks to my supervisor, Professor Meier, for giving me the invaluable opportunity to join the research team. Throughout the research process, you not only provided me with academic guidance, valuable suggestions, and direction for my research, but also gave me support and encouragement whenever I encountered difficulties. The academic spirit and passion for scientific research that you have demonstrated has provided me with a deeper understanding of its significance and the responsibility it entails. I am especially grateful for your unwavering support during moments of uncertainty and your help has been an indispensable part of my journey in scientific research.

I would also like to express my gratitude to my colleagues, Qianyu, Bohn, Jonas, Clara, Anja, Francesca, Roma, Daniel, Maxi, Michi and the rest of my group, for their academic support, for engaging in problem-solving discussions, sharing experiences and advice, and helping me in daily life. The times spent working together with you have been among the most valuable experiences of my research career. Whether in lab work or routine chores, your company and assistance have helped me through many challenging moments.

To all my dear friends - Jing, Maike, Kaiwen, Kun, Xing, Yumeng, Qiming and others - who have been the unsung heroes of this journey, I want to say a heartfelt thank you for the incredible support you've given me. The laughter you brought into my life, the comfort offered during times of hardship, and the advice you provided as I looked toward the future have been invaluable as I faced the pressures of research. Our irreplaceable friendship has made my life away from home richer and more colorful.

I would not have come this far without the steadfast support of my closest partner over

the past two years, my rock of our family, the love of my life, my fiancé, Hansen. Meeting you in Karlsruhe opened a new chapter in my life. Thank you for your boundless understanding, patience, and support throughout this journey. You have opened a window to a new world and held my hand, encouraging me to face challenges with courage. You have been an indispensable partner every step of the way. By your side, I feel an unprecedented sense of security and warmth, and I am deeply thankful for the happiness and strength you have brought into my life.

Though they are not here with me in Karlsruhe, I feel my family's presence with me. To my parents, a hardworking, kind, and gentle couple who have made me who I am, thank you for raising me and for all the care and education you have provided. I am endlessly grateful to you. To my sisters, Runhong and Yan, you have become the strongest backbone of our family. Without your unwavering encouragement and support, I would not have been able to pursue my dreams without doubt or fear. To Xinyue and Yaoyu, my niece and nephew, thank you for the joy and happiness you bring to my life. Your presence has been a delightful source of energy and inspiration throughout this journey. To all my dearest family members, I am profoundly grateful and want you to know that I miss you all more than you could imagine. I love you all!

Finally, I would like to express my heartfelt gratitude to my country. It is her prosperity and strength that have provided me with the opportunity to study in Germany and the resources necessary to pursue my dreams. I wish her continued growth and prosperity, and may her people live in health and happiness.

As I conclude this research journey, my heart is filled with gratitude and a sense of accomplishment. I would like to thank everyone who has supported me; it is your companionship and encouragement that have shaped who I am today. The road ahead may be long, and the climb may be steep, but with all of your encouragement and support, I have never been more hopeful than I am now that we can create an even brighter future for scientific research and our lives.

Thank you once again!

Abstract

Inspired by the highly complex and sequence-defined structures of biological macromolecules found in nature, such as DNA and peptides, the synthesis of sequence-defined macromolecules has become a new research field. Sequence definition often affects the structure-property relationship of macromolecules, which is important for their application. Therefore, over time, research on the relationship between the structure and properties of sequence-defined macromolecules evolved.

In this work, isocyanide based multicomponent reactions, particularly the Passerini three component reaction, was used to prepare two different architectures of monodisperse macromolecules, mainly because of its versatility and the possibility it offers to introduce side chains into sequence-defined macromolecules. First, a benzoate-protected isocyanide monomer was prepared. The monomer was used to synthesize a sequence-defined pentamer via repeated Passerini reactions and subsequent deprotection steps. In a specific growth-step, 2-phenylpropionaldehyde was used to synthesize each permutation of the sequence-defined pentamer with an aromatic group at a different position. Here, the yield of each step was above 90%, and the amount of the obtained pentamer was higher than 3 g. All oligomers were characterized by NMR and IR spectroscopy, SEC and HR-ESI-MS mass spectrometry. The thermal properties were analyzed by DSC and TGA. Tandem electron spray ionization mass spectrometry (ESI-MS/MS) measurements were analyzed for each Passerini product and the fragmentation patterns were assigned accordingly. Only analyzing the fragmentation patterns in MS/MS experiments, the structures of the macromolecules could be distinguished.

In the second part of the work, cyclic macromolecules were synthesized via the Passerini reaction investigating five diacids with different chain lengths, different aldehydes as well as two different diisocyanides. The obtained products were characterized by NMR, GPC, mass spectrometry, and infrared spectroscopy. Investigation of the reaction's crude mixtures allowed in some case to draw conclusions related to cyclic molecule yield a monomer structure used.

Table of Contents

1 Introduction

In nature, DNA, peptides and proteins are high-precision macromolecules with perfectly defined primary structures. DNA, for instance, carries the genetic information of living organisms and provides the information necessary for the generation of essential proteins for biochemical processes, such as self-replication, biocatalysis, self-assembly and molecular recognition, which play an important role in living organisms. Inspired by the highly defined structures of these biomolecules, scientists have explored a new field of research: the synthesis and characterization of sequence-defined macromolecules. In 2013, sequence-controlled polymers were first defined in a review by Lutz, Ouchi and Sawamoto as follows: "…macromolecules in which monomer units of different chemical nature are arranged in an ordered fashion."

Initially, the synthesis of these defined and structurally complex macromolecules was the focus of attention, and scientists have researched and developed different synthetic routes and improved the degree of precision and control. Three different strategies are mainly used: the iterative stepwise method, the two-way (i.e. bidirectional) growth method and the iterative exponential growth method. The iterative stepwise method allows each monomer unit to be controlled as much as possible. The exponential growth strategy (IEG) and the two-way growth strategy can more quickly construct uniform macromolecules, but are limited in terms of the degree of definition. Different synthetic strategies can be carried out in solution, in the solid phase or in the fluorine phase.

Multicomponent reactions are ideal for synthesizing sequence-defined oligomers due to their high yields and selectivity. Furthermore, due to their highly modular nature, it is straightforward to introduce different functionalities in the side chains or main chains to increase the structural diversity of the oligomers. A common multicomponent reaction for synthesizing sequence-defined oligomers is the Passerini three-component reaction. It can be used alone or in combination with other reactions to provide an efficient route for synthesizing different structures and sequences. After reporting many different sequence-defined oligomer synthesis methods, some research groups have

used tandem mass spectrometry, single mass spectrometry and other analytical methods to read out the sequence, proving its application in the field of data storage.

2 Theoretical Background

2.1 Multicomponent reaction

Multicomponent reactions (MCRs) are an efficient method for organic synthesis. Three or more starting materials are reacted in a one-pot method to produce a single product containing most of the atoms of the reactants.[1-3] These reactions offer significant advantages compared to conventional multistep synthesis. Firstly, MCRs are one-pot reactions, so there is no need to separate or purify intermediates, which usually saves time. Secondly, the reactions show highly modular character, with individual components allowing the introduction of different functional groups and often being available on large scales and in great variety. Furthermore, high yields are usually achieved, and the starting materials are often easy to obtain or commercially available.[2, 4] Because of these advantages, MCRs are useful tools in drug discovery, peptide and protein chemistry, polymer chemistry, click chemistry, and the preparation of sequence-defined structure.[5-11] In general, MCRs can be divided into three different types depending on their reaction mechanism, as shown in Scheme 1.[1]

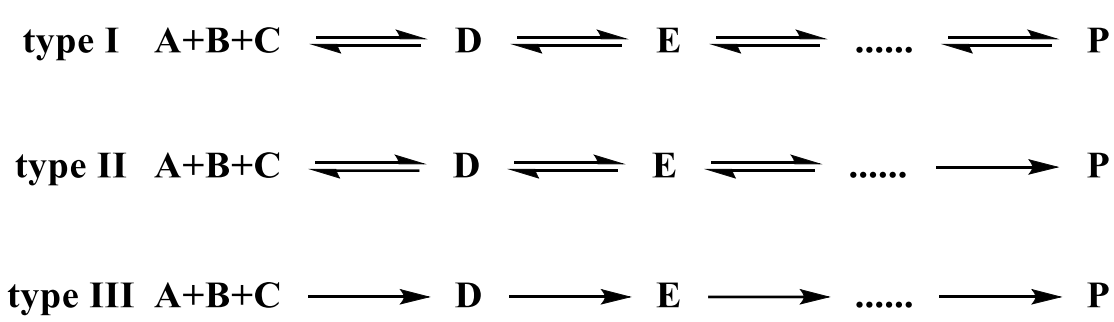

Scheme 1: Types of MCRs according to reversible reaction steps: A, B, and C are starting materials, D, E, etc. are intermediates, and P is the product.[1]

In Type I MCRs, all reaction steps are reversible, and the starting materials, intermediates and final products are in equilibrium, thus the product mixture contains intermediates and starting materials. Moreover, the incomplete conversion of Type I reactions may also result in side reactions, thereby further complicating the isolation process of the desired product. In synthesis, the attainment of high yields in Type I reactions is really difficult. In contrast, the final step of type II MCRs is irreversible.

The advantage of this type is that the equilibrium is strongly shifted towards the product side. Examples of irreversible steps may be formation of stable products, irreversible ring closure, aromatization or highly exothermic reactions, etc. All steps are irreversible in a type III reaction. This type of MCR is very rare in synthetic chemistry, but normal in biochemical processes. The transitions between these three subtypes of MCRs are very simple and smooth, so it is often not possible to exactly classify always.

2.1.1 History

In the following section, some multicomponent reactions that marked important milestones in organic synthesis are introduced (Scheme 2). In 1850, Strecker introduced the first MCR.[12] It involves the reaction of an aldehyde, ammonia (or amine), and hydrogen cyanide to produce an α-amino nitrile, which can be hydrolyzed to give an α-amino acid. Arthur Hantzsch had two important work progress in MCR.[13, 14] In 1882, he produced 1,4-dihydropyridine from an aldehyde, β-keto ester, and ammonia.[13] In 1890, he reacted a β-keto ester, α-haloketone and ammonia to form a pyrrole structure.[14] Dihydropyridine is the precursor of drugs such as nifedipine, and pyrrole is an important heterocyclic compound in the synthesis of many drugs and materials. So Hantzsch's work advanced the development of drug synthesis. In 1891, Biginelli published the heterocyclic dihydropyrimidinones formed by the reaction of urea, aldehydes and β-keto esters.[15] This reaction is valuable for the synthesis of heterocyclic compounds. In 1912, Mannich synthesized β-aminocarbonyl compounds by the amino alkylation of an acidic proton next to a carbonyl functional group (aldehydes or ketones) by formaldehyde and amine (or ammonia).[16] In 1921, Passerini combined an isocyanide, a carboxylic acid, and an aldehyde (or ketone) to form α-acyloxy amides.[17] Details will be introduced in later chapter 2.1.3. In 1952, Kabachnik and Fields synthesized aminophosphonates by using amines, carbonyl functional groups (aldehydes or ketones) and dialkylphosphonate. Aminophosphonates are synthetic targets of importance as phosphorus analogues of α-amino acids (a bioisostere).[18] Asinger synthesized thiazoline derivatives in 1956 from elemental sulfur, ketones, and ammonia.[19] This reaction can used to prepare D-penicillamine and DL-cysteine. In1959, Ugi extended

the Passerini reaction to a four-component reaction that includes an isocyanide, a carbonyl compound (aldehyde or ketone), an amine, and a carboxylic acid.[20] This reaction is widely used in drug discovery and development. These reactions paved the way for the formation of new molecules that ca be used in various fields, such as natural products,[21-25] drugs,[26-32] materials,[33-39] and others.[40-45]

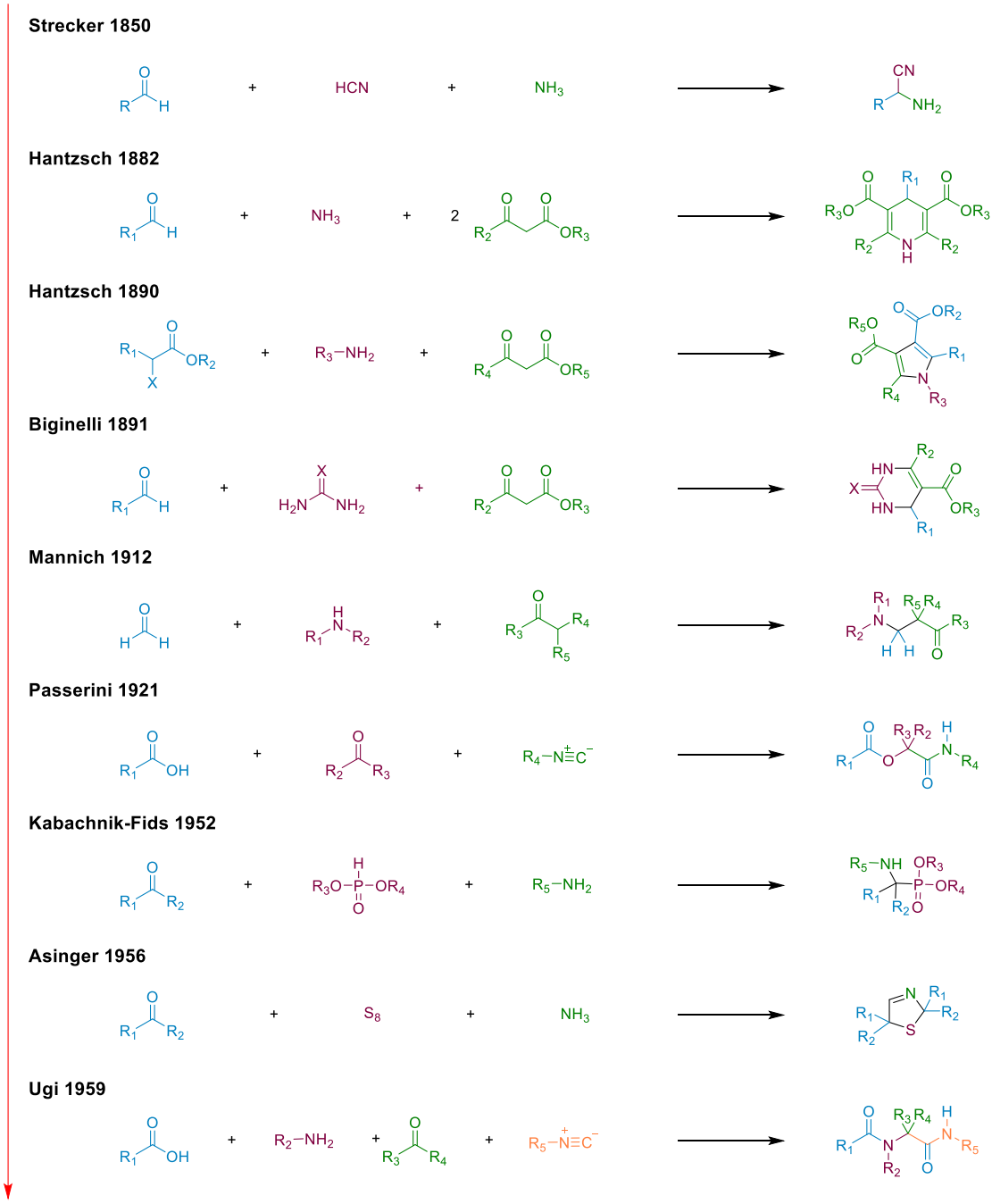

Scheme 2: A chronological list of some historically significant MCRs.[13-20]

2.1.2 IMCR (Isocyanide-based multicomponent reactions)

IMCRs are a special class of MCRs,[46] because of the inherent and unique reactivity of the isocyanide functional group, such as α-additions, α-acidity and carbene-like properties. In this chapter, the synthesis, inherent reactivity type and properties of isocyanides will be presented. Finally, the most relevant reaction for this thesis, the Passerini three-component reaction (P-3CR) is presented, which is used to synthesize the sequence-defined macromolecules herein.

2.1.2.1 Isocyanides

Isocyanides are one of the few functional group with a formal divalent carbon atom.[47, 48] Apart from isocyanide, only carbon monoxide and carbenes have this structural feature. The Scheme 3 shows two resonance structures of an isocyanide, the ionic structure on the one hand and the carbene structure on the other. In this case, the negatively charged carbon in the zwitterionic ion resonance structure is able to react as a nucleophilic reagent, and after a nucleophilic attack it becomes an electrophilic reagent, which is able to react with a nucleophile on the same carbon atom. This process is called α-addition. The α-acidity can be explained by the positively charged nitrogen atoms in the amphiphilic ion resonance structure and can be increased by the ability to attach electron-withdrawing groups (EWGs) to the α-site or to form free radicals. This property may lead to polymerization or cyclisation. Isocyanides are stable under alkaline conditions but are hydrolyzed to the corresponding *N*-formamide under acidic conditions.[1]

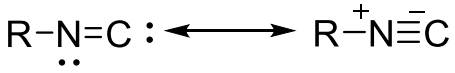

Scheme 3: Resonance structure of the isocyanide: zwitterionic and carbenoid structure.[48]

The synthesis of isocyanides is presented in terms of synthetic routes from different precursors, as shown in Scheme 4 for details. The first successful synthesis of an isocyanide was in 1859, when Lieke obtained the product by reacting an alkyl halide with silver cyanide.[49] It was not until 1868 that the isocyanide structure was proven to be real by Gautier.[50] In 1867, Hoffmann was able to convert primary amines to

isocyanides via the formation of the dichlorocarbene reagent from chloroform and potassium hydroxide.[51] In 2020, Zhang *et al.* decarboxylated chlorodifluoroacetate to produce difluorocarbene, which reacts efficiently with primary amines to form isocyanides. A variety of primary amines can be converted, including aryl, heteroaryl, benzyl and alkyl amines, as well as amine residues in amino acids and peptides.[52] Kitano reported the conversion of benzyl alcohols or tertiary alcohols to isocyanides using trimethylsilyl cyanide as a conversion reagent.[53] In addition to alcohols, this method can also be applied to epoxides.[54] Nowadays, the most common synthetic method is the use of *N*-formamides as a starting material for the reaction and the formation of isocyanides by the addition of a dehydrating reagent. This method was first used by Ugi in 1958 to synthesize isocyanides by dehydrating n-formamide using phosgene.[55] However, in the laboratory, due to the high toxicity of phosgene, it has been replaced by a number of other reagents including triphosgene, diphosgene, organochlorine phosphate derivatives, toluenesulfonyl chloride, phosphoryl chloride, trifluoromethyl sulfonic acid anhydride, or tosyl chloride.[48, 56-61] In 1992, Guirado *et al*. first used electrochemistry to reduce carbodiimide dichlorides to prepare isocyanides.[62] In 2021, Lam *et al.* reported an electrochemical method for the preparation of isocyanides from readily available aminotetrazole derivatives. This method tolerates an unprecedented variety of functional groups and can be easily scaled up by flow electrochemistry, expanding its applicability in both academic and industrial scale laboratories.[63]

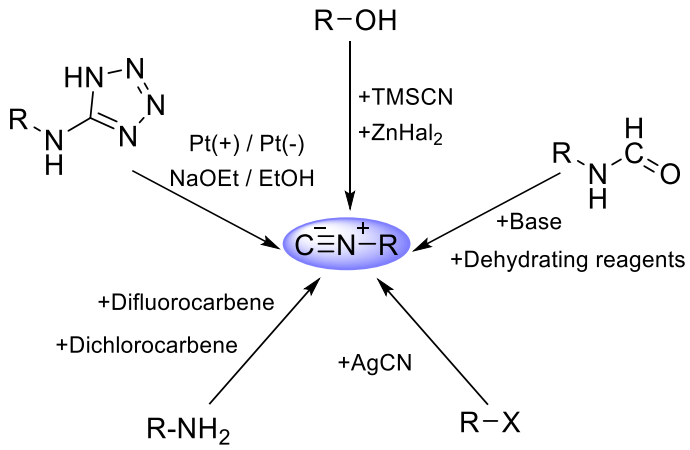

Scheme 4: Summary of described isocyanide synthesis procedures.[48-63]

2.1.2.2 Isocyanide based multicomponent reactions (IMCRs)

The large-scale preparation of isocyanides in the laboratory as well as in industry has facilitated a variety of applications for isocyanides. Naturally occurring isocyanides can exhibit antibiotic, bactericidal, antitumor or antifouling effects.[64-66] Most commonly, isocyanides are used in isocyanide-based multicomponent reactions (IMCRs) with a wide range of applications such as organic synthesis,[67-69] drug discovery[70-73] and polymer science.[74-78] In Scheme 5, several different IMCRs are outlined, and the reactions and their applications are discussed later.

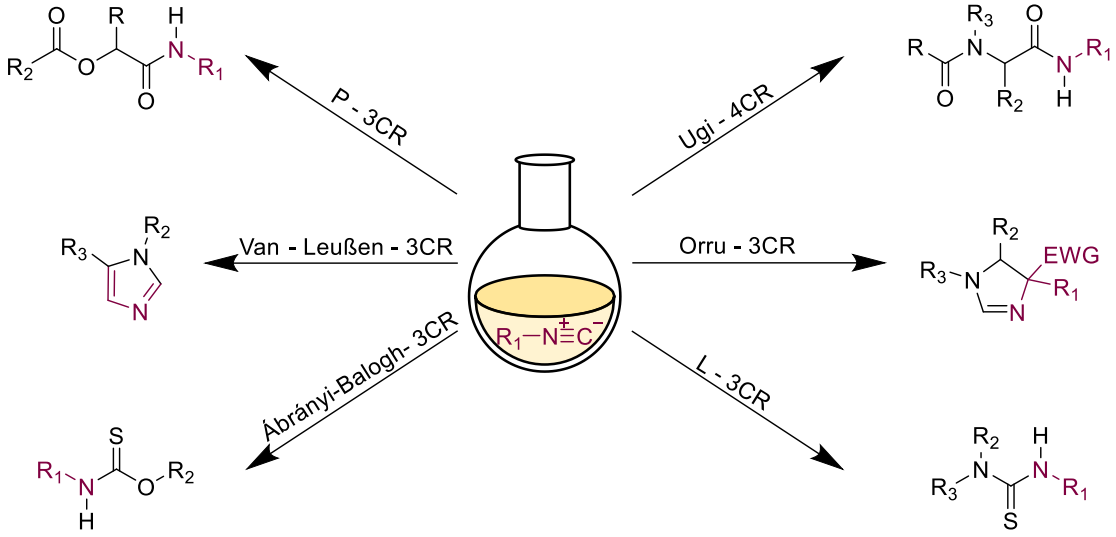

Scheme 5: Overview of several different IMCRs.[17, 20, 79-82]

The most common IMCRs are the P-3CR and U-4CR, and both reactions rely on the above described α-addition as the key reaction step. The part of Passerini will be described in detail in the next section. The Ugi four-component reaction was proposed by Ivar Karl Ugi in 1959.[20] In this reaction, the oxygen component condenses with an amine to form an imine, which reacts with an isocyanide and a carboxylic acid and undergoes an irreversible Mumm rearrangement to form an α-aminoacyl amide.

By varying the components, various variants of the Ugi reaction can be formed, yielding a variety of frameworks. In addition to carboxylic acids, Ugi investigated useful acidic components soon after describing the U-4CR process, such as hydrazoic acid, cyanate, thiocyanate, thiosulfate, water or hydrogen sulfide.[83-86] For example, hydrazoic acid combined with isocyanides, oxo-components and amines will form 1,5-substituted

tetrazoles.[87] The first report on the Ugi five-component reaction (U-5CR) was published by Ugi *et al.* in 1961, using an alcohol, an amine, a carbonyl compound, an isocyanide, and carbon dioxide to yield an α-(alkoxylcarbonylamino)amide in one step.[88] The Ugi five-component condensation reaction (U-5CC) was formed by using alcohols and CO_2, COS or CS_2 instead of carboxylic acids and was demonstrated to be an effective tool for the synthesis of *N*-(alkoxylcarbonyl)aminoamides.[89] For example, substituted diurethanes are generated by the U-5CC between diamines, isobutyraldehyde, tert-butyl isocyanate, methanol and carbon dioxide, which can be used to synthesize polyurethanes.[90] In the presence of alcohol, α-amino acids can undergo a Ugi five-center four-component reaction (U-5C-4CR) to combine with aldehydes, alcohols and isocyanides to yield α-aminoacyl carboxylates. This method can also produce iminodicarboxylic acid monoamide monoesters, which is used for the industrial synthesis of clinical oxytocin receptor antagonists Epelsiban and Atosiban.[91, 92] The carboxylic acid can be replaced by o-nitrophenol, p-nitrophenol or salicylic acid to participate in the U-4CR reaction, the last step of which is the Smiles rearrangement, so the variant is also called the Ugi-Smiles reaction.[93-95]

As the amine component, primary amine, secondary amine, hydroxylamine, hydrazine, hydrazine derivatives, etc. can be used. The Joullie-Ugi three-component reaction (JU-3CR) is a modified version of the Ugi reaction.[96] Cyclic imines can replace the amine and oxo-components in U-4CR and react with carboxylic acids and isocyanides to generate N-heterocycles attached to oxazoles or tetrazoles. JU-3CR is a useful tool for the synthesis of natural products and important pharmaceutical compounds.[97, 98]

There are many other important isocyanide-based multicomponent reactions. The GGB-3CR for the synthesis of imidazole heterocycles as core structures was discovered by three independent groups (Groebke - Blackburn - Bienaym) in 1998.[99-101] In this reaction, heterocyclic amidines such as 2-amino pyridine, pyrazine or pyrimidine react with aldehydes and isocyanides to generate 3-aminoimidazo (1,2-a) -pyridine, pyrazine or pyrimidine. Nowadays, the GGB-3CR is often used to synthesize bioactive molecules such as kinase inhibitors, antibacterial agents or HIV-1 reverse transcriptase inhibitors.[102-104] In 2000, Dömling discovered a reaction similar to U-4CR, using a vinyl

isocyanide containing both a tertiary amine and an ester group to react with aldehydes, amines and thiocarboxylic acids to form α-acylaminocarboxythioamides after Mumm-rearrangement. As thionoamides have inherent nucleophilicity at the sulfur atom, further 5-exo-trig cyclization occurs to form α-acylaminothiazoles.[105]

IMCRs can also rely on the reactivity of the acidic α-CH_2 group of the isocyanide group. A relevant reaction was reported by Van-Leußen in 1977,[79] the reaction of aldehydes, amines and methyl tolyl isocyanate to form imidazoles. Base-induced cycloaddition of tosylmethyl isocyanide (TosMIC) to aldimines in protic medium occurs with subsequent elimination of *p*-toluenesulfinic acid to give the otherwise difficulty accessible 1,4-disubstituted imidazoles. Addition of TosMIC to imidoyl chlorides is accompanied by the loss of HCl, and leads to 1,4,5-trisubstituted imidazoles. In 2003, Orru *et al.* discovered that nitrogen-containing heterocyclic imidazolines can be synthesized by a similar reaction in the process of studying the synthesis of 2-imidazoline.[80] The three raw materials are amines, isocyanides and aldehydes. Ketones can also participate in the reaction as oxo-components instead of aldehydes. When isocyanides contain additional ester or amide groups, oxazoles can be obtained through the α-addition pathway. Imidazolinium itself is less important, but its derivatives, especially 2-imidazoline derivatives, play an important role in medicine and pesticides.[106]

Another reaction is formed by the formation of a double bond between the isocyanide carbon and a chalcogen such as sulfur or selenium. In 1959, Lipp *et al.* used elemental sulfur, amines and isocyanates to yield thioureas through multicomponent reactions.[81, 107] This product is often used in polymer chemistry. When alcohols are used instead of amines, *O*-thiocarbamates can be prepared.[82] Hu *et al.* reported in 2018 that when amines and isocyanates both contain two effective functional groups, they can react at room temperature to generate polythioureas.[108] Furthermore, Ábranyi-Balogh *et al.* reported that amines can be replaced by alcohols or thiols in alkaline environments to form thiocarbamates or dithiocarbamates.[82]

2.1.3 Passerini Reaction

In 1921, Mario Passerini discovered the P-3CR, which is the first known IMCR.[17] P-3CR describes the reaction of carboxylic acids, oxygenates, and isocyanides to form α-acyloxy carboxamides (Scheme 6). Usually, simple reaction conditions, such as room temperature, high concentration, and the use of aprotic solvents such as dichloromethane (DCM), can achieve excellent yields.

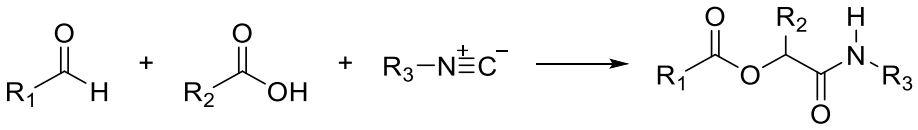

Scheme 6: Reaction equation of the Passerini reaction, a carboxylic acid, an oxo-compound, and an isocyanide to yield an α-acyloxy amine.[17]

Although the P-3CR has been discovered more than 100 years ago, the reaction mechanism has not yet been fully elucidated. Passerini himself proposed a reasonable mechanism (shown in Scheme 7), and further research by Baker and Ugi also supported this view.[109, 110]

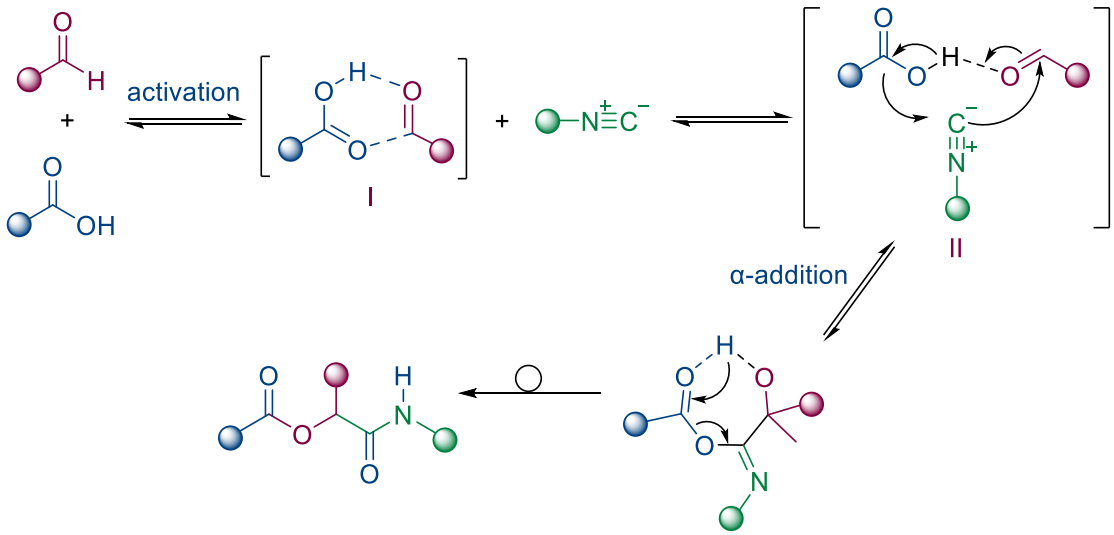

Scheme 7: Commonly accepted mechanism of the P-3CR, first, activation of the oxo-component by hydrogen-bonding (I), α-addition of the isocyanide yielding intermediate (II), Subsequently, the irreversible rearrangement takes place to form the Passerini product.[109]

First, the oxo-component is activated by hydrogen bonding with the carboxylic acid, and then the isocyanide undergoes an α-addition reaction with the hydrogen-bonded

adduct I. The isocyanide first reacts as a nucleophile with the carbonyl center of the activated aldehyde and is then attacked by the carboxylic acid at the electrophilic carbon atom formed, forming a cyclic transition state II. As an azo analog of an anhydride, in the final irreversible rearrangement, an intramolecular transacylation reaction occurs, and an α-acyloxy amide is obtained as final product.

As mentioned earlier, the mechanism of P-3CR is still in doubt. In 1965, Eholzer *et al.* proposed another mechanism whereby isocyanide is protonated by a carboxylic acid in the first step.[111] This hypothesis was based on their observation that the Passerini reaction is faster in the presence of an inorganic acid as a catalyst. This result is consistent with the description in Pirrung's publication that the Passerini reaction is accelerated in water,[112] and contradicts Ugi's statement that the Passerini reaction proceeds best in nonparetic, nonpolar solvents.[84]

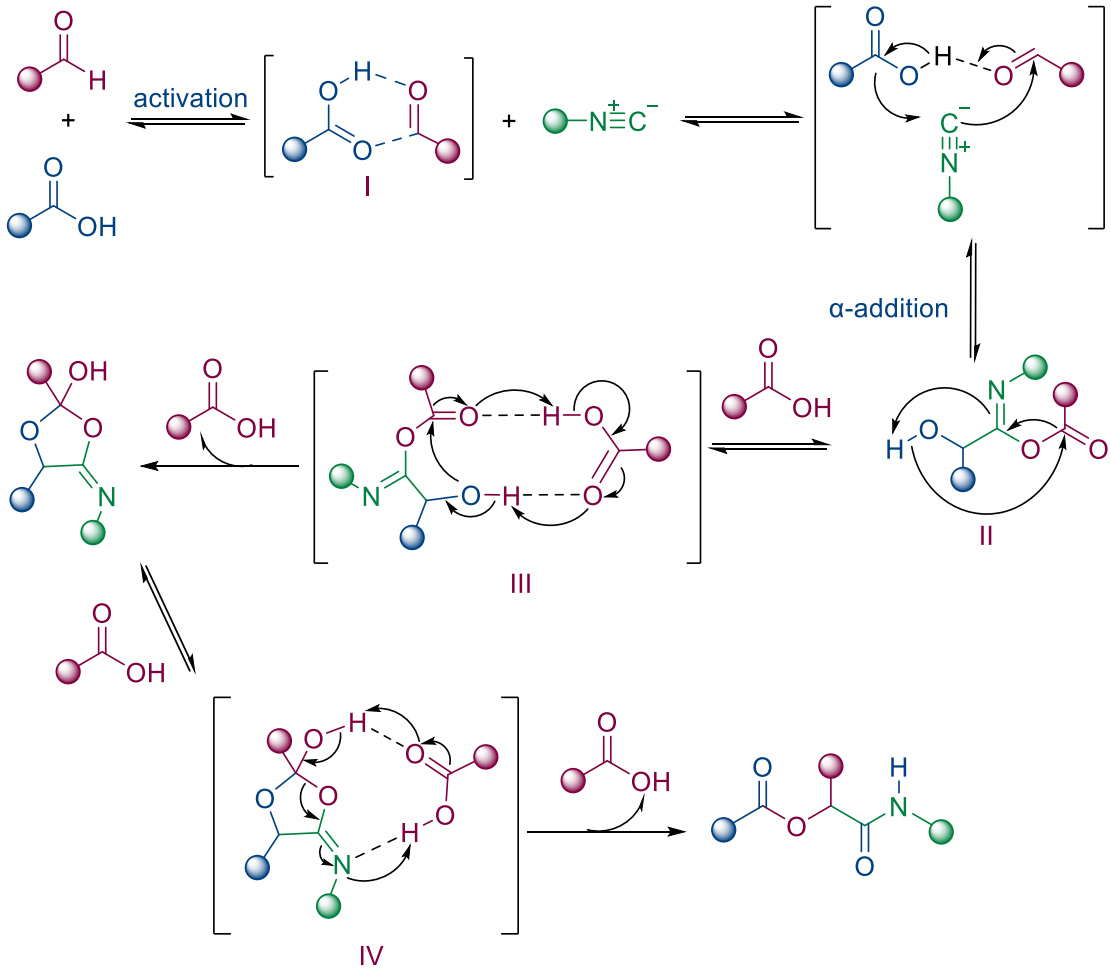

Scheme 8: Postulated mechanism of P-3CR involving two carboxylic acid molecules.[113, 114]

In 2011, Maeda *et al.* introduced another mechanism based on quantum chemical calculations in the gas phase, suggesting that the P-3CR is a four-component reaction involving two carboxylic acid molecules (shown in Scheme 8).[115] The additional carboxylic acid molecule acts as a catalyst, so that P-3CR can be described as an organocatalytic three-component reaction. Firstly, the activation and α-addition steps are similar to the mechanism proposed by Passerini. But the rearrangement is assumed to be acid-catalyzed because the transition state (TS) involving another carboxylic acid molecule is significantly lower in energy (III). The resulting cyclic intermediate then undergoes a carboxylic acid-catalyzed rearrangement via another four-component TS (IV) to produce P-3CR. Later on, density functional theory (DFT) calculations support this postulated mechanism.[113]

Due to the structural diversity resulting from the one-step synthesis and its easy availability, a wide range of variants can be obtained through this MCR reaction by substituting carboxylic acid or oxo-components. Several different variants of P-3CR are shown in Scheme 9.

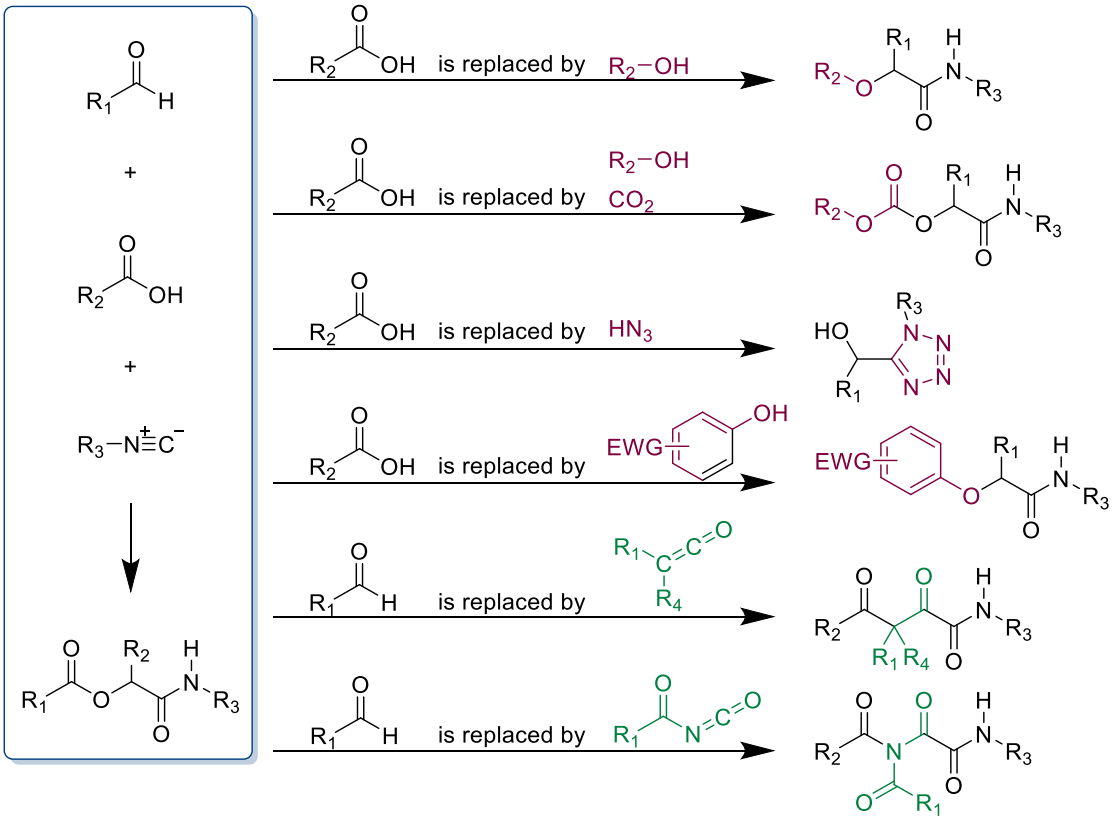

Scheme 9: Variations of the carboxylic acid or oxo-components of the Passerini reaction produced a variety of different variants.[114, 116-120]

Using alcohols instead of carboxylic acids to synthesize α-alkoxy amide derivates is one of the commonly used methods to generate variants.[114] Aldehydes are air sensitive and easily oxidised to form the corresponding carboxylic acid, producing by-products. Moreover, alcohols are more readily available and less expensive than aldehydes. Therefore, alcohols and 2-iodoxybenzoic acid (IBX, as oxidation agent) in place of carboxylic acids to produce α-hydroxyamines or normal Passerini products. Soeta *et al.* used silanols instead of carboxylic acids in the P-3CR. The silyl group is coordinated to the oxygen of the carbonyl group, which made it susceptible to nucleophilic attack by isocyanide. The alcohol functional group of the silanol then captured the nitrile ion within the molecule, thereby synthesizing α-siloxyamides.[121] The same group also reported a one-pot synthesis of α-(sulfonyloxy)amides using the oxidative Passerini reaction. Sulfinic acid instead of carboxylic acid reacts with aldehydes and isocyanides, and then meta-chloroperoxybenzoic acid (mCPBA) is added to generate the product in high yield.[122] This group reported for the first time a multicomponent reaction using phosphinic acids instead of carboxylic acids. The reaction is based on the reaction of an aldehyde, an isocyanide and a phosphonic acid followed by the addition of a second aldehyde. The nucleophilic phosphinate group allows for a subsequent catalytic Pudovik-type reaction to form the corresponding α-(phosphinoylxy)amide derivatives.[123] By replacing the carboxylic acid component with alcohol and CO_2, it can be converted into a Passerini four-component reaction (P-4CR) to yield carbonate ester amides.[116] In addition, carboxylic acids can be substituted with hydrazoic acids or trimethylsilyl azide to form tetrazole derivatives.[117, 124] The electron-deficient phenol derivative is used to replace the carboxylic acid and react with aldehydes and isocyanides to form *O*-arylamides.[118, 125] The key to the reaction is that the bond intermediate undergoes an irreversible smile rearrangement, which is similar to the rearrangement in the Ugi-smiles reaction.[93] In addition to replacing carboxylic acids, the oxo-component can be replaced by acyl isocyanates to form *N,N*-diacyloxamides,[120] or the oxo-component can be replaced by ketenes to form α, γ-diketocarboxamides.[119]

In the context of this work, the versatility of the Passerini reaction has been exploited to synthesize a wide variety of molecules for applications in various fields, such as

medicinal chemistry,[126] polymer chemistry,[127-130] or the synthesis of designed molecules.[131-134] In the next chapter, we will focus on the important application of the multicomponent reaction (especially P-3CR) in the field of sequence defined structures.[135-137]

2.2 Sequence-definition in chemistry

In nature, DNA carries the genetic information for the evolutionary, growth and reproductive functions of organisms.[138-141] The genetic instructions are transcribed into mRNA, which is translated into polypeptides, which fold into functional proteins. DNA, polypeptides and proteins are all high-precision macromolecules with perfectly defined primary structures. These complex structures allow organisms to have essential properties for biochemical processes such as self-replication, biocatalysis, self-assembly and molecular recognition, which play important roles in organisms. Inspired by the structures of these highly defined biomolecules, scientists have explored a new area of research: the synthesis and characterization of sequence-defined macromolecules. Over time, synthetic and purification methods were developed and the relationship between their structures and properties was probed.

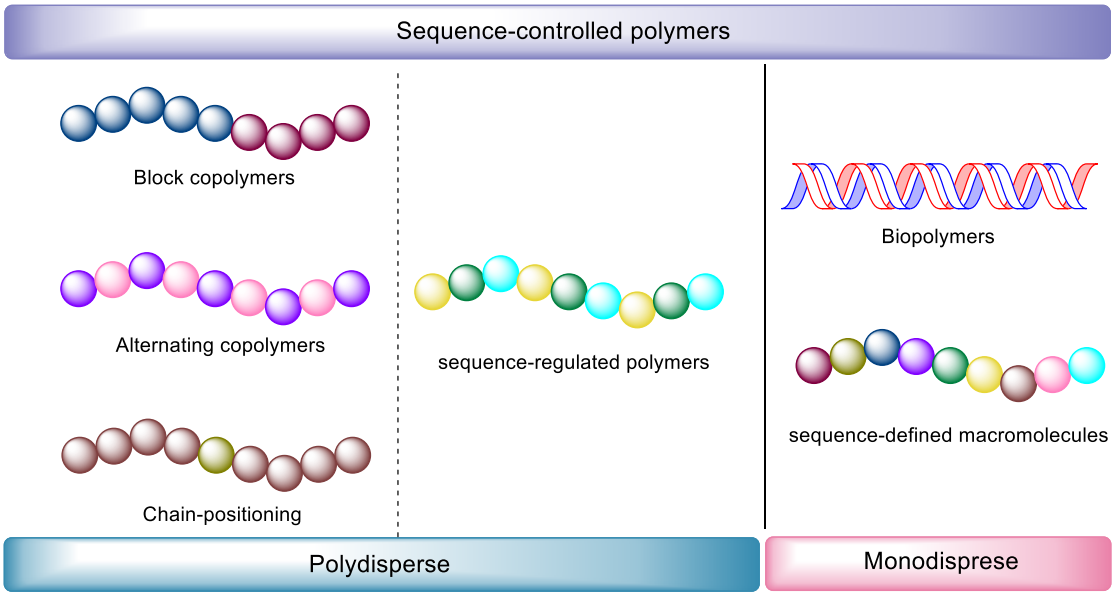

Figure 1: Classification and examples of different types of sequence-controlled polymers.[142, 143]

In 2013, sequence-controlled polymers were first defined in a review by Lutz, Ouchi and Sawamoto as follows: “Sequence-controlled polymers are macromolecules in which monomer units of different chemical nature are arranged in an ordered fashion.”[144] This definition covers polymers with any degree of control over the sequence of monomers. According to the 1996 International Union of Pure and Applied Chemistry (IUPAC) definition of the various types of copolymers, these sequence-

controlled polymers can be divided into two broad categories: polydisperse polymers and monodisperse polymers (see Figure 1).[142] Included in polydisperse, sequence-controlled polymers are alternating copolymers, block copolymers, chain-positioned polymers, and sequence-regulated polymers. These polymers have a dispersed chain length distribution in composition and molecular weight with a dispersibility index Đ > 1.00. Sequence-defined macromolecules on the contrary are strictly homogeneous in size and composition, they have a fully controlled sequence of monomers, and the dispersibility index Đ = 1.00, and are therefore monodisperse macromolecules.

2.2.1 Synthetic sequence-defined macromolecules

The synthesis of sequence- defined macromolecules and their applications will be discussed in detail in the following content. The methods for the preparation of sequence-defined macromolecules can, for instance, be classified as solid-phase synthesis, liquid-phase synthesis, fluorous-phase synthesis, and polymeric tethered methods. There are various synthesis strategies for macromolecules, three prominent ones being linear iterative growth, bidirectional growth and iterative exponential growth (IEG), as shown in Figure 2.[145] In addition to the main approaches, there are other strategies and methods for synthesizing sequence-defined molecules. However, these will not be further discussed in this work.

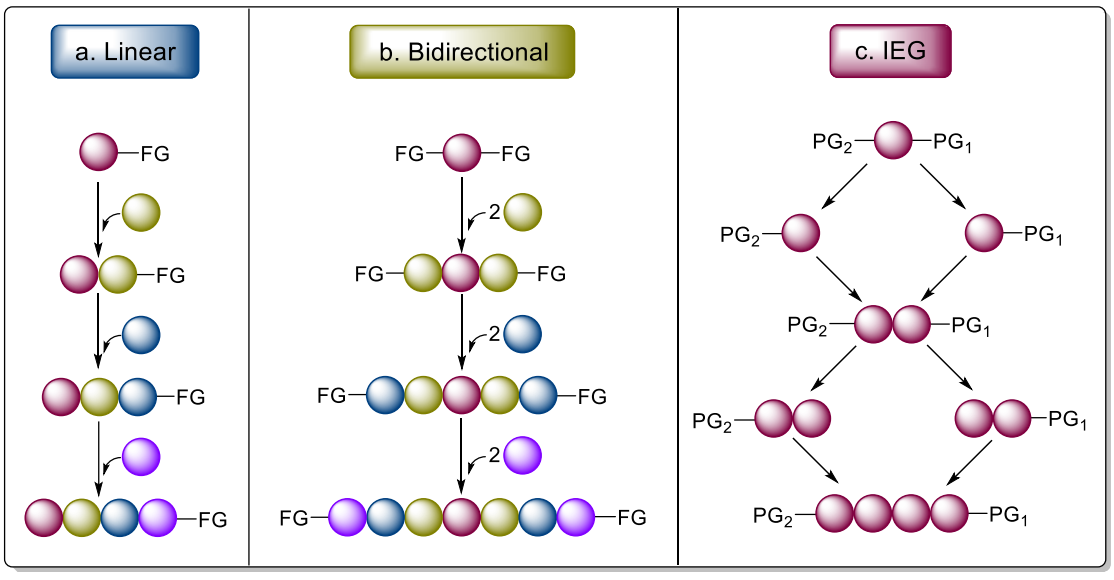

Figure 2: The main three synthesis strategies for sequence-defined macromolecules. a. Linear iterative

growth. b. Bidirectional growth. c. Iterative exponential growth. (PG = protecting group, FG = functional group)[145]

The strategy of linear synthesis focuses on the stepwise addition of monomers or units to growing polymer chains, which can be performed in solution, in solid phase, fluorous-phase synthesis, and polymeric tethered methods. In contrast to unidirectional growth, bidirectional growth starts not only from one but also from two reaction sites, leading to higher polymerization and symmetric macromolecules more quickly. Multidirectional growth formed by multiple reaction sites is also possible, resulting in star-shaped macromolecules. The most rapid strategy for molecular weight increase is iterative exponential growth, often referred to as the divergence/convergence approach, which comes with minimal control over the sequence obtained.

The most prominent example of the unidirectional chain growth concept was proposed in 1963 by Merrifield, who described the first sequence-defined synthetic method, solid-phase peptide synthesis (SPPS). For this achievement, he was awarded the Nobel Prize in 1984.[146, 147] The synthesis usually consists of iterative cyclic steps, including both coupling and deprotection steps, as show in Scheme 10. In this concept, the peptide is constructed from the C-terminus to the N-terminus. For the coupling of two amino acids, a protecting group needs to be configured on the amino acid to avoid an undesirable reaction between the carboxylic acid and the amine, resulting in a mixture of products. In the first step of the synthesis, the N-terminal protected amino acid reacts with a linker molecule via the C-terminus *via* in S_N2 reaction, thereby being coupled to the resin. Subsequently, the amine protecting group is cleaved and reacts with the activated carboxylic acid group of another N-terminally protected amino acid. A second deprotection is then performed and so on. In the final step, the peptide is cleaved from the solid carrier and the protecting group is cleaved to obtain the sequence-defined molecule.

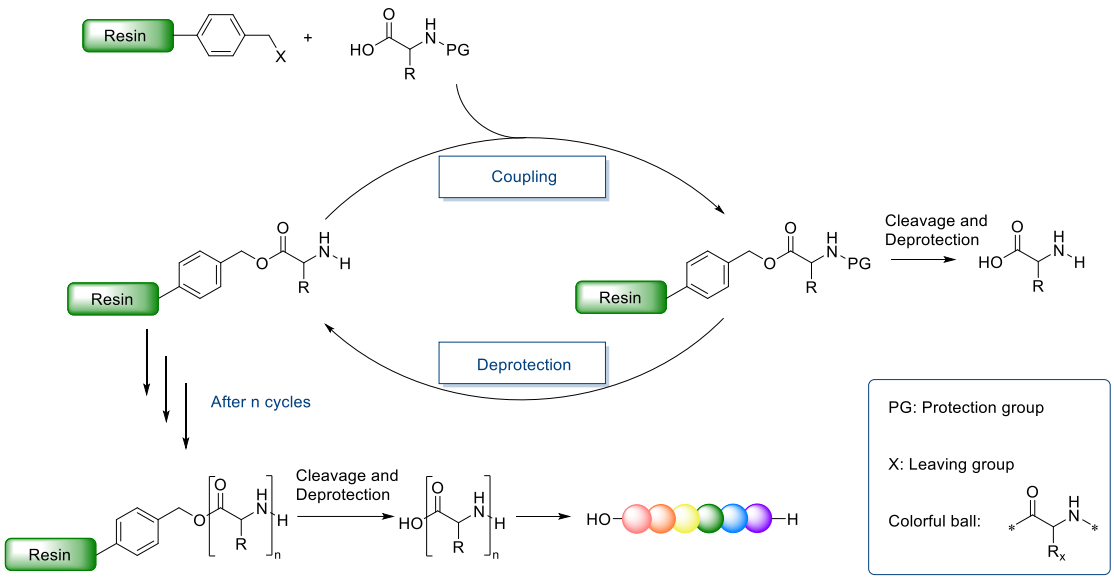

Scheme 10: General reaction scheme of the SPPS by Merrifield. [146, 147]

Most of the resins commonly used for SPPS consist of highly cross-linked copolymers of styrene and 1,4 divinylbenzene, or polyacrylamide resins. The resin has to be swollen in an organic solvent to solubilize the growing peptide well enough for diffusion reagents to have access to it. In the second step, the carboxyl function of the amino acid needs to be activated. This activation can be achieved by synthesizing specific feedstocks or by using activators based on, for example, synthetic anhydrides, acyl azides, *N,N*-bicyclohexylcarbodiimide etc. The activators can be used as benzotriazol-1-yloxytripyrrolidinophosphonium hexafluorophosphate (PyBOP) and hexafluorophosphate benzotriazole tetramethyl uronium (HBTU). After successful coupling of the amino acids, the N-terminal temporary protecting group is cleaved, usually fluorenylmethyloxycarbonyl protecting group.

In 1966, Merrifield reported the automation of the process, because SPPS could get product by simple separation operations (i.e., filtration and washing) of the product and that the entire process was suitable for automation. This report makes rapid synthesis of longer sequences a reality.[148]

The solid-phase concept is not limited to the synthesis of peptides, but can also be used for the synthesis of oligoamines, oligonucleotides and oligosaccharides, peptide nucleic acids, as well as for the synthesis of sequence-defined macromolecules.

In 2013, the Du Prez group demonstrated an example of the synthesis of sequence-defined macromolecules based on thiolactone chemistry, using solid-phase chemistry with a unidirectional growth strategy.[149] In the initial approach, a thiolactone building blocks in combination with Michael acceptors were used. As first, the amine acts as a nucleophile and introduces the side chain definition, and the thiolactone undergoes a ring-opening reaction to form a thiol. The resulting thiol reacted with another reactive thiolactone building block in a thia-Michael addition or nucleophilic sunsttution reaction to complete the reaction cycle. Continuing these steps, trimers and tetramers with different sequence definitions and different side chains were synthesized. The variation of the side chain was achieved by introducing different primary amines through the reaction of the amine function in an aminolysis.

In 2016, Du Prez *et al.* expanded and improved the reaction system.[150] Two thiolactones were synthesized to be the initial building blocks, one containing an alcohol function and the other containing an isocyanate group. The reaction cycle begins with the ring-opening of thiolactone with amino alcohol to form thiol, which reacts with acrylamide or acrylate in a thia-Michael addition. The use of different amino alcohols leads to changes in the main chain, and different acrylates and acrylamides introduce different side chains. Next, the hydroxyl group reacts with the isocyanate group of the thiolactone. Continuing these iterative reactions, oligomers with different functionalized sequence definitions were synthesized. Among them, the definition of the side chain can be achieved by modifying the thiol through thiol-ene reaction or nucleophilic substitution.[151-154] In addition, the initial building block was replaced by α-isocyanate-γ-thiolactone, and the thiolactone motif was incorporated into the main chain structure of the growing chain as a thioether.[155, 156] The alcohol functionality was introduced by thia-Michael addition or epoxide nucleophilic ring opening to introduce the second side chain. In the next step, the alcohol reacted with the isocyanate of the thiolactone to complete the reaction cycle. In the overall reaction, the side chain changes were achieved by synthesizing with different resins, replacing acrylate or acrylamide with n-hydroxyethyl acrylamide, and using different amines.

In an iterative stepwise approach, monofunctional starting materials are stepwise elongated and monomer units are coupled one by one.

In 2014, Livingston *et al.* achieved a unidirectional synthesis of heterofunctional uniform oligo (ethylene glycol) using a three-armed phenyl star as the core.[157] They used a monoprotected octa (ethylene glycol) in a nucleophilic substitution reaction with the core for iterative chain extension to form a linear oligo (ethylene glycol). The protecting groups were then removed by dichloroacetic acid, pyrrole and DCM, exposing hydroxyl groups, which were then coupled with formylated monoprotected octa ethylene glycol. By repeating this cycle, a three-armed star-shaped 24-mer was finally synthesized. In 2019, using a similar experimental concept, the team employed a liquid-phase synthesis approach to generate uniform sequence-defined PEGs.[158] Firstly, monomers with functionalized terminals were synthesized with hydrophilic tetrahydropyran-1-yl acetals on one end and toluene sulfonate groups on the other side. During the reaction the hydroxyl group of the core unit reacts with the toluene sulfonate group of the monomer in a Williamson ether synthesis, which then deprotected protecting group of the THP to produce the hydroxyl group again. At the end of the iterative reaction, the benzyl ether bond between the polyether chain and the core molecule can be broken. This approach defines a strategy for the synthesis of multifunctional polyether based on sequences purified from molecular sieves. This strategy is used in industry for the synthesis of oligonucleotides, peptides, homopolymers and sequence defined polymers (show in Scheme 11).

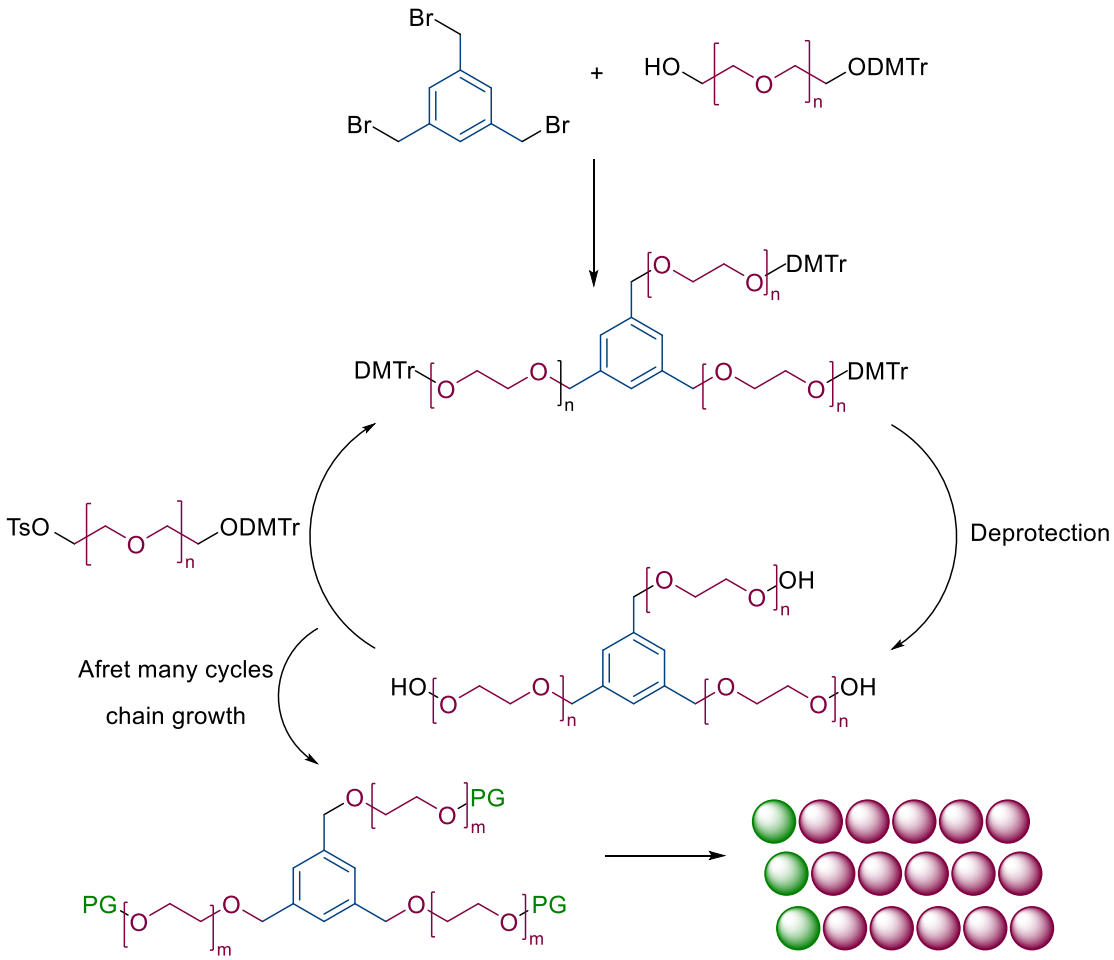

Scheme 11: Synthesis of uniform PEG with a benzylic core.[157, 158]

Lutz also has demonstrated numerous possibilities on synthesizing sequence-defined macromolecules and using them for data storage.

In 2014, the Lutz team reported the chemically selective iterative synthesis of an oligomer (triazole amide) encoded by two bifunctional groups AB and CD.[159] In 2015, the team published a review detailing the use of iterative strategies to synthesize sequence-defined polymers on the solid phase (summarized in Scheme 12).[160] For clarity, all these concepts are drawn on solid-supports (yellow blocks). The first one is the traditional approach employing AB building blocks. Functional R_1 reacts with R_2 in coupling step, in which functional R_1 of the monomer is protected during that step. The iterative cycle is completed afterwards by deprotection. The second example is an AA + BB approach, in which function R_1 reacts with R_2. Bifunctional monomers are used in large excess in the coupling step. The third approach relies on an AA + BC reactions. Functional R_1 reacts only with R_2 in coupling conditions. Function R_1 reacts only with

R_3 in another coupling condition. Bifunctional monomer AA is used in large excess in every coupling step. The last example consists of an AB + CD approach. Function R_1 reacts only with R_3. Function R_2 reacts only with R_4. Coupling steps are chemo selective. After many cycles, sequence-defined oligomers can be obtained.

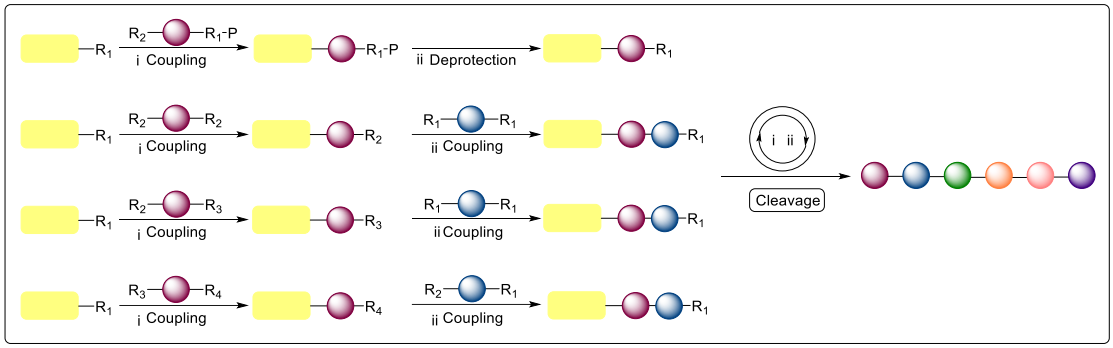

Scheme 12: The first is a traditional method using AB building blocks. The last three are protecting group-free methods.[159, 160]

In 2016, they used a solid-phase orthogonal "AB + CD" iterative strategy to synthesize peptide triazole nucleic acids (PTzNA).[161] In this method, AB and CD molecules containing carboxylic acid, azide, alkyne, and primary amine functional groups were assembled together through consecutive copper-catalyzed azide-alkyne cycloaddition (CuAAC) and acid-amine coupling steps to prepare molecules with different sequences. In the same year, they introduced chemical selectivity into the two-step iterative method.[162] First, the reaction of alcohol with *N,N'*-disuccinimidyl carbonate got activated carbonates. Then, the selective formation of carbamates was carried out using different amino alcohols. By using amino alcohols with or without methyl side chains, oligo-carbamates with the potential to contain information-rich molecules were synthesized, implementing the binary code of "1" and "0" into the sequence.

In 2019, the team upgraded the synthesis scheme by combining the formation of reactive carbonates with their chemo selective reaction with the secondary amine groups of the amino alcohol building blocks.[163] Using four coded molecules (i.e. 2-(methylamino) ethanol, 2-(ethyl amino) ethanol, 2-(propyl amino) ethanol and 2- (butyl amino) ethanol) to write binary information on the formed polymers, representing the

binary dyads 00, 01, 10 and 11, respectively. Again, homogeneous oligomers and polymers with controlled lengths and sequences of digital information were synthesized. In 2020, Lutz *et al.* prepared sequence-defined poly(alkoxyamine phosphodiester) by orthogonal iterative solid-phase method and carried out a detailed study of the fragmentation mechanism.[164] The experiment involved two different types of bifunctional building blocks, namely phosphor amidite monomers with alkyl bromide and hydroxyl functional group nitroxides. Two different phosphor amidite monomers were used to incorporate molecular information into the polymer chain. In positive and negative mode ESI-MS/MS, the CH_2-O bond breaks instead of the O-(CO) bond in N-R oligourethanes, as opposed to N-H oligourethanes. The different rearrangements result in up to four product ions per carbamate, which results in complex fragment patterns.

Beyond these, Prof. Lutz has many more publications of synthesizing sequence-defined macromolecules that can be digitally encoded or exploit fragmentation patterns alone.[165-171] Of course, there are also more and more researchers using step-by-step iterative methods to synthesize the desired well-defined macromolecules.

In 2016, Grate *et al.* successfully synthesized a triazine-based sequence-defined hexamer.[172] By changing the reaction temperature, the melamine can be activated or deactivated, and iterative coupling reactions can be completed without the need for special protective groups. In 2017, Fang *et al.* synthesized a 12-mer-PEG by synthesizing a tetraethylene glycol monomer with a methoxy group on one side and a dimethoxy trimethyl group on the other side, and gradually adding it to a solid support in combination with a phenyl group containing a benzene-protected building block.[173]

Iterative stepwise synthesis is a common method for synthesizing sequence-defined macromolecules. The group of Prof. Meier has reported on different methods of iterative stepwise synthesis, mainly based on MCR. We discuss these methods in more detail in 2.2.2 on MCR in sequence definition.

As already mentioned in Figure 2, bidirectional growth is also an important method for synthesizing sequence defined oligomers. In bidirectional growth, bifunctional starting

molecules react with two monomer units per step, and higher molecular weights can be obtained in fewer steps than with unidirectional iterative step synthesis.

The synthesis of polyethylene glycols can be carried out by means of a bidirectional growth process. In 1992, Jenneskens *et al.* synthesized a dodeca(ethylene glycol) by means of a bidirectional growth process from a mono-protected and di-alkylated tetraethylene glycol.[174] First, a ditosylated ethylene glycol was synthesized, then it was reacted with mono-protected glycols to couple three OEGs in a single reaction step. After deprotection, the resulting glycol can be ditosylated, then reacted again with mono-protected glycol. Repeating of the synthesis cycle leads to higher molecular weights. In 1999, Baker *et al.* synthesized OEGs in a greener way by replacing dichloromethane with an aqueous solution based on Jenneskens' method.[175] In 2006, Tanaka *et al.* synthesized 44-mer PEGs by reacting two equivalents of mono-protected and tosylated tetraethylene glycol with another glycol, followed by deprotection and iterative reactions, resulting in multiple cycles.[176] In 2008, Springer *et al.* obtained a 29-mer PEGs in six steps by growing in both directions from hexa(ethylene glycol).[177] First, hexa(ethylene glycol) was mono-protected with benzyl protecting groups followed by reaction with penta(ethylene glycol)-di-(p-tosylate) to obtain the doubly protected PEG-17-mer. Next, the monoprotected monomer was reacted with the deprotected PEG-17-mer and deprotection to obtain the PEG-29-mer. In 2014, Bruce *et al.* used Tanaka's experimental procedure to obtain a dimethyl-protected 24-mer with the highest purity reported to date.[178]

In 2015, Jiang *et al.* used a new strategy to synthesize monodisperse PEG.[179] Glycol was added to two macrocyclic monomers in a single reaction step. The macrocyclic monomers were converted from tetra(ethylene glycol) to macrosulfoxylate by thionyl chloride in a one-pot reaction. Bidirectional growth was carried out using the ring-opening of tetra(ethylene glycol) as a cyclic sulfite. Using this simple iterative method, PEG-36-mer was synthesized in four steps. PEG-64 monomethyl ether was synthesized in 8 steps using sodium methoxide as the nucleophile and the macrocycle octamer as the iterative ring-opening.

In the same year, Barner-Kowollik *et al.* synthesized sequence-defined macromolecules using a two-way photochemical method.[180] First, a monomer containing a photoenol and a sorbitol group, a monomer with a phenyl sulfide group and a protected maleimide group were prepared. Next, a Diels-Alder reaction was carried out between the photoenol with the sorbitol end group using a symmetric core unit containing two maleimides as a raw material. The sorbitol end group reacts with the photochemically activated phenacyl sulfide to form a Diels-Alder adduct. Finally, thermal reduction of the Diels-Alder, liberation of the maleimide functionality, removal of the furan under vacuum, and reaction with the latest products. By repetition of the steps, a symmetric sequence-defined decamer was obtained (show in Figure 3).

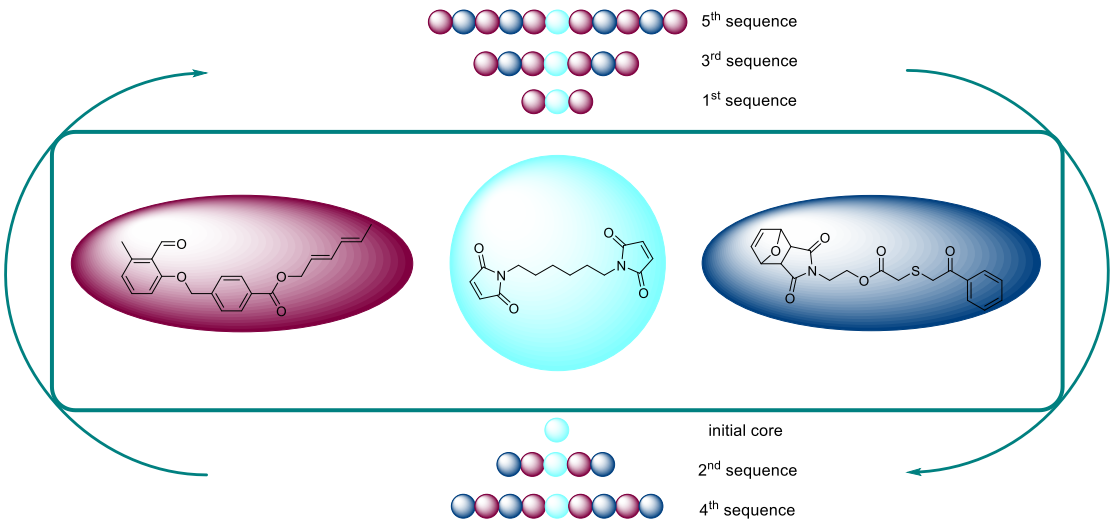

Figure 3: Overview of the photochemical reaction approach for the synthesis of sequence-defined macromolecules.[180]

In 2016, the team used a similar experimental scheme to obtain a variety of sequence-defined polymers through two-way growth. [181, 182] First, a monomer is synthesized with a photoreactive benzaldehyde at one end and a furan-protected maleimide at the other. Next, the dimaleimide core reacts with the photoreactive benzaldehyde, and finally the deprotection of the furan protective group prepares the next reaction. The iterative cycle is repeated to synthesize oligomers with a defined sequence, and it was successfully decoded by MALDI tandem MS. In 2019, the team published the synthesis of sequence-defined macromolecules without protective groups using precise orthogonal photochemistry.[183] Two monomers were first synthesized, one consisting of a pyrene-

functionalized visible-light-responsive tetrazole and a diene, and the other consisting of a carboxylic acid and a fumarate. The symmetrical core molecule reacted with the tetrazole of the monomer in a nitrile-imine-carboxylic acid reaction, and the remaining diene group reacted with the fumarate group in a Diels-Alder cycloaddition reaction. After several cycles, a sequence-defined decamer was synthesized using selective photochemistry.

The iterative exponential growth (IEG) (also known as divergence/convergence methods) strategy is an effective method for the rapid synthesis of large sequence-defined macromolecules. The synthesis uses orthogonal protection groups containing two parts, orthogonally protected and activated functional groups. The two parts are orthogonally deprotected or activated separately and then combined in a coupling reaction. In this way, two monomers react to form a dimer, two dimers to form a tetramer, two tetramers to form an octamer, and so on and so forth, achieving exponential growth. The synthesis of highly defined macromolecules using IEG methods with the introduction of defined side chains is difficult and challenging and is usually limited to repetitive sequences.

The first sample about iterative exponential growth for the synthesis of long aliphatic chain compounds by the IEG method was reported by Whiting *et al.* in 1982 (show in Scheme 13).[184]

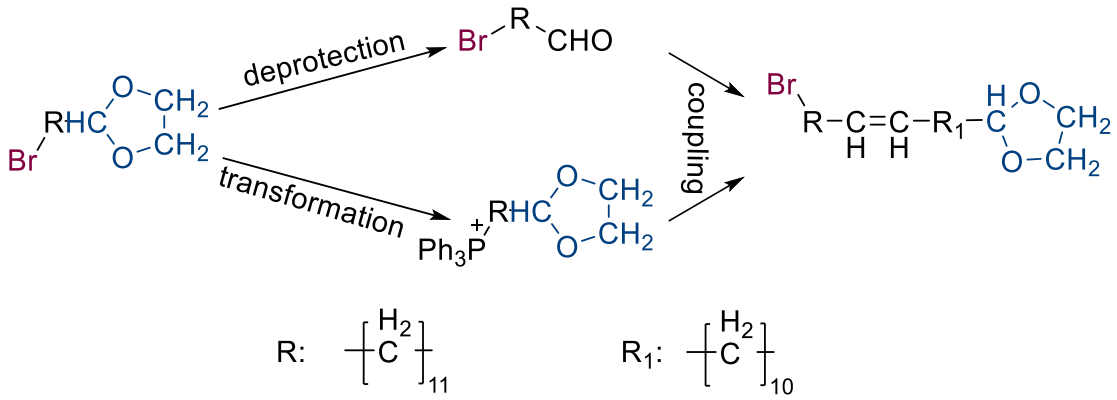

Scheme 13: Schematic diagram of dimer generation using IEG by Whiting.[184]

They used C_{12} -bromoacetal as the reactant monomer, which was split into two parts, with one half of the bromine converted to phosphine and the other half deprotecting the

acetal. Subsequently, the phosphine moiety reacted with the aldehyde to produce a dimer, which also contained the bromine and acetal functions. These steps are repeated to obtain the octamer. In the final step, the bromine and acetal are removed and the double bond is hydrogenated to give a pure aliphatic chain. This report showed that highly defined molecules can be synthesized using IEG, and the group further synthesized different highly defined macromolecules such as pure paraffins with different chain lengths,[185] and ultra-long straight-chained alkanes of specific lengths using this method.[186]

In 2008, Hawker *et al.* reported the synthesis of uniform oligomers by an iterative exponential growth strategy (Scheme 14).[187] 6-Hydroxyhexanoic acid generated from ε-caprolactone via a ring opening reaction was used as a starting material, which was converted into two parts, half of which was protected with *tert*-butyl dimethyl silyl (TBDMS) to protect the alcohol functional group, and half of which was protected with benzyl ester to protect the carboxyl group. The monomer was then subjected to Steglich esterification to give an orthogonally protected dimer. The dimer was also divided into two parts, the benzyl ester was reductively hydrogenated and the silyl ether was treated by tetra-n-butyl ammonium fluoride (TBAF). Afterwords, carboxyl-terminated or hydroxyl-terminated dimers can be obtained. The dimer was coupled again in a Steglich esterification reaction to give a tetramer, and so on to synthesize a uniform 64-mer oligo(ε-caprolactone). In the same year, this group synthesized uniform (L)-lactic acid oligomers according to a similar reaction scheme.[188]

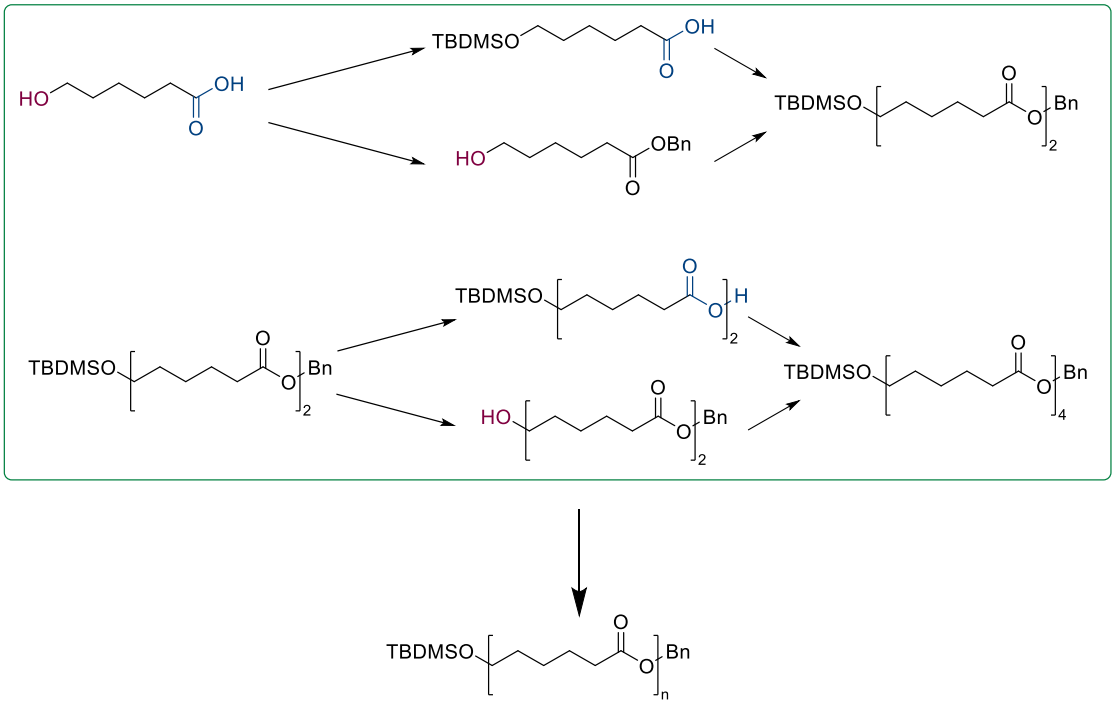

Scheme 14: Overview of the synthesis of ε-caprolactone oligomers. The monomer 6-hydroxyhexanoic acid was prepared via ring opening of ε-caprolactone.[187]

In 1995, Huang and Hermes applied an IEG strategy to synthesize alternating oligomers.[189] Alternating oligomers of (L)-lactic-co-glycolic acid (La-co-Gl), which are isosteric with polypeptides, were synthesized through solution-phase methodologies involving the protection, coupling, and deprotection of hydroxyl and carboxylic acid functional groups. The carboxylic acid moiety was protected via benzyl ester formation and subsequently deprotected through hydrogenation. The hydroxyl group was protected as a methoxyethoxyethyl (MEE) ether and deprotected using a combination of sodium iodide and trimethylsilyl chloride. The coupling reaction was facilitated by dicyclohexylcarbodiimide (DCC).

IEG method is also a good way to synthesized PEG. In 1999, Burns *et.al* synthesized PEGs by the reaction of a protected ethylene glycol with another ethylene glycol building block containing a protecting group and a leaving group.[190] Later, Hill *et al*. synthesized asymmetric polyethylene glycols by iterative exponential growth using orthogonal protecting groups in 2004.[191] In 2009, a refinement of the IEG strategy by Davis *et al.* resulted in the syntheses of 16-, 32-, and 48-mers of ethylene glycol.[192]

In the field of conjugated molecules, IEG methods are usually employed to synthesize oligomers such as oligoacetylenes, oligo(p-phenylene), oligofluorene and oligophenylene ethylene. Since 1992, the synthesis of several conjugated oligomers in solution and solid phase has been reported by Moore *et al.* Scheme 15 shows the synthesis of sequence-defined poly(phenylacetylene) in combination with solid-phase synthesis.[193] The terminal acetylene and aryl halides were orthogonally masked as (trimethylsilyl)-acetylene and 1-aryl-3.3-dialkyltriazene groups. Subsequently, the product was divided into two parts. One part was deprotected with potassium carbonate and from the other part the phenyl iodine was obtained by cleaved from the solid carrier with methyl iodide via ipso substitution. These two parts were then reacted in a Sonogashira coupling to obtain dimers. Following this cycle, phenylacetylene oligomer with 32-mer was obtained. Later,Moore's team synthesized oligomers of phenylacetylene of different structural types according to a similar reaction scheme.[194-197]

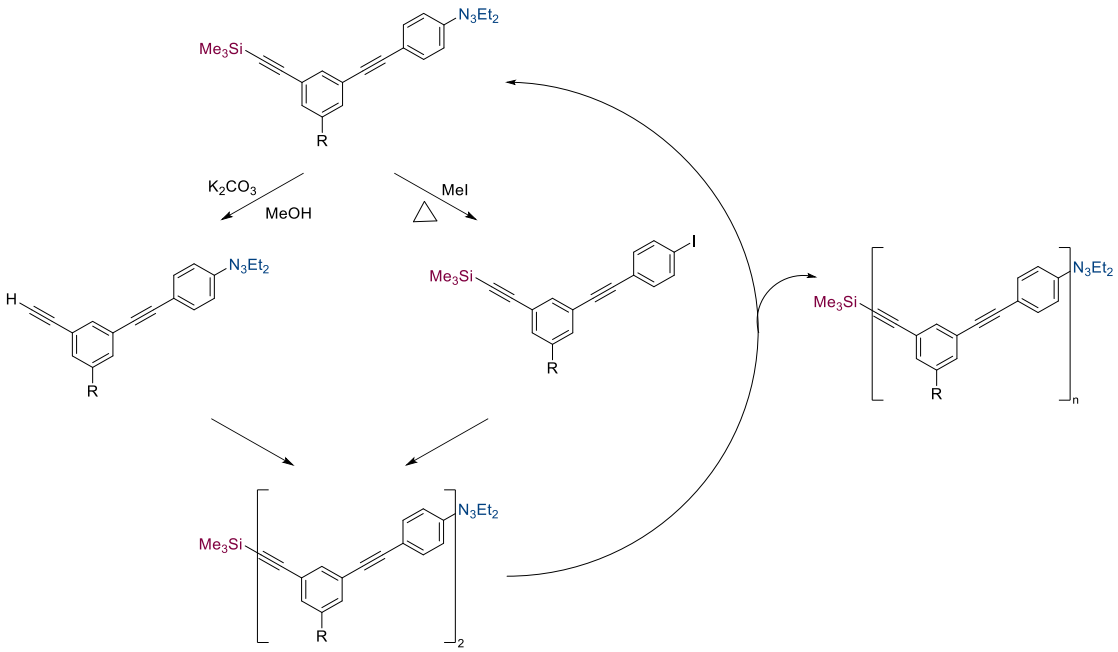

Scheme 15: IEG approach of Moore et al. for the oligoacetylenes synthesis with the Sonogashira reaction in solid phase. [193]

Conjugated oligomers with precise lengths and structures can be used both as models for native-like polymers and as candidates for molecular wires and molecular-level electronic devices, and as a result, more and more publications report the synthesis

conjugated oligomers. Combining the IEG reaction mechanism with the Suzuki cross-coupling reaction, Schlüter *et al*. synthesized oligo(para-phenylene) in 1996,[198] and Chen *et al*. synthesized oligofluorenes in 2002.[199] Tour *et al*. successfully synthesized a variety of conjugated oligomers by IEG methods, including oligo(thiophene-ethynylene) derivatives, phenyl alkyne oligomers, oligo(2,5-thiophene ethynylene)s, oligo(phenylene ethynylene) and so on.[200-203] In 2005, Wang *et al*. developed a new strategy to synthesize oligo(1,4-phenyleneethynylene)s,[204] the strategy combining the advantages of the iterative divergent/convergent strategy and the in situ desilication/coupling strategy based on Tour's study.[205]

In 2015, Johnson et.al reported a semi-automated, scalable IEG method for the synthesis of sequence-defined macromolecules (shown in Scheme 16.A).[206] The IEG method typically utilizes an orthogonal deprotection reaction that permits the coupling of α-ω-terminal functionalized molecules, thereby doubling the molecular weight of the resulting product. This new approach describes the semi-automated coupling of ester monomers. A monomer was first synthesized in an esterification reaction to give a bromine and a triisopropylsilyl-protected alkyne monomer. The bromine was converted to an azide in a nucleophilic substitution reaction and the protected alkyne can be orthogonally deprotected using a fluorine reagent such as tetrabutylammonium fluoride (TBAF). The IEG semi-automated system allows the monomer to be separated into two parts, converted orthogonally to alkyne and azide, purified on-line, and then subjected to the coupling step of deprotecting the monomer.

In the same year, they refined this strategy, offering the possibility of controlling the chain length, sequence and stereo configuration of the aimed for macromolecule, which is now commonly referred to as IEG+ strategy.[207] The previously reported method was modified. A three-step iterative cycle was carried out using a monomer building block with an epoxide at one terminal and a TBS-protected alkyne at the other, where the chiral tert-butyldimethylsilyl (TBS)-protected epoxy-alkyne is selectively ring-opened by the azide anion to provide the azide group and the secondary hydroxyl functional group. The secondary hydroxyl group can be esterified to introduce the desired side chain, while the azide and alkyne to the CuAAC of the corresponding tetrazole dimer

allow chain elongation. By repeating this reaction cycle, macromolecules of consistent arrangement and stereo configuration are obtained (show in Scheme 16.B).

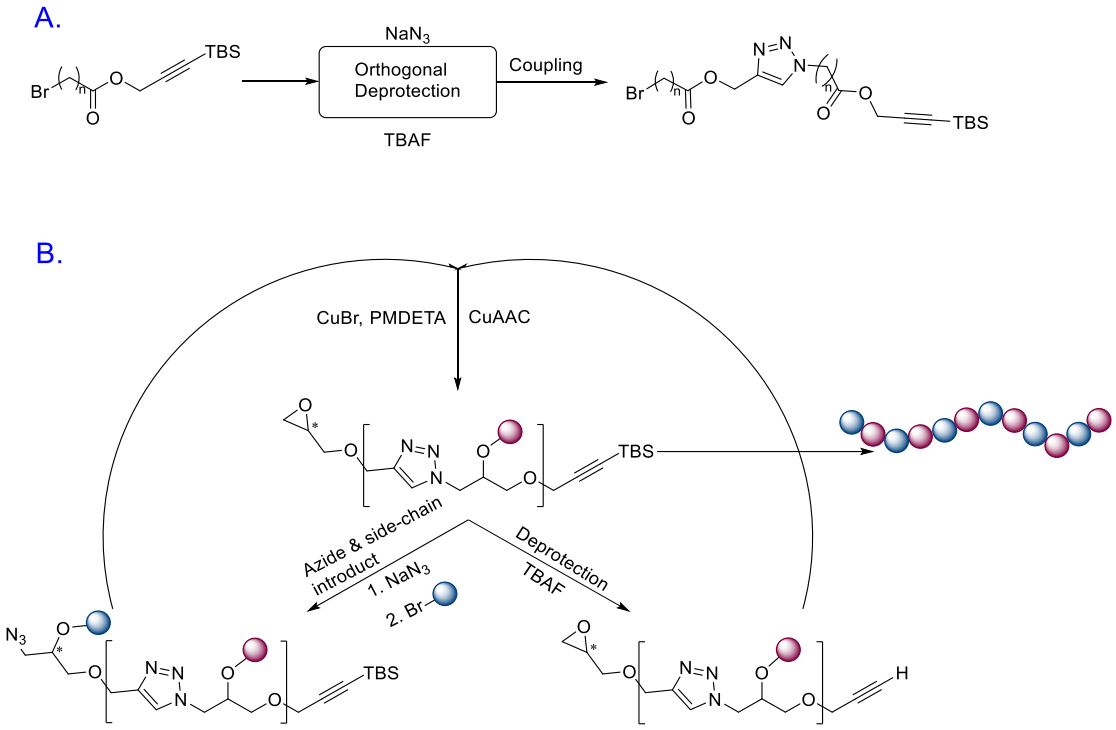

Scheme 16: Overview of the different strategy by Johnson *et.al*, A. Flow-IEG strategy.[206] B. IEG+ strategy. [207]

In 2006, the team further improved the IEG+ strategy by forming a new strategy, allyl-IEG, which takes advantage of efficient thiol-alkene addition reactions with side-chain olefinic functional groups that are capable of efficient post-polymerization functionalization, increasing side-chain diversity.[208] This approach is widely used to produce homogeneous, sequence-defined macromolecules.[209-212]

Nowadays, the IEG strategy is widely used in the synthesis of sequence-defined macromolecules. [213-217]

2.2.2 MCRs in sequence-defined macromolecules

Multicomponent reactions offer a wide range of applications, as discussed earlier. They play an important role in the field of sequence definition due to their advantages such as high efficiency, high atom economy, and raw material diversity. Several groups have studied the application of MCR in the field of sequence definition. In this section, some examples of MCR will be introduced, especially Passerini Three component reaction.

In 2014, the Meier group reported the synthesis of a sequence-defined macromolecule via P-3CR.[218] Stearic acid, as a starting material, reacted with 10-undecenal and an isocyanide to form a Passerini product with a terminal double bond and a side-chain depending on the used isocyanide. The double bond can undergo a Thiol-Ene addition with 3-mercapto propionic acid to regenerate a carboxylic acid, allowing further P-3CR to be achieved. By continuing the iterative cycle, sequence-defined macromolecules were synthesized. The definition of the side chains is achieved using different isocyanides (Show in Scheme 17. left). In 2015, the U-4CR, was used for the same approach, i.e. amines were used as an additional fourth component, providing a change in the amine group in the reaction, thus achieving the definition of double side chains (Show in Scheme 17. right).[219]

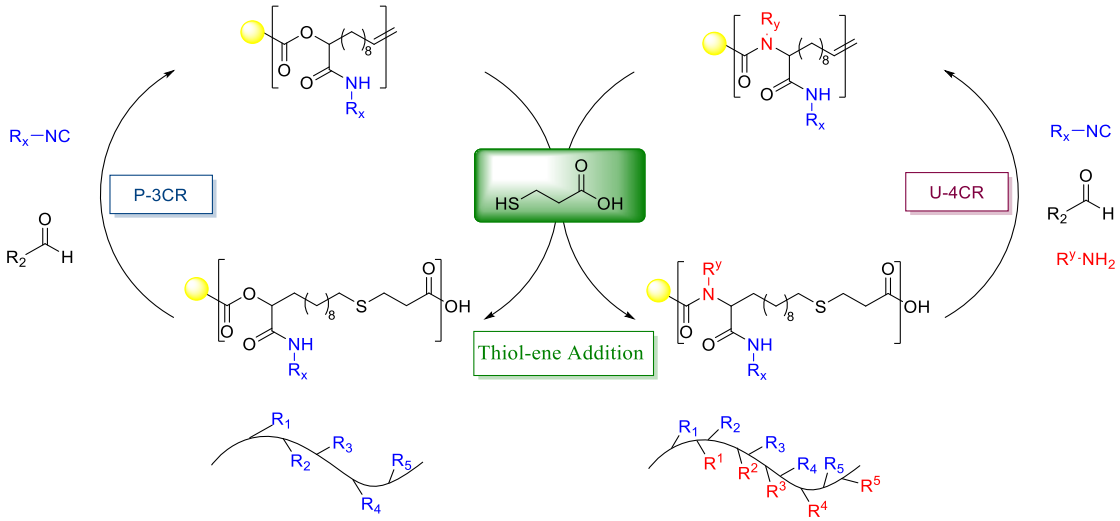

Scheme 17: Overview of the synthesis of sequence-defined macromolecules via multicomponent reactions by Meier group. The reaction cycle on the left describes the P-3CR and the subsequent Thiol-Ene reaction to introduce a carboxylic acid to complete the reaction cycle. The side chain is defined by changing the isocyanate component.[218] In the reaction cycle on the right was U-4CR, the isocyanate and

amine components are used to define a double side chain.[219]

Several research groups have studied the use of the Passerini multicomponent reaction in tandem with other reactions for the synthesis of sequence-defined macromolecules. In 2015, Barner-Kowollik and Meier *et al.* combined the P-3CR with a Diels-Alder reaction to generate oligomers with different functionalities using photochemical induction to initiate a two-way reaction.[180] Hong *et al.* used the Passerini three-component reaction in tandem with a three-component amine-thiol-ene conjugation reaction to synthesize sequence-defined polymers. The Passerini reaction between methacrylic acid, adipaldehyde and 2-isocyanobutyrate yields a new molecule containing two olefin units. Subsequently, the addition of an amine and a thiolactone to the reaction system results in a three-component amine-thiol-olefin conjugation reaction and a sequence-defined polymer.[220]

In 2016, the Meier group reported the synthesis of sequence-defined macromolecules using an improved P-3CR methodology. First, a single-protected AB monomer with isocyanide and a benzyl ester were synthesized, which is also an important raw material for this thesis. Stearic acid as the starting acid reacted with this AB monomer and an aldehyde, the first Passerini product was synthesized. Palladium on charcoal with hydrogen was used to cleave the benzyl ester on carbon with hydrogen to deprotect. The resulting free carboxylic acid can undergo a further Passerini reaction. By continuing this iterative two-step reaction cycle, a high-purity sequence-defined decamer with nine different side chains was synthesized. The side chains were defined by using different aldehydes in each Passerini step.[221]

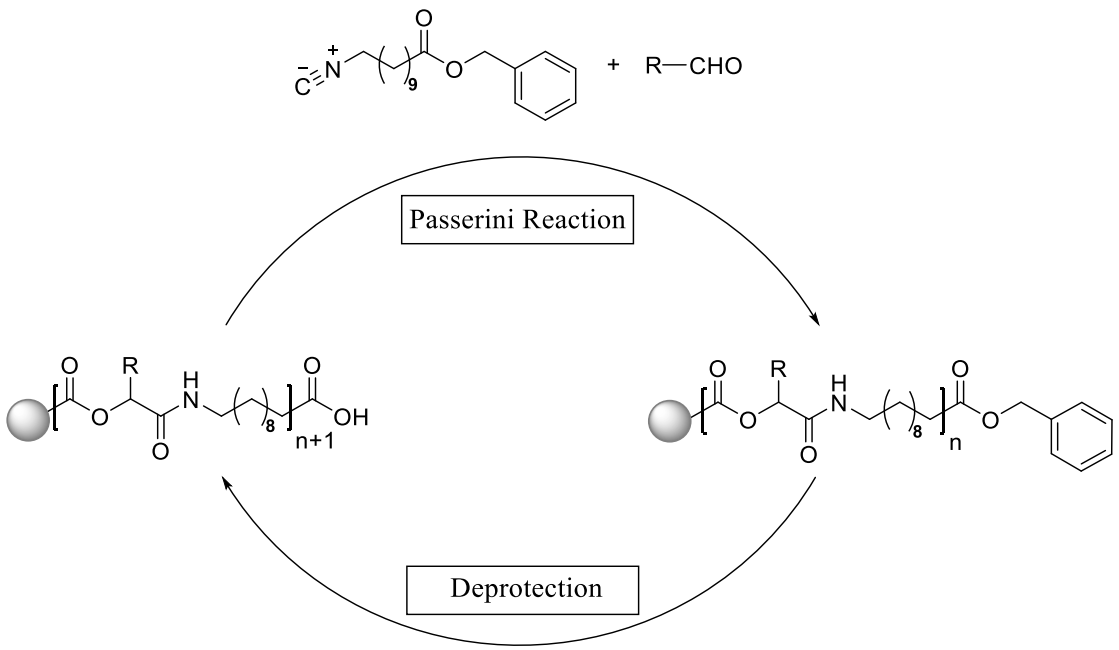

Scheme 18: Overview of the use of the improved P-3CR method to synthesize defined macromolecules by Meier group in 2016.[221]

As mentioned earlier, Du Prez used the thia-Michael addition reaction to synthesize a sequence-defined macromolecule based on a thiolactone via a one-way growth strategy.[149] In 2014, Alabi et.al described the iterative thiol-alkene addition and Thia-Michael reaction on soluble and cleavable fluorous tags, permitting the synthesis of sequence-defined oligomers with tailor-made side chains without protecting groups.[222] In 2017, the Meier and Du Prez groups opened up a novel synthetic method by combining the P-3CR and thiolactone chemistry.[223] Thioacetate acid is used as the starting acid to participate in the iterative cycle of P-3CR and the thia-Michael addition reaction to form oligomers. The thiolactone end group in the product is directly reacted with the isocyanate-functional acrylate in a thia-Michael addition reaction via ammonolysis, this step forms a building block with an isocyanate functional group and an end double bond. The isocyanate functional group undergoes a Passerini reaction, followed by a thiol addition. By means of such iterative cycle reactions, macromolecules with up to 15 optional side chains were successfully synthesized.

In 2018, the Meier group combined the Passerini reaction with the Biginelli monomer synthesis reaction to explore new sequence-defined materials.[224] First, Biginelli acid was synthesized from aldehydes, urea carboxylic acids and benzyl acetoacetate. The

acid was reacted with different aldehydes and diisocyanides in a P-3CR reaction to obtain monomers with a benzyl group and isocyanide. The monomers were reacted via P-3CR via the isocyanide group, and then the benzyl group was deprotected to form an acid, which was used again in a P-3CR with the monomer and aldehyde. After several of these iterative cyclic reactions, macromolecules with defined sequences and encode information for data storage materials were synthesized.

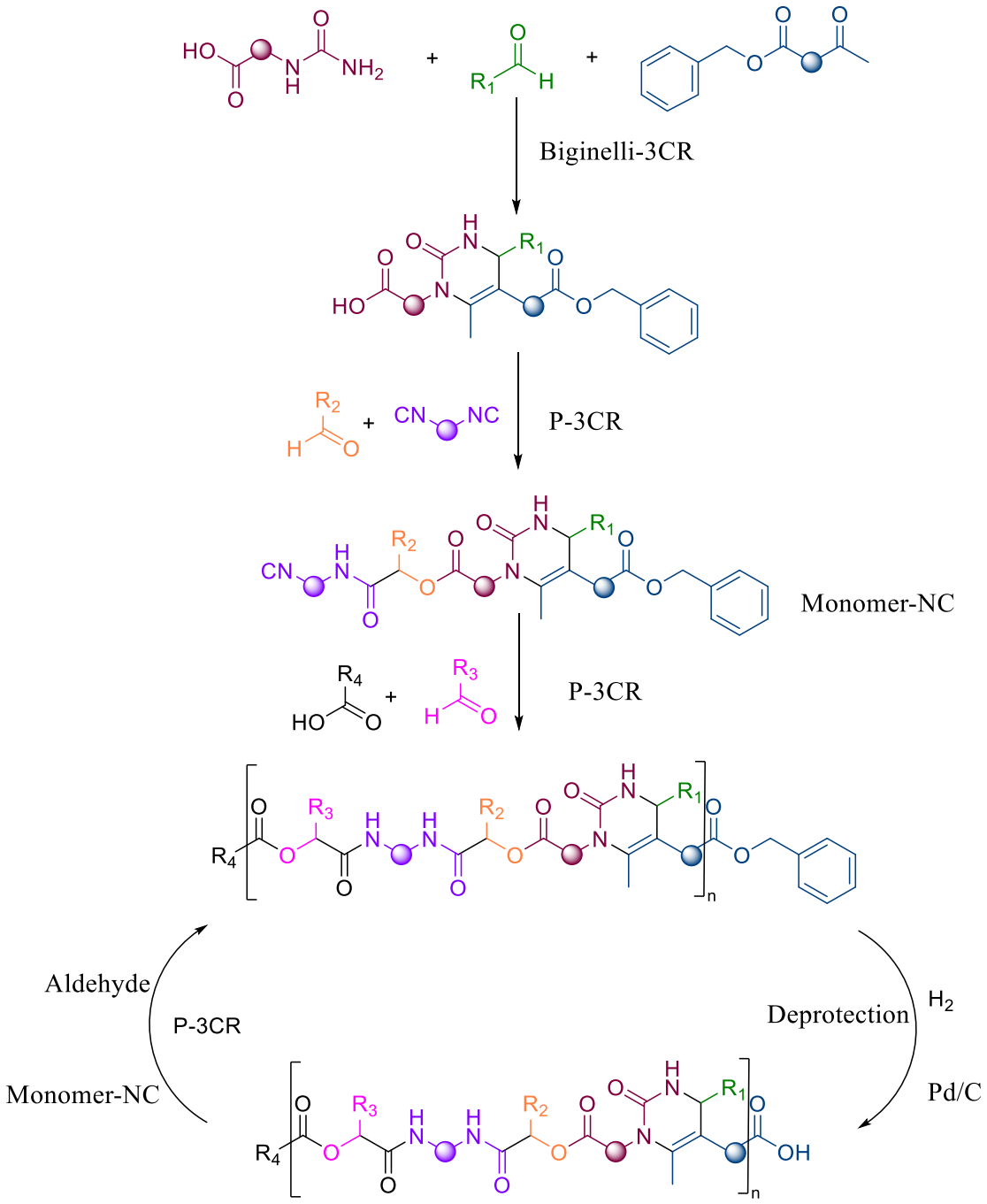

Scheme 19: Macromolecules defined by a synthetic sequence via the Biginelli and P-3CR. In the

Biginelli reaction, urea, an aromatic aldehyde and an acetoacetate react to form Biginelli acid, which then reacts with an aldehyde and diisocyanides to form isocyanate monomer (monomer-NC). The monomer is polymerized repeatedly via the following Passerini reaction, with the addition of aldehydes and carboxylic acids. After hydrolytic benzyl deprotection, the growing macromolecule is equipped with a free carboxylic acid, allowing the addition of the next monomer-NC in the next Passerini step.[224]

In the next year, Du Prez and Meier combined click chemistry with P-3CR to study and compare the processes of synthesizing sequence-defined oligomers in the solid state and in solution.[225] In solution synthesis, stearic acid is used as a starting material, reacted with aldehydes and molecules which containing isocyanides and conjugated dienes, to form Passerini product. The double bonds in the resulting product continues to react with TAD, and the unreacted carboxylic acid group is subjected to P-3CR with aldehydes and molecules with isocyanides and conjugated dienes. By repeating this cycle, a macromolecule with a defined sequence can be synthesized in solution. In solid-phase synthesis, the 2-chlorotriphenylmethyl chloride functionalization resin reacted with TAD first to introduce a carboxylic functional group. Subsequent reactions are similar to those in solution (comparation in Scheme 20). In solution, the Passerini reaction takes longer and requires purification by methods such as column chromatography. Purification in this way can yield a product of much higher purity(>99%). The synthesis in solution can be easily scaled up to multi-gram quantities in theory. The main advantage of solid-phase chemistry is that it is possible to use large excesses of reagents to ensure 100% conversion, and the product is purified by a simple washing procedure. Purification is much faster than with methods such as column chromatography and, in principle, the reaction can be automated. Working on a solid support therefore greatly simplifies and accelerates the synthesis and post-treatment procedures, with shorter reaction times.

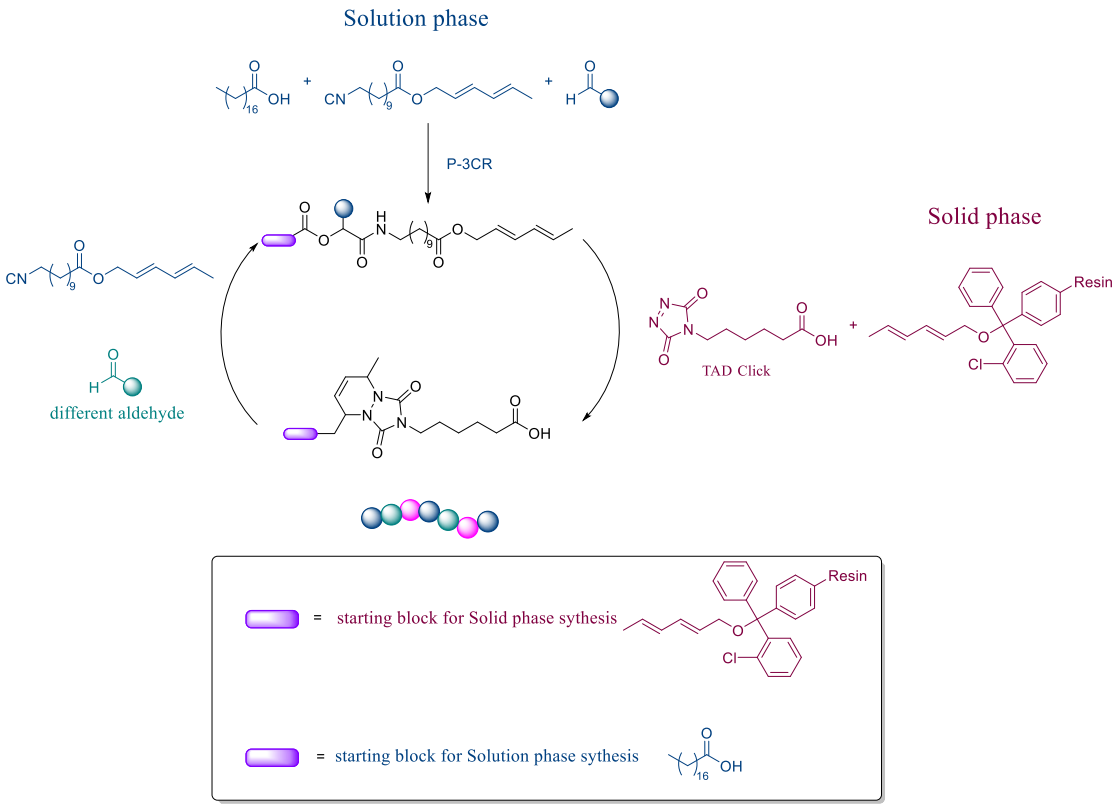

Scheme 20: A two-step iterative reaction cycle consisting of a P-3CR and a TAD Diels-Alder reaction can be used to synthesize sequence-defined macromolecules in the solid phase and in solution.[225]

In 2019, Tao *et al.* researched the process of synthesizing sequence-defined peptides via U-4CR.[226] First, acetic acid as the starting acid reacted with aldehydes, isocyanates and acid-protected amino acids, to form an Ugi product. The resulting products were deprotected with trifluoroacetic acid to obtain free acids, which were reacted in the next Ugi reaction with isocyanides, aldehydes and amino acids. By carrying out the reaction in multiple cycles and using different aldehydes, decamers with different sequences of side chains were obtained. The main chain was defined by changing the amino acids. In the same year, Barner-Kowollik *et al.* described the visible light-induced synthesis of poly(amide thioester)s.[227] The polymers are prepared by in situ generation of thioalcohol, which is then used as an oxygenated component in Passerini polymerization. These polymers can then be cleaved by ammonolysis or chain-extended by inserting thietanes.

In 2020, the Meier group successfully synthesized twelve different sequence-defined tetramers and three hexamers with different mass tags and side chains by iteratively

Passerini three-component reactions and subsequent deprotection steps. Using mass tags as starting compounds simplified MS/MS data and allows the sequence of the synthesized oligomers to be clearly read. By writing a simple Python script for ESI-MS/MS analysis, the information stored in these oligomers can be quickly sequenced and read.[228] Rosenstein *et al.* used U-4CR to synthesize a variety of macromolecules, with each molecule representing a piece of information. An 880,000-pixel Picasso painting was written and read out using fragment mass analysis.[229] Many similar articles had published in recent years.[229-235]

Recently, the same group used P-3CR to synthesize the first-generation dendrimer with a uniform structure by the divergent method. Three oligo (phenyl ethynyl) homopolymers (OPEs) with different lengths and low solubility were used as focal points to achieve self-assembly of the dendrimer solution. This was confirmed by fluorescence spectroscopy and diffusion-ordered NMR (DOSY NMR) spectroscopy.[236] These studies suggest that multicomponent reactions (MCRs) are highly effective for the synthesis of sequence-defined macromolecules due to their versatility, efficiency, and ability to generate complex and diverse structures.

3 Aim

In the first part of work, the aim was to investigate possible structure-property relationships and to determine the structure of sequence-defined macromolecules by fragmentation patterns. For the synthesis of the macromolecules, a well-established iterative cycle consisting of a P-3CR and subsequent deprotection steps was used as a powerful toolbox for sequence-defined molecules. The stepwise synthesis of sequence-defined macromolecules in solution led to complete conversion of the reactions and high yields, ideally without side reactions, and the products were isolated in high purity. The products are measured using common analytical tools for purity determination and structure elucidation (NMR, SEC, ESI-MS), as well as tools for the investigation of thermal properties (DSC and TGA). The results are discussed to explore the structure-property relationship of the molecules. The results of the ESI-MS/MS measurements of the Passerini products are analyzed and the fragment patterns are assigned accordingly. The structure of the formed pentamers was determined based on the values of the detected fragments. Only this MS/MS analysis allowed to distinguish the different sequences prepared.

The aim of the second part of work was to vary the components of the Passerini reaction with the aim to prepare defined macrocycles. A diisocyanides as the core component, reacted with a diacid and isobutyraldehyde under highly diluted conditions in a one-pot reaction, resulted in cyclic macromolecules. The selectivity was determined by combining the SEC profiles with the SEC peak fitting of the crude product and the most highly purified product obtained. The structure of the final product was determined by NMR, IR, and ESI-MS. Even with the same reaction conditions and reactant ratios, the final products will result in either monocyclic or bicyclic compounds due to their different structures.

4 Results and Discussion

4.1 Accurate synthesis of pentamers with phenyl groups at specific positions *via* Passerini reactions

Abstract

Stearic acid was reacted with an α-isocyano ω-benzyl ester AB building block and two different aldehydes containing an isopropyl or a α-methylphenyl group, respectively, in an iterative Passerini three-component reaction (P-3CR) and subsequent deprotection approach. Thus, each permutation of sequence-defined pentamers bearing an aromatic side group at different positions of the synthesized pentamers was realized. All oligomers were obtained in overall yields between 30% and 45% and were characterized by NMR and IR spectroscopy, SEC, and HR-ESI-MS mass spectrometry. The thermal properties were analyzed with DSC and TGA. This series of sequence-defined macromolecules does not show any sequence-related property changes, thus each individual macromolecule was only unambiguously distinguishable by ESI-MS/MS.

4.1.1 Synthesis

An iterative synthesis scheme involving the Passerini reaction and subsequent deprotection was used to synthesize the pentamer. For this iterative cycle, monoprotected monomer was necessary. An AB building block bearing an isocyanide and a benzyl ester was prepared according to a previously reported procedure.[221] In the initial P-3CR, stearic acid (C_{17} portion represented as blue sphere in Scheme 21) was reacted with the AB building block and the aldehyde component. After stirring at room temperature for 1 day and purification by column chromatography, the Passerini product was obtained. The resulting product can be subjected to another P-3CR after Pd-catalyzed hydrogenolysis of the benzyl ester protecting group and a simple workup by filtration (Scheme 21), closing the iterative synthesis cycle. Using this strategy, the monomer, dimer, trimer, and tetramer were then synthesized iteratively, and six

different pentamers (**P0-P5**) were obtained after five Passerini reactions and four deprotection steps, respectively, with a total yield of 30-45%. Two different aldehydes (isobutyl- and 2-phenylpropionaldehyde) were used, and the position of the aromatic moiety was varied systematically. A pentamer only derived from isobutyraldehyde (**P0**) was prepared as a reference. For the other five pentamers, 2-phenylpropanal was used as the aldehyde component in one of the iterative cycles. This allowed the α-methylphenyl side chain to be installed in each possible position of the pentamers, as depicted in Scheme 21 as orange spheres (**P1 - P5**). The products of all steps were fully characterized, as detailed in chapter 6.3.1.

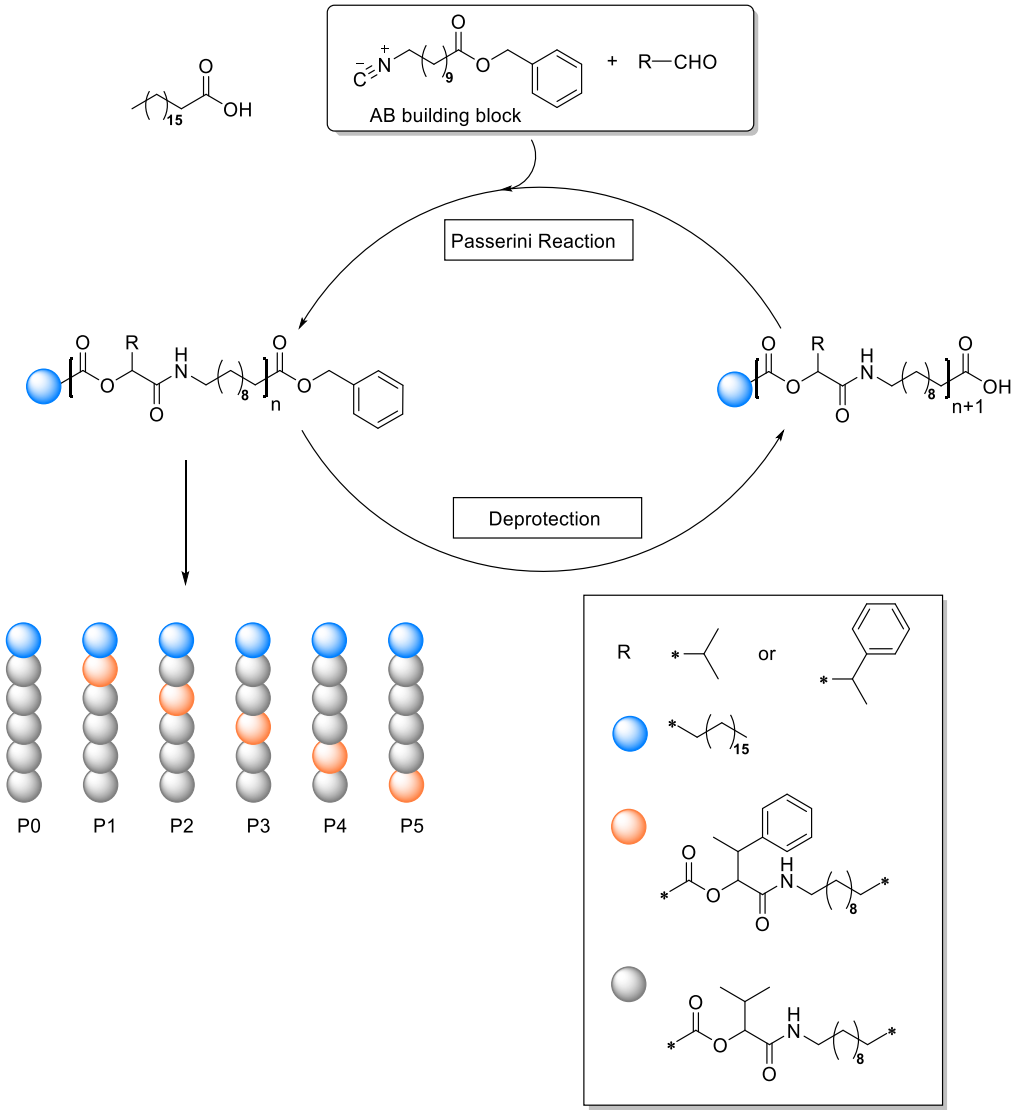

Scheme 21: Iterative step approach with a P-3CR and deprotection. Synthesis strategy towards sequence-defined macromolecules using the monoprotected AB building block (left). Schematic structures of the sequence-defined pentamers differing in the position of the aromatic side chains (right).

4.1.2 Comparison

Each of the Passerini reactions was monitored *via* IR spectroscopy, which is exemplarily shown for one P-3CR (in Figure 4) in comparison with the AB building block. According to the vanishing of the characteristic NC stretching vibration around 2250 cm^{-1} after 12 hours and the observation of the N-H vibration around 3330 cm^{-1}, and the formation of the C=O vibration around 1600 cm^{-1}, a quantitative conversion of the isocyanide and the formation of the α-acyl amide was assumed.

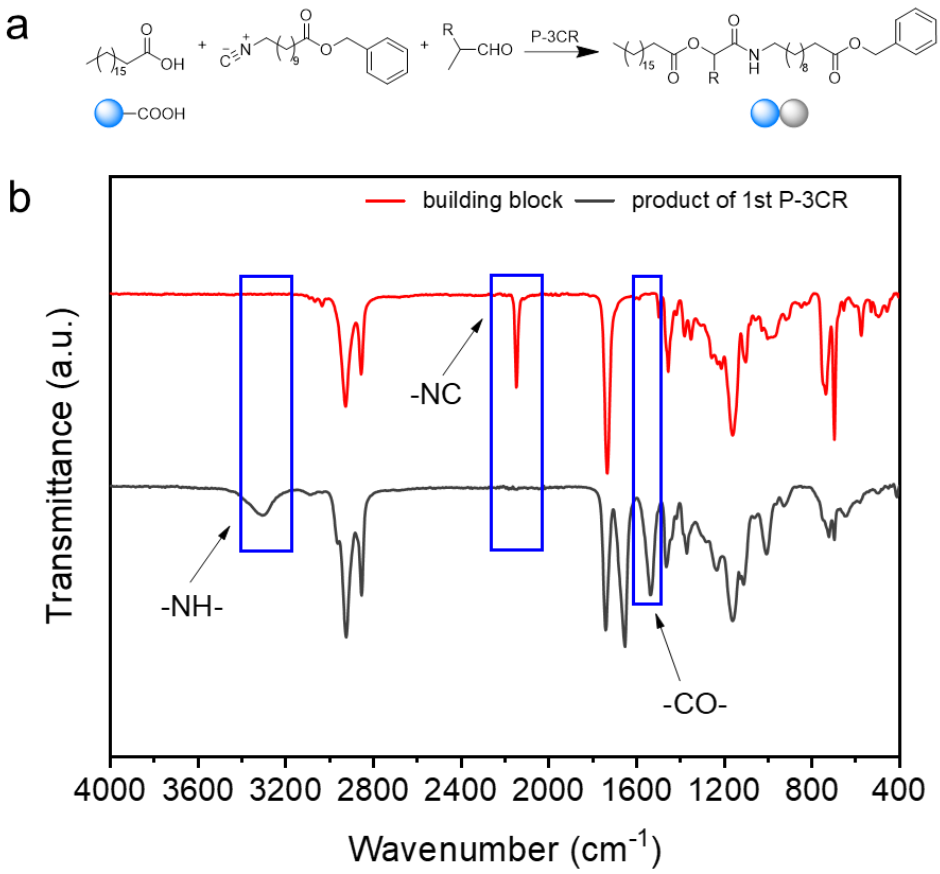

Figure 4: a) Synthesis scheme of the first Passerini product. b) Comparison of the IR spectra of the building block M1 (red, upper graph) and Passerini product (black, lower graph).

P1, which is the pentamer with the α-methylphenyl side chain in the first position of the side chain, was taken as example and analyzed thoroughly. During its synthesis, 2-phenylpropionaldehyde was used in the first Passerini reaction, and isobutyl propionaldehyde was used in subsequent Passerini reactions. Figure 5 shows the characterization of the products obtained during the synthesis of the sequence-defined

pentamer **P1**, including the structure of the sequence-defined pentamer **P1** (Figure 5, top) the SEC traces of all P-3CR products during the synthesis of **P1** (Figure 5, bottom), and the exact mass values found in ESI-MS experiments. As the number of repeating units increases in the iterative synthesis process, the molecular weight of the oligomers increases and thus also their hydrodynamic volume, as observed in the SEC traces showing a decrease in retention time with increasing oligomer size (Figure 5). Detailed characterization data of all oligomers formed in the described iterative synthesis is provided in the chapter 6.3.1.

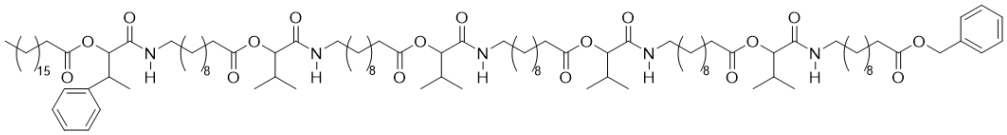

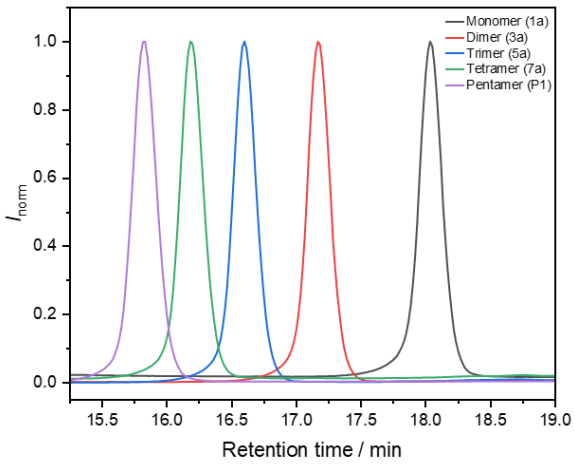

Product	Calc. / Da	Detected / Da
Monomer	720.5564	720.5562
Dimer	1003.7700	1003.7709
Trimer	1286.9870	1286.9856
Tetramer	1570.2025	1570.2024
Pentamer	1853.4168	1853.4151

Figure 5: SEC traces of monomer, dimer, trimer, tetramer and pentamer formed during the synthesis process and the corresponding ESI-MS values.

Figure 6 shows the ^{1}H-NMR spectrum of each product synthesized by P-3CR during the synthesis of **P1**. Except for the first P-3CR product, the remaining products show additional signals around 5.05-4.95 ppm for methine groups. This is due to the implementation of the aldehyde groups in the P-3CR. Apart from this, there are no significant differences in the other signals, which indicates that the chemical environment of most other hydrogen atoms is similar during synthesis.

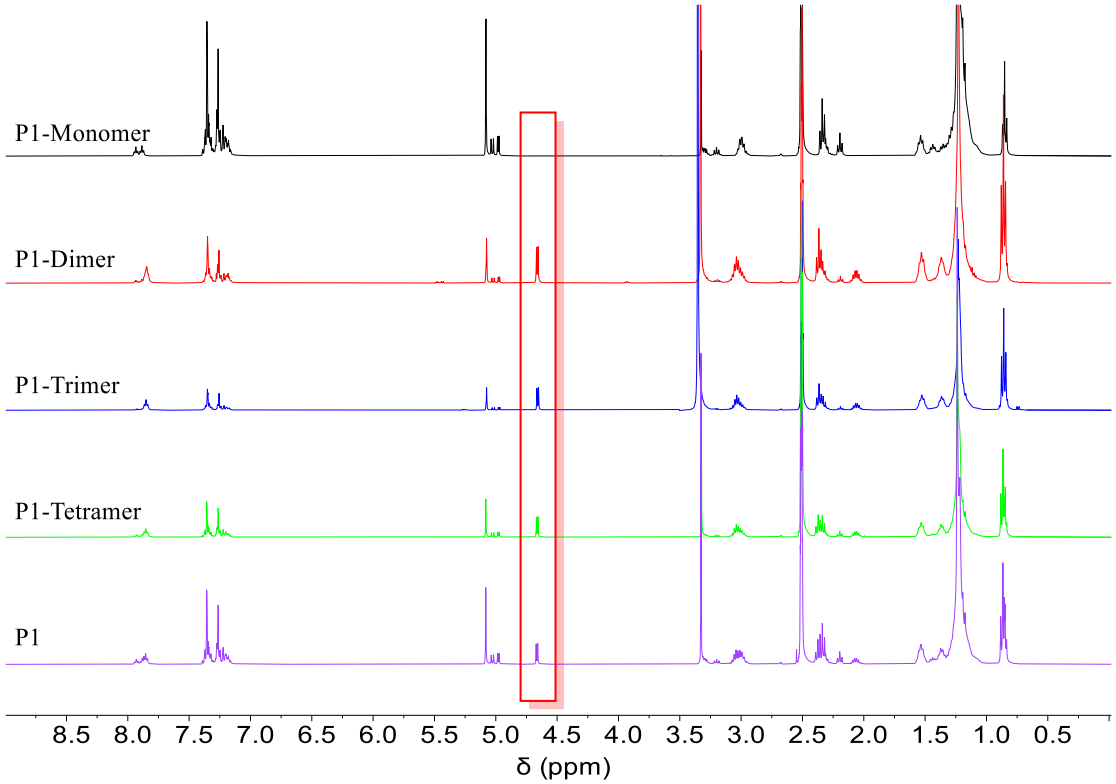

Figure 6: The ^{1}H-NMR of each Passerini product during the synthesis process.

Next, ^{1}H, ^{13}C-NMR and diffusion ordered- and IR spectroscopy, HR-ESI-MS and SEC measurements of all products were preformed and evaluated. In summary, all analytic data confirm that sequence-defined, uniform macromolecules were obtained.

Since pentamers **P1** to **P5** are constitutional isomers to each other, their IR spectra are very similar (Figure 7.a). However, due to the lack of a 2-phenylethyl side chain in **P0**, a small difference in the aromatic C=C stretching vibration at 1535 cm^{-1} can be observed (~2.5% difference in normalized signal intensity, Figure 7.b). This shows that **P0** can be distinguished by IR spectroscopy, while **P1** to **P5** cannot be distinguished by this method.

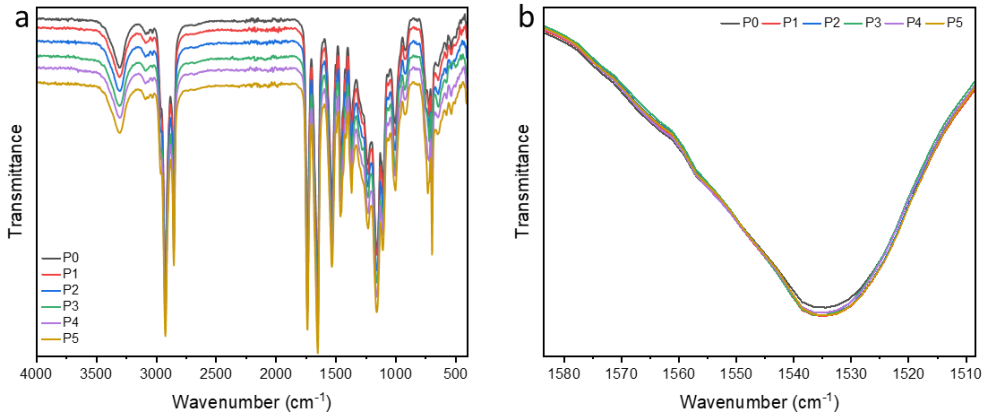

Figure 7: a) IR-spectrum of pentamers **P0-P5** in the range from 4000 to 500 cm^{-1}. b) IR vibrations at 1535 cm^{-1}.

Distinguishing **P0** from **P1** to **P5** is obviously much easier by ^{1}H NMR, as there is no aromatic in side chain present in **P0** (Figure 8.e, signal c). In the range from 7.3 to 7.1 ppm of the ^{1}H NMR spectra (Figure 8.b), additional aromatic signals for **P1** to **P5** compared to that of oligomer **P0** were observed. In the range from 5.5 to 4.9 ppm (Figure 8.c), benzylic proton signal of the end group is observed at around 5.07 ppm. Moreover, oligomers **P1** to **P5** show additional signals around 5.05-4.95 ppm for methine groups (CH), marked yellow in Figure 8.e. The addition of the 2-phenylpropionaldehyde results in the formation of diastereomers and enantiomers. Therefore, there are two doublet signals in the range of 5.5 - 4.9 ppm visible for **P1** to **P5**. The spectra of **P1** to **P4** show a higher consistency in comparison to that of **P5**, for which a shift to lower fields was observed (Figure 8.c), indicating that the 2-phenyl ethyl moiety at the last position in **P5** observed a different chemical environment than for all other positions.

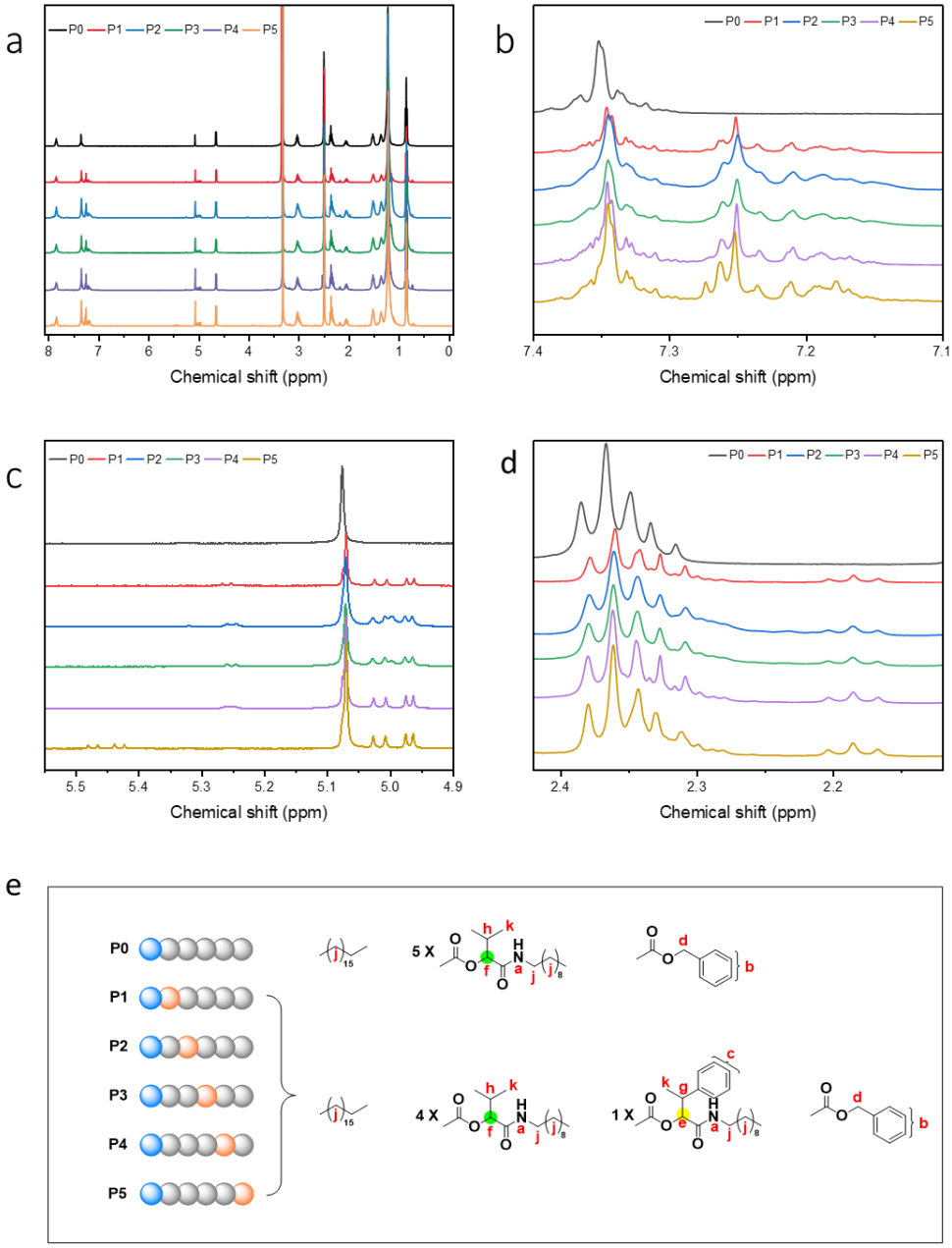

Figure 8: a) ^{1}H - NMR spectra of pentamers **P0-P5** in the whole range. b) ^{1}H-NMR signals between 7.4 - 7.1 ppm. c) ^{1}H - NMR signals between 5.5 - 4.9 ppm. d) ^{1}H-NMR signals between 2.4 - 2.1 ppm e) Highlighted parts of molecule and assignment of the signals.

Interestingly, the retention time (peak maximum) of **P1** to **P5** is 15.85 minutes, indicating that the position of the phenethyl group has no effect on the hydrodynamic volume on this oligomer series (Figure 9, inset). Comparing **P1** to **P5** with **P0** shows that the introduction of an aromatic moiety results in a small but clear change in the hydrodynamic volume of the oligomers, but its position cannot be distinguished by SEC. (Figure 9).

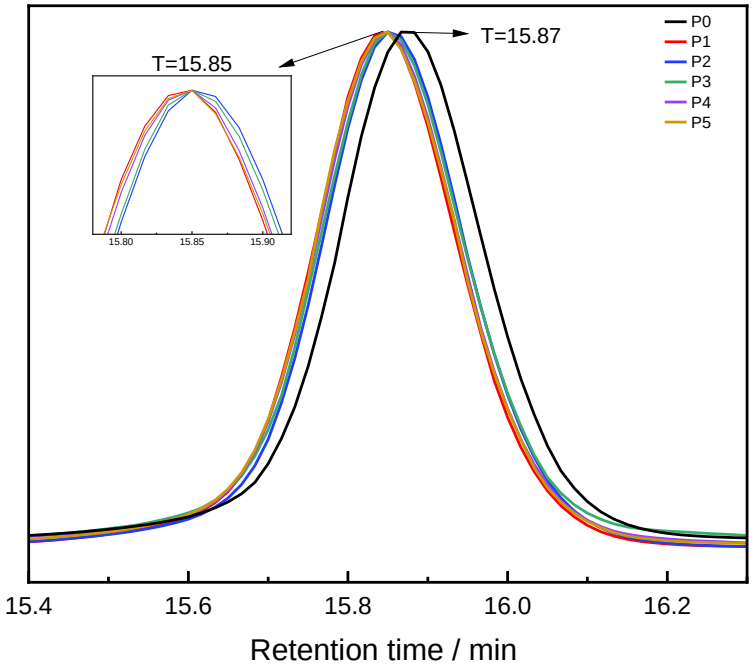

Figure 9: SEC traces of final oligomers.

To investigate the impact of the side-chains on the thermal properties, thermogravimetric analysis (TGA) and differential scanning calorimetry (DSC) were conducted. The onset of decomposition observed by TGA of **P1** to **P5** ranged from 285 to 295 °C, and the decomposition end ranges from 490 to 495 °C, whereas the decomposition end of **P0** is 500°C. Thus, the pentamers with 2-phenylethyl group at different position decompose at a somewhat lower temperature than **P0**. The remaining mass of **P0** is 5.8%, and the remaining mass of **P1** to **P5** is 2.5%. (Figure 10), thus, the remaining mass of **P0** is a 3.2% higher than pentamers with 2-phenylethyl groups at specific positions. The pentamers with 2-phenylethyl groups at different position were more easily decomposed than **P0**. The slight differences between pentamers **P1-P5** were within experimental error and show that a change of the position of the aromatic moiety resulted in no measurable effect on the thermal stability.

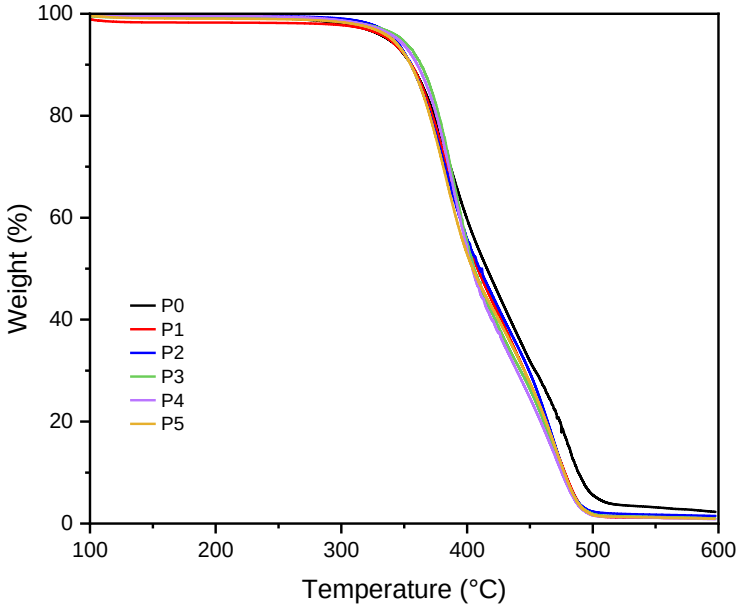

Figure 10: TGA of pentamers **P0-P5**.

Concerning differential scanning calorimetry (DSC), T_g values of each pentamer, ranging from -26 to -20 °C (Figure 11) were observed, a clear relationship between the presence and position of the aromatic moiety and the glass transition temperature was not observed.

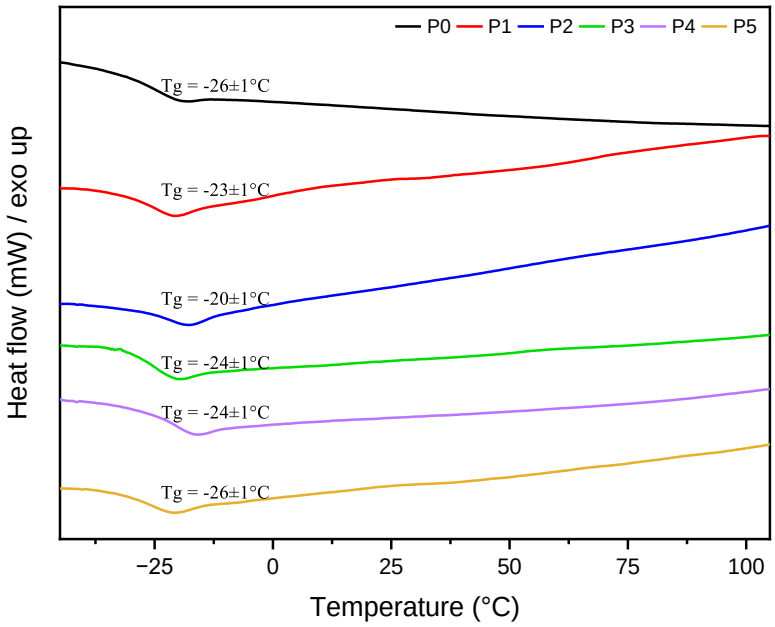

Figure 11: DSC curves of pentamers **P0-P5**.

In summary, it was found to be difficult to distinguish pentamers containing a 2-pehnylethyl side chain by ^{1}H-NMR, ^{13}C-NMR, IR, GPC, ESI-MS or thermal properties.

4.1.3 Identification via ESI MS/MS

So far, using common analytical tools, **P1** to **P5** were indistinguishable. Since our group has expertise in determination of the sequence of Passerini oligomers, MS/MS analysis to decode the different oligomers were performed.[237-240] In Figure 12, the two observed fragmentation pathways of the Passerini motif are shown, which were already reported in a previous study from our group.[239] According to fragment ion notation of Katzenmeyer *et. al.*,[241] the stearic acid moiety is labeled as α-end and the benzylester as ω-end. The fragments formed *via* an α-cleavage of the (C=O)-O ester bond, carrying the α-end, are labeled as **a** or $\mathbf{b_i}^+$ for the acylium ions and $\mathbf{y_j}^+$ for the corresponding protonated alcohols, where **i** is the number of the repeating unit of the macromolecule. On the other side, a McLafferty-type rearrangement can occur, yielding the protonated carboxylic acid $\mathbf{a_i}^+$ or the corresponding Michael-type fragment $\mathbf{z_j}^+$. Since both fragment pairs were detected for each of the repeating unit of the Passerini motif, the structure of the pentamers **P1-P5** can be deciphered from the α-end (blue sphere) as well as the ω-end.

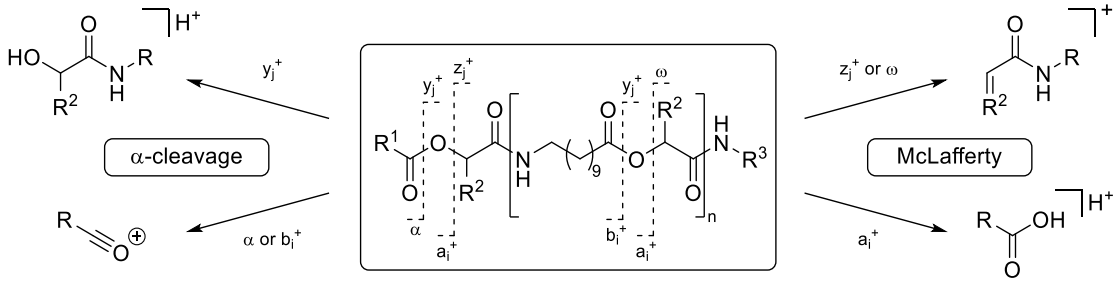

Figure 12: Proposed fragmentation pattern for the Passerini motif. On the left side, the α-cleavage of the (C=O)-O ester bond yielding the acylium ion or the corresponding protonated alcohol is shown. On the right side, the McLafferty-type rearrangement yielding the protonated carboxylic acid or the Michael-type fragment is depicted.

Since the pentamers **P1-P5** exhibit the same chemical formula of $C_{110}H_{189}N_5O_{17,}$ and thus are of the same molecular weight of 1852.4078 g/mol, ESI-MS/MS analysis was performed to differentiate the isomers according to their characteristic fragmentation

pattern.

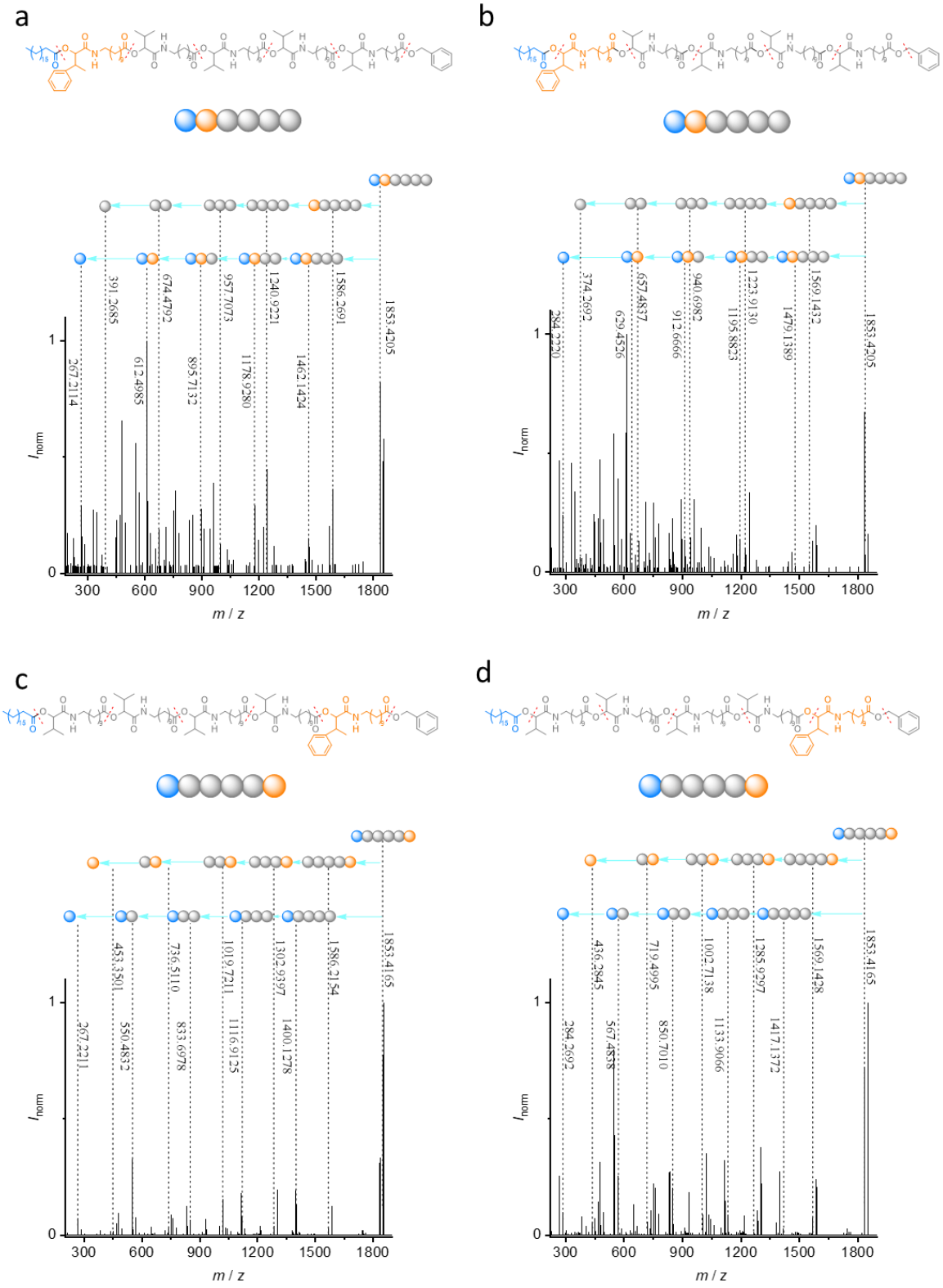

Figure 13: a and b show MS/MS fragmentation patterns of **P1** at *m/z* = 1853.4205 Da recorded in positive mode. a) α-cleavage of the (C=O)-O bond (with an NCE of 19), b) cleavage *via* McLafferty rearrangement (with an NCE of 20). c and d show MS/MS fragmentation patterns of **P5** at m/z = 1853.4165 Da recorded in positive mode. c) α-cleavage (with an NCE of 19), d) McLafferty

rearrangement (with an NCE of 20).

Figure 13 exemplarily shows the mass spectra of **P1** and **P5** after fragmentation, similar figures for all oligomers can be found in the supporting information. The fragmentation points and the corresponding fragments are schematically depicted as red dashed lines and colored spheres, respectively, which are assigned to the respective detected mass. In Figure 13 a and c, the identification of the molecular structure according to the MS/MS spectra observed from α-cleavage, or McLafferty rearrangement (Figure 13 b and c) of **P1** and **P5**, is shown as an example for all synthetized pentamers. The detected masses of all fragments are summarized in chapter 6.3.1. Thus, ESI-MS/MS confirmed that five different and sequence-defined oligomers were obtained, which was not possible via IR and NMR spectroscopy, SEC, ESI-MS or thermal analysis.

4.2 Effects of component structure on macrocyclization *via* the Passerini reaction

Abstract

Cyclic macromolecules find applications in pharmaceutical chemistry, materials science and environmental science, among other fields, and can be synthesized by intramolecular cyclization reactions. The isocyanide-based Passerini three-component reaction (P-3CR) provides multifunctionalized compounds in a one-pot approach, minimizing the total number of synthetic steps. Here, two series of five macrocyclic compounds are described, in which the P-3CR was used to generate macrocyclic compounds. The influence of the structure of the components on the formation of cyclic compounds was explored, and it was found that cyclic macromolecules containing only aliphatic chains could be synthesized more efficiently than macromolecules containing carbazole units.

4.2.1 Synthesis and analysis of building block

To investigate a small scope of different building block structures for macrocycle synthesis, two different diisocyanides were combined with five different diacids (Scheme 24, bottom). As building blocks, one diisocyanide was synthesized from 9-ethyl-9H-carbazole, thus containing a rigid backbone. Another diisocyanide was obtained from hexyl-1,6-diamine with a more flexible aliphatic chain. Therefore, two different diisocyanides with considerable structural differences were used, which allows to investigate the effect of molecular flexibility on the synthesis of cyclic macromolecules.

Carbazole has a highly conjugated structure, and its core structure allows for targeted functionalization at various positions. The 9-ethyl-9H-carbazole molecule was modified by nitration and subsequent reduction to form the diamine **3** (Scheme 22), which was then converted to the diisocyanide **5** (Scheme 22) by the subsequent formylation and dehydration of the corresponding diformamide **4** (Scheme 22).

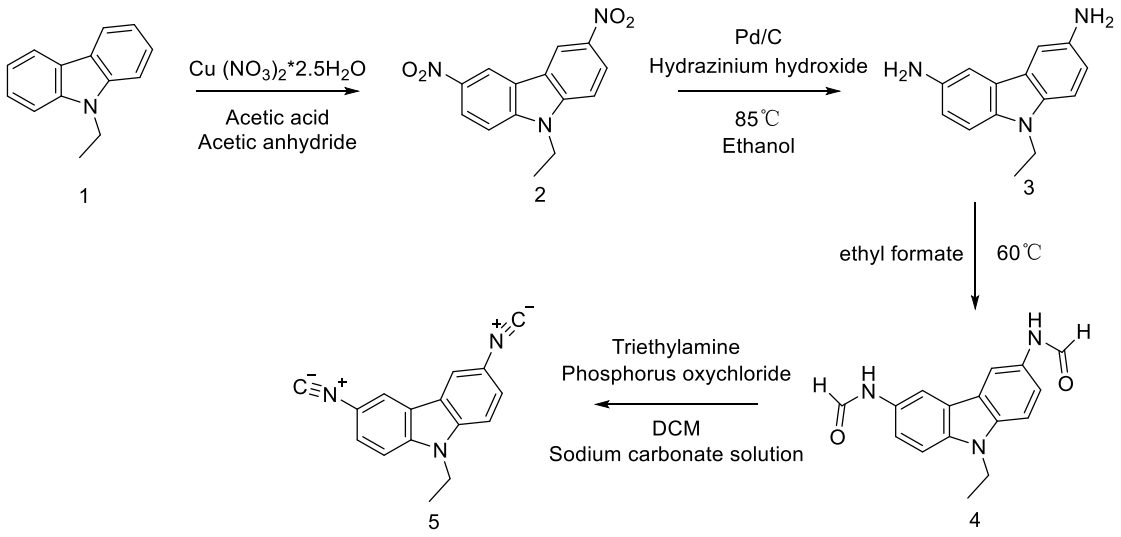

Scheme 22: Flow chart for the synthesis of 9-ethyl-3,6-diisocyano-9H-carbazole (**5**) from 9-ethyl-9H-carbazole (**1**).

The nitrated carbazole was prepared by reacting carbazole with an acidic copper nitrate solution. Purification was achieved via precipitation in water and washing with water, methanol, and dichloromethane, yielding 80% of the product **2**. Nitro compounds **2** are reduced to amine compounds by hydrazine hydrate under the catalysis of Pd/C. The crude product was purified by column chromatography and the product **3** was obtained as grey solid with a yield of 60%. Mix product **3** with ethyl formate and reflux overnight. Product **4** can be used without further purification. $POCl_3$ acted as a dehydrating agent to dehydrate N-formamide to get isocyanide. The crude product was purified by filtration and column chromatography, and obtained a pink solid product **5** with a yield of 45%.

The synthesis process was monitored by different characterization techniques, such as NMR, IR, ESI-MS, and analyzing and comparing the results. Characterization data of all products show in chapter 6.3.2.

Figure 14 shows the ^{1}H-NMR of all intermediates in the synthesis of **5**. The nitro group is strongly electron-withdrawing, containing an oxidized nitrogen atom that forms a large conjugated system with the benzene ring. Due to the mesmeric effect and the electronegativity of the heteroatom, the electron density of the remaining hydrogen atoms in the benzene ring decreases, that is, the corresponding signals shift to lower

field. The isonitrile group decreases the electron group similarly to the nitro group in **2**, but to a lower extend.

The next intermediate **3** contains amino groups. Due to the p-π conjugation between the unpaired electrons of the saturated heteroatom and the delocalized electrons of the benzene ring, the electron density of the benzene ring increases, which is reflected in the ^{1}H-NMR spectrum by a shift of the peaks of the remaining hydrogen atoms of the benzene ring to higher field.

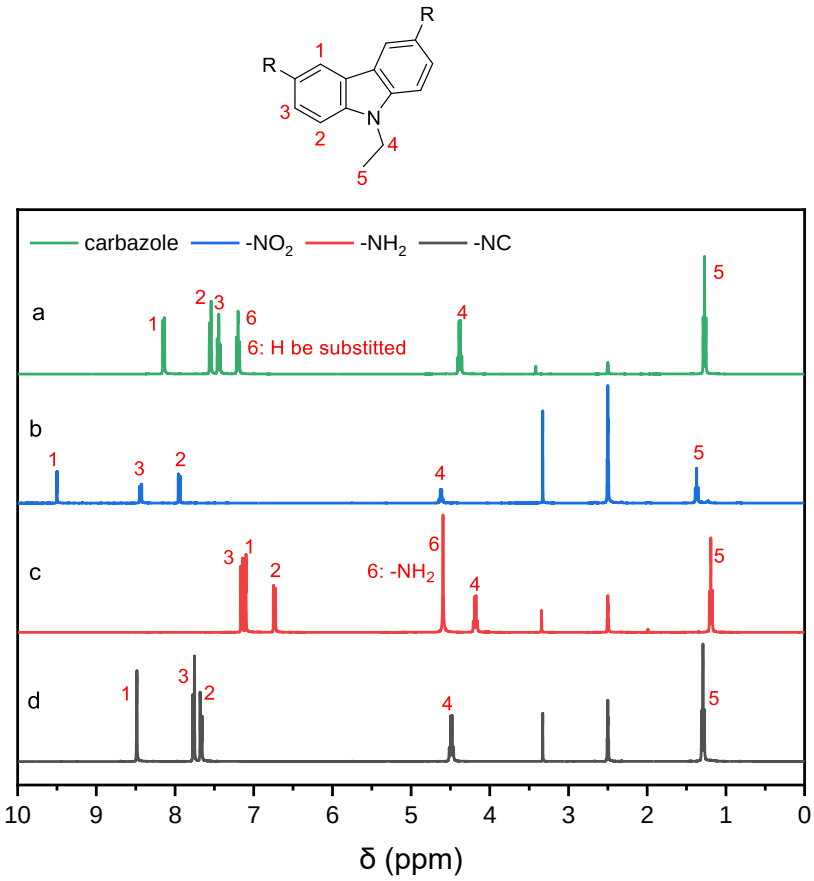

Figure 14: The ^{1}H-NMR spectra of intermediates **2** and **3** and the final product **5**.

Hydrogen atoms in formamides (especially N-H hydrogen) may undergo rapid hydrogen exchange with surrounding solvent molecules (such as water or other hydrogen-containing solvents). Since the rate of this hydrogen exchange is usually faster than the time scale of nuclear magnetic resonance, this can lead even disappearance of the N-H signal. Therefore, the ^{1}H-NMR of the formamide **4** is not shown.

The reaction process can further be monitored with IR spectroscopy. In the aromatic nitro compound **2**, the ν NO_2 asymmetric stretching vibration and symmetric stretching vibration produce two strong peaks near 1540 cm^{-1} and 1350 cm^{-1}, respectively, with the symmetric stretching vibration being stronger. In the diamine **3**, the amino groups exhibit a ν N-H vibration between 3500 and 3100 cm^{-1}. The formamide **3** shows a strong absorption between 1680 and 1630 cm^{-1}, which is ν C=O, and the coupling between N-H stretching vibration and C-N stretching vibration causes the amide band, which can be found at approximately 1570 to 1510 cm^{-1}. Especially the appearance of the characteristic NC stretching vibration near 2250 cm^{-1} confirms the formation of the product **5** (Figure 15) These data indicate that the target product **5** was successfully synthesized.

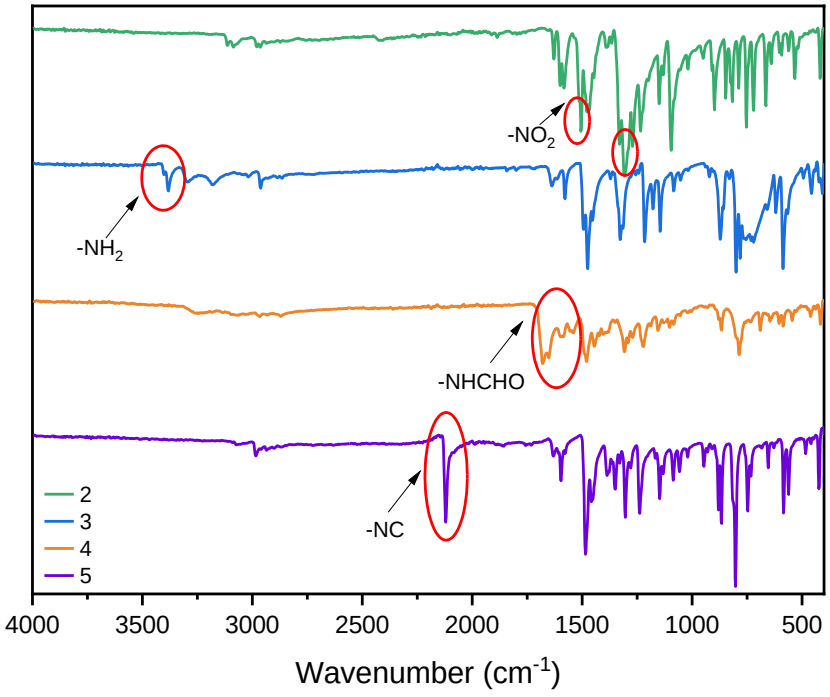

Figure 15: The IR spectra of each step's product.

In combination with spectroscopic methods which can confirm the presence of certain functional groups, ESI-MS represents a useful tool to confirm the constitution of the molecule. For the final product, an m/z value of 246.1025, which is close to the calculated m/z of $[M+H]^+$= 246.1026 can be found in ESI-MS (Figure 16). These data indicate that the target product **5** was successfully synthesized.

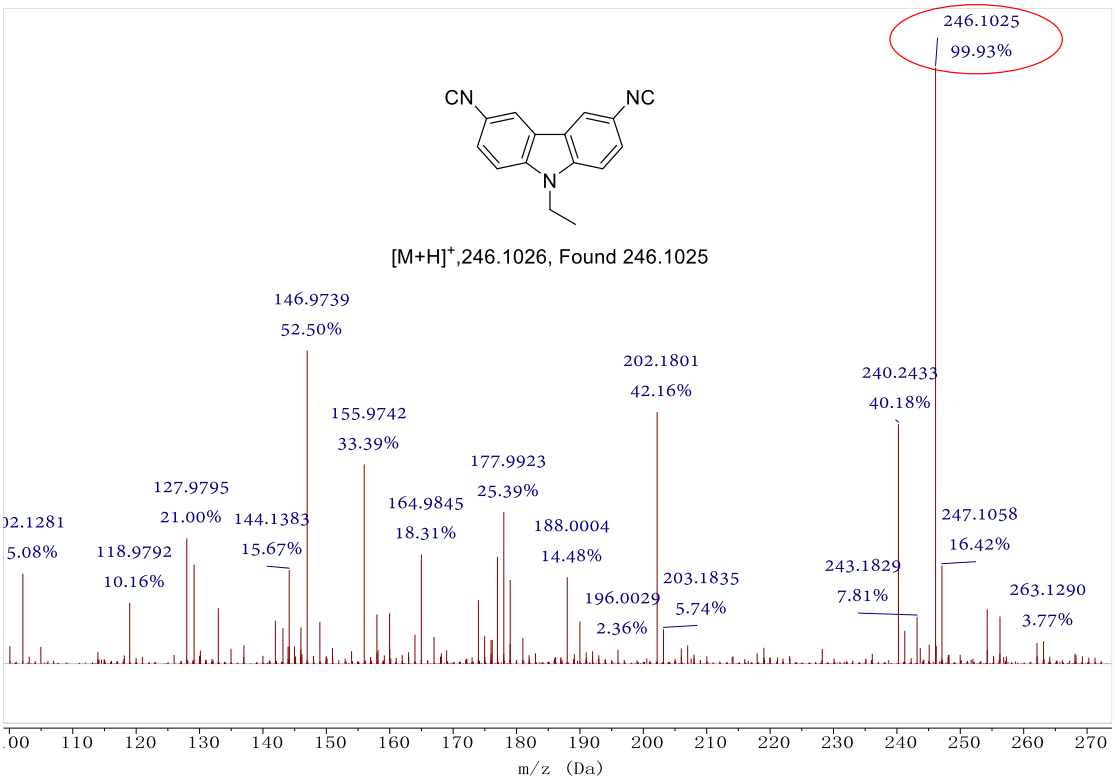

Figure 16: ESI-MS spectrum of diisocyanide **5.**

Similarly, 1,6-diisocyanohexane was prepared from 1,6-N,N′-diformamido hexane by formylation and subsequent dehydration, as was published by our group before.[56] (Scheme 23)

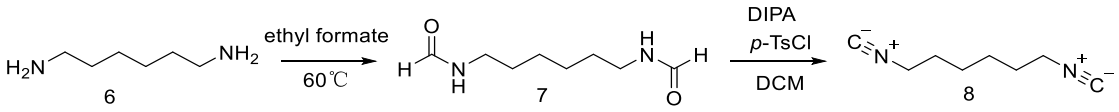

Scheme 23: Flow chart for the synthesis of 1,6-diisocyanohexane.

Our team investigated and optimized a synthetic route for the conversion of N-formamides to isocyanide. For aliphatic foramides, *p*-TsCl was the reagent of choice, due to less toxic compared to other dehydration reagents and easier and greener access to aliphatic isocyanide functionalities, the yields up to 98%.

4.2.2 Synthesis and analysis of cyclic macromolecules

Scheme 24 shows the synthesis plan of cyclic macromolecules using diisocyanides, diacids and a monofunctional aldehyde as the Passerini-MiBs. Generally, depending of the used components, two different cyclic macromolecules or more different cycles may form.

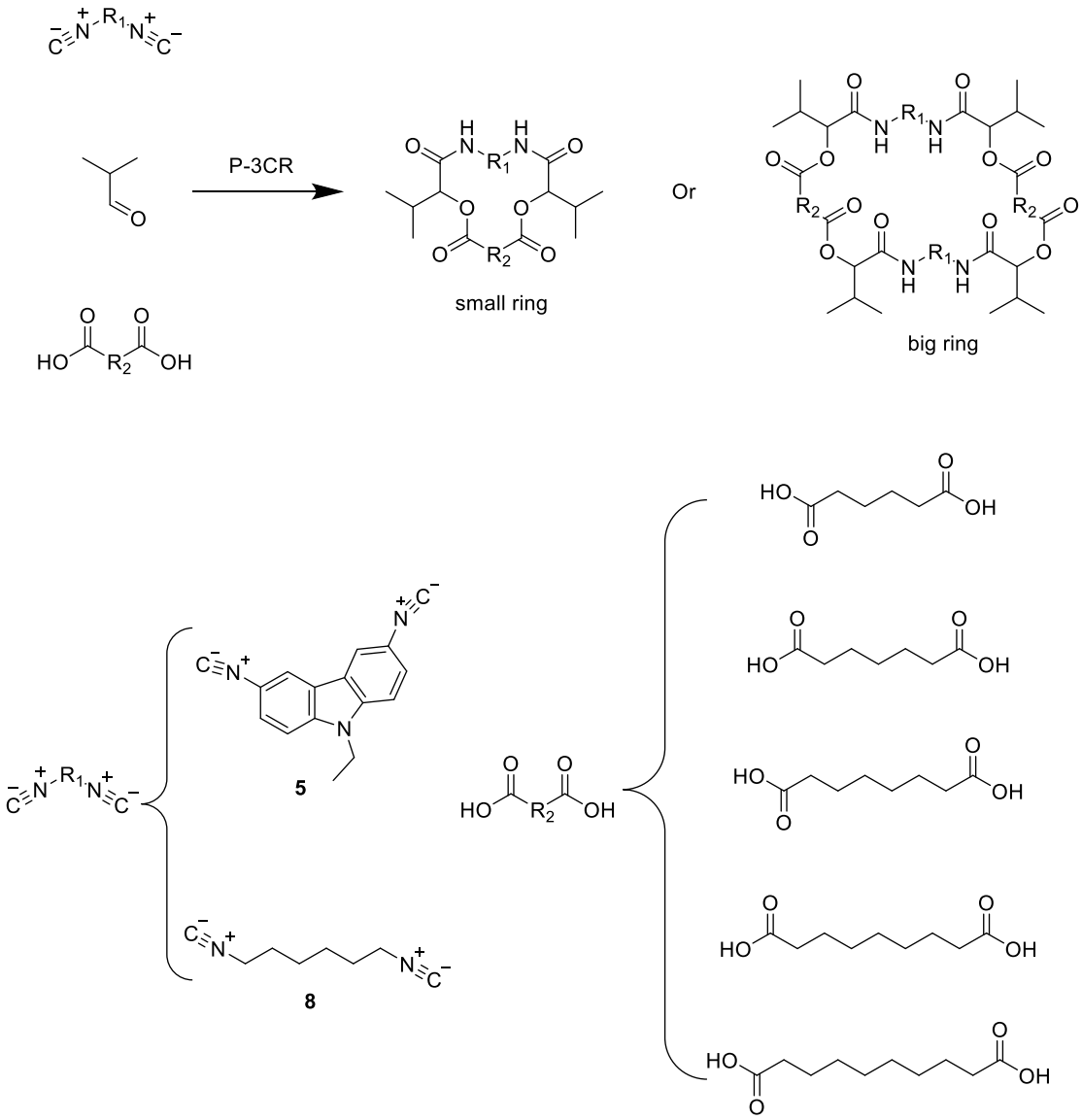

Scheme 24: Reaction scheme for the synthesis of macromolecules *via* the P-3CR (top) performed within this work. The lower part of the scheme shows the investigated components.

Since high dilution favors the formation of macrocycles, the diacid component and the diisocyanide were dissolved in dichloromethane (2 mM), the mixture was dropwise to the mixture solution of isobutyraldehyde and dichloromethane over 24 h and reacted last 96 hours at room temperature. The solvent was removed under reduced pressure. The crude product was purified by multiple column chromatography to afford the final product.

For the synthesis of carbazole-based macrocycles, diisocyanide **5** was reacted with isobutyraldehyde and different diacids (see Scheme 25 for investigated structures).

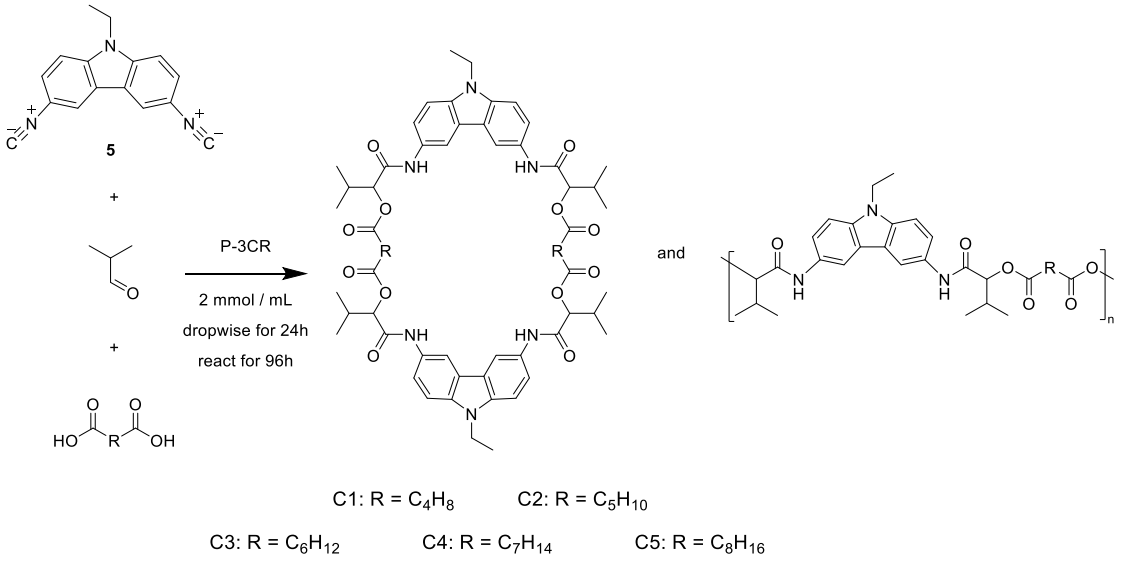

Scheme 25: P-3CR of carbazole-based diisocyanide **5** with isobutyraldehyde and different diacids, allowing for the formation of macrocycles and polymeric species.

The crude products obtained after solvent removal were analyzed by SEC (see Figure 17.a). In all cases, a signal between 18.5 and 20.0 min can be observed, which is assumed to correspond to a macrocyclic species. With increasing chain length of the diacid involved, the signal is shifted to a lower retention time, related to a higher hydrodynamic volume of the cyclic species. At the same time, the signals between 15 and 18.5 min indicate the formation of polymers. It is visible that shorter aliphatic chains within the diacid led to an increased formation of polymers (see Figure 17.a).

In the final products, **C3-C5** containing longer chain diacids, a narrow signal assigned to the macrocycle was obtained after multiple purifications by column chromatography (see Figure 17.b). If the aliphatic chain of the dibasic acid was shorter on the other hand, as in **C1** and **C2**, repeated purification did not result in a successful isolation of the cyclic macromolecules without polymers (see Figure 17.b). Thus, three of the five macrocycles could be obtained and already this observation of practicable isolation showed a clear correlation with size of the aliphatic R-group in Scheme 25. Moreover, the narrow and monomodal SEC traces of **C3-C5** clearly show the high molecular definition of the obtained cyclic compounds. From the SEC traces of the purified compounds, also the retention times of the final macrocycles could be confirmed.

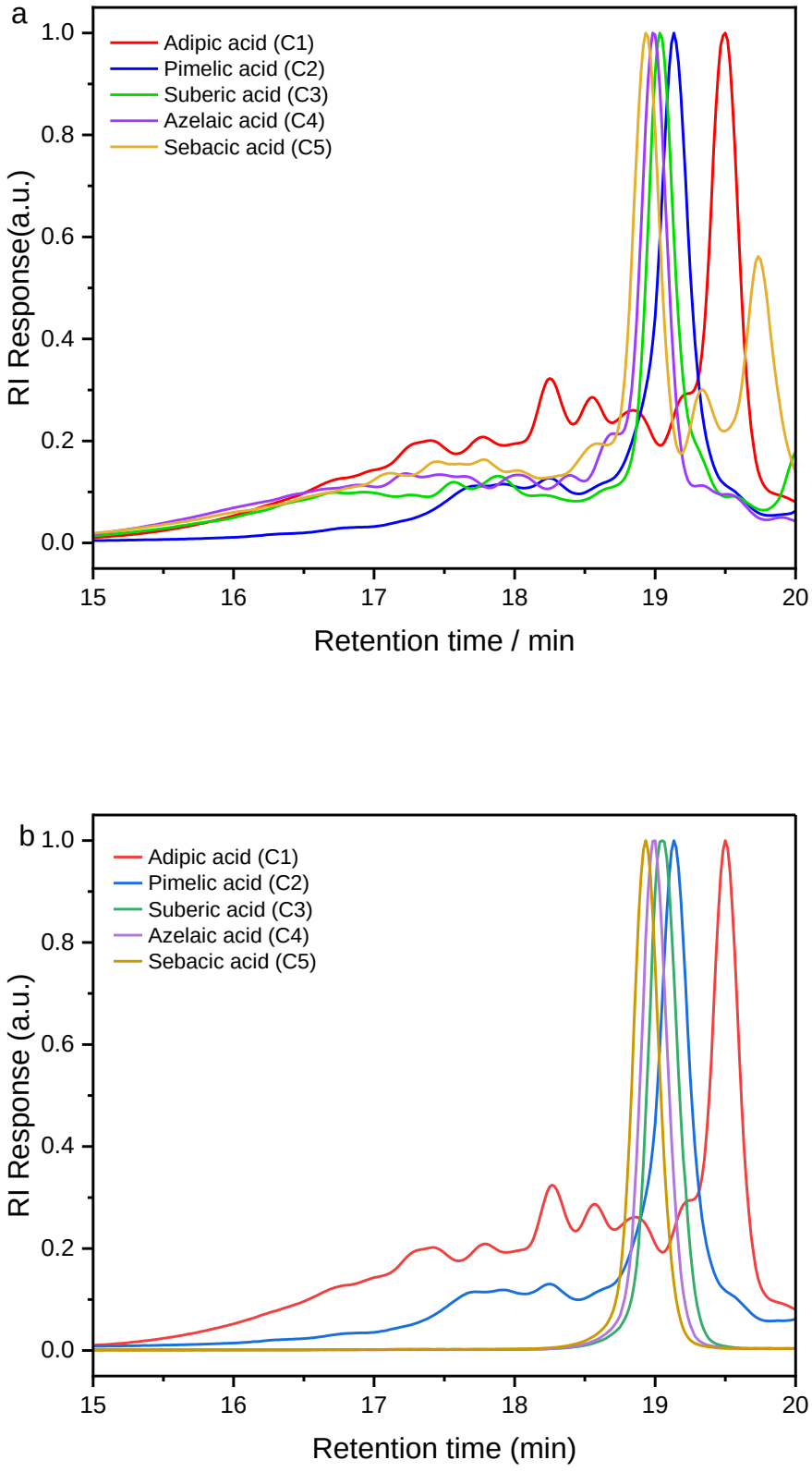

Figure 17: a) SEC traces of crude products of the P-3CR of diisocyanides **5** with isobutyraldehyde and different diacids. b) SEC traces of purified products.

In order to obtain a quantitative measure of the ratio between macrocycle and polymer formation, i.e. information regarding the macrocyclization selectivity, the SEC trace of the crude products was fitted using a peak deconvolution method (see Figure 18 for an example, i.e. for the formation of **C4**) in order to determine the content of cyclic compounds in the crude product.

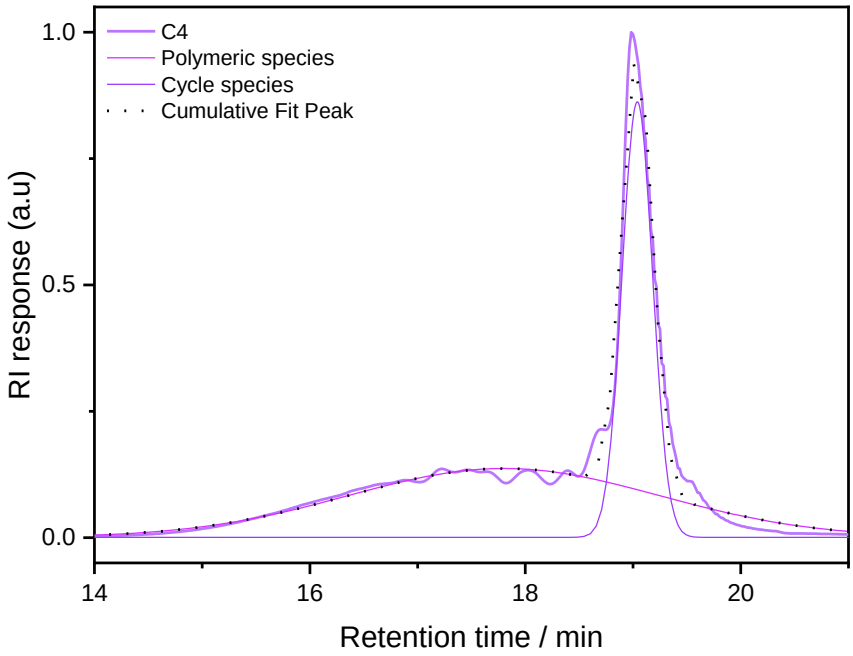

Figure 18: Peak deconvolution of SEC chromatogram from crude product **C4**.

Product	Polymeric species	Cycle species
C1	76%	24%
C2	71%	29%
C3	65%	35%
C4	62%	38%
C5	70%	30%

Table 1: Determination of signal areas of polymeric products and macrocycles for products **C1-C5** using a peak deconvolution.

For an estimation of cyclic compound content, deconvoluted peaks were integrated and a cyclic compound content is given as a percentage.

From ESI-MS measurements, it could be stated that the area at higher retention times corresponds to dimeric cyclic macromolecules. Table 1 shows the ratios of both areas

in the crude samples after peak deconvolution for all investigated diacids. The sample containing the highest content of cyclic macromolecules was obtained by using azelaic acid (**C4**), while the crude product synthesized by adipic acid contained only 24% of the target molecule. ESI-MS confirmed the formation of macrocycles with "ring selectivity", shown in Table 2 together with the calculated yields after purification.

Diisocyanides **5** reacted in P-3CR

Diacid / Product	Theoretical $[M+H]^+$	Experimental $[H]^+$	yield
Adipic acid (**C1**)	1071.5421	n. d.	0%
Pimelic acid (**C2**)	1099.5751	1099.5727	0%
Suberic acid (**C3**)	1127.6063	1127.6063	5%
Azelaic acid (**C4**)	1155.6376	1155.6357	15%
Sebacic acid (**C5**)	1183.6689	1183.6657	7%

Table 2: Theoretical m/z values of the cyclic macromolecules and the values detected in ESI-MS, as well as the final yield.

In each case, the reaction mixtures were purified by multiple column chromatography, obtaining yields of 5% to 15% of the desired macrocyclic compounds, as shown in 6.3.2. Here, the process of the purification of **C4** is used as an example, with Figure 19 showing the SEC trace of the product obtained after each column chromatography purification, and Table 3 showing the determination of signal areas of polymeric products and macrocycles with a peak deconvolution**.**

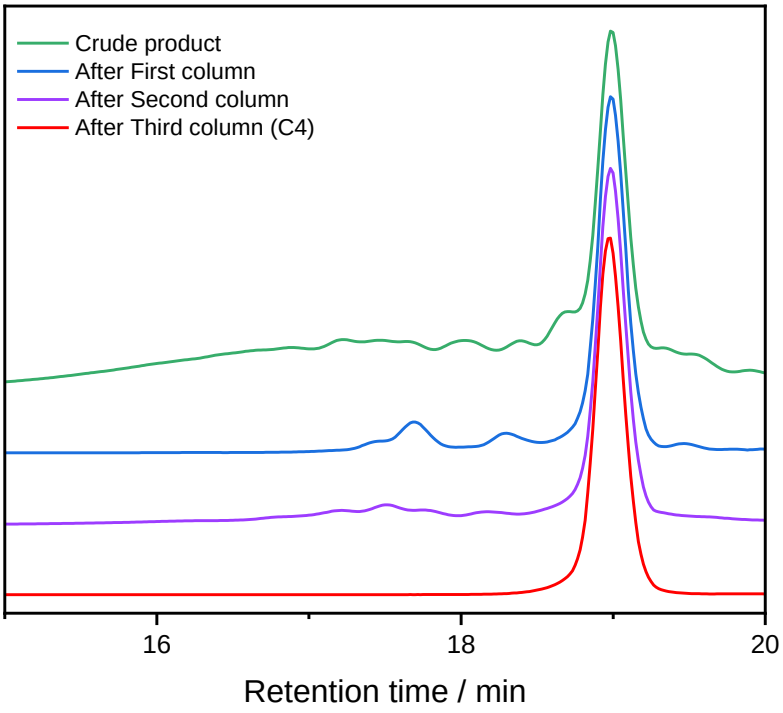

Figure 19: The mixtures of **C4** were purified by 3 times column chromatography.

Peak deconvolution.

Operation	Product	Polymeric species	Cycle species
Remove solvent	Crude product	62%	38%
First column Cy:EA = 7:3	After first column	35%	65%
Second column Cy:EA = 4:6	After twice column	11%	87%
Third column Cy:EA = 5:5	**C4**	0%	100%

Table 3: Determination of signal areas of polymeric products and macrocycles for products using a peak deconvolution after the purification step of **C4.**

As the number of purification steps increases, the signal area of the polymer product gradually decreases, while the area of the macrocyclic product gradually increases until it reaches 100%, obtaining a macrocyclic molecule with high purity.

To further confirm the successful formation of Passerini adducts, the isolated products

were also characterized by infrared spectroscopy. The conversion of the diisocyanide **5** can be observed exemplarily from the IR spectrum of **C4** from azelaic acid (Figure 20). According to the disappearance of the characteristic NC stretching vibration near 2250 cm^{-1} and the formation of the N-H vibration near 3330 cm^{-1}, quantitative conversion can be assumed.

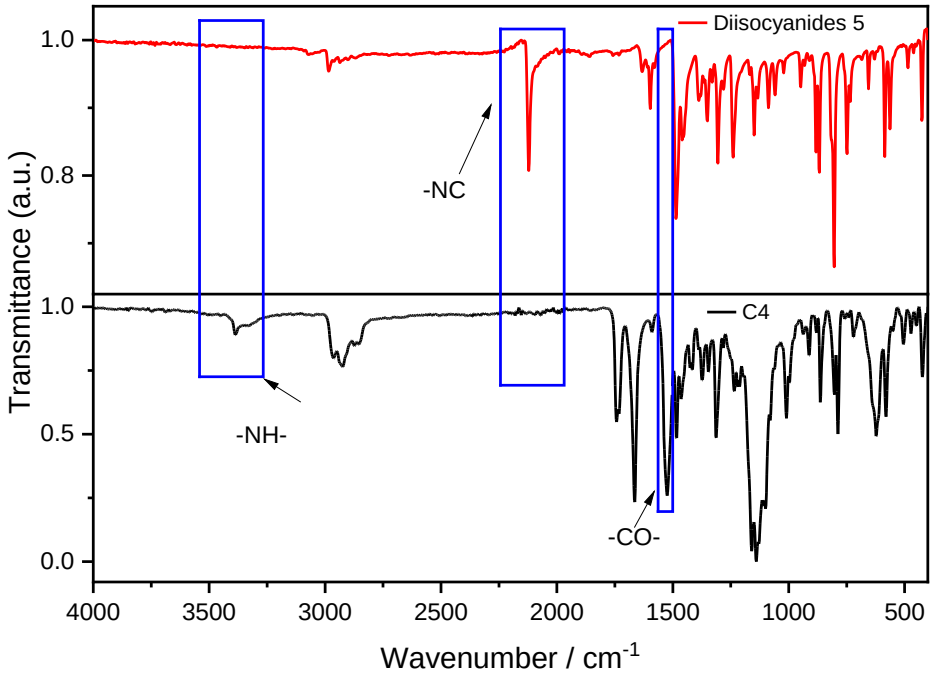

Figure 20: Cyclic macromolecule **C4** synthesized from diisocyanide **5**, isobutyraldehyde and azelaic acid, as well as comparison of the IR spectra of **5** (red, upper graph) and **C4** (black, lower graph)

The product **C4** with the highest yield in the crude reaction mixture is discussed here as a model regarding macrocycle characterization. Figure 21 shows the ^{1}H-NMR spectrum of **C4**, with the signal assignment fitting to a dimeric macrocyclic structure. The NMR data of **C4** show the success by the appearance of characteristic signals and appropriate integrals for the introduced amide protons after the P-3CR. When the isocyanide is converted to α-acyloxy amide, the electron density of the remaining hydrogen atom in the benzene ring increases slightly, and the spectral peaks of the hydrogen atom in the benzene ring all shift to little higher fields.

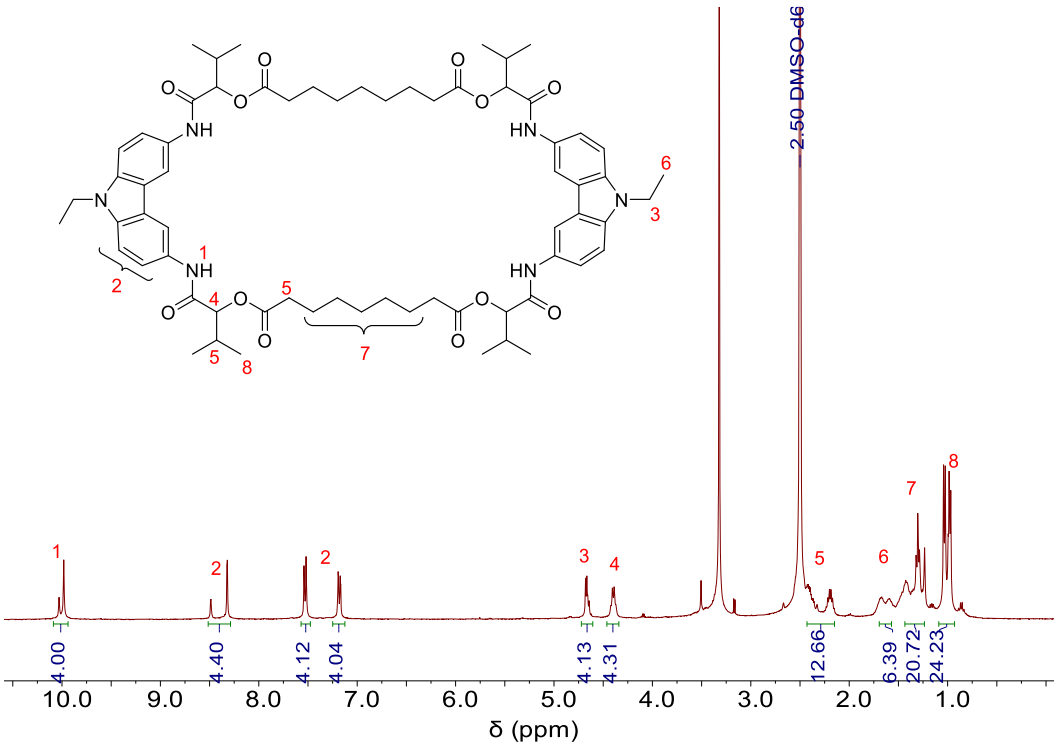

Figure 21: The assigned ^{1}H-NMR spectrum of **C4**.

The formation of the cyclic product was also confirmed via ESI-MS measurements. Figure 22 shows the ESI-MS spectrum of the **C4**. The assigned mass corresponds to the protonated structure (1155.63 m/z) . No other cycle macromolecules larger or smaller than **C4** was found in other ranges.

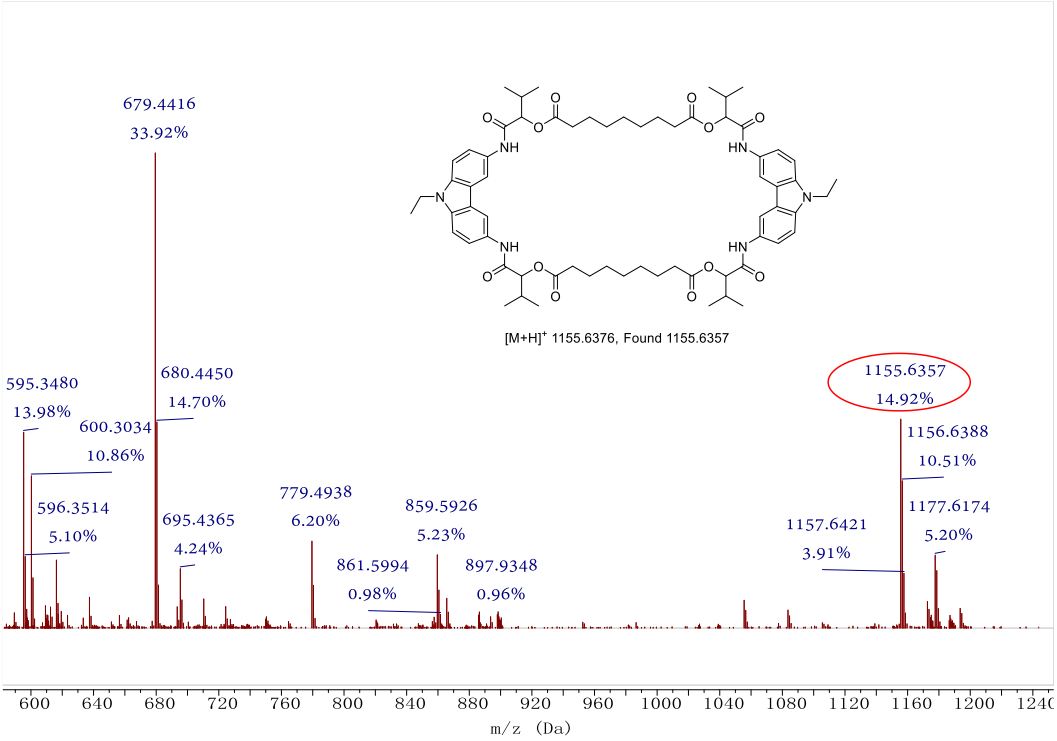

Figure 22: The ESI-MS spectrum of **C4**.

According to the experimental results obtained, after analysis by ^{1}H-NMR, ^{13}C-NMR, IR and MS, cyclic macromolecules with two core units formed in all cases of **C3**-**C5**. For a second set of investigated macrocycles, the aliphatic 1,6-diisocyanohexane **8**, as a more flexible replacement for **5**, was reacted with isobutyraldehyde and different diacids to synthesize cyclic macromolecules (show in Scheme 26).

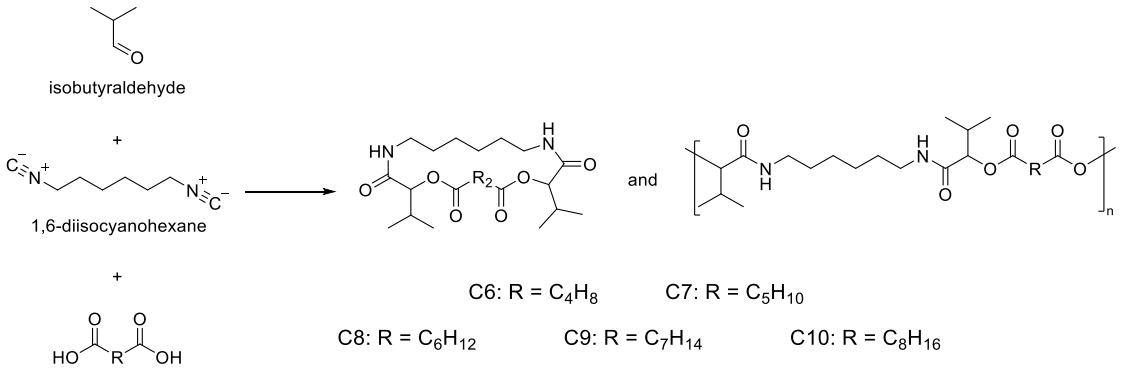

Scheme 26: Reaction of aliphatic 1,6-diisocyanohexane with isobutyraldehyde and different diacids.

As described before, SEC measurements were performed both for the crude products and the purified product after one separation and purification by column chromatography. The SEC traces of the crude products are shown in Figure 23.a, and the SEC traces of the final products in Figure 23.b. In all cases, narrowly distributed and highly pure compounds could be obtained after purification (see Figure 23.b).

In combination with the SEC traces of the isolated products, the area between 16- and 18-minutes retention time can be assumed to show oligomeric higher molecular weight species. ESI-MS measurements indicated that the signals between 19 and 20 minutes correspond to monomeric cyclic macromolecules, as shown in Scheme 25. This represents a clear difference to the use of the carbazole-based diisocyanides **5**, which led to the formation of dimeric macrocycles **C1-C5**.

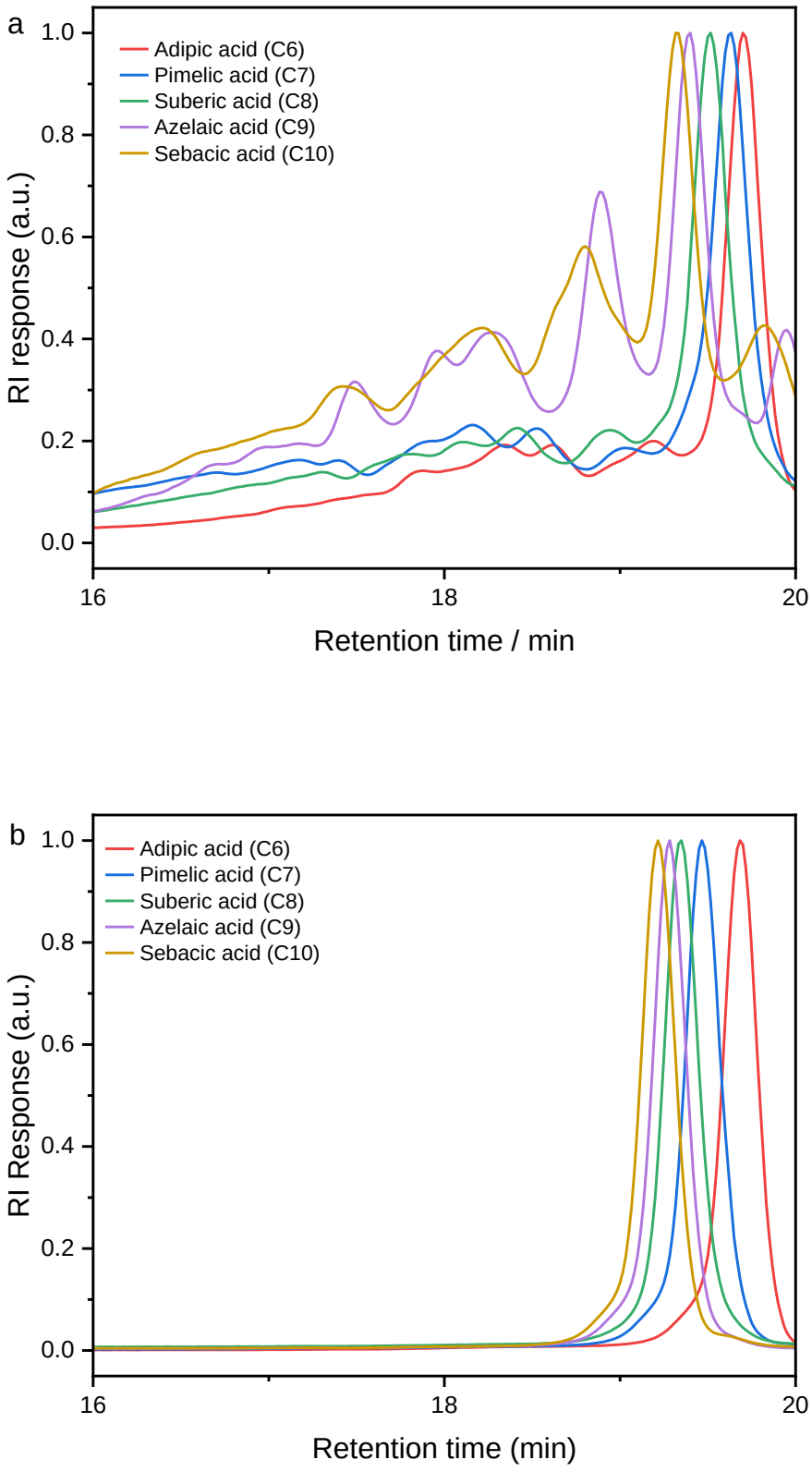

Figure 23: SEC traces of a.) crude and b.) purified products from the reaction of 1,6-iisocyanohexane **8** with isobutyraldehyde and different diacids, forming the products **C6-C10**.

The product **C6-C10** can be separated by one-time column chromatography to obtain a high purity product.

In analogy to the carbazole-containing P-3CR products, the SEC traces of the crude products were evaluated using peak deconvolution (Figure 24). Table 4 shows the ratio of polymeric products to macrocyclic compounds after peak deconvolution and integration. In case of the reaction with suberic acid, **C8**, the highest selectivity towards the formation of the macrocyclic compound was observed.

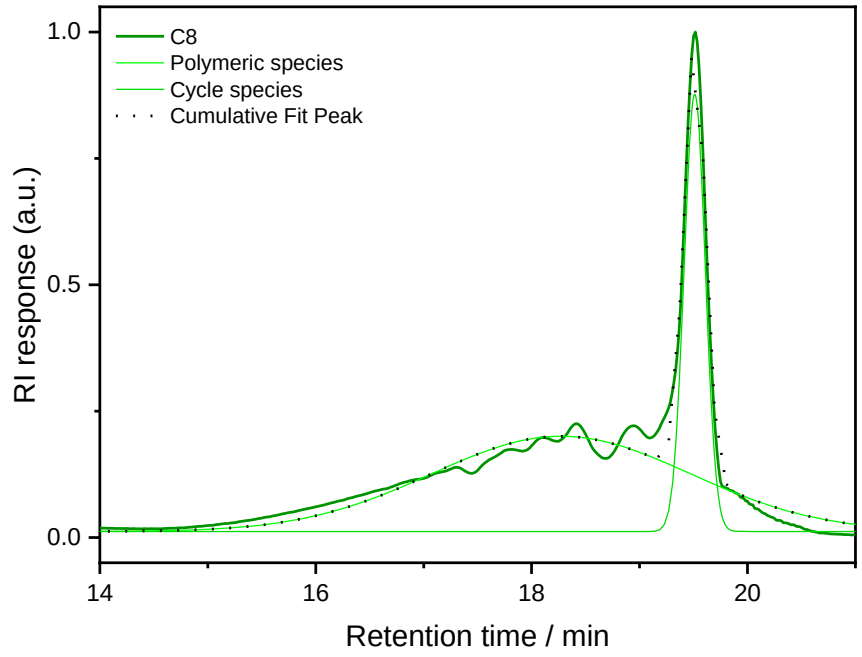

Figure 24: Peak fitting of SEC traces from crude products **C8**.

Product	Polymeric species	Cycle species
C6	69%	31%
C7	66%	34%
C8	63%	37%
C9	74%	26%
C10	76%	24%

Table 4: Determination of signal areas of polymeric products and macrocycles for products **C6-C10** using a peak deconvolution.

Figure 25 shows the IR spectra of the five purified products. All of them don't display a visible characteristic peak of the isocyanide peak near 2500 cm^{-1} and show NH

vibration peaks at 3300 cm^{-1} as well as the C=O stretching vibration at 1600 cm^{-1}. This hints at a successful P-3CR.

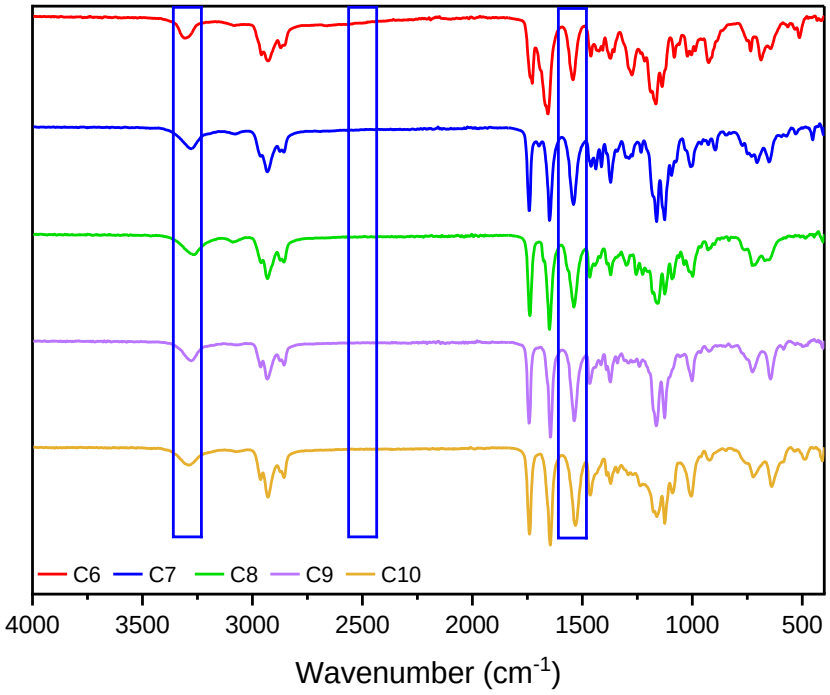

Figure 25: IR spectra of purified products **C6-C10**.

One of these products is analyzed and presented as model herein for all prepared cycles. Figure 26 shows the ^{1}H-NMR spectrum of **C8**, showing the successful reaction by the appearance of characteristic signals and appropriate integrals for the introduced amide protons after the P-3CR. The saturated straight-chain structure, compared to the carbazole structure, causes the peak of the adjacent NH atom to shift to a higher field. Figure 27 shows the ESI-MS spectrum of **C8**. The assigned mass corresponds to the protonated species (455.31 m/z) . No masses fitting to larger ring sizes were observed. Data for **C6, C7, C9** and **C10** are reported in 6.3.2.

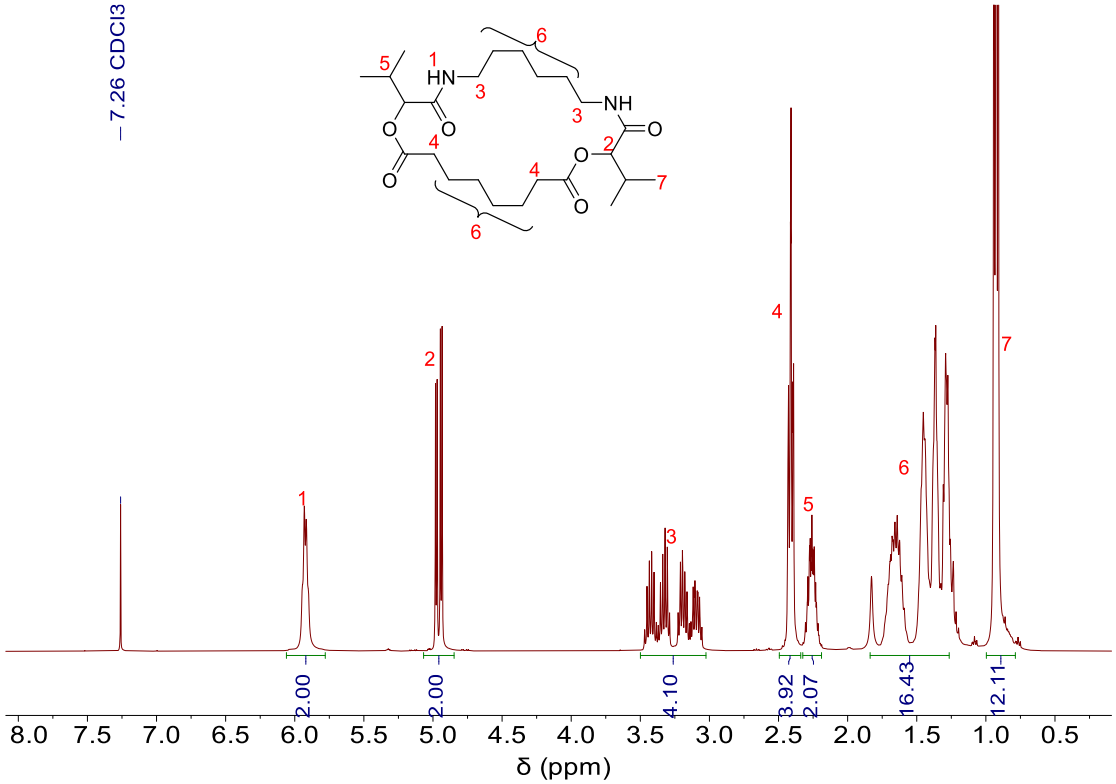

Figure 26: ^{1}H-NMR spectrum of **C8**, with the characteristic signals assigned.

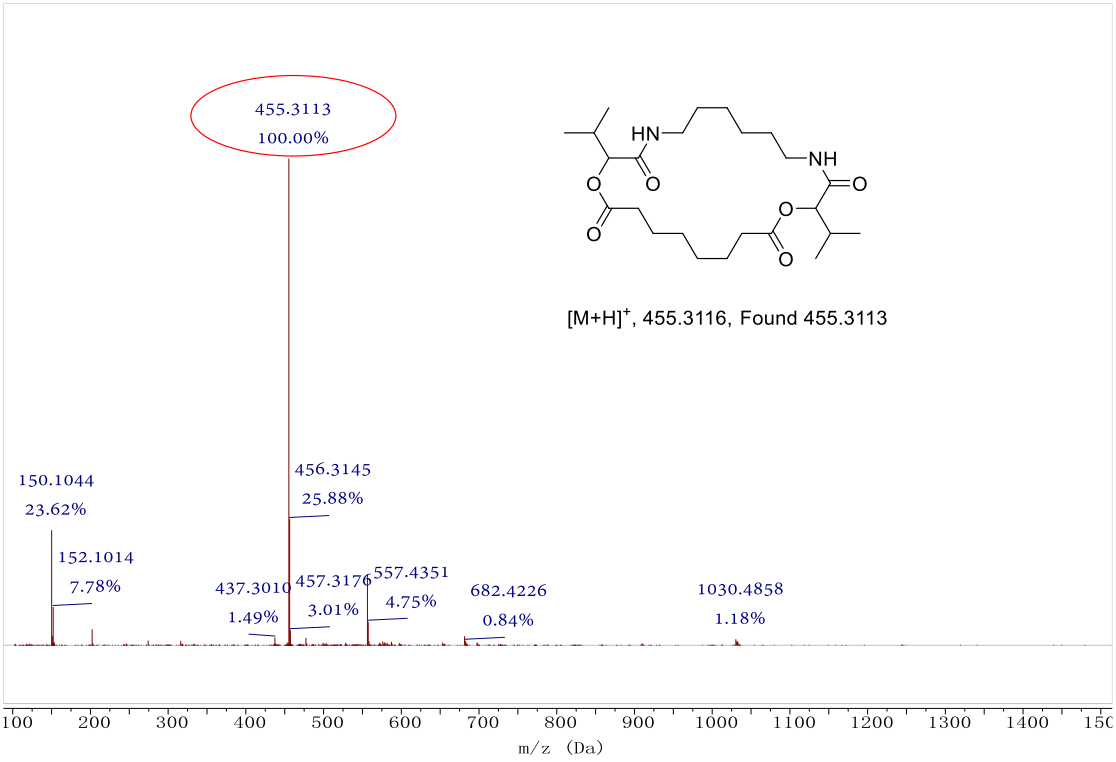

Figure 27: ESI-MS spectrum of **C8**.

According to the experimental results obtained, after testing and analysis by ^{1}H-NMR, ^{13}C-NMR, IR and MS, cyclic macromolecules with one core unit were formed in the case of **C6-C10**.

4.2.3 Conclusion

Through the above two sets of experiments, macrocyclic compounds were synthesized via the Passerini reaction using a rigid diisocyanide or a more flexible aliphatic structure in combination with isobutyraldehyde and diacids of varying chain length.

It was found that using a carbazole-based diisocyanide led to the formation of dimeric macrocyclic structures, of which **C3-C5** could be isolated in yields of 5-15%. The structure of carbazole is relatively rigid and rotation is limited. This results in the isocyanide groups at both ends being relatively fixed in position, thus geometrically leading to larger cycles upon reaction with the diacids.

On the other hand, 1,6-diisocyanohexane and the selected diacids are both straight-chain molecules that can rotate relatively easily in space. Therefore, the two ends can more easily react with each other in order to enable ring-closure **C6-C10**. A clear and pronounced trend on the macrocyclization selectivity depending on the used diacid was not observed.

Regarding the same diacid, for instance comparing C3 and C8, cyclization selectivity to the macrocycles of different size was also very comparable, leading to the overall conclusion that the choice of diacid for cyclization was less important within the set of herein investigated components.

5 Conclusion

The P-3CR reaction is valuable for the synthesis of sequence-defined macromolecules. For the synthesis of sequence-defined oligomers, a well-established iterative cycle was used, consisting of a P-3CR and a deprotection step. Using stearic acid as the starting acid, two different aldehydes (containing either an isopropyl or an α-methylphenyl group) and the α-isocyano ω-benzyl ester AB as building blocks, sequence-defined pentameters with aromatic groups at specific positions in the prepared pentamers were obtained via a one-pot growth process. The molecular structure and thermal properties were investigated by NMR and IR spectroscopy, thermogravimetric analysis, HR-ESI-MS, DSC and SEC analysis. These methods clearly showed that the analytical methods could not distinguish between the obtained isomers. All products were analyzed by ESI-MS/MS, where the fragmentation of the Passerini macromolecule always followed a fixed scheme and two distinct fragmentation patterns were observed. The exact structure was determined by detecting the two common fragment patterns.

In addition, the influencing factors for the synthesis of cyclic macromolecules were investigated by varying the isocyanide component and the diacid component in P-3CR. Here, two diisocyanides with different spatial structures and five diacids with different chain lengths were introduced using isobutyraldehyde as the third component of the P-3CR, and reacted at low concentrations for a long time. The crude products obtained by simply removing the reaction solvent were subjected to SEC analysis and peak fitting. Combined with the final product's SEC and ESI-MS, the final product was determined, as well as its composition in the crude product, to explore the influence of the component's structure on the selectivity towards macrocyclization.

6 Experimental Section

6.1 Materials

11-Aminoundecanoic acid (>97%, Sigma Aldrich), ethyl formate (98+%, thermo scientific), benzyl bromide (99%, abcr), pyridine (>98%, Acros Organics), 4-toluenesulfonyl chloride (>99%, Acros Organics), Na_2CO_3 (>99%, Sigma Aldrich), stearic acid (>97%, Sigma Aldrich), 2-phenylpropionaldehyde (98%, Sigma Aldrich), palladium on activated charcoal (10% Pd basis, Sigma Aldrich), isobutyraldehyde (>99%, Sigma Aldrich), cyclohexane (>99%, Fisher Chemical), hydrogen (>99.999%, Air Liquide), sodium sulfate (>99% anhydrous, Acros Organics), silica gel 60 (Sigma Aldrich), TLC silica gel F254 (Thin layer chromatography, Merck), dichloromethane (>99%, Fisher Chemical), ethyl acetate (>99.5%, Fisher Chemical), methanol (>99%, VWR Chemicals), ethanol (>99%, Fisher Chemical), triethylamine (99.9%, Acros Organics), N-ethyl-carbazole (>97%, Sigma Aldrich), hydrazinium hydroxide (>99%, Sigma Aldrich), phosphorus oxychloride (>99%, Sigma Aldrich), Acetic acid (technical grade), Acetic anhydride (99.5%, Sigma Aldrich), Hexanedioic acid (>99%, Sigma Aldrich), Heptanedioic acid (>99%, Sigma Aldrich), Octanedioic acid (>99%, Sigma Aldrich), Nonanedioic acid (>99%, Sigma Aldrich), Decanedioic acid (>99%, Sigma Aldrich), chloroform-*d* ($CDCl_3$, 99.8 at% D, Armar Chemicals), DMSO-d_6 (99.9% at% D, Fisher Chemical), dimethylformamide (>99%, VWR Chemicals). All solvents and chemicals were used without further purification.

6.2 Instrumentation

Nuclear Magnetic Resonance (NMR) Spectroscopy

^{1}H NMR spectra were recorded using a Bruker Ascend spectrometer at 400 MHz with 16 scans and a delay time D_1 of 1 s at 298 K. The chemical shift was reported in parts per million (ppm) and referenced to characteristic signals of deuterated solvents, e.g. DMSO-d_6 at 2.50 ppm or $CDCl_3$ at 7.26 ppm. ^{13}C NMR spectra were recorded using a Bruker Ascend spectrometer at 101 MHz with 1024 scans and a delay time D_1 of 2 s at 298 K. The chemical shift was reported in parts per million (ppm) and referenced to the solvent signal of DMSO-d_6 at 39.52 ppm or $CDCl_3$ at 77.16 ppm. Additionally, 2D NMR methods, e.g. heteronuclear multiple quantum coherence (HMQC), heteronuclear multiple bond correlation (HMBC) and correlated spectroscopy (COSY), were carried out, if necessary, for signal assignment and structure elucidation. The following abbreviations are used to describe the proton splitting pattern: s = singlet, d = doublet, t = triplet, m = multiple. All coupling constants *J* are given in Hz and decreasing order.

Infrared Spectroscopy (IR)

Infrared spectra of the samples were recorded using a Bruker ALPHA attenuated total reflection (ATR) IR spectrometer in a frequency range from 4000 to 400 cm^{-1}.

Thermogravimetric analysis (TGA)

Thermogravimetric analysis was performed using a TGA Q5500 from TA instruments. 5mg of a sample was placed in a aluminum pan and heated from 25 to 600 °C under a nitrogen atmosphere at a heating rate of 10 °C/min. The onset temperature (T_{Onset}) is the temperature extrapolated at the intersection point of inflectional tangents to the degradation curve.

Differential Scanning Calorimetry (DSC)

DSC measurements were performed using a Mettler Toledo DSC 3 STARe system. Aluminum crucibles (40 µL) were used to weigh a precise amount of each sample, between 2 and 8 mg. Measurements were performed under nitrogen flow (50 mL min^{-1}) in three consecutive heating-cooling cycles: from 25 to 200, 200 to -50, and -50 to

200 °C. T_g values were determined as the onset of the transition in the second heating cycle.

Electrospray Ionization with Mass Spectrometry (ESI-MS)

Electrospray ionization (ESI) experiments were recorded using a Q-Exactive (Orbitrap) mass spectrometer (Thermo Fisher Scientific) equipped with a HESI II probe to record high resolution spectra. This mass spectrometer is equipped with an atmospheric pressure ionization source operating in the nebulizer assisted electrospray mode. The instrument was calibrated in the m/z-range 150-2000 using a standard containing caffeine, Met-Arg-Phe-Ala acetate (MRFA) and a mixture of fluorinated phosphazenes (Ultramark 1621, all from Sigma Aldrich). A constant spray voltage of 3.5 kV, a dimensionless sheath gas of 6, and a sweep gas flow rate of 2 were applied. The capillary voltage and the S-lens RF level were set to 68.0 V and 320 °C, respectively. For the interpretation of the spectra, molecular peaks $[M]^+$, peaks of pseudo molecules $[M+H]^+$ and $[M+Na]^+$ characteristic fragment peaks are indicated with their mass to charge ratio (m/z) and their intensity in percent, relative to the most intense peak (100%). For the fragmentation of the compounds, the parent ion was preselected in the quadrupole and fragmentated in the collision ion cell applying a collision energy (CE).

Size exclusion chromatography (SEC)

SEC measurements were performed using a PSS SECcurity^2 SEC-system with the Agilent infinity 1260 II hardware. The system consists of a refractive index detector SECcurity² RI, a column oven “(Bio)SECcurity² Column Chamber TCC6500", a "standard SECcurity²" autosampler, and an isocratic pump "SECcurity² Isocratic Pump". The used column system consists of two PSS SDV analytical columns (3 µm, 300 × 8.0 mm, 1000 Å) with a PSS SDV analytical precolumn (3 µm, 50 × 8.0 mm). For the calibration, narrow linear poly (methyl methacrylate) standards (Polymer Standards Service, PSS, Germany) ranging from 2000 to 62200 Da were used. Anhydrous tetrahydrofuran (THF) stabilized with 250 ppm butylated hydroxytoluene was used as the mobile phase at a flow rate of 1.0 mL min^{-1} and a temperature of 30 °C. The compound samples were dissolved in THF at a concentration of 1 mg mL^{-1} in the eluent

and filtered over a 0.2 μL filter prior to the measurement.

6.3 Experimental procedures

6.3.1 Accurate synthesis of pentamers with phenyl groups at specific positions *via* Passerini reactions

Benzyl 11-isocyanoundecanoate (AB building block)

The AB building block was synthesized according to the reported procedure from Meier *et al*.

In a 500 mL three necked flask, 15.0 g 11-aminoundecanoic acid (74.5 mmol, 1.00 eq.) were suspended in 75 mL THF and 96.7 g benzyl alcohol (895 mmol, 12.0 eq.) were added. The suspension was cooled in an ice bath and subsequently 16.5 mL thionyl chloride (27.1 g, 231 mmol, 3.10 eq.) were added dropwise at 0 °C. After the addition of thionyl chloride, the solution was warmed to room temperature and stirred overnight. The yellow solution was then poured into 500 mL diethylether and stored in the freezer for one hour. The product was then filtered off and dried under high vacuum. The 11-(benzyloxy)-11-oxoundecan-1-aminium chloride was obtained as a white solid in a yield of 90% (22g, 67 mmol).

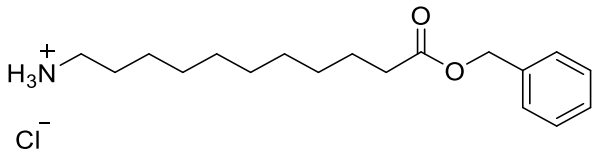

The next step, in a 250 mL round bottom flask, 17.6 g 11-(benzyloxy)-11-oxoundecan-1-aminium chloride (53.9 mmol, 1.00 eq.) were dissolved in 58.9 mL trimethyl orthoformate (57.2 g, 539 mmol, 10.0 eq.) and heated to 100 °C for 12 hours. Trimethyl orthoformate was removed under reduced pressure and benzyl 11-formamidoundecanoate was obtained in quantitative yield (17.24 g, 53.9 mmol).

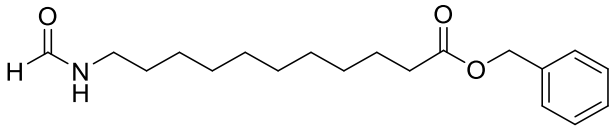

In a 500 mL three necked flask, 17.2 g of benzyl 11-formamidoundecanoate (53.8 mmol, 1.00 eq.) were dissolved in 200 mL DCM and 24.7 mL diisopropylamine 8 (17.7 g, 167

mmol, 3.10 eq.) were added and the reaction mixture was cooled to 0 °C. Subsequently, 6.54 mL phosphorus oxychloride (10.7 g, 69.9 mmol, 1.30 eq.) were added dropwise, and the reaction mixture was then stirred at room temperature for two hours. The reaction was quenched by addition of sodium carbonate solution (20 %, 75 mL) at 0 °C. After stirring this mixture for 30 min, water (50 mL) and DCM (50 mL) were added. The aqueous phase was separated, and the organic layer was washed with water (3 × 80 mL) and brine (80 mL). The combined organic layers were dried over sodium sulfate and the solvent was evaporated under reduced pressure. The crude product was then purified by column chromatography (cyclohexane / ethyl acetate 10:1 → 4:1). The building block was obtained as slightly yellow oil in total yield of 51.4%. (8.35g, 27.7mmol)

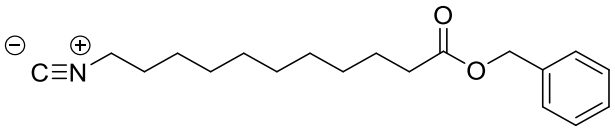

^{1}H NMR: (400 MHz, $CDCl_3$): δ / ppm = 7.44-7.27 (m, 5H, aromatic, ^{1}), 5.12 (s, 2H, CH_2, ^{2}), 3.43-3.30 (m, 2H, CH_2, ^{3}), 2.35 (t, J = 7.5 Hz, 2H, CH_2, ^{4}), 1.72-1.60 (m, 4H, 2 CH_2, ^{5}), 1.48-1.23 (m, 12H, 6 CH_2, ^{6}).
^{13}C NMR: (400 MHz, $CDCl_3$): δ / ppm = 173.63, 155.77, 155.72, 155.66, 136.18, 128.56, 128.18, 66.06, 41.62, 41.56, 41.50, 34.31, 29.28, 29.18, 29.11, 29.08, 28.68, 26.31, 24.94.
IR (ATR platinum diamond): ν / cm^{-1} = 3033.9, 2924.7, 2853.3, 2144.2, 1728.1, 1450.6, 1380.8, 1345.6, 1155.1, 1095.2, 996.7, 913.8, 734.9, 692.2, 573.2, 495.2, 448.4.
ESI-MS m/z: $[M+H]^+$ calculated $C_{19}H_{28}NO_2$ = 302.2015, found: 302.2110.

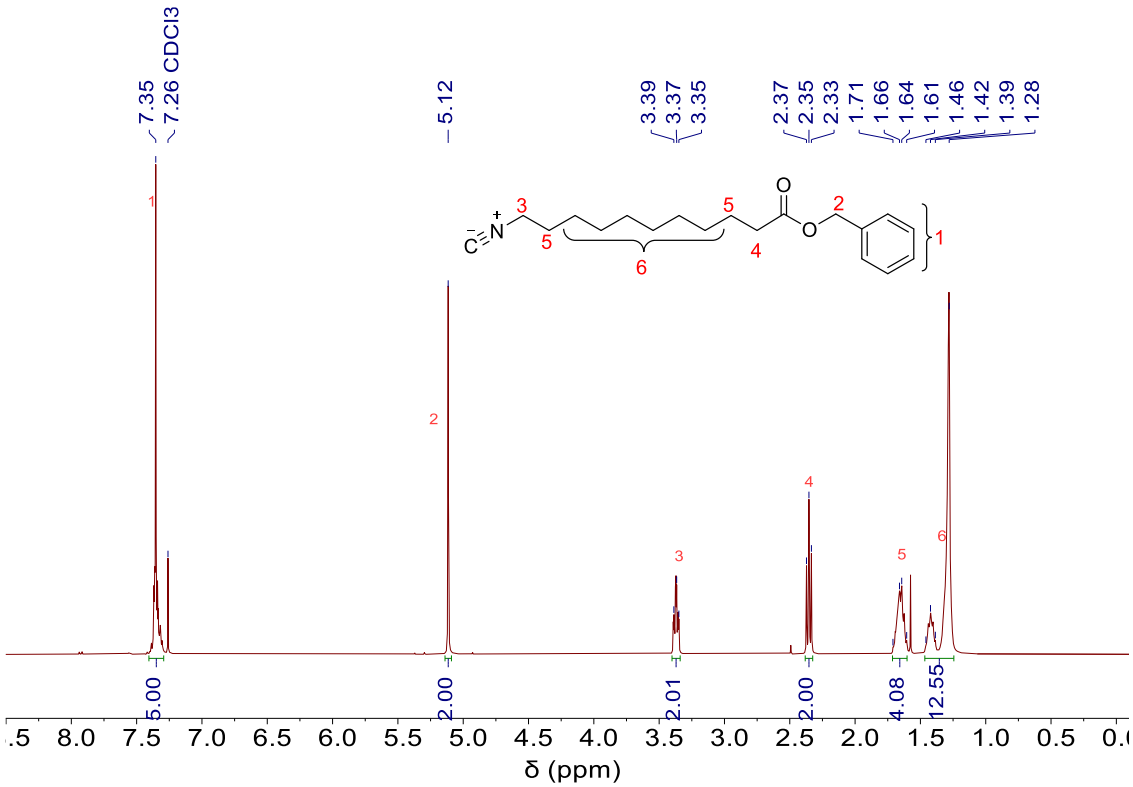

General Methods

Passerini Reaction

The carboxylic acid component (1.0 eq.) was dissolved in dichloromethane (1.0 M) and isobutyraldehyde (or 2-phenylpropionaldehyde) (1.5 eq.) and the AB building block (1.5 eq.) were added. The mixture was stirred at room temperature for 24 hours and subsequently, the solvent was removed under reduced pressure. The crude product was purified by column chromatography to afford the Passerini product.

Deprotection

The benzyl ester was dissolved in a 2:1 mixture of ethyl acetate and methanol (0.5 M) and palladium on activated charcoal (9 wt%) were added. Subsequently, the mixture was purged with hydrogen (balloon) and stirred under a hydrogen atmosphere overnight. The heterogeneous catalyst was filtered off, and the solvent was evaporated under reduced pressure. The product was used without any purification.

Passerini reaction (1a of P1)

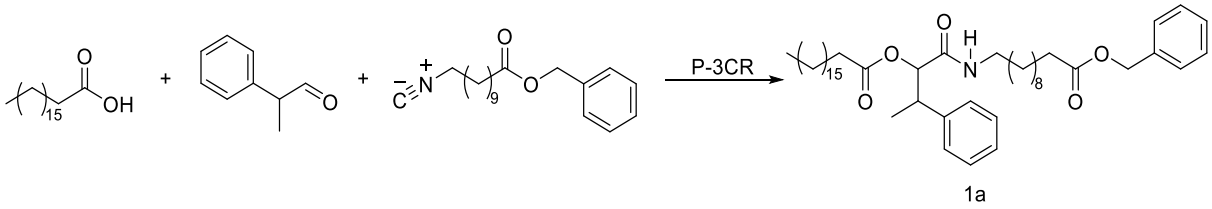

Product 1a was obtained as a white solid in a yield of 94% (6.88 g).

^{1}H NMR (400 MHz, DMSO-d_6) δ / ppm: 7.94 – 7.86 (m, 1H, NH, ^{1}), 7.36 – 7.15 (m, 10H, aromatic, ^{2}), 5.07 (s, 2H, CH_2, ^{3}), 5.03 – 4.97 (2d, J^a = 7.7Hz, J^b = 4.7 Hz, 1H, 1 CH, ^{4}), 3.32 – 3.16 (m, 1H, 1 CH, ^{5}), 3.05 – 2.93 (m, 2H, 1 CH_2, ^{6}), 2.35 – 2.17 (m, 4H, 2 CH_2, ^{7}), 1.57 – 1.17 (m, 49H, 23 CH_2, 1 CH_3, ^{8}), 0.86 – 0.83 (t, 3H, 1 CH_3, ^{9}).
^{13}C NMR (101 MHz, DMSO-d_6) δ / ppm: 172.71, 172.16, 172.08, 167.96, 167.78, 142.35, 142.22, 136.28, 128.37, 128.05, 127.99, 127.93, 127.87, 127.71, 127.64, 126.48, 126.39, 77.06, 76.82, 65.24, 40.90, 40.55, 38.24, 33.45, 33.39, 33.36, 31.27, 29.01, 28.93, 28.88, 28.83, 28.80, 28.69, 28.65, 28.61, 28.41, 28.27, 28.19, 26.21, 26.19, 24.45, 24.26, 22.07, 17.90, 14.78, 13.91.
IR (ATR platinum diamond): ν [cm^{-1}] = 3309.6, 2922.9, 2852.9, 1738.1, 1657.8, 1536.5, 1454.2, 1378.1, 1230.1, 1158.1, 1112.8, 1022.3, 911.2, 748.7, 697.3, 577.9, 536.8.
ESI-MS m/z: $[M+H]^+$ calculated for $C_{46}H_{73}NO_5$ = 720.5562, found: 720.5560.

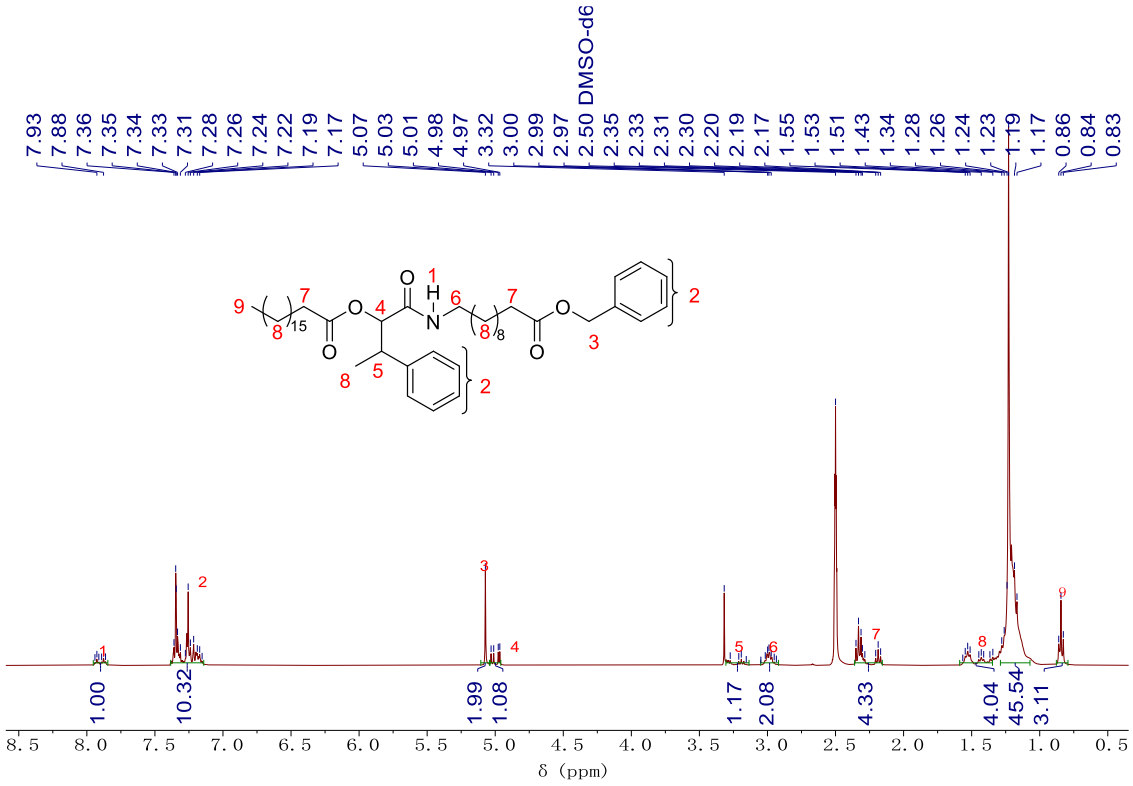

Deprotection (2a of P1)

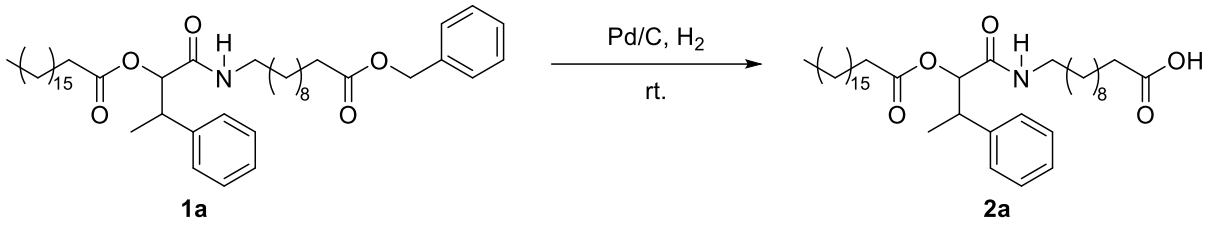

1a **2a**

Product 2a was obtained in quantitative yield as a white solid (5.23g)

^{1}H NMR (400 MHz, DMSO-d_6) δ / ppm: 7.94 – 7.86 (m, 1H, NH, ^{1}), 7.29 – 7.16 (m, 5H, aromatic, ^{2}), 5.03 – 4.96 (2d, J^a = 7.7 Hz, J^b = 4.7 Hz, 1H, 1 CH, ^{3}), 3.21 – 3.17 (m, 1H, 1 CH, ^{4}), 3.02 – 2.95 (m, 2H, 1 CH_2, ^{5}), 2.33 – 2.16 (m, 4H, 2 CH_2, ^{6}), 1.50 – 1.16 (m, 49H, 23 CH_2, 1 CH_3, ^{7}), 0.86 – 0.83 (t, 3H, 1 CH_3, ^{8}).

^{13}C NMR (101 MHz, DMSO-d_6) δ / ppm: 172.15, 172.08, 167.97, 167.79, 142.35, 142.23, 128.05, 127.98, 127.73, 127.64, 126.47, 126.39, 77.06, 76.82, 40.91, 40.57, 38.27, 33.66, 33.41, 33.38, 31.30, 29.04, 28.96, 28.92, 28.88, 28.83, 28.78, 28.72, 28.67, 28.65, 28.58, 28.30, 28.22, 26.23, 24.50, 24.28, 17.90, 14.78, 13.91.

IR (ATR platinum diamond): ν [cm^{-1}] = 3305.5, 2920.8, 2852.9, 1738.1, 1709.3, 1649.6, 1540.6, 1454.2, 1378.1, 1230.1, 1160.1, 1112.8, 1022.3, 911.2, 763.1, 719.91, 699.3, 538.9.

ESI-MS m/z: $[M+H]^+$ calculated for $C_{39}H_{67}NO_5$ = 630.5092, found: 630.5083.

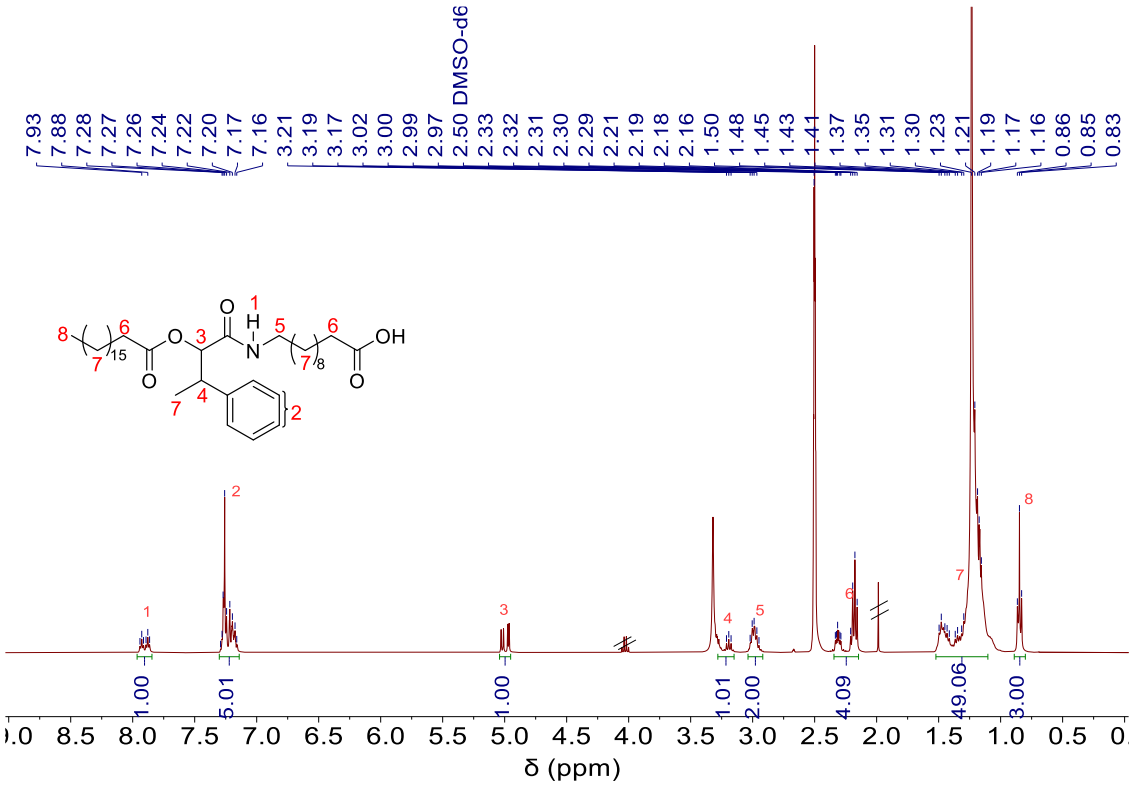

Passerini reaction (3a of P1)

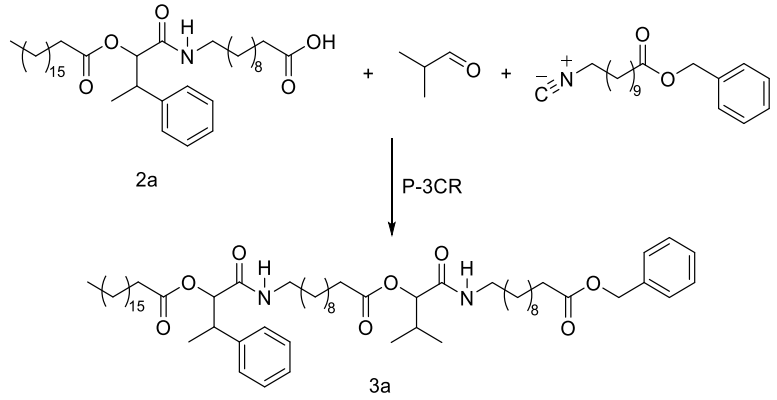

The target product 3a was obtained as a white solid in a yield of 89% (7.15g)

^{1}H NMR (400 MHz, DMSO-d_6) δ / ppm: 7.92 – 7.83 (m, 2H, 2 NH, ^{1}), 7.38 – 7.16 (m, 10H, aromatic, ^{2}), 5.07 (s, 2H, 1 CH_2, ^{3}), 5.03 – 4.96 (2d, J^a = 7.7Hz, J^b = 4.7Hz, 1H, 1CH, ^{4}), 4.66 (d, J = 5.1 Hz, 1H, 1CH, ^{5}), 3.29 – 3.15 (m, 1H, 1CH, ^{6}), 3.06 – 2.98 (m, 4H, 2 CH_2, ^{7}), 2.38 – 2.17 (m, 6H, 3 CH_2, ^{8}), 2.08 – 2.03 (m, 1H, 1 CH, ^{9}), 1.54 – 1.14 (m, 65H, 31 CH_2, 1 CH_3, ^{10}), 0.87 – 0.83 (m, 9H, 3 CH_3, ^{11}).

^{13}C NMR (101 MHz, DMSO-d_6) δ / ppm: 172.71, 172.44, 172.16, 172.08, 168.37, 167.98, 167.80, 142.35, 142.22, 136.29, 128.38, 128.05, 127.99, 127.94, 127.88, 127.72, 127.64, 126.48, 126.40, 77.39, 77.07, 76.82, 65.24, 40.91, 40.56, 38.25, 38.18, 33.46, 33.41, 31.29, 29.87, 29.02, 28.94, 28.91, 28.84, 28.79, 28.70, 28.65, 28.42, 28.29, 28.21, 26.23, 24.46, 24.41, 24.27, 22.09, 18.58, 17.90, 17.10, 14.77, 13.91.

IR (ATR platinum diamond): ν [cm^{-1}] = 3305.5, 2922.9, 2852.9, 1738.1, 1655.8, 1534.5, 1456.3, 1376.1, 1230.1, 1158.1, 1110.7, 1003.8, 911.2, 721.9, 697.3, 577.9, 536.8.

ESI-MS m/z: $[M+H]^+$ calculated for $C_{62}H_{102}N_2O_8$ = 1003.7709, found: 1003.7700.

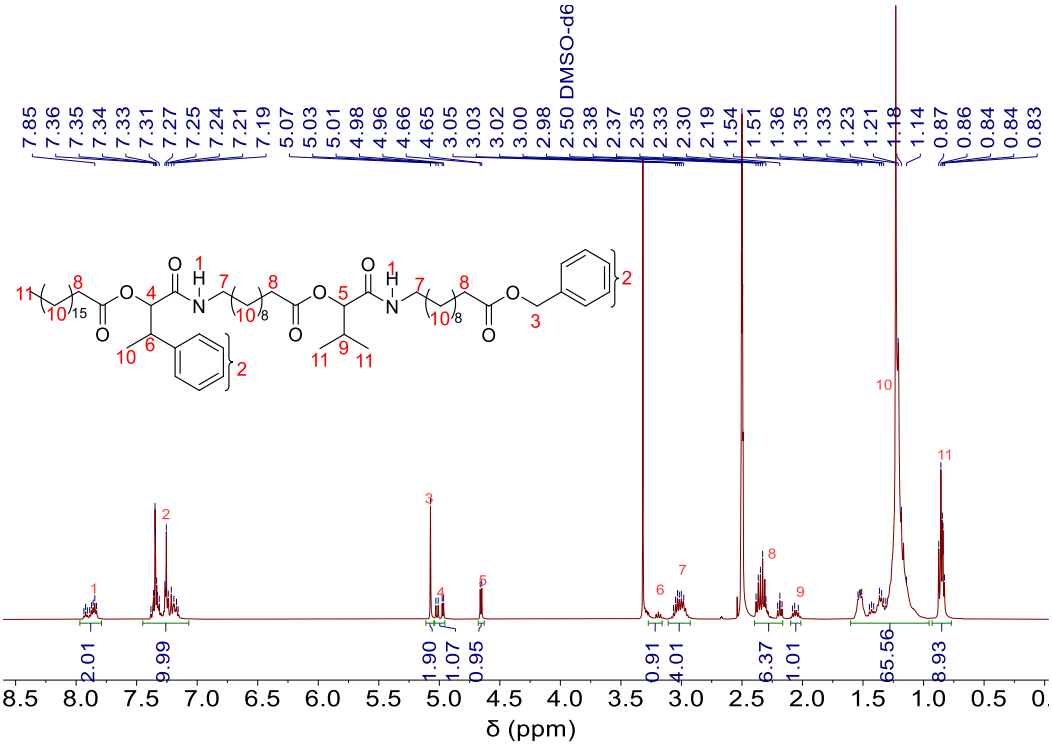

Deprotection (4a of P1)

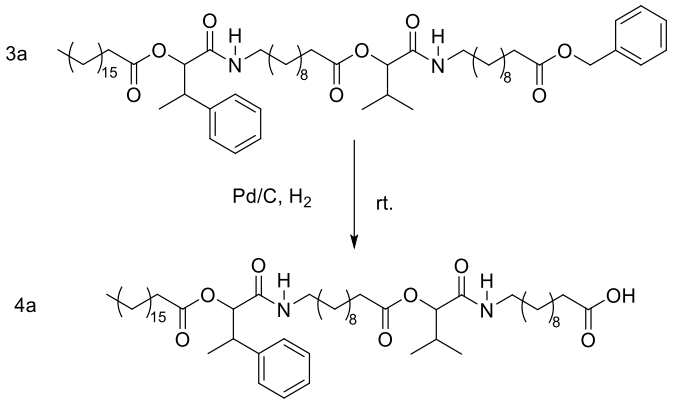

The target product 4a was obtained in quantitative yield as a white solid (4.81g).

^{1}H NMR (400 MHz, DMSO-d_6) δ / ppm: 7.93 – 7.83 (m, 2H, 2 NH, ^{1}), 7.27 – 7.15 (m, 5H, aromatic, ^{2}), 5.03 – 4.97 (2d, J^{a} = 7.7 Hz, J^{b} = 4.6 Hz, 1H, 1 CH, ^{3}), 4.66 (d, J = 5.1 Hz, 1H, 1 CH, ^{4}), 3.21 – 3.17 (m, 1H, 1 CH, ^{5}), 3.07 – 2.97 (m, 4H, 2 CH_2, ^{6}), 2.39 – 2.15 (m, 6H, 3 CH_2, ^{7}), 2.08 – 2.04 (m, 1H, 1 CH, ^{8}), 1.53 – 1.17 (m, 65H, 31 CH_2, 1 CH_3, ^{9}), 0.88 – 0.83 (m, 9H, 3 CH_3, ^{10}).

^{13}C NMR (101 MHz, DMSO-d_6) δ / ppm: 174.43, 172.15, 168.36, 167.97, 167.78, 128.05, 127.98, 127.72, 127.64, 126.48, 126.39, 77.38, 77.06, 76.82, 40.90, 40.55, 38.25, 38.19, 33.65, 33.40, 31.28, 29.87, 29.02, 28.94, 28.91, 28.84, 28.75, 28.70, 28.62, 28.56, 28.43, 28.28, 28.20, 26.25, 24.49, 24.40, 24.27, 22.08, 18.58, 17.90, 17.09, 14.78, 13.91.

IR (ATR platinum diamond): ν [cm^{-1}] = 3305.5, 2922.9, 2852.9, 1740.1, 1651.7, 1538.6, 1462.5, 1369.9, 1230.0, 1164.2, 1110.7, 1020.2, 963.1, 763.1, 699.3, 649.9, 538.9.

ESI-MS m/z: $[M+H]^{+}$ calculated for $C_{55}H_{96}N_2O_8$ = 913.7239, found: 913.7232.

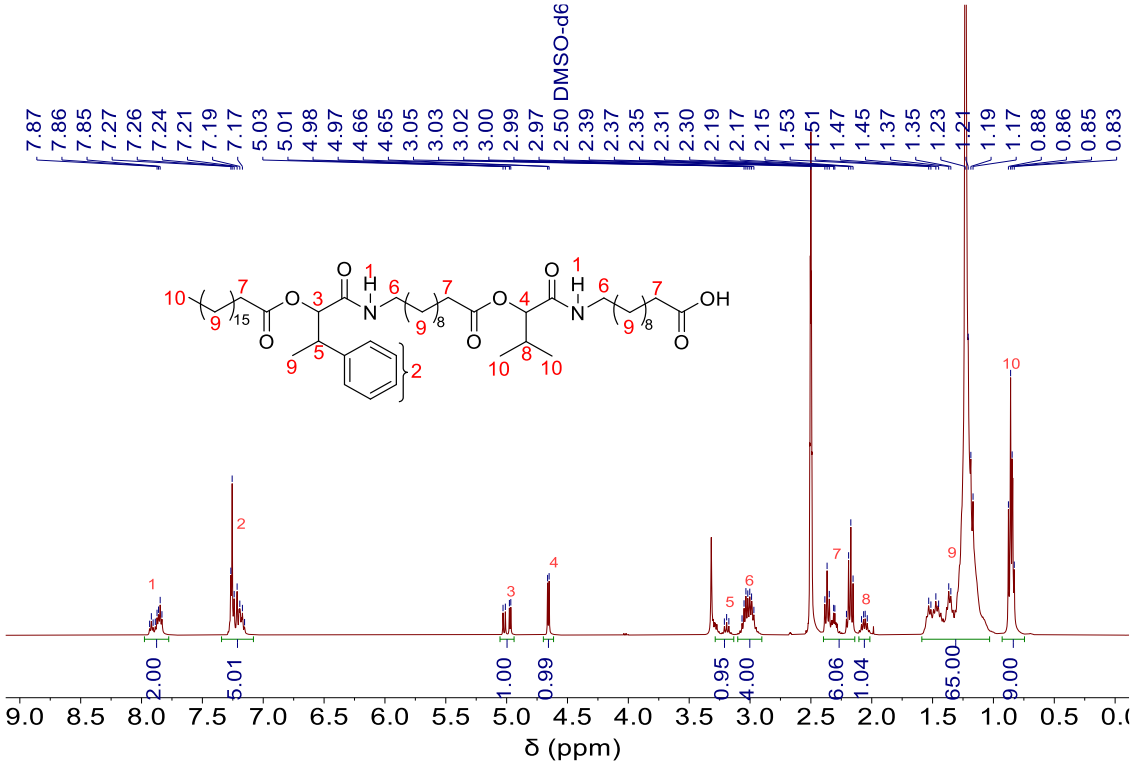

Passerini reaction (5a of P1)

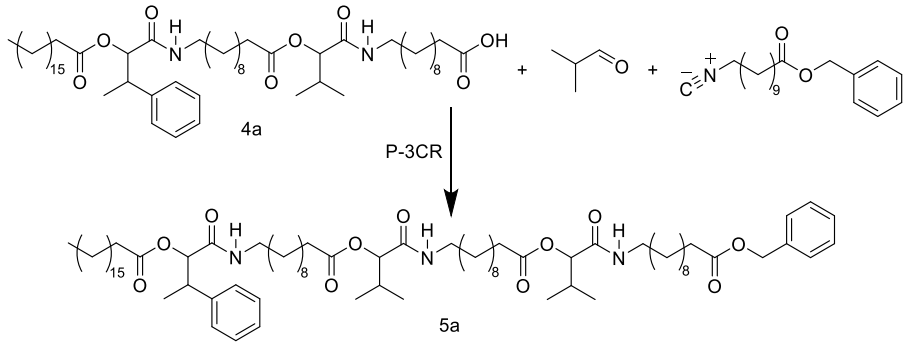

The target product 5a was obtained as a yellow oil in a yield of 88% (4.92g).

^{1}H NMR (400 MHz, DMSO-d_6) δ / ppm: 7.94 – 7.83 (m, 3H, 3 NH, ^{1}), 7.38 – 7.16 (m, 10H, aromatic, ^{2}), 5.07 (s, 2H, 1 CH_2, ^{3}), 5.03 – 4.96 (2d, J^a =7.7Hz, J^b = 4.6Hz, 1H, 1CH, ^{4}), 4.65 (d, J = 5.1 Hz, 2H, 2CH, ^{5}), 3.27 – 3.15 (m, 1H, 1CH, ^{6}), 3.06 – 2.98 (m, 6H, 3 CH_2, ^{7}), 2.38 – 2.17 (m, 8H, 4 CH_2, ^{8}), 2.10 – 2.03 (m, 2H, 2 CH, ^{9}), 1.54 – 1.17 (m, 81H, 39 CH_2, 1 CH_3, ^{10}), 0.87 – 0.78 (m, 15H, 5 CH_3, ^{11}).

^{13}C NMR (101 MHz, DMSO-d_6) δ / ppm: 172.71, 172.44, 172.15, 172.08, 168.36, 167.97, 142.35, 128.37, 128.05, 127.99, 127.93, 127.88, 127.72, 127.63, 126.47, 77.39, 77.07, 76.82, 65.24, 40.90, 40.55, 38.25, 33.45, 33.40, 31.28, 29.86, 29.01, 28.93, 28.90, 28.83, 28.79, 28.69, 28.42, 28.28, 28.20, 26.23, 24.45, 24.40, 24.27, 18.58, 17.90, 17.09, 14.77.

IR (ATR platinum diamond): ν [cm^{-1}] = 3305.5, 2922.9, 2852.9, 1738.1, 1653.8, 1536.5, 1456.3, 1369.9, 1232.1, 1158.1, 1110.7, 1003.8, 917.4, 721.9, 697.3, 577.9, 536.8.

ESI-MS m/z: $[M+H]^+$ calculated for $C_{78}H_{131}N_3O_{11}$ = 1286.9856, found: 1286.9870.

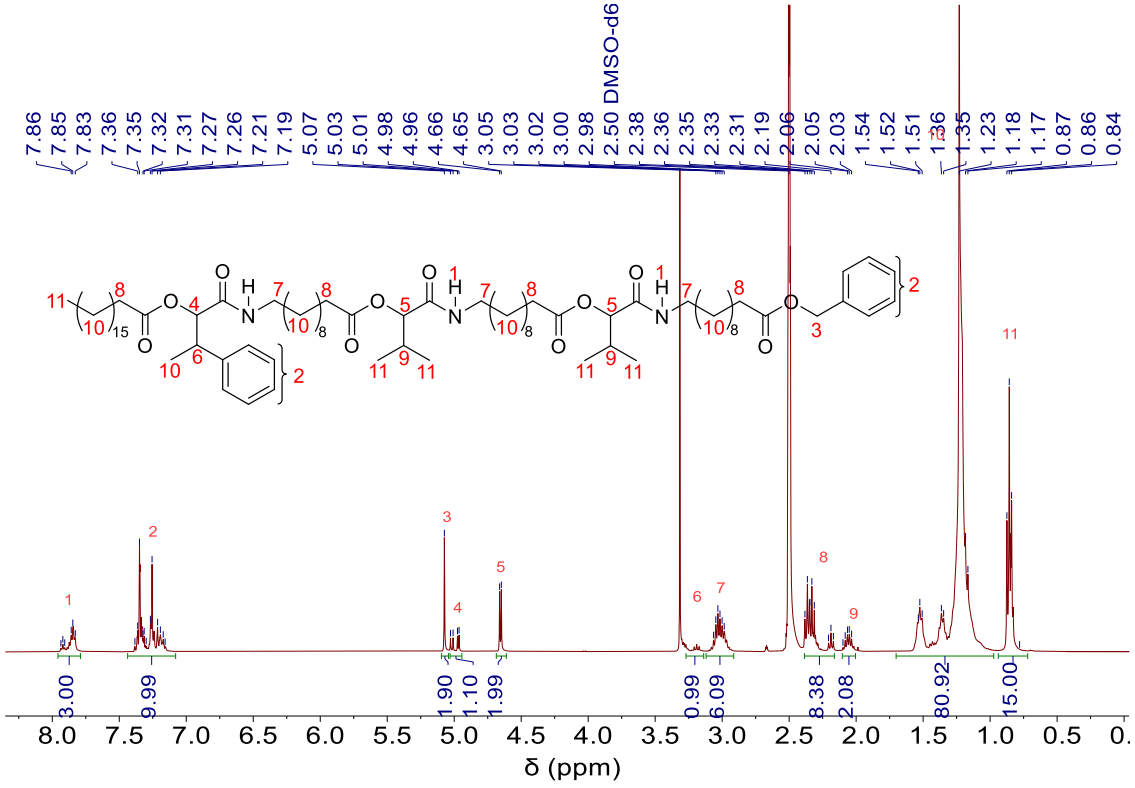

Deprotection (6a of P1)

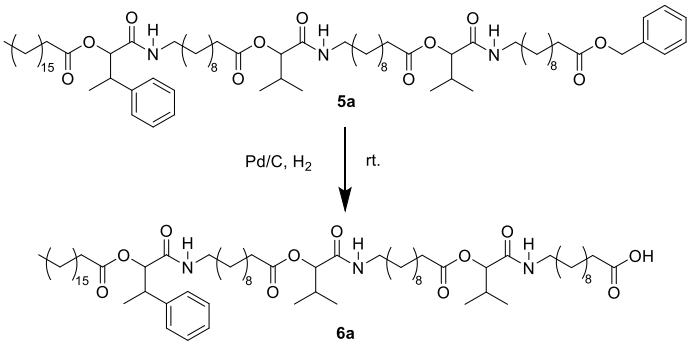

The target product 6a was obtained in quantitative yield as a white solid. (4.23g)

^{1}H NMR (400 MHz, DMSO-d_6) δ / ppm: 7.93 – 7.83 (m, 3H, 3 NH, ^{1}), 7.26 – 7.15 (m, 5H, aromatic, ^{2}), 5.03 – 4.97 (2d, J^a =7.7Hz, J^b = 4.6Hz, 1H, 1CH, ^{3}), 4.66 (d, J = 5.0 Hz, 2H, 2CH, ^{4}), 3.21 – 3.17 (m, 1H, 1CH, ^{5}), 3.07 – 2.97 (m, 6H, 3 CH_2, ^{6}), 2.38 – 2.15 (m, 8H, 4 CH_2, ^{7}), 2.07 – 2.02 (m, 2H, 2 CH, ^{8}), 1.53 – 1.17 (m, 81H, 39 CH_2, 1 CH_3, ^{9}), 0.88 – 0.83 (m, 15H, 5 CH_3, ^{10}).

^{13}C NMR (101 MHz, DMSO-d_6) δ / ppm: 174.43, 172.42, 172.13, 172.05, 168.36, 167.96, 167.79, 142.34, 142.22, 128.03, 127.97, 127.71, 127.63, 126.46, 126.38, 77.38, 77.06, 76.81, 40.91, 40.55, 38.25, 38.19, 33.68, 33.41, 31.29, 29.87, 29.03, 28.95, 28.85, 28.76, 28.71, 28.58, 28.43, 28.29, 28.21, 26.25, 24.50, 24.40, 24.27, 22.09, 18.58, 17.88, 17.08, 14.76, 13.90.

IR (ATR platinum diamond): ν [cm^{-1}] = 3305.5, 2922.9, 2852.9, 1740.1, 1651.7, 1538.6, 1464.5, 1371.9, 1232.1, 1162.2, 1110.7, 1009.9, 921.5, 763.1, 721.9, 699.3, 577.9, 536.8.

ESI-MS m/z: $[M+H]^+$ calculated for $C_{71}H_{125}N_3O_{11}$ = 1196.9387, found: 1196.9393.

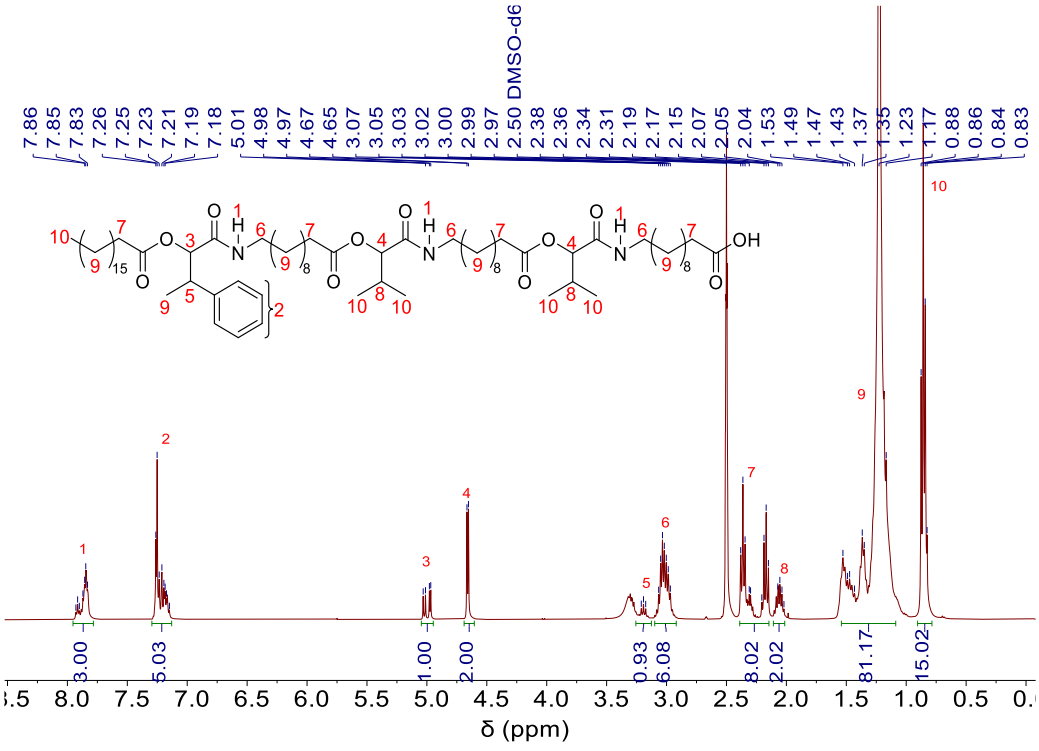

Passerini reaction (7a of P1)

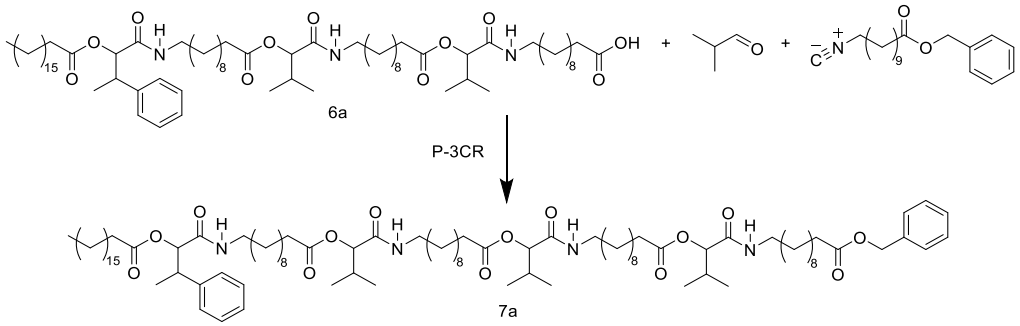

The target product 7a was obtained as a yellow oil in a yield of 92% (5.05g).

^{1}H NMR (400 MHz, DMSO-d_6) δ / ppm: 7.91 – 7.83 (m, 4H, 4 NH, ^{1}), 7.38 – 7.17 (m, 10H, aromatic, ^{2}), 5.07 (s, 2H, 1 CH_2, ^{3}), 5.03 – 4.97 (2d, J^a = 7.7Hz, J^b = 4.7 Hz, 1H, 1CH, ^{4}), 4.66 (d, J = 5.0 Hz, 3H, 3 CH, ^{5}), 3.27 – 3.17 (m, 1H, 1 CH, ^{6}), 3.06 – 2.97 (m, 8H, 4 CH_2, ^{7}), 2.38 – 2.17 (m, 10H, 5 CH_2, ^{8}), 2.10 – 2.02 (m, 3H, 3 CH, ^{9}), 1.52 – 1.17 (m, 97H, 47 CH_2, 1 CH_3, ^{10}), 0.87 – 0,84 (m, 21H, 7 CH_3, ^{11}).

^{13}C NMR (101 MHz, DMSO-d_6) δ / ppm: 172.69, 172.41, 172.12, 168.35, 167.96, 167.77, 142.33, 142.21, 136.27, 128.36, 128.03, 127.96, 127.86, 127.70, 127.62, 77.37, 77.05, 76.80, 65.23, 40.90, 40.54, 38.24, 38.17, 33.44, 33.39, 31.28, 29.85, 29.01, 28.93, 28.90, 28.78, 28.69, 28.42, 28.28, 28.20, 26.24, 24.44, 24.39, 24.26, 18.57, 17.88, 17.07, 14.76, 13.90.

IR (ATR platinum diamond): ν [cm^{-1}] = 3305.5, 2922.9, 2852.9, 1738.1, 1653.7, 1534.5, 1464.5, 1369.9, 1236.2, 1162.2, 1110.7, 1003.8, 921.5, 721.9, 699.3, 647.9, 538.9, 409.3.

ESI-MS m/z: $[M+H]^+$ calculated for $C_{94}H_{160}N_4O_{14}$ = 1570.2204, found: 1570.2025.

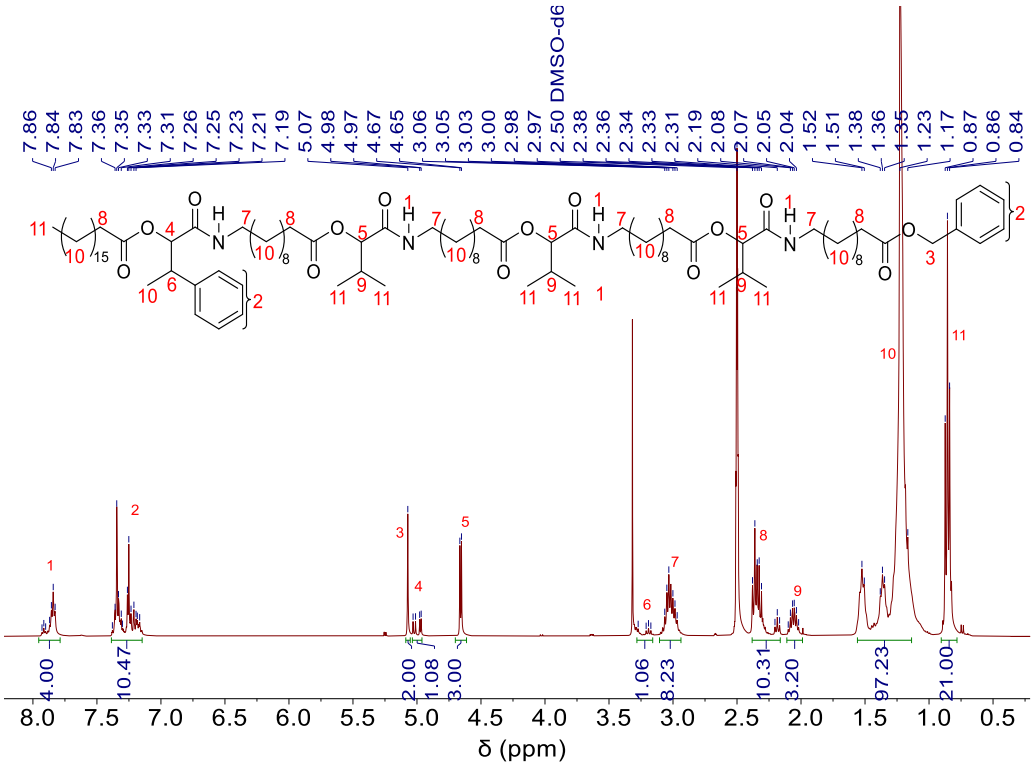

Deprotection (8a of P1)

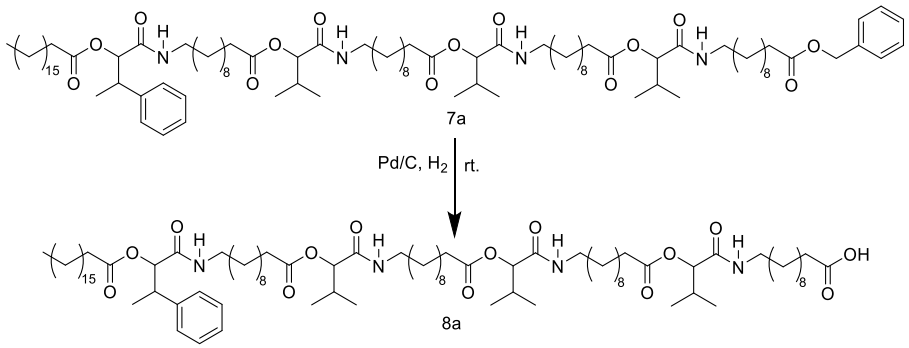

The target product 8a was obtained in quantitative yield as a white solid. (3.85g).

^{1}H NMR (400 MHz, DMSO-d_6) δ / ppm: 7.93 – 7.84 (m, 4H, 4 NH, ^{1}), 7.26 – 7.15 (m, 5H, aromatic, ^{2}), 5.03 – 4.97 (2d, J^a = 7.7Hz, J^b = 4.7Hz, 1H, 1 CH, ^{3}), 4.66 (d, J = 5.0 Hz, 3H, 3 CH, ^{4}), 3.28 – 3.17 (m, 1H, 1 CH, ^{5}), 3.08 – 2.97 (m, 8H, 4 CH_2, ^{6}), 2.38 – 2.15 (m, 10H, 5 CH_2, ^{7}), 2.08 – 2.02 (m, 3H, 3 CH, ^{8}), 1.53 – 1.17 (m, 97H, 47 CH_2, 1 CH_3, ^{9}), 0.87 – 0.82 (m, 21H, 7 CH_3, ^{10}).

^{13}C NMR (101 MHz, DMSO-d_6) δ / ppm: 174.42, 172.42, 172.13, 172.05, 168.37, 167.97, 167.79, 142.34, 142.22, 128.04, 127.97, 127.71, 127.63, 126.46, 126.38, 77.38, 77.06, 76.81, 40.91, 40.56, 38.25, 38.19, 33.66, 33.40, 31.29, 29.87, 29.03, 28.95, 28.85, 28.76, 28.68, 28.57, 28.43, 28.29, 28.21, 26.25, 24.49, 24.40, 24.27, 22.09, 18.58, 17.88, 17.08, 14.76, 13.90.

IR (ATR platinum diamond): ν [cm^{-1}] = 3309.6, 3089.5, 2922.9, 2852.9, 1740.1, 1651.7, 1536.5, 1462.5, 1369.9, 1234.1, 1160.1, 1110.7, 1007.9, 921.5, 761.1, 719.9, 699.3, 647.9, 540.9, 409.3.

ESI-MS m/z: $[M+H]^+$ calculated for $C_{87}H_{154}N_4O_{14}$ = 1480.1534, found: 1480.1534.

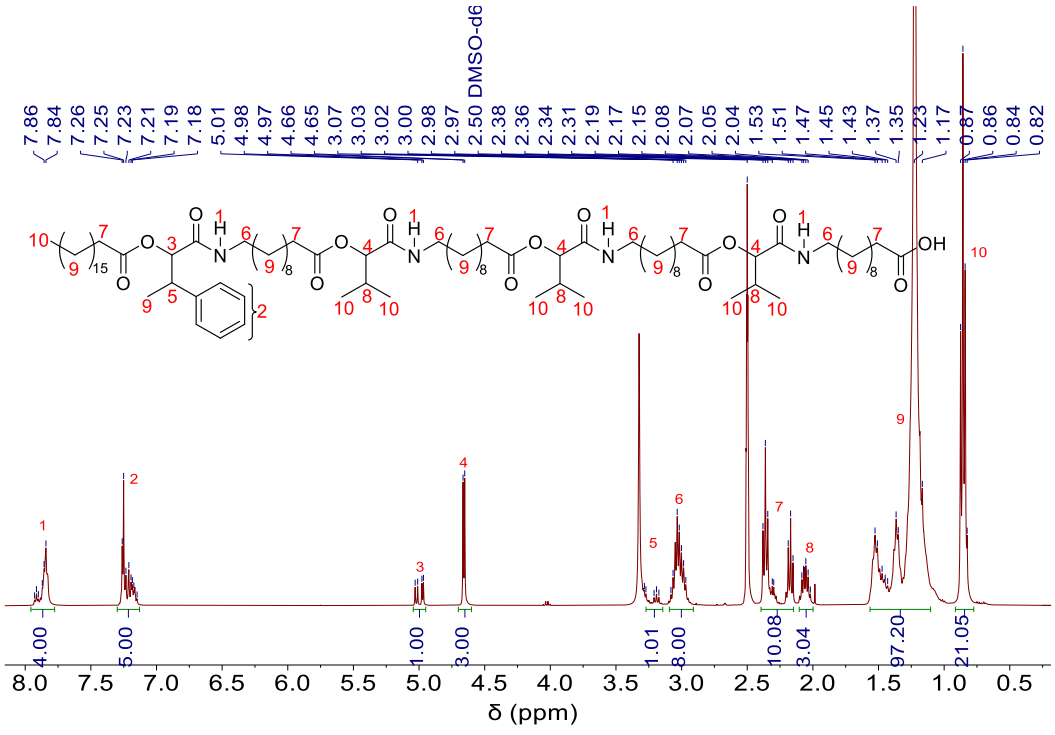

Passerini reaction to synthesize P1

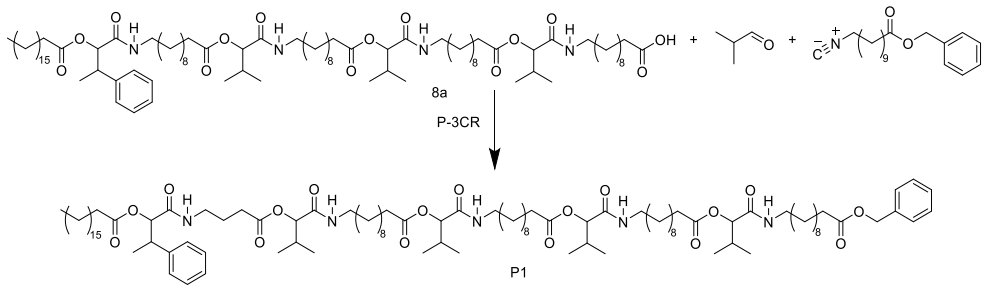

P1 was obtained as a yellow oil in a yield of 91% (4.05g).

^{1}H NMR (400 MHz, DMSO-d_6) δ / ppm: 7.92 – 7.83 (m, 5H, 5 NH, ^{1}), 7.38 – 7.17 (m, 10H, aromatic, ^{2}), 5.07 (s, 2H, 1 CH_2, ^{3}), 5.03 – 4.96 (m, J^a = 7.7Hz, J^b = 4.6Hz, 1H, 1 CH, ^{4}), 4.65 (d, J = 5.1 Hz, 4H, 4 CH, ^{5}), 3.21 – 3.17 (m, 1H, 1 CH, ^{6}), 3.06 – 2.97 (m, 10H, 5 CH_2, ^{7}), 2.38 – 2.17 (m, 12H, 6 CH_2, ^{8}), 2.10 – 2.02 (m, 4H, 4 CH, ^{9}), 1.54 – 1.18 (m, 115H, 56 CH_2, 1 CH_3, ^{10}), 0.89 – 0.73 (m, 27H, 9 CH_3, ^{11}).

^{13}C NMR (101 MHz, DMSO-d_6) δ / ppm: 172.70, 172.42, 168.36, 142.22, 136.28, 128.37, 128.04, 127.93, 127.87, 127.71, 127.63, 77.38, 65.24, 59.73, 38.18, 33.40, 31.28, 29.86, 29.01, 28.93, 28.90, 28.83, 28.79, 28.69, 28.67, 28.64, 28.42, 24.45, 22.08, 17.89, 17.08, 14.77, 14.07, 13.91.

IR (ATR platinum diamond): ν [cm^{-1}] = 3303.4, 2922.9, 2852.9, 1738.1, 1653.7, 1534.5, 1462.5, 1369.9, 1236.2, 1162.2, 1110.7, 1005.8, 923.6, 721.9, 699.3, 644.9, 538.9, 413.4.

ESI-MS m/z: $[M+H]^+$ calculated for $C_{110}H_{189}N_5O_{17}$ = 1853.4151, found: 1853.4168.

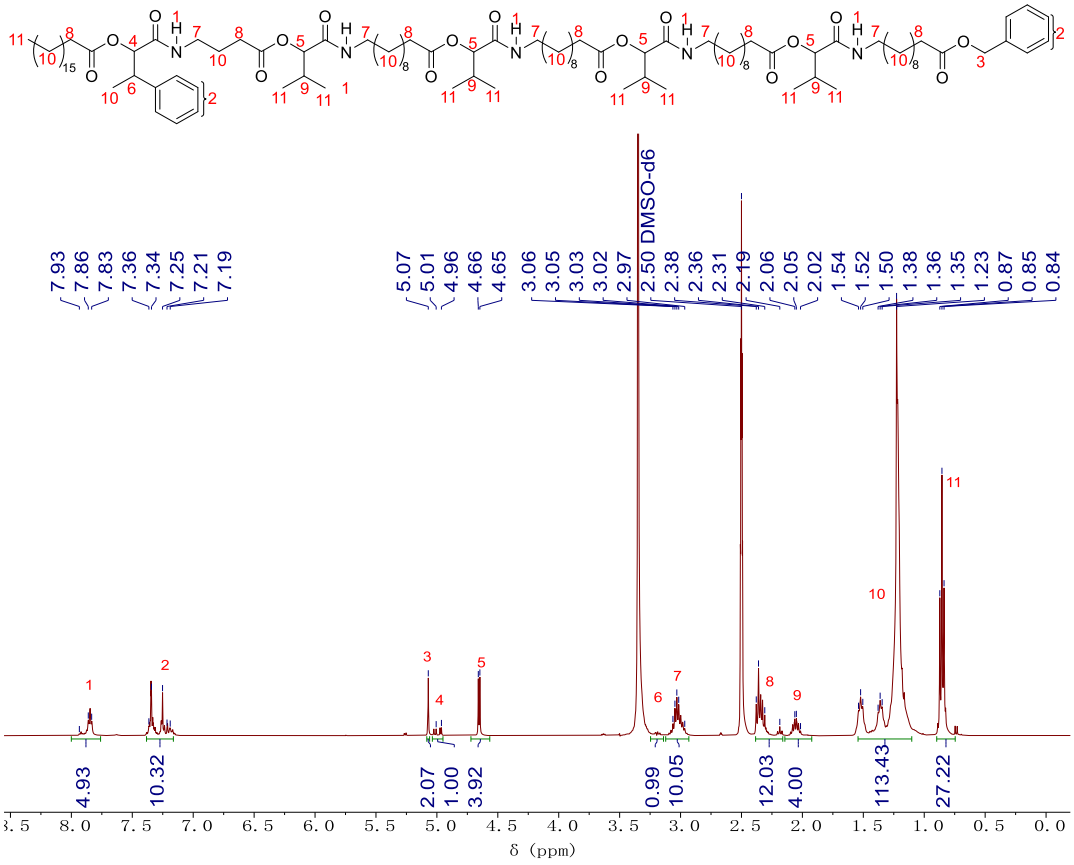

Passerini reaction (1b of P2)

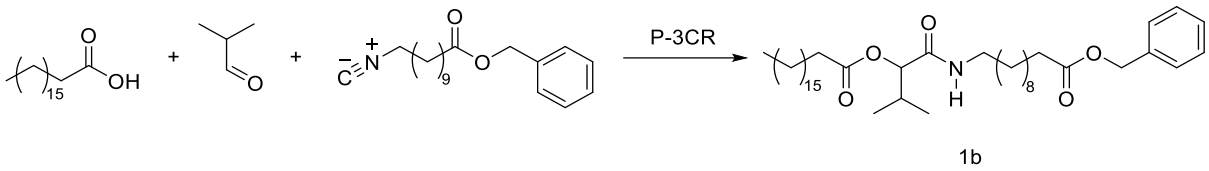

1b

The target product 1b was obtained as a white solid in a yield of 95% (8.74g).

^{1}H NMR: (400 MHz, $CDCl_3$) δ / ppm: 7.39 – 7.29 (m, 5H, aromatic, ^{1}), 5.92 (t, J = 5.9Hz, 1H, NH, ^{2}), 5.11 (s, 2H, CH_2, ^{3}), 5.07 – 5.06 (d, J = 4.4 Hz, 1H, CH, ^{4}), 3.30 – 3.18 (m, 2H, CH_2, ^{5}), 2.42 – 2.26 (m, 5H, CH, 2 CH_2, ^{6}), 1.70 –1.25 (m, 46H, 23 CH_2, ^{7}), 0.95 – 0.86 (m, 9H, 3 CH_3, ^{8}).

^{13}C NMR (101 MHz, $CDCl_3$) δ / ppm: 173.80, 172.67, 169.39, 136.28, 128.67, 128.29, 78.03, 66.20, 39.28, 34.46, 32.06, 30.65, 29.84, 29.82, 29.79, 29.74, 29.72, 29.61, 29.57, 29.50, 29.48, 29.41, 29.34, 29.31, 29.24, 26.98, 25.19, 25.07, 22.83, 18.92, 17.06, 14.26.

IR (ATR platinum diamond): ν [cm^{-1}] = 3260.2, 2916.7, 2848.8, 1742.2, 1649.6, 1567.4, 1466.6, 1384.3, 1254.0, 1160.1, 1104.0, 993.5, 927.7, 721.7, 695.2, 580.0, 485.4.

ESI-MS m/z: $[M+H]^+$ calculated for $C_{41}H_{71}NO_5$ = 658.5405, found: 659.5404.

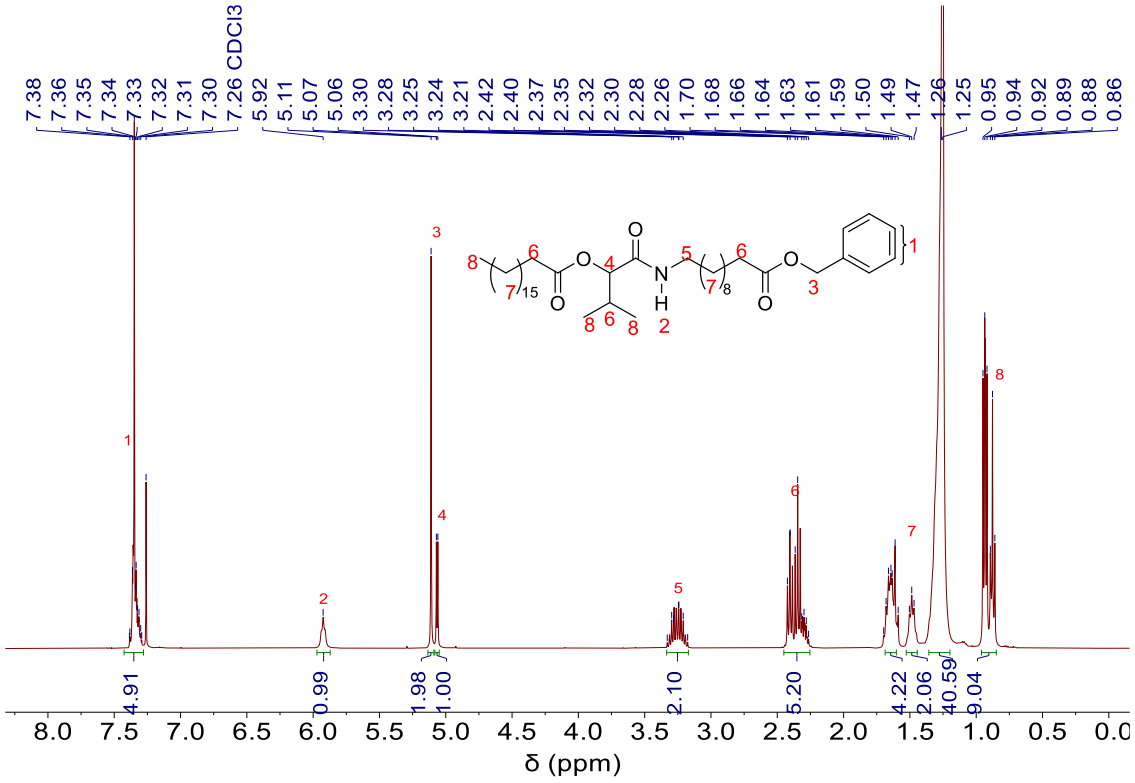

Deprotection (2b of P2)

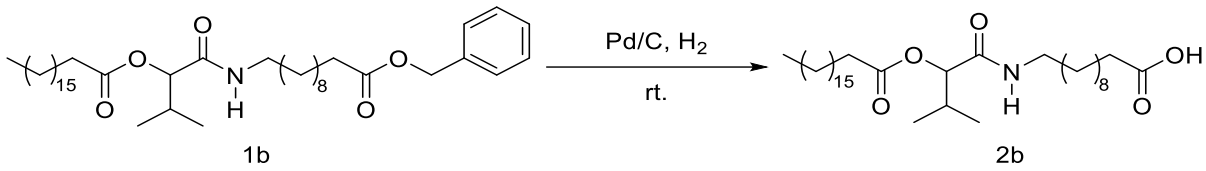

1b 2b

The target product 2b was obtained in quantitative yield as a white solid. (6.76 g)

^{1}H NMR: (400 MHz, $CDCl_3$) δ / ppm: 6.01 - 5.99 (t, J = 5.9 Hz, 1H, NH, ^{1}), 5.06 – 5.05(d, J = 4.4 Hz, 1H, CH, ^{2}), 3.64– 3.20 (m, 2H, CH_2, ^{3}), 2.42 – 2.29 (m, 5H, 2 CH_2, CH, ^{4}), 1.68 – 1.25 (m, 46H, 23 CH_2, ^{5}), 0.93 – 0.86 (m, 9H, 3 CH_3, ^{6}).
^{13}C NMR (101 MHz, $CDCl_3$) δ / ppm: 179.19, 172.75, 169.54, 78.04, 39.31, 34.45, 32.06, 30.63, 29.83, 29.79, 29.74, 29.65, 29.60, 29.49, 29.41, 29.39, 29.30, 29.26, 29.25, 29.16, 26.93, 25.18, 24.95, 22.82, 18.90, 17.07, 14.25.
IR (ATR platinum diamond): ν [cm^{-1}] = 3282.8, 2916.7, 2848.8, 1742.2, 1703.1, 1651.7, 1542.7, 1466.6, 1369.9, 1293.8, 1234.1, 1213.6, 1190.9, 1162.2, 1112.8, 1011.9, 927.7, 721.9, 676.7, 475.1.
ESI-MS m/z: $[M+H]^+$ calculated for $C_{34}H_{65}NO_5$ = 568.4936, found: 568.4938.

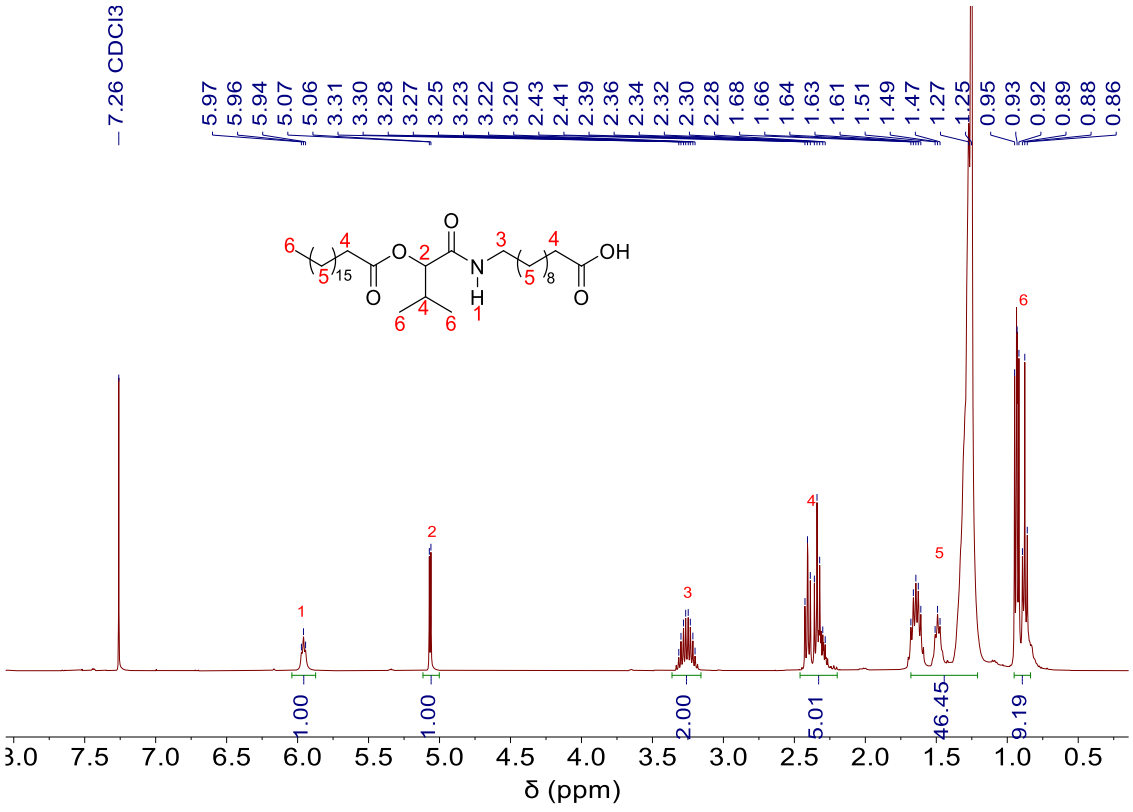

Passerini reaction (3b of P2)

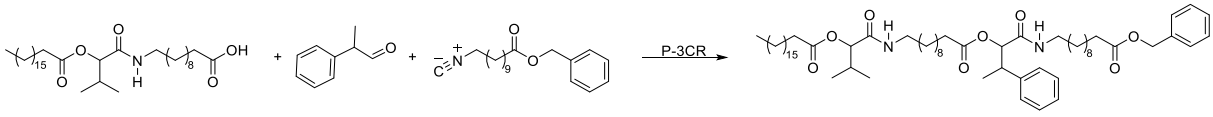

2b 3b

The target product 3b was obtained as a white solid in a yield of 89% (6.24 g)

^{1}H NMR (400 MHz, DMSO-d_6) δ / ppm: 7.94 – 7.83 (m, 2H, 2 NH, ^{1}), 7.38 – 7.15 (m, 10H, aromatic, ^{2}), 5.07 (s, 2H, 1 CH_2, ^{3}), 5.03 – 4.97 (2d, J^a = 7.7 Hz, J^b = 4.7 Hz, 1H, 1CH, ^{4}), 4.66 (d, J = 5.1 Hz, 1H, 1CH, ^{5}), 3.29 – 3.16 (m, 1H, 1CH, ^{6}), 3.09 – 2.94 (m, 4H, 2 CH_2, ^{7}), 2.38 – 2.17 (m, 6H, 3 CH_2, ^{8}), 2.09 – 2.05 (m, 1H, 1CH, ^{9}), 1.55 – 1.17 (m, 65H, 31 CH_2, 1 CH_3, ^{10}), 0.88 – 0.83 (m, 9H, 3 CH_3, ^{11}).

^{13}C NMR (101 MHz, DMSO-d_6) δ / ppm: 172.73, 172.46, 172.15, 168.39, 167.98, 167.81, 142.35, 142.22, 136.29, 128.38, 128.06, 127.99, 127.94, 127.88, 127.72, 127.64, 126.49, 126.41, 77.42, 77.07, 76.81, 65.25, 40.93, 40.56, 38.26, 38.19, 33.46, 33.40, 31.30, 29.87, 29.02, 28.94, 28.88, 28.70, 28.42, 28.39, 28.34, 26.25, 26.21, 24.47, 24.40, 24.29, 22.09, 18.59, 17.91, 17.12, 14.74, 13.92.

IR (ATR platinum diamond): ν [cm^{-1}] = 3307.5, 3031.8, 2922.9, 2852.9, 1738.1, 1655.8, 1536.5, 1456.3, 1374.0, 1232.1, 1160.1, 1110.7, 1003.7, 913.3, 724.1, 697.3, 645.9, 538.9, 411.4.

ESI-MS m/z: $[M+H]^+$ calculated for $C_{62}H_{102}N_2O_8$ = 1003.7709, found: 1003.7695.

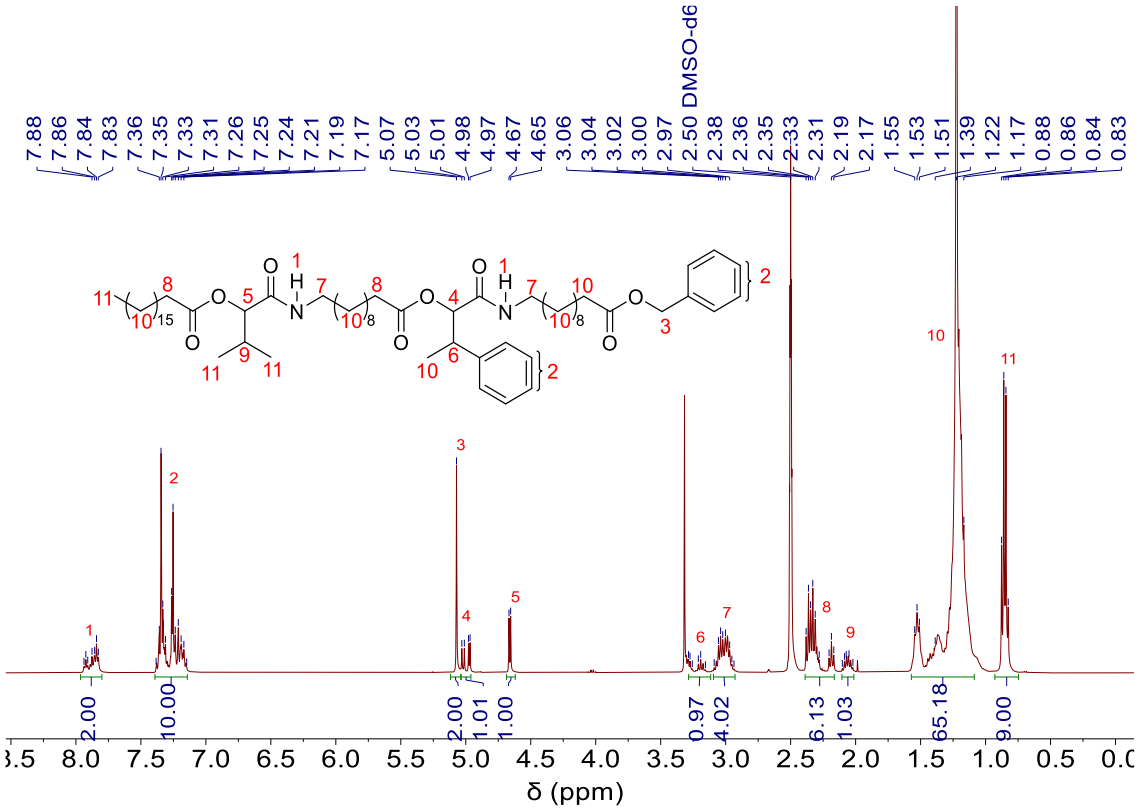

Deprotection (4b of P2)

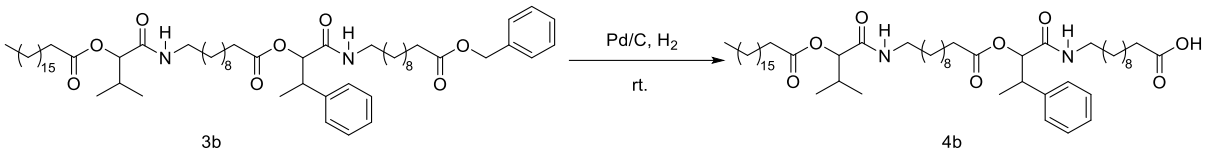

The target product 4b was obtained in quantitative yield. (3.97 g)

^{1}H NMR (400 MHz, DMSO-d_6) δ / ppm: 7.94 – 7.83 (m, 2H, 2 NH, ^{1}), 7.29 – 7.15 (m, 5H, aromatic, ^{2}), 5.03 – 4.97 (2d, J^{a} = 7.6 Hz, J^{b} = 4.7 Hz, 1H, 1CH, ^{3}), 4.66 (d, J = 5.1 Hz, 1H, 1CH, ^{4}), 3.27 – 3.11 (m, 1H, 1CH, ^{5}), 3.07 – 2.92 (m, 4H, 2 CH_2, ^{6}), 2.38 – 2.16 (m, 6H, 3 CH_2, ^{7}), 2.06 – 2.04 (m, 1H, 1 CH, ^{8}), 1.54 – 1.08 (m, 65H, 31 CH_2, 1 CH_3, ^{9}), 0.88 – 0.83 (m, 9H, 3 CH_3, ^{10}).

^{13}C NMR (101 MHz, DMSO-d_6) δ / ppm: 174.45, 172.46, 172.15, 172.08, 168.40, 167.99, 167.81, 142.35, 142.22, 128.06, 127.99, 127.73, 127.65, 126.50, 126.42, 77.42, 77.07, 76.82, 40.94, 40.58, 38.28, 38.20, 33.67, 33.41, 31.31, 29.87, 29.04, 28.96, 28.89, 28.78, 28.72, 28.59, 28.40, 28.26, 26.26, 24.51, 24.41, 24.30, 22.11, 18.59, 17.91, 17.12, 14.75, 13.92.

IR (ATR platinum diamond): ν [cm^{-1}] = 3299.3, 2922.9, 2852.9, 1740.1, 1651.7, 1538.6, 1464.5, 1369.9, 1232.1, 1160.1, 1110.7, 1020.2, 911.2, 763.1, 721.9, 699.3, 645.9, 538.9, 413.4.

ESI-MS m/z: $[M+H]^+$ calculated for $C_{55}H_{96}N_2O_8$ = 913.7239, found: 913.7224.

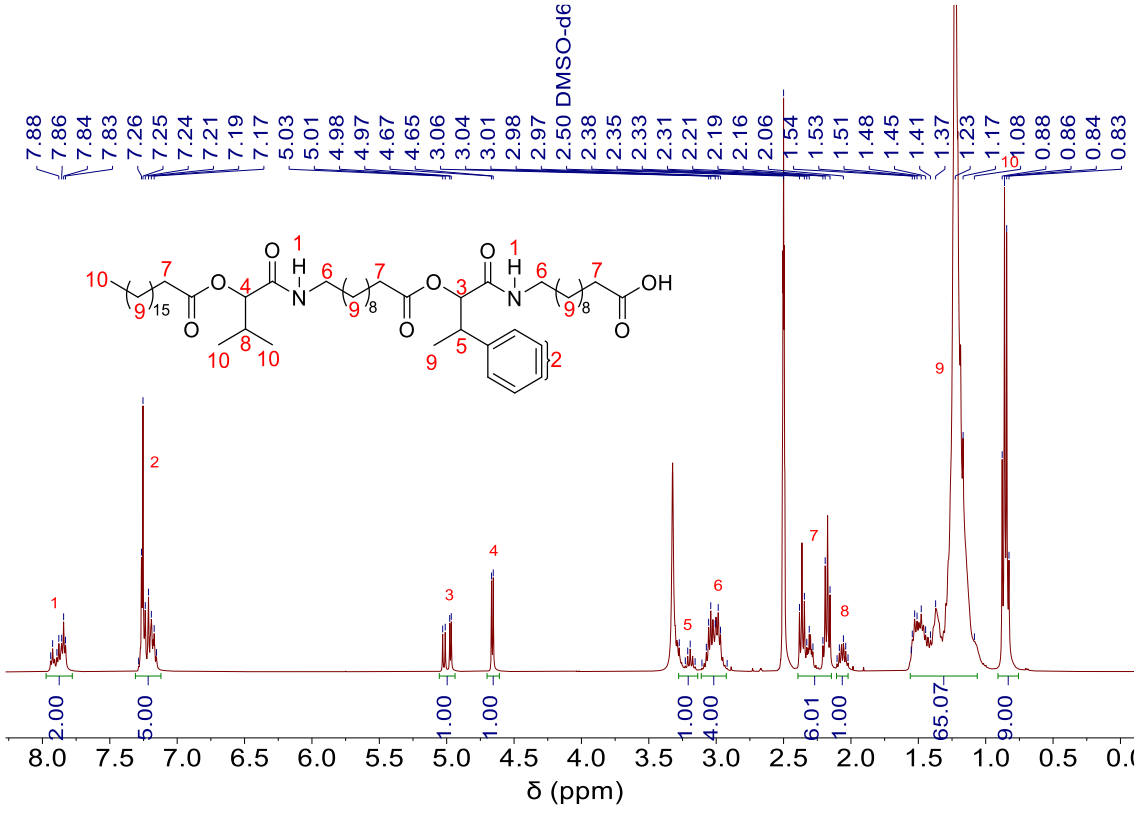

Passerini reaction (5b of P2)

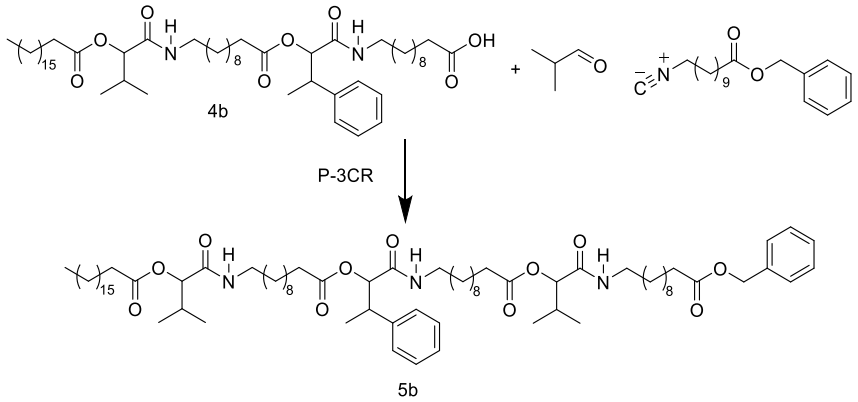

The target product 5b was obtained as a white solid in a yield of 88% (4.52 g)

^{1}H NMR (400 MHz, DMSO-d_6) δ / ppm: 7.92 – 7.83 (m, 3H, 3 NH, ^{1}), 7.38 – 7.15 (m, 10H, aromatic, ^{2}), 5.07 (s, 2H, 1 CH_2, ^{3}), 5.03 – 4.97 (2d, J^a = 7.6Hz, J^b = 4.6Hz, 1H, 1CH, ^{4}), 4.65 (d, J = 5.1 Hz, 2H, 2 CH, ^{5}), 3.27 – 3.17 (m, 1H, 1 CH, ^{6}), 3.05 – 2.93 (m, 6H, 3 CH_2, ^{7}), 2.38 – 2.17 (m, 8H, 4 CH_2, ^{8}), 2.08 – 2.02 (m, 2H, 2 CH, ^{9}), 1.56 – 1.17 (m, 81H, 39 CH_2, 1 CH_3, ^{10}), 0.88 – 0.83 (m, 15H, 5 CH_3, ^{11}).

^{13}C NMR (101 MHz, DMSO-d_6) δ / ppm: 172.70, 172.43, 172.12, 172.05, 168.36, 167.95, 167.78, 142.33, 142.21, 136.28, 128.36, 128.04, 127.87, 127.71, 127.62, 126.46, 77.39, 76.80, 65.24, 40.91, 40.55, 38.25, 38.18, 33.45, 33.39, 31.28, 29.86, 29.01, 28.90, 28.86, 28.79, 28.70, 28.64, 28.41, 28.38, 28.23, 26.23, 24.45, 24.39, 24.27, 22.08, 18.57, 17.89, 17.11, 14.72, 13.90.

IR (ATR platinum diamond): ν [cm^{-1}] = 3305.5, 2922.9, 2852.9, 1738.1, 1651.7, 1536.5, 1456.3, 1369.9, 1232.1, 1160.1, 1108.7, 1003.8, 915.3, 763.1, 721.9, 697.3, 647.9, 538.9, 409.3.

ESI-MS m/z: $[M+H]^+$ calculated for $C_{78}H_{131}N_3O_{11}$ = 1286.9856, found: 1286.9856.

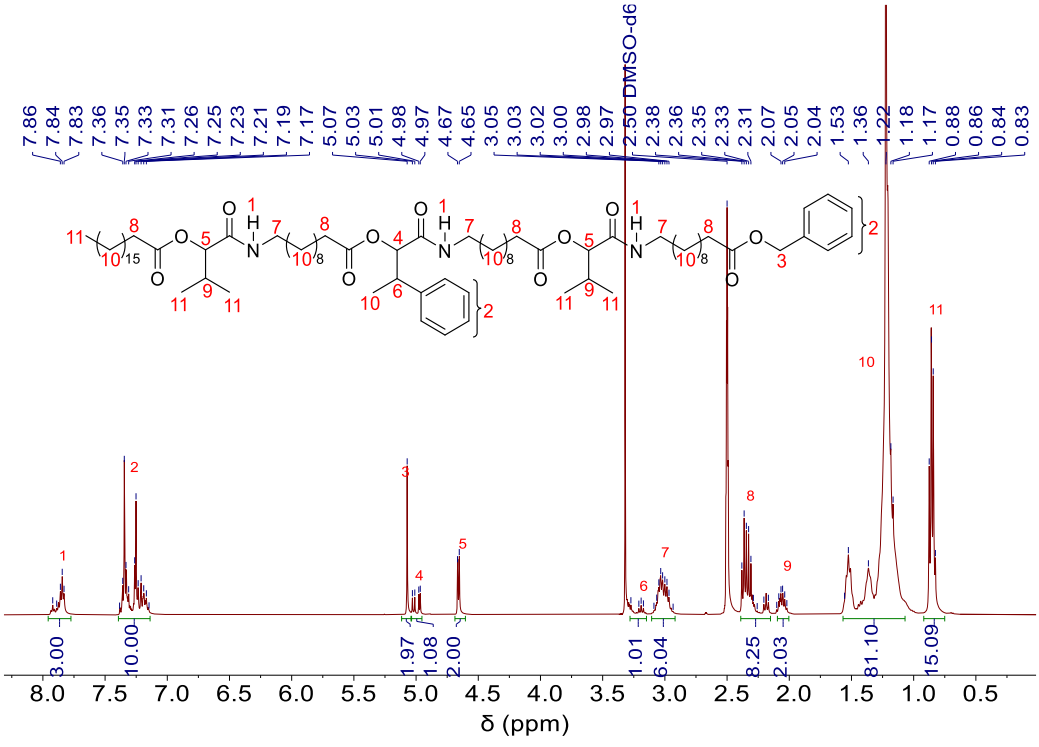

Deprotection (6b of P2)

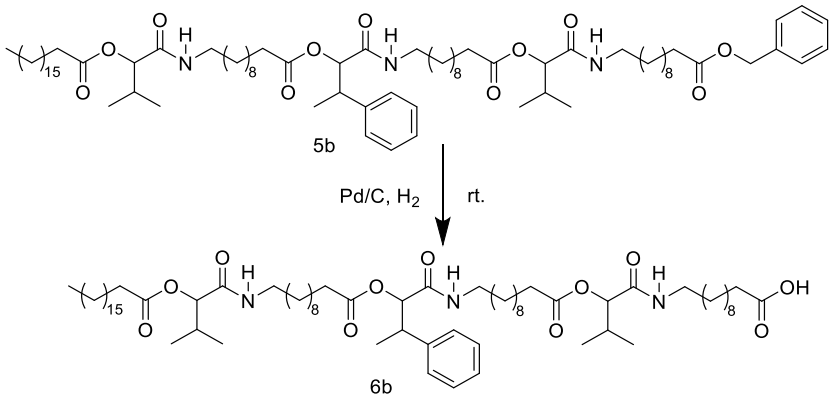

The target product 6b was obtained in quantitative yield as a white solid (2.94g).

^{1}H NMR (400 MHz, DMSO-d_6) δ / ppm: 7.94 – 7.84 (m, 3H, 3 NH, ^{1}), 7.26 – 7.16 (m, 5H, aromatic, ^{2}), 5.03 – 4.97 (2d, J^a = 7.6 Hz, J^b = 4.7 Hz 1H, 1 CH, ^{3}), 4.66 (d, J = 5.0 Hz, 2H, 2 CH, ^{4}), 3.27 – 3.21 (m, 1H, 1 CH, ^{5}), 3.05 – 2.96 (m, 6H, 3 CH_2, ^{6}), 2.39 – 2.16 (m, 8H, 4 CH_2, ^{7}), 2.11 – 2.04 (m, 2H, 2 CH, ^{8}), 1.55 – 1.17 (m, 81H, 39 CH_2, 1 CH_3, ^{9}), 0.88 – 0.83 (m, 15H, 5 CH_3, ^{10}).

^{13}C NMR (101 MHz, DMSO-d_6) δ / ppm: 174.43, 172.44, 172.13, 172.05, 168.37, 167.96, 167.78, 142.34, 142.21, 128.04, 127.98, 127.72, 127.63, 126.48, 77.39, 77.05, 76.80, 40.92, 40.56, 38.26, 38.18, 33.65, 33.40, 31.29, 29.86, 29.02, 28.94, 28.87, 28.70, 28.57, 28.43, 28.23, 26.25, 24.49, 24.39, 24.28, 22.08, 18.58, 17.89, 17.11, 17.09, 14.73, 13.91.

IR (ATR platinum diamond): ν [cm^{-1}] = 3301.3, 2922.9, 2852.9, 1740.1, 1651.7, 1538.6, 1464.5, 1369.9, 1232.1, 1162.2, 1110.7, 1011.9, 921.5, 763.1, 721.9, 699.3, 649.9, 538.9, 411.4.

ESI-MS m/z: $[M+H]^+$ calculated for $C_{71}H_{125}N_3O_{11}$ = 1196.9387, found: 1196.9365.

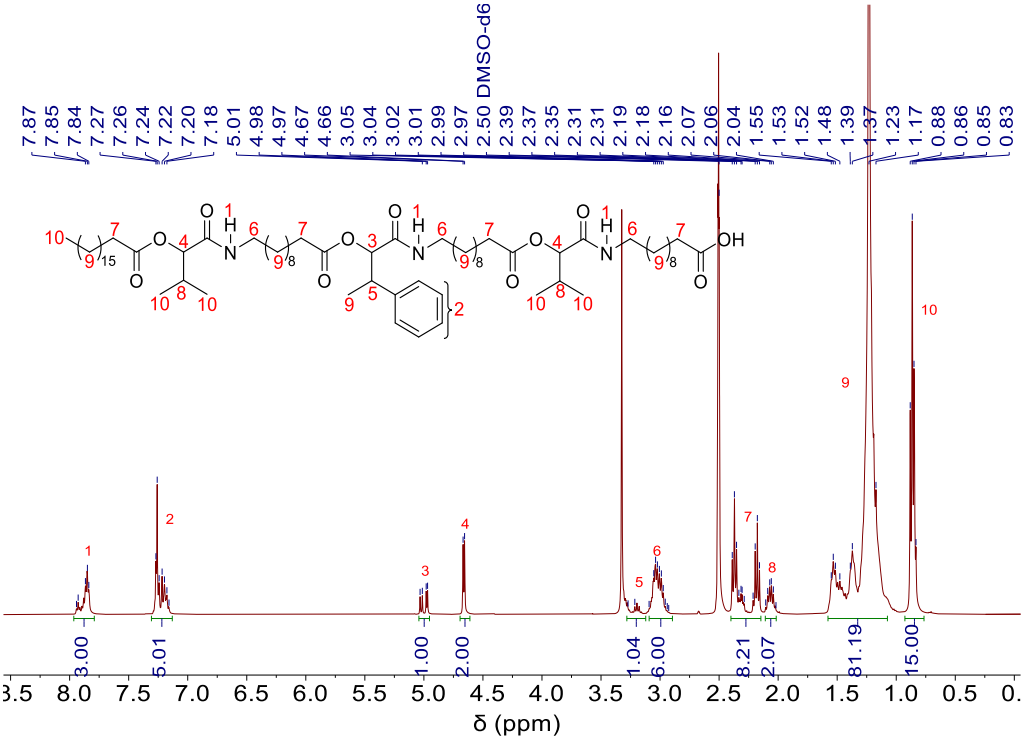

Passerini reaction (7b of P2)

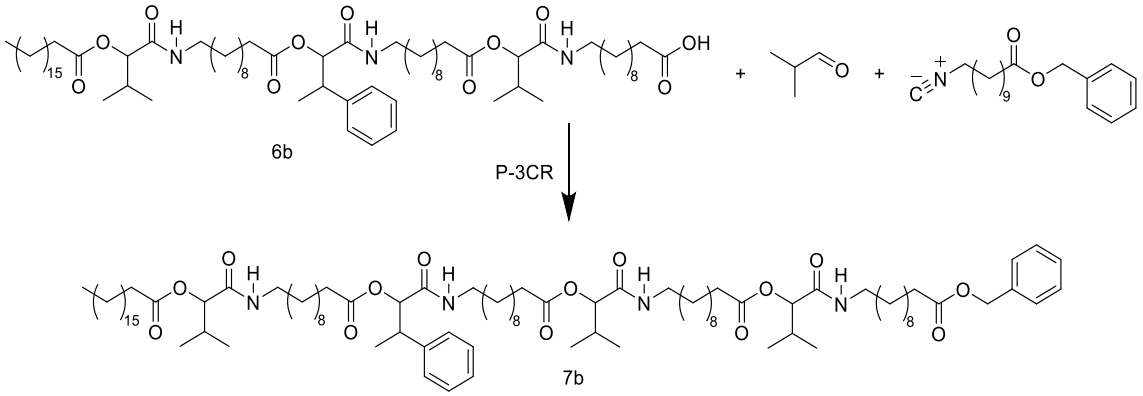

The target product 7b was obtained as a yellow oil in a yield of 92% (2.88g).

^{1}H NMR (400 MHz, DMSO-d_6) δ / ppm: 7.94 – 7.83 (m, 4H, 4 NH, ^{1}), 7.38 – 7.17 (m, 10H, aromatic, ^{2}), 5.06 (s, 2H, 1 CH_2, ^{3}), 5.03 – 4.97 (2d, J^a = 7.7 Hz, J^b = 4.8 Hz, 1H, 1CH, ^{4}), 4.66 (d, J = 5.0 Hz, 3H, 3 CH, ^{5}), 3.27 – 3.17 (m, 1H, 1 CH, ^{6}), 3.08 – 2.97 (m, 8H, 4 CH_2, ^{7}), 2.38 – 2.17 (m, 10H, 5 CH_2, ^{8}), 2.08 – 2.03 (m, 3H, 3 CH, ^{9}), 1.54 – 1.17 (m, 97H, 47 CH_2, 1 CH_3, ^{10}), 0.87 – 0,84 (m, 21H, 7 CH_3, ^{11}).

^{13}C NMR (101 MHz, DMSO-d_6) δ / ppm: 172.72, 172.43, 172.12, 172.05, 168.37, 167.96, 167.78, 136.28, 128.37, 128.04, 127.93, 127.87, 127.70, 127.62, 126.40, 77.38, 65.24, 40.79, 38.18, 33.45, 33.40, 31.28, 29.86, 29.00, 28.93, 28.82, 28.78, 28.69, 28.69, 28.45, 28.23, 26.24, 24.45, 24.39, 24.27, 21.71, 18.57, 17.89, 17.09, 14.73, 13.91.

IR (ATR platinum diamond): ν [cm^{-1}] = 3303.4, 2922.9, 2852.9, 1738.1, 1651.7, 1534.5, 1462.5, 1369.9, 1232.1, 1160.1, 1110.7, 1003.8, 923.5, 721.9, 699.3, 647.9, 538.9, 411.4.

ESI-MS m/z: $[M+H]^+$ calculated for $C_{94}H_{160}N_4O_{14}$ = 1570.2024, found: 1570.2002.

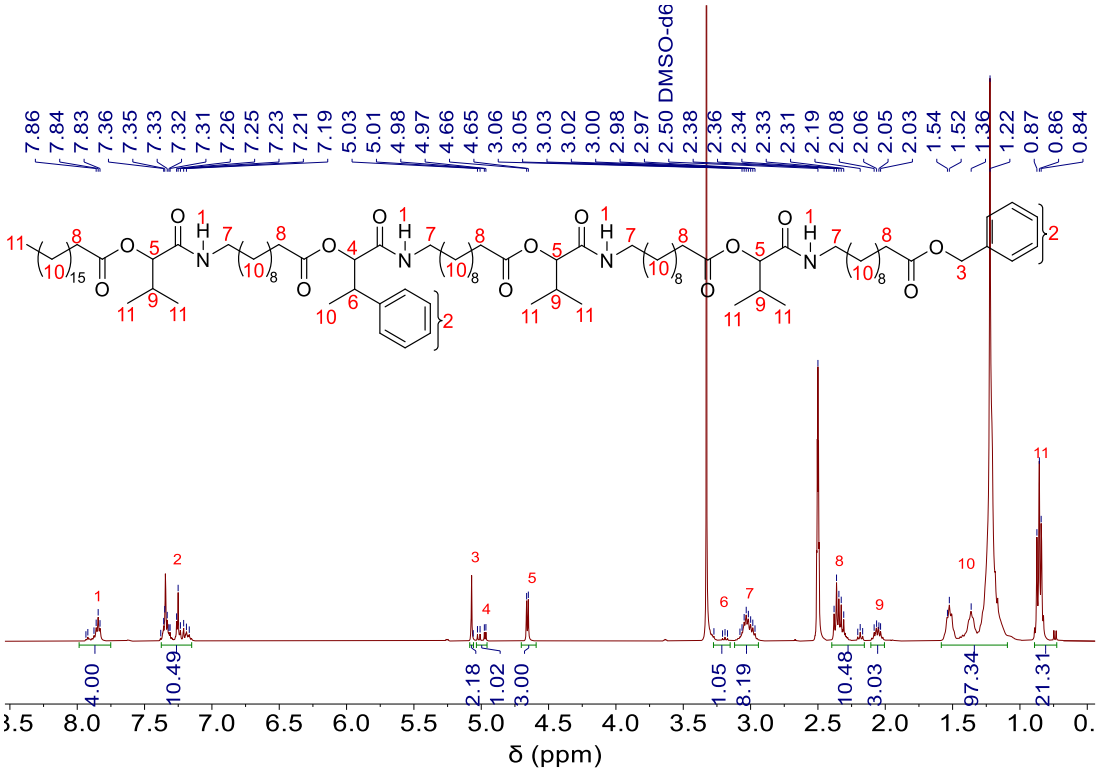

Deprotection (8b of P2)

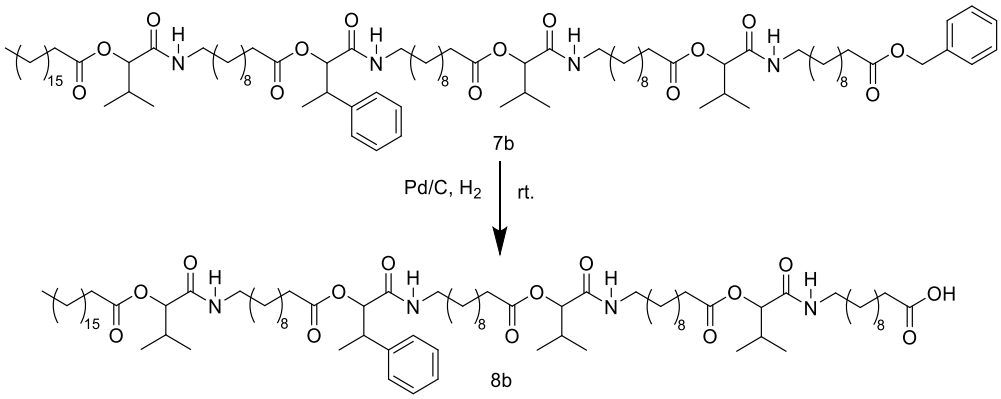

The target product 8b was obtained in quantitative yield as a white solid (2.02 g).

^{1}H NMR (400 MHz, DMSO-d_6) δ / ppm: 7.93 – 7.83 (m, 4H, 4 NH, ^{1}), 7.26 – 7.15 (m, 5H, aromatic, ^{2}), 5.03 – 4.97 (2d, J^{a} = 7.6 Hz, J^{b} = 4.7 Hz, 1H, 1 CH, ^{3}), 4.66 (d, J = 5.0 Hz, 3H, 3 CH, ^{4}), 3.21 – 3.17 (m, 1H, 1 CH, ^{5}), 3.05 – 2.97 (m, 8H, 4 CH_2, ^{6}), 2.38 – 2.15 (m, 10H, 5 CH_2, ^{7}), 2.08 – 2.02 (m, 3H, 3 CH, ^{8}), 1.53 – 1.17 (m, 97H, 47 CH_2, 1 CH_3, ^{9}), 0.87 – 0.81 (m, 21H, 7 CH_3, ^{10}).

^{13}C NMR (101 MHz, DMSO-d_6) δ / ppm: 174.42, 172.43, 172.12, 172.04, 168.36, 167.96, 167.78, 142.33, 142.21, 128.04, 127.97, 127.71, 127.62, 126.39, 77.38, 77.06, 76.75, 40.91, 40.55, 38.25, 38.18, 33.65, 33.40, 31.28, 29.86, 28.93, 28.83, 28.69, 28.56, 28.42, 28.23, 26.24, 24.49, 24.39, 24.27, 22.08, 18.58, 17.09, 17.89, 17.09, 14.73, 13.91.

IR (ATR platinum diamond): ν [cm^{-1}] = 3307.5, 2922.9, 2852.9, 1740.1, 1651.7, 1538.6, 1464.5, 1369.9, 1232.1, 1162.1, 1110.7, 1009.9, 917.4, 763.1, 721.9, 699.3, 652.0, 538.9, 405.2.

ESI-MS m/z: $[M+H]^+$ calculated for $C_{87}H_{154}N_4O_{14}$ = 1480.1534, found: 1480.1532.

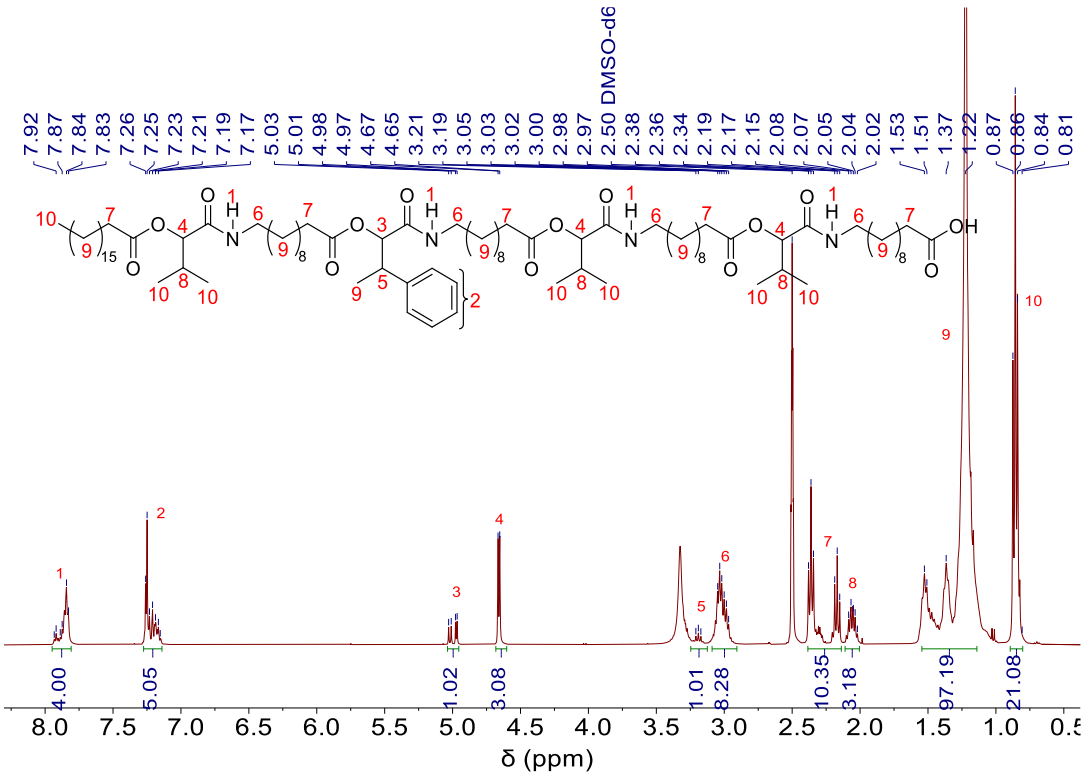

Passerini reaction to synthesize P2

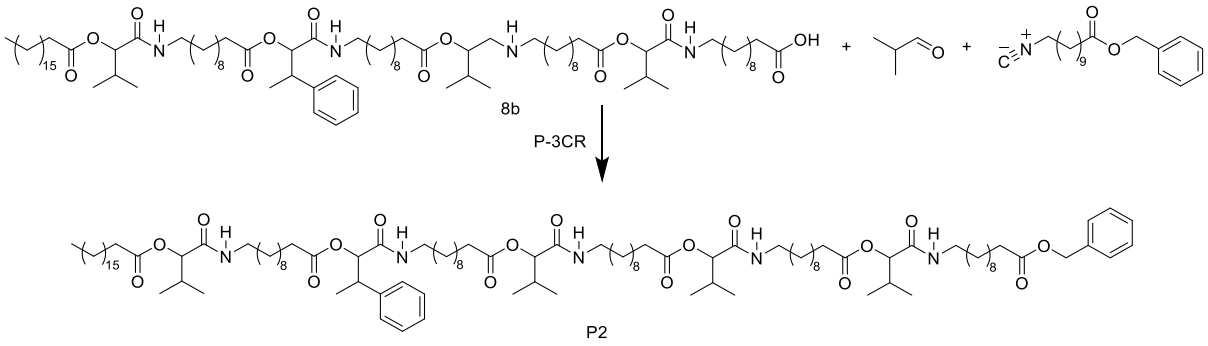

P2 was obtained as a yellow oil in a yield of 85% (1.91g).

^{1}H NMR (400 MHz, DMSO-d_6) δ / ppm: 7.93 – 7.83 (m, 5H, 5 NH, ^{1}), 7.34 – 7.19 (m, 10H, aromatic, ^{2}), 5.07 (s, 2H, 1 CH_2, ^{3}), 5.03 – 4.97 (2d, J^a = 4.4 Hz, J^b = 4.7 Hz, 1H, 1 CH, ^{4}), 4.65 (d, J = 5.1 Hz, 4H, 4 CH, ^{5}), 3.21 – 3.17 (m, 1H, 1 CH, ^{6}), 3.05 – 2.98 (m, 10H, 5 CH_2, ^{7}), 2.38 – 2.17 (m, 12H, 6 CH_2, ^{8}), 2.05 – 2.02 (m, 4H, 4 CH, ^{9}), 1.52 – 1.16 (m, 115H, 56 CH_2, 1 CH_3, ^{10}), 0.87 – 0.84 (m, 27H, 9 CH_3, ^{11}).

^{13}C NMR (101 MHz, DMSO-d_6) δ / ppm: 172.70, 172.43, 172.12, 172.05, 168.37, 167.96, 167.78, 136.28, 128.37, 128.04, 127.93, 127.87, 127.70, 127.62, 126.40, 77.38, 65.24, 40.79, 38.18, 33.45, 33.40, 31.28, 29.86, 29.00, 28.93, 28.82, 28.78, 28.69, 28.42, 28.23, 26.24, 24.45, 24.39, 24.27, 21.71, 18.57, 17.89, 17.09, 14.73, 13.91.

IR (ATR platinum diamond): ν [cm^{-1}] = 3305.5, 2922.9, 2852.9, 1740.1, 1651.7, 1534.5, 1462.5, 1369.9, 1234.1, 1162.2, 1110.7, 1005.8, 923.6, 721.9, 699.3, 647.9, 538.9, 411.4.

ESI-MS m/z: $[M+H]^+$ calculated for $C_{110}H_{189}N_5O_{17}$ = 1853.4151, found: 1853.4191.

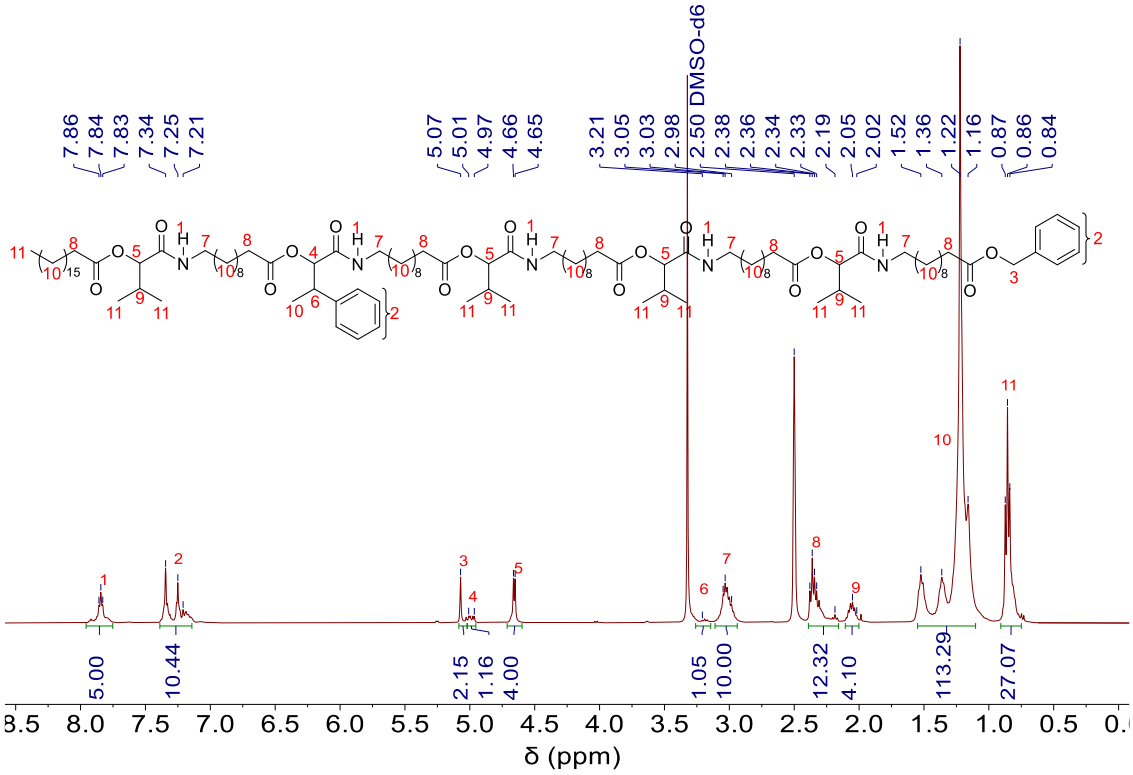

Passerini reaction (3c of P3)

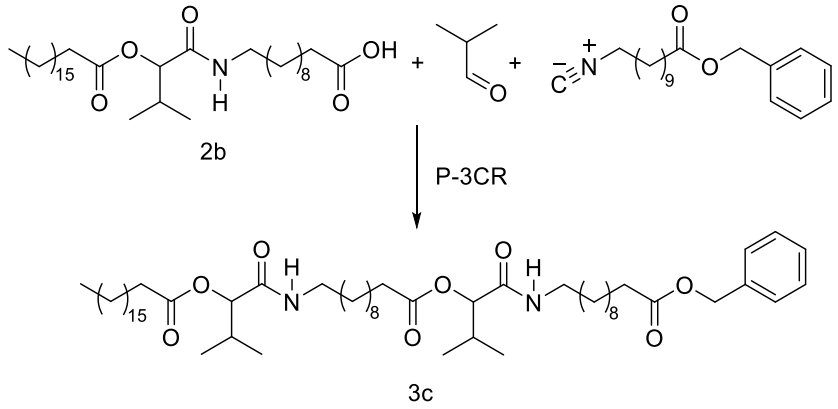

The product 3c was obtained as a white solid in a yield of 82% (7.70 g).

^{1}H NMR: (400 MHz, $CDCl_3$) δ / ppm: 7.38 – 7.31 (m, 5H, aromatic, ^{1}), 5.95 – 5.94 (m, 2H, 2 NH, ^{2}), 5.11 (s, 2H, CH_2, ^{3}), 5.06 –5.05(d, J = 6.3 Hz, 2H, 2 CH, ^{4}), 3.33 – 3.17 (m, 4H, 2 CH_2, ^{5}), 2.42 – 2.24 (m, 8H, 2 CH, 3 CH_2, ^{6}), 1.69 – 1.25 (m, 62H, 31 CH_2, ^{7}), 0.95 – 0.86 (m, 15H, 5 CH_3, ^{8}).
^{13}C NMR (101 MHz, $CDCl_3$) δ / ppm: 173.80, 172.68, 172.66, 169.40, 169.37, 136.27, 128.67, 128.28, 78.05, 78.03, 66.19, 39.28, 39.26, 34.45, 34.42, 32.05, 30.64, 29.83, 29.80, 29.78, 29.72, 29.60, 29.56, 29.49, 29.47, 29.40, 29.33, 29.30, 29.25, 29.23, 26.96, 25.18, 25.14, 25.06, 22.82, 18.91, 17.08, 17.07, 14.25.
IR (ATR platinum diamond): ν [cm^{-1}] = 3307.5, 2922.9, 2852.9, 1736.0, 1653.8, 1534.5, 1462.5, 1369.9, 1232.1, 1160.1, 1110.7, 1003.8, 927.7, 724.0, 697.3, 580.0, 501.9.
ESI-MS m/z: $[M+H]^+$ calculated for $C_{57}H_{100}N_2O_8$ = 941.7552, found: 941.7548.

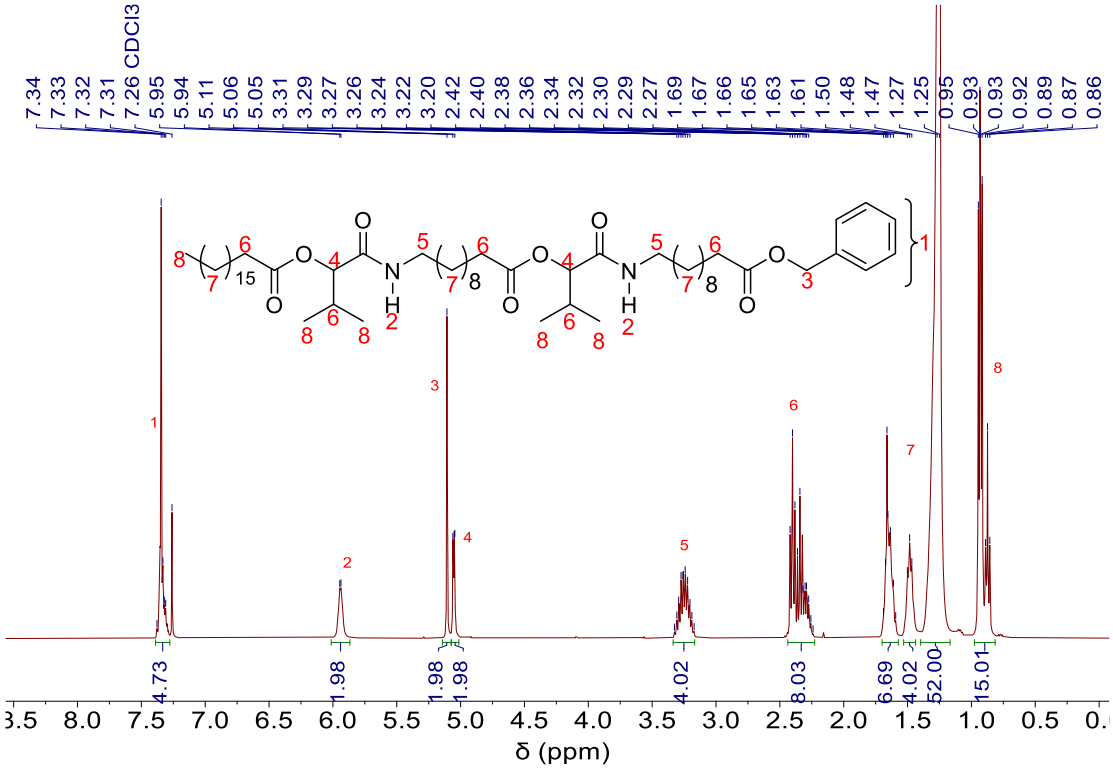

Deprotection (4c of P3)

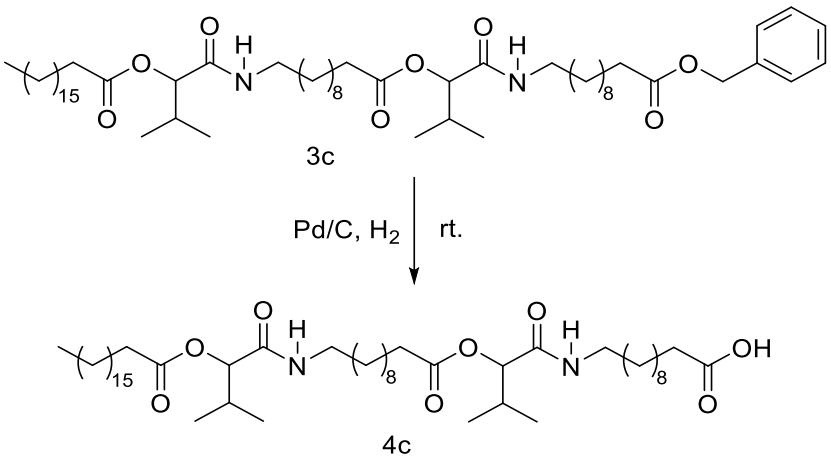

The target product 4c was obtained in quantitative yield as a white solid. (5.92 g).

^{1}H NMR (400 MHz, $CDCl_3$) δ / ppm: 6.02 – 5.96 (m, 2H, NH, ^{1}), 5.06 – 5.05 (d, J = 4.5 Hz, 2H, 2 CH, ^{2}), 3.32 – 3.20 (m, 4H, 2 CH_2, ^{3}), 2.42 – 2.26 (m, 8H, 2 CH, 3 CH_2, ^{4}), 1.69 – 1.25 (m, 62H, 31 CH_2, ^{5}), 0.94 – 0.85 (m, 15H, 5 CH_3, ^{6}).
^{13}C NMR (101 MHz, $CDCl_3$) δ / ppm: 178.09, 172.78, 172.69, 169.59, 169.49, 78.07, 78.05, 39.34, 39.27, 34.45, 34.43, 34.02, 32.06, 30.62, 29.83, 29.81, 29.78, 29.74, 29.70, 29.60, 29.58, 29.49, 29.45, 29.40, 29.35, 29.30, 29.27, 29.22, 29.10, 26.97, 26.90, 25.16, 24.85, 22.82, 18.90, 17.08, 14.25.
IR (ATR platinum diamond): ν [cm^{-1}] = 3307.5, 2922.8, 2852.9, 1740.1, 1651.7, 1538.6, 1464.5, 1369.9, 1234.1, 1162.2, 1112.8, 1007.9, 927.7, 721.9, 649.9, 411.4.
ESI-MS m/z: $[M+H]^+$ calculated for $C_{50}H_{94}N_2O_8$ = 851.7083, found: 851.7079.

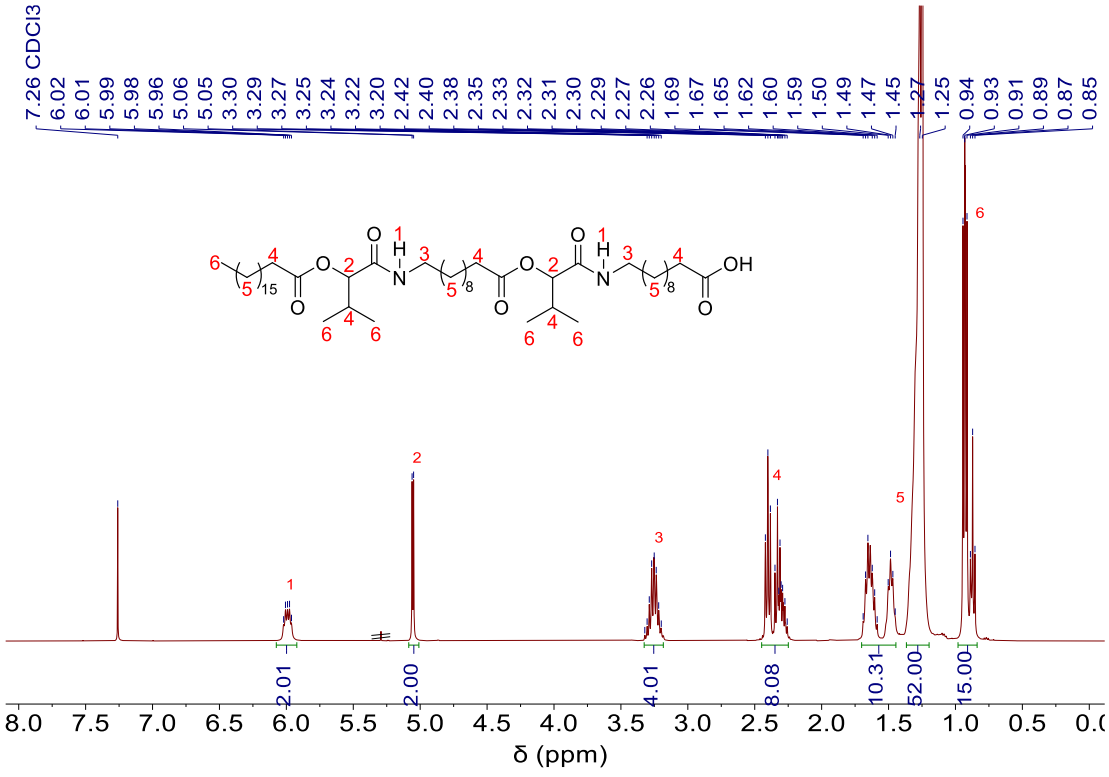

Passerini reaction (5c of P3)

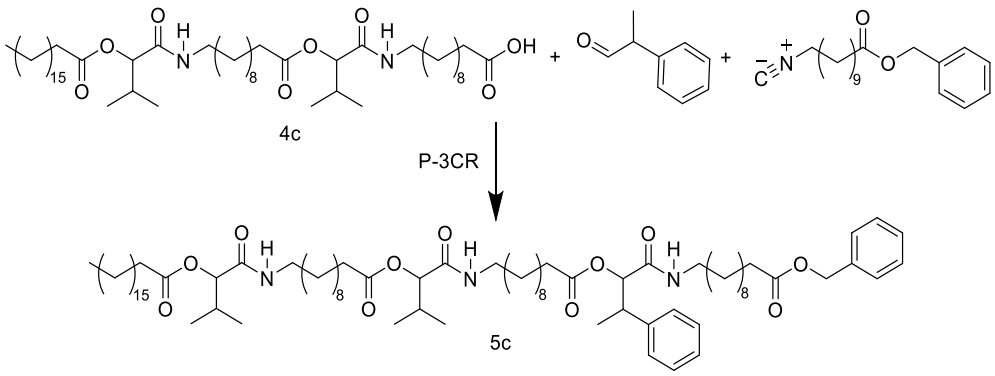

The target product 5c was obtained as a yellow oil in a yield of 92% (5.9g).

^{1}H NMR (400 MHz, DMSO-d_6) δ / ppm: 7.94 – 7.84 (m, 3H, 3 NH, [1]), 7.38 – 7.17 (m, 10H, aromatic, [2]), 5.07 (s, 2H, 1 CH_2, [3]), 5.03 – 4.97 (2d, J^a = 7.6 Hz, J^b = 4.6 Hz, 1H, 1 CH, [4]), 4.65 (d, J = 5.1 Hz, 2H, 2 CH, [5]), 3.21 – 3.17 (m, 1H, 1 CH, [6]), 3.05 – 2.98 (m, 6H, 3 CH_2, [7]), 2.38 – 2.17 (m, 8H, 4 CH_2, [8]), 2.10 – 2.03 (m, 2H, 2 CH, [9]), 1.54 – 1.17 (m, 81H, 39 CH_2, 1 CH_3, [10]), 0.87 – 0.84 (m, 15H, 5 CH_3, [11]).
^{13}C NMR (101 MHz, DMSO-d_6) δ / ppm: 172.71, 172.45, 172.43, 172.15, 172.07, 168.38, 167.98, 167.81, 142.35, 142.22, 136.29, 128.38, 128.05, 127.99, 127.94, 127.88, 127.72, 127.64, 126.49, 77.42, 77.39, 77.07, 76.82, 65.25, 38.26, 38.18, 33.46, 33.39, 31.29, 29.87, 29.02, 28.94, 28.88, 28.82, 28.70, 28.43, 28.38, 28.24, 26.24, 24.46, 24.40, 24.29, 22.09, 18.58, 17.90, 17.11, 17.09, 14.74, 13.91.
IR (ATR platinum diamond): ν / cm^{-1} = 3309.6, 3093.6, 2922.9, 2852.9, 1738.1, 1653.7, 1534.5, 1456.3, 1369.9, 1232.1, 1160.1, 1110.7, 1003.8, 917.4, 763.1, 721.9, 697.3, 538.9, 409.3.
ESI-MS m/z: $[M+H]^+$ calculated for $C_{78}H_{131}N_3O_{11}$ = 1286.9856, found: 1286.9844.

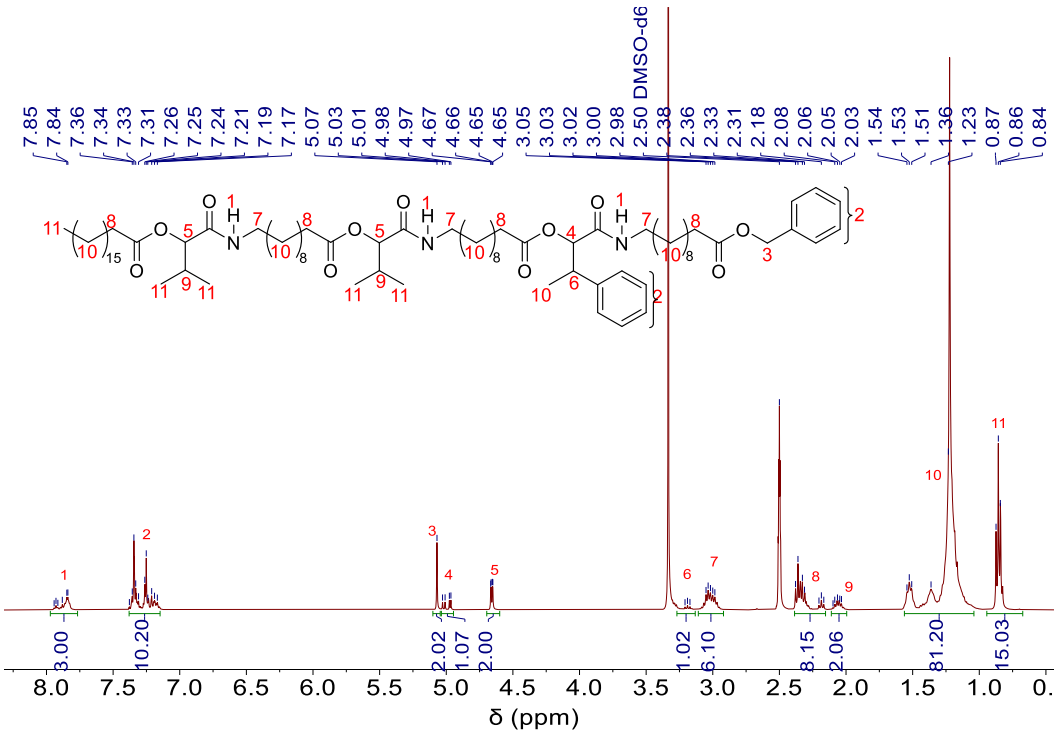

Deprotection (6c of P3)

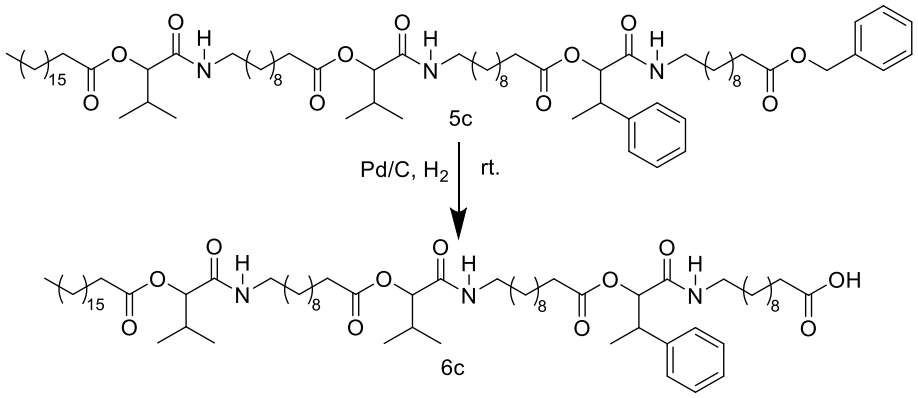

The target product 6c was obtained in quantitative yield as a white solid. (4.74g)

^{1}H NMR (400 MHz, DMSO-d_6) δ / ppm: 7.94 – 7.84 (m, 3H, 3 NH, ^{1}), 7.26 – 7.15 (m, 5H, aromatic, ^{2}), 5.03 – 4.97 (2d, J^{a} = 7.7Hz, J^{b} = 4.7 Hz,1H, 1 CH, ^{3}), 4.66 (d, J = 5.0 Hz, 2H, 2 CH, ^{4}), 3.23 – 3.17 (m, 1H, 1 CH, ^{5}), 3.08 – 2.97 (m, 6H, 3 CH_2, ^{6}), 2.38 – 2.15 (m, 8H, 4 CH_2, ^{7}), 2.09 – 2.04 (m, 2H, 2 CH, ^{8}), 1.53 – 1.17 (m, 81H, 39 CH_2, 1 CH_3, ^{9}), 0.88 – 0.84 (m, 15H, 5 CH_3, ^{10}).

^{13}C NMR (101 MHz, DMSO-d_6) δ / ppm: 174.43, 172.43, 172.14, 172.06, 168.37, 167.97, 167.79, 142.33, 142.21, 128.05, 127.98, 127.72, 127.63, 126.40, 77.41, 77.38, 77.05, 76.81, 40.92, 40.56, 38.27, 38.18, 33.66, 33.41, 31.29, 29.86, 29.02, 28.93, 28.86, 28.76, 28.70, 28.578, 28.43, 28.38, 28.23, 26.24, 24.50, 24.39, 24.28, 22.08, 18.58, 17.90, 17.11, 17.08, 14.75, 13.91.

IR (ATR platinum diamond): ν / cm^{-1} = 3297.2, 3087.4, 2922.9, 2852.9, 1740.1, 1651.7, 1538.6, 1464.5, 1369.9, 1232.1, 1160.1, 1108.7, 1009.9, 923.6, 763.1, 721.9, 699.3, 536.9, 405.2.

ESI-MS m/z: $[M+H]^+$ calculated for $C_{71}H_{125}N_3O_{11}$ = 1196.9387, found: 1196.9379.

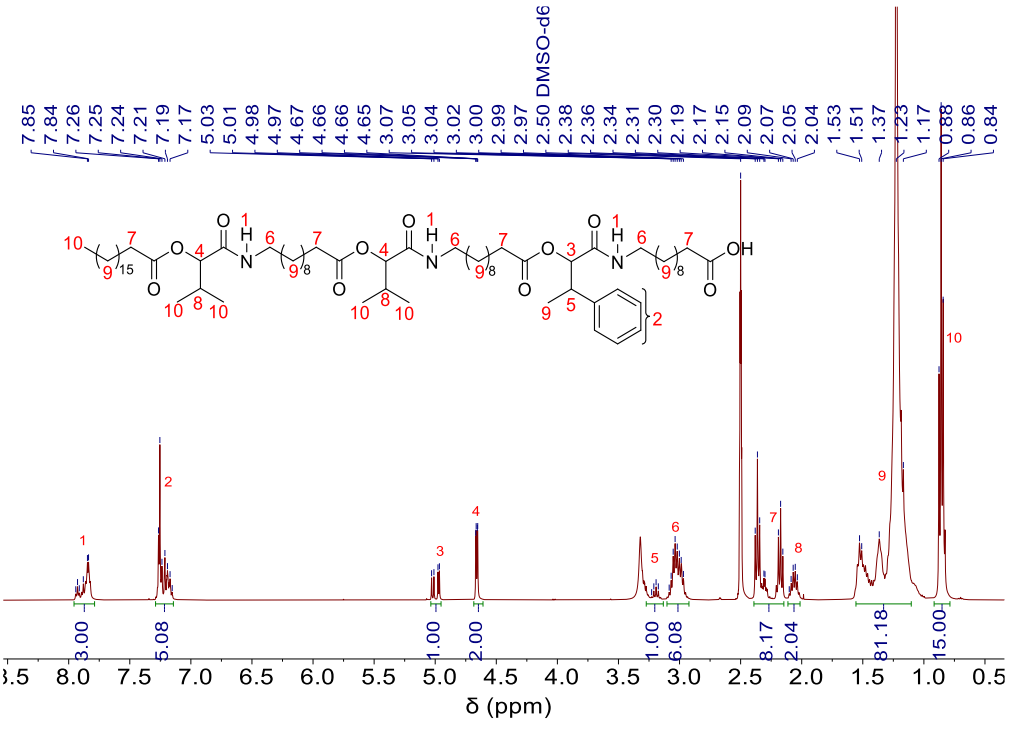

Passerini reaction (7c of P3)

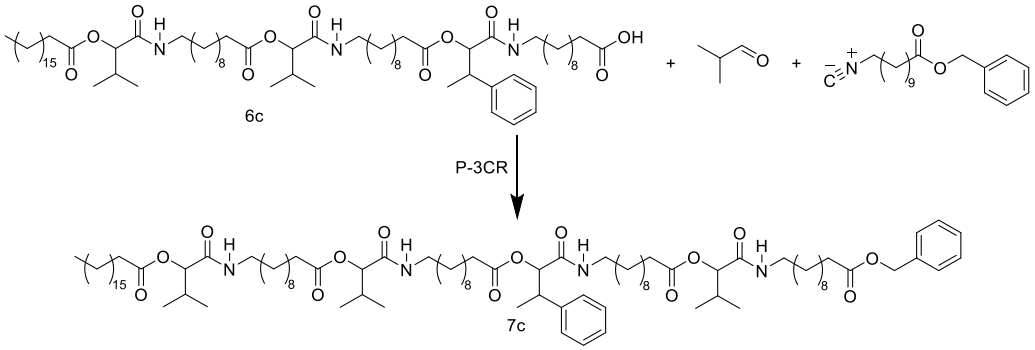

The target product 7c was obtained as a yellow oil in a yield of 90% (5.0g).

^{1}H NMR (400 MHz, DMSO-d_6) δ / ppm: 7.92 – 7.84 (m, 4H, 4 NH, [1]), 7.36 – 7.17 (m, 10H, aromatic, [2]), 5.07 (s, 2H, 1 CH_2, [3]), 5.03 – 4.96 (2d, J^a = 7.7Hz, J^b = 4.8 Hz, 1H, 1 CH, [4]), 4.66 (d, J = 5.0 Hz, 3H, 3 CH, [5]), 3.27 – 3.17 (m, 1H, 1 CH, [6]), 3.07 – 2.98 (m, 8H, 4 CH_2, [7]), 2.38 – 2.17 (m, 10H, 5 CH_2, [8]), 2.08 – 2.02 (m, 3H, 3 CH, [9]), 1.52 – 1.16 (m, 97H, 47 CH_2, 1 CH_3, [10]), 0.87 – 0,84 (m, 21H, 7 CH_3, [11]).
^{13}C NMR (101 MHz, DMSO-d_6) δ / ppm: 172.70, 172.43, 172.13, 172.05, 168.36, 167.96, 167.78, 142.33, 142.21, 136.28, 128.37, 128.04, 127.97, 127.92, 127.87, 127.71, 127.62, 126.41, 77.38, 77.05, 76.80, 65.24, 59.73, 40.92, 40.56, 38.25, 38.18, 33.45, 33.40, 31.28, 29.86, 29.01, 28.93, 28.86, 28.79, 28.69, 28.42, 28.32, 28.23, 26.23, 24.45, 24.39, 24.27, 22.08, 20.74, 18.57, 17.89, 17.11, 17.08, 14.73, 14.07, 13.90.
IR (ATR platinum diamond): ν / cm^{-1} = 3305.5, 3091.5, 2922.9, 2852.9, 1738.1, 1653.8, 1534.5, 1462.5, 1369.9, 1232.1, 1162.2, 1112.8, 1005.8, 917.4, 763.1, 721.9, 699.3, 536.9, 409.3.
ESI-MS m/z: $[M+H]^+$ calculated for $C_{94}H_{160}N_4O_{14}$ = 1570.2004, found: 1570.2019.

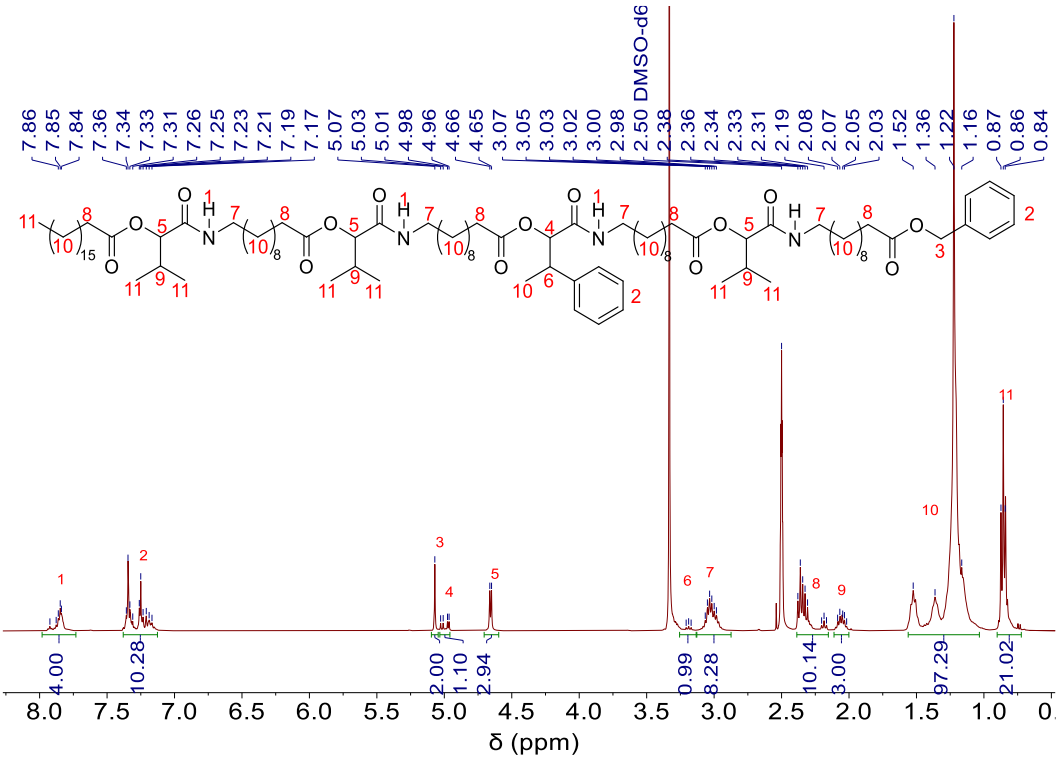

Deprotection (8c of P3)

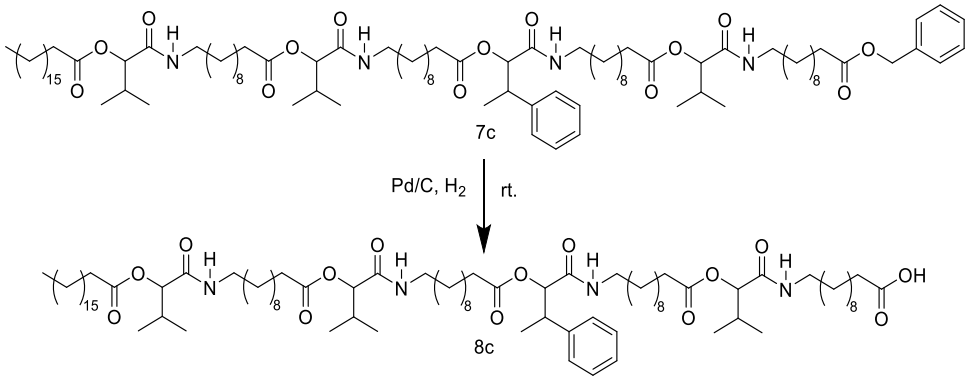

The target product 8c was obtained in quantitative yield as a white solid. (2.56g)

^{1}H NMR (400 MHz, DMSO-d_6) δ / ppm: 7.92 – 7.84 (m, 4H, 4 NH, ^{1}), 7.26 – 7.17 (m, 5H, aromatic, ^{2}), 5.03 – 4.96 (2d, J^a = 7.7 Hz, J^b = 4.6 Hz, 1H, 1 CH, ^{3}), 4.66 (d, J = 5.0 Hz, 3H, 3 CH, ^{4}), 3.21 – 3.17 (m, 1H, 1 CH, ^{5}), 3.07 – 2.98 (m, 8H, 4 CH_2, ^{6}), 2.38 – 2.15 (m, 10H, 5 CH_2, ^{7}), 2.10 – 2.04 (m, 3H, 3 CH, ^{8}), 1.53 – 1.17 (m, 97H, 47 CH_2, 1 CH_3, ^{9}), 0.86 – 0.84 (m, 21H, 7 CH_3, ^{10}).

^{13}C NMR (101 MHz, DMSO-d_6) δ / ppm: 174.44, 172.44, 172.42, 172.13, 172.05, 168.39, 167.99, 167.81, 142.33, 142.21, 128.04, 127.98, 127.72, 127.63, 126.48, 126.40, 77.39, 77.06, 76.81, 40.94, 40.57, 40.43, 38.27, 38.20, 33.67, 33.40, 31.31, 29.87, 29.02, 28.96, 28.86, 28.77, 28.72, 28.70, 28.45, 28.40, 28.25, 26.35, 26.26, 24.51, 24.42, 24.29, 22.10, 18.58, 17.89, 17.09, 14.73, 13.90.

IR (ATR platinum diamond): ν / cm^{-1} = 3305.5, 3089.5, 2922.9, 2852.9, 1740.1, 1651.7, 1536.5, 1464.5, 1369.9, 1234.1, 1162.2, 1108.7, 1007.9, 923.6, 763.1, 721.9, 699.3, 647.9, 536.9, 411.4.

ESI-MS m/z: $[M+H]^+$ calculated for $C_{87}H_{154}N_4O_{14}$ = 1480.1534, found: 1480.1537.

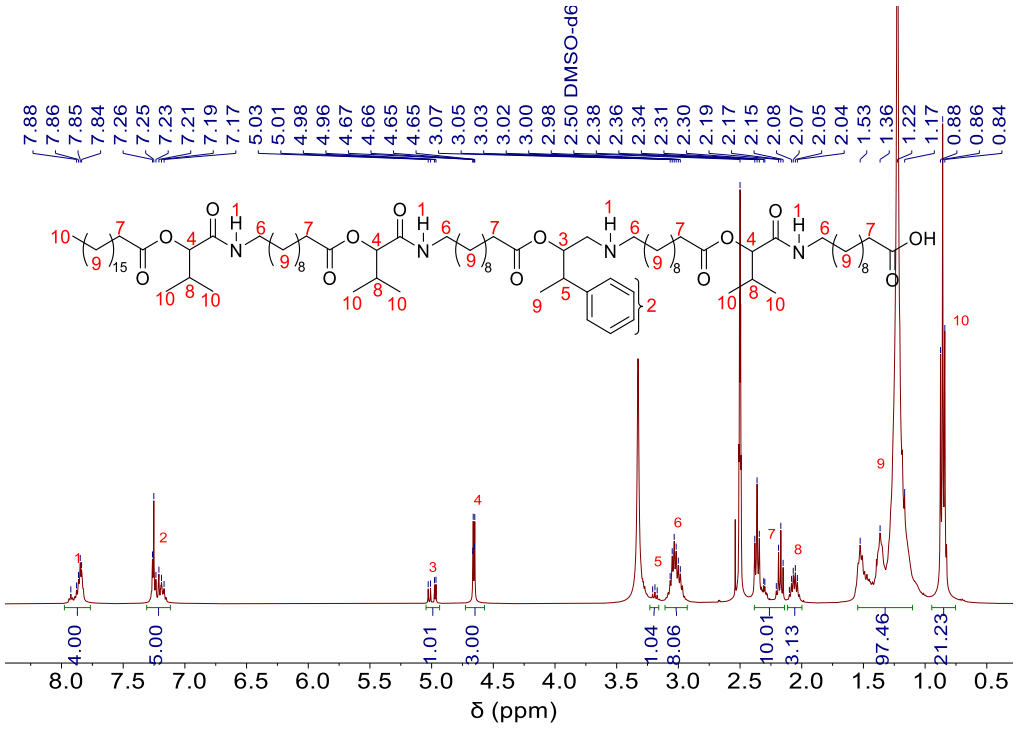

Passerini reaction to synthesize P3

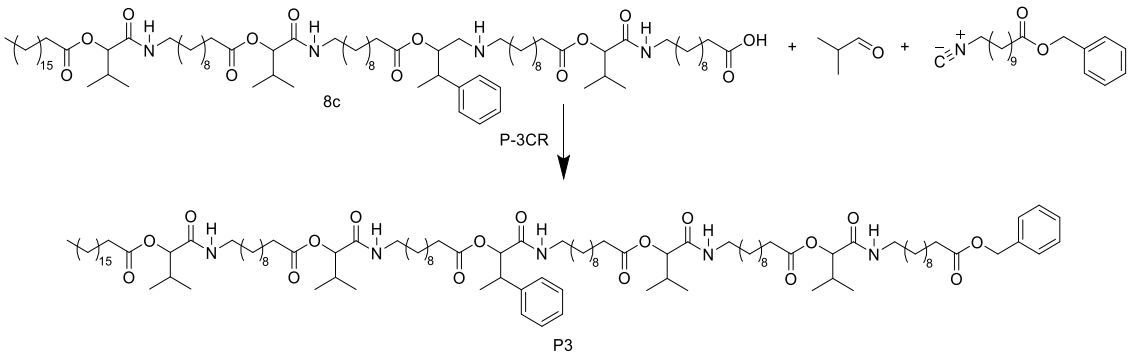

P3 was obtained as a yellow oil in a yield of 91% (2.52g).

^{1}H NMR (400 MHz, DMSO-d_6) δ / ppm: 7.94 – 7.85 (m, 5H, 5NH, ^{1}), 7.38 – 7.15 (m, 10H, aromatic, ^{2}), 5.07 (s, 2H, 1 CH_2, ^{3}), 5.03 – 4.97 (2d, J^a = 7.6 Hz, J^b = 4.8 Hz, 1H, 1CH, ^{4}), 4.65 (d, J = 5.1 Hz, 4H, 4CH, ^{5}), 3.21 – 3.17 (m, 1H, 1 CH, ^{6}), 3.10 – 2.97 (m, 10H, 5 CH_2, ^{7}), 2.38 – 2.17 (m, 12H, 6 CH_2, ^{8}), 2.08 – 2.03 (m, 4H, 4 CH, ^{9}), 1.52 – 1.16 (m, 115H, 56 CH_2, 1 CH_3, ^{10}), 0.87 – 0.84 (m, 27H, 9 CH_3, ^{11}).

^{13}C NMR (101 MHz, DMSO-d_6) δ / ppm: 172.71, 172.43, 168.36, 136.28, 128.37, 128.04, 127.93, 127.87, 127.71, 127.62, 77.38, 65.24, 38.18, 33.45, 33.40, 31.28, 29.86, 29.00, 28.93, 28.86, 28.82, 28.69, 28.42, 28.37, 26.23, 24.45, 24.39, 24.27, 22.08, 18.57, 17.09, 14.78, 13.91.

IR (ATR platinum diamond): ν / cm^{-1} = 3303.4, 3091.5, 2922.9, 2852.9, 1738.1, 1651.7, 1534.5, 1462.5, 1369.9, 1232.1, 1160.1, 1110.7, 1009.9, 923.6, 724.1, 697.3, 645.9, 543.1, 409.3.

ESI-MS m/z: $[M+H]^+$ calculate for $C_{110}H_{189}N_5O_{17}$ = 1853.4151, found: 1853.4155.

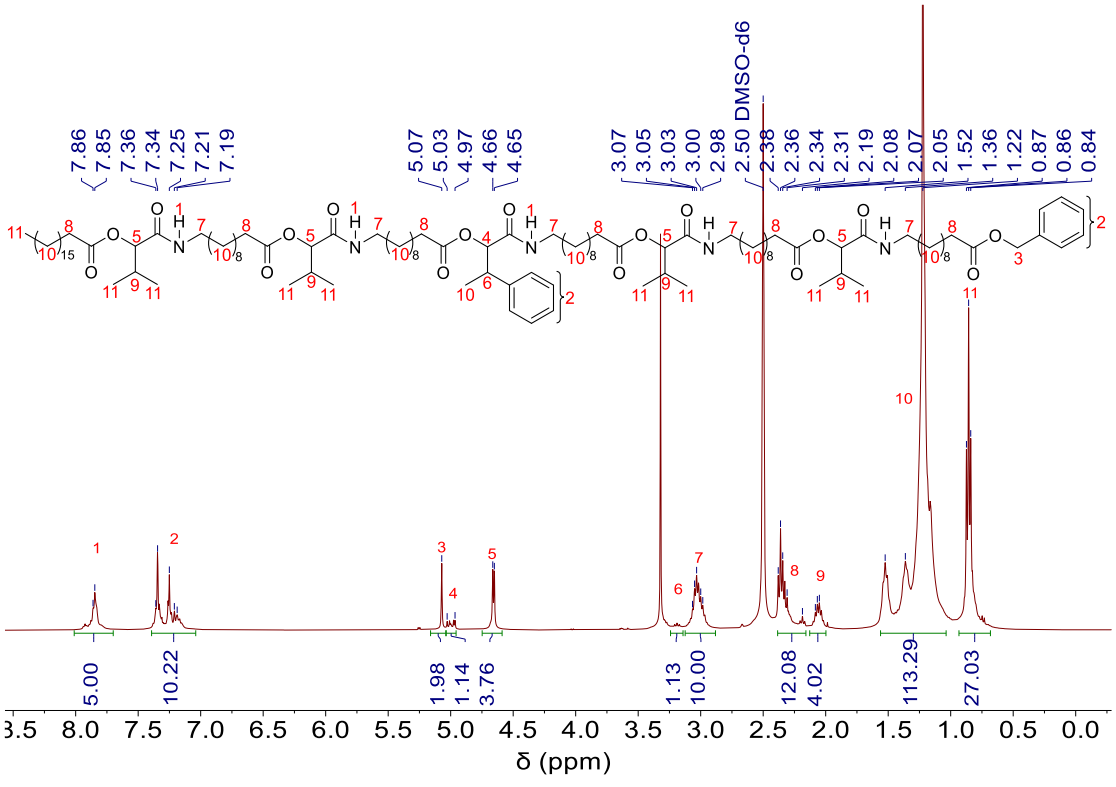

Passerini reaction (5d of P4)

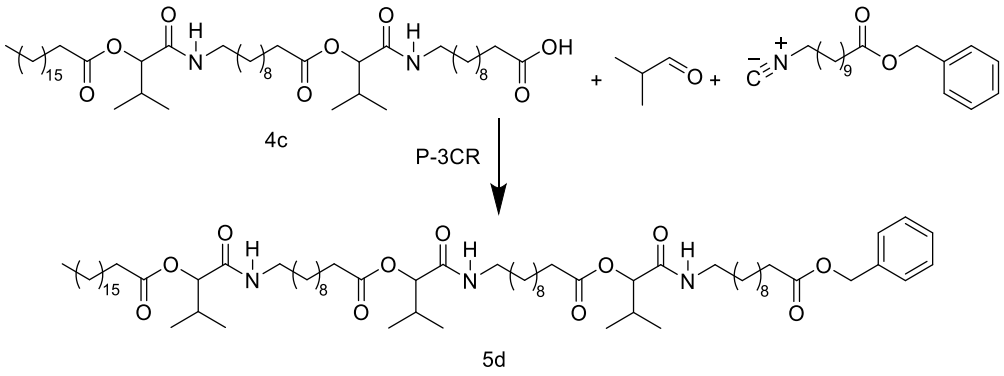

The target product 5d as a white solid in a yield of 96% (7.41g).

^{1}H NMR (400 MHz, $CDCl_3$) δ / ppm: 7.38 – 7.30 (m, 5H, aromatic, ^{1}), 5.95 (s, 3H, NH, ^{2}), 5.11 (s, 2H, CH_2, ^{3}), 5.06 – 5.04 (m, 3H, 3 CH, ^{4}), 3.32 – 3.17 (m, 6H, 3 CH_2, ^{5}), 2.42 – 2.24 (m, 11H, 4 CH_2, 3 CH, ^{6}), 1.67 – 1.25 (m, 78H, 39 CH_2, ^{7}), 0.94 – 0.86 (m, 21H, 7 CH_3, ^{8}).

^{13}C NMR (101 MHz, $CDCl_3$) δ / ppm: 173.80, 172.70, 172.67, 169.41, 169.39, 169.37, 136.27, 128.67, 128.28, 78.06, 78.03, 66.19, 39.29, 39.27, 34.45, 34.42, 32.05, 30.65, 29.83, 29.81, 29.78, 29.73, 29.60, 29.56, 29.47, 29.40, 29.33, 29.30, 29.26, 29.23, 26.97, 25.18, 25.14, 25.07, 22.82, 18.91, 17.09, 17.07, 14.25.

IR (ATR platinum diamond): ν / cm^{-1} = 3315.7, 3091.5, 2922.9, 2852.9, 1740.1, 1651.7, 1534.5, 1464.5, 1369.9, 1234.1, 1160.1, 1112.8, 1005.8, 927.7, 722.0, 697.3, 641.7, 493.7, 411.4.

ESI-MS *m/z*: $[M+H]^+$ calculated for $C_{73}H_{129}N_3O_{11}$ = 1224.9700, found: 1224.9699.

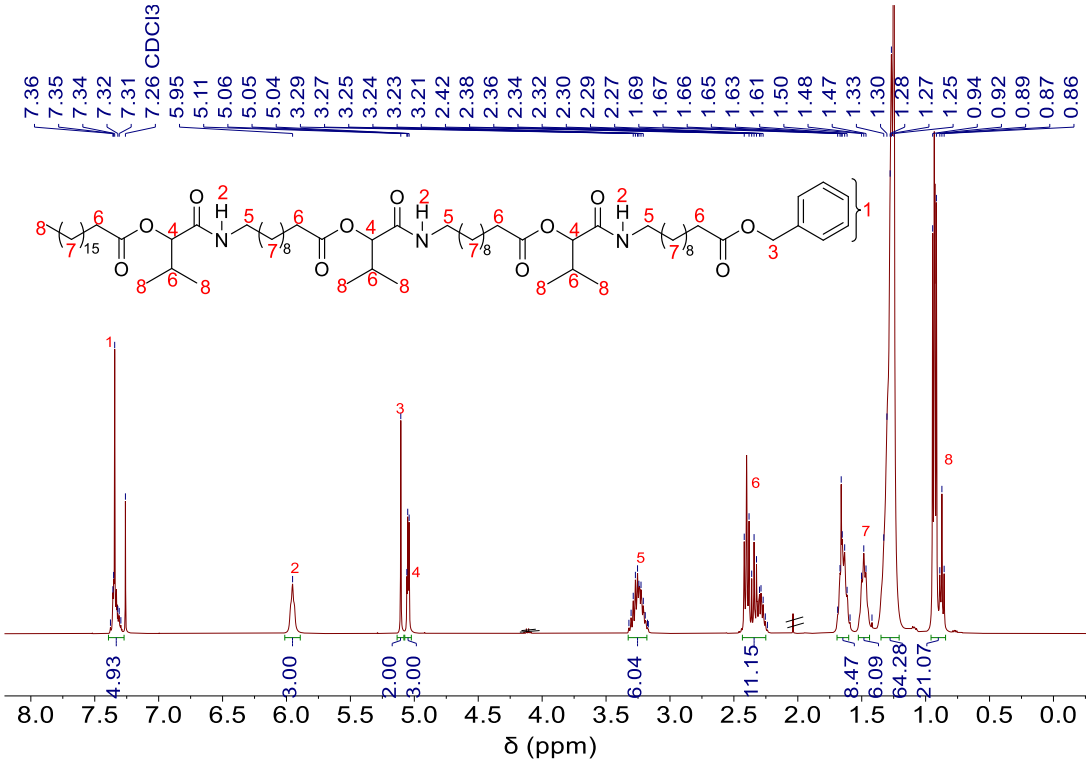

Deprotection (6d of P4)

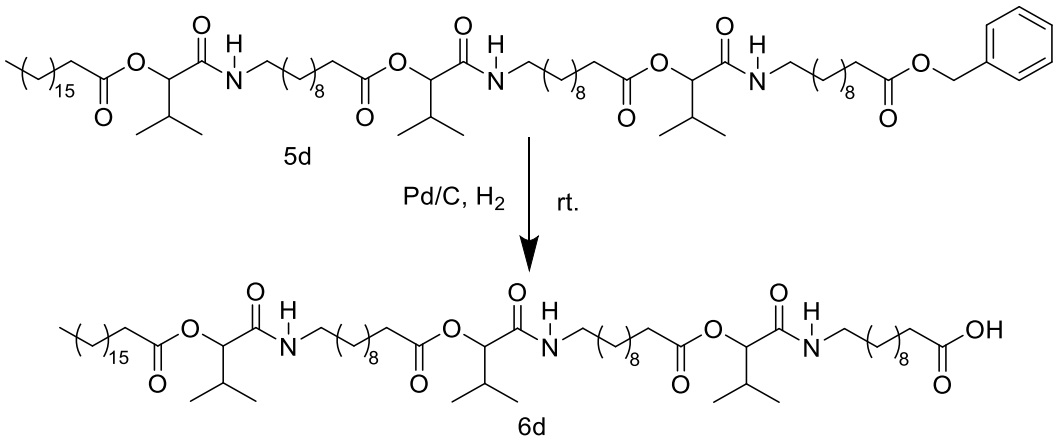

The target product 6d was obtained in quantitative yield as a white solid. (5.22g)

^{1}H NMR (400 MHz, $CDCl_3$) δ / ppm: 6.08 – 5.96 (m, 3H, NH, ^{1}), 5.06 - 5.04 (m, 3H, 3 CH, ^{2}), 3.32 – 3.18 (m, 6H, 2 CH_2, ^{3}), 2.42 – 2.24 (m, 11H, 3 CH, 4 CH_2, ^{4}), 1.68 – 1.25 (m, 80H, 40 CH_2, ^{5}), 0.95 – 0.86 (m, 21H, 7 CH_3, ^{6}).
^{13}C NMR (101 MHz, $CDCl_3$) δ / ppm: 172.80, 172.73, 169.58, 169.50, 78.09, 78.04, 39.35, 39.31, 39.26, 34.46, 34.43, 34.34, 32.06, 30.64, 29.83, 29.79, 29.74, 29.59, 29.50, 29.41, 29.33, 29.28, 29.22, 29.13, 26.97, 26.89, 25.18, 25.13, 25.01, 22.83, 18.91, 17.11, 17.08, 14.26.
IR (ATR platinum diamond): ν / cm^{-1} = 3303.4, 3089.5, 2922.9, 2852.9, 1740.1, 1651.7, 1536.5, 1462.5, 1369.9, 1234.1, 1162.2, 1110.7, 1009.9, 931.7, 721.9, 645.9, 413.4.
ESI-MS *m/z*: $[M+H]^+$ calculated for $C_{66}H_{123}N_3O_{11}$ = 1134.9230, found: 1134.9225.

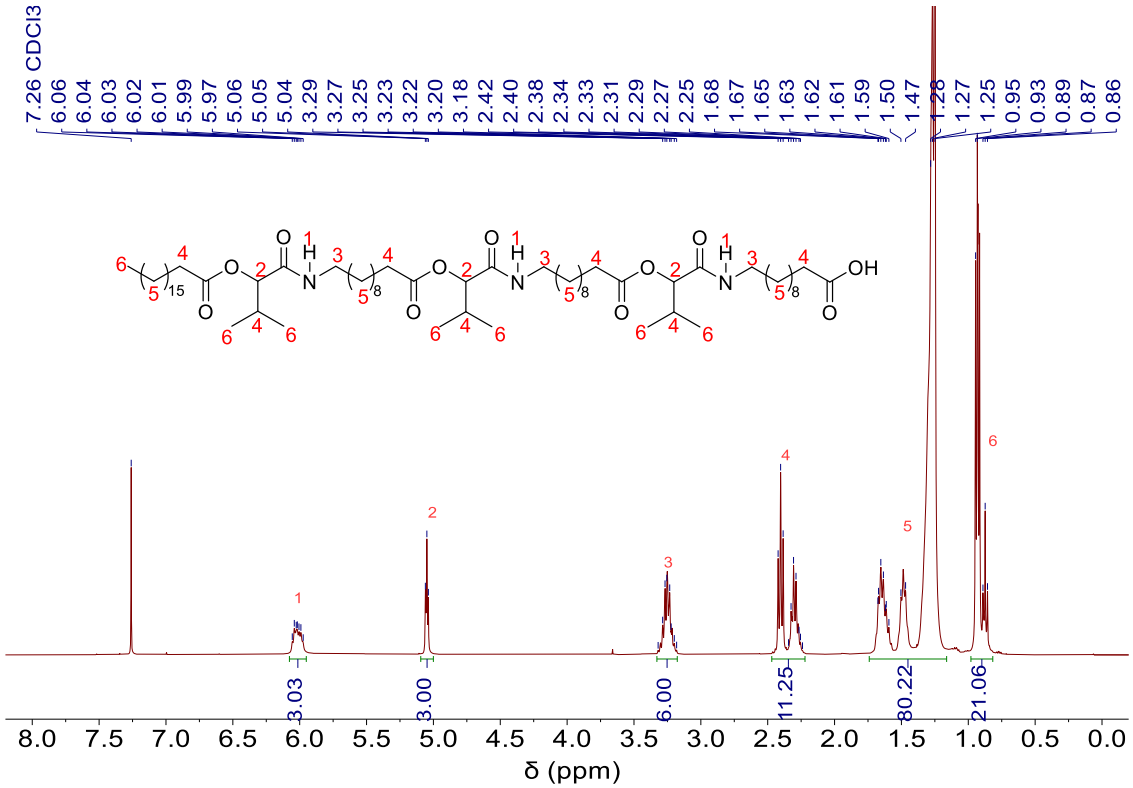

Passerini reaction (7d of P4)

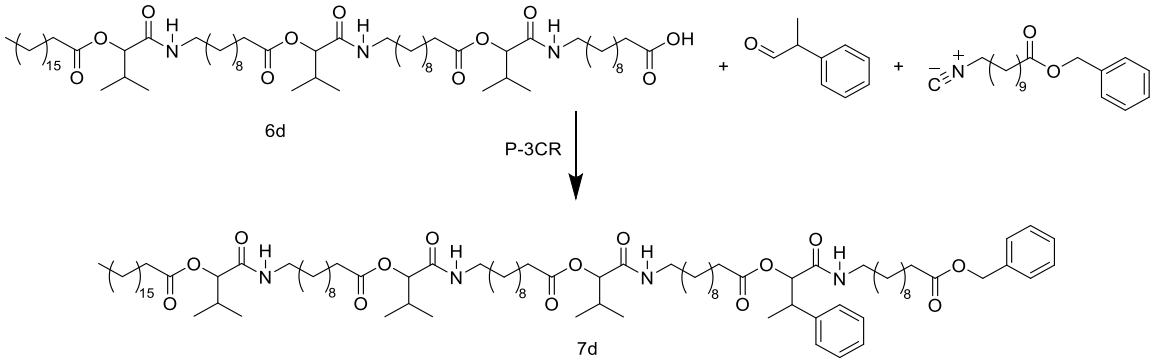

The target product 7d as a white solid in a yield of 94% (6.65g).

^{1}H NMR (400 MHz, DMSO-d_6) δ / ppm: 7.93 – 7.83 (m, 4H, 4 NH, [1]), 7.36 – 7.17 (m, 10H, aromatic, [2]), 5.07 (s, 2H, 1 CH_2, [3]), 5.03 – 4.96 (2d, J^a = 7.7 Hz, J^b = 4.7 Hz, 1H, 1 CH, [4]), 4.66 (d, J = 5.1 Hz, 3H, 3 CH, [5]), 3.21 – 3.17 (m, 1H, 1 CH, [6]), 3.05 – 2.98 (m, 8H, 4 CH_2, [7]), 2.38 – 2.17 (m, 10H, 5 CH_2, [8]), 2.10 – 2.02 (m, 3H, 3 CH, [9]), 1.52 – 1.16 (m, 97H, 47 CH_2, 1 CH_3, [10]), 0.87 – 0,84 (m, 21H, 7 CH_3, [11]).

^{13}C NMR (101 MHz, DMSO-d_6) δ / ppm: 172.91, 172.63, 172.34, 172.26, 168.57, 168.17, 167.99, 142.42, 136.49, 128.57, 128.25, 128.18, 128.13, 128.07, 127.92, 127.83, 126.60, 77.61, 65.44, 55.93, 55.09, 40.76, 38.46, 38.38, 33.66, 33.60, 31.49, 30.07, 29.21, 29.14, 29.02, 28.88, 28.63, 28.53, 28.43, 26.44, 24.66, 24.60, 24.48, 22.29, 20.94, 18.78, 18.10, 17.31, 14.94, 14.27, 14.11

IR (ATR platinum diamond): ν / cm^{-1} = 3305.5, 3089.5, 2922.9, 2852.9, 1738.1, 1653.7, 1536.5, 1462.5, 1369.9, 1232.1, 1158.1, 1110.7, 1003.8, 927.7, 724.1, 699.3, 645.9, 538.9, 411.4.

ESI-MS m/z: $[M+H]^+$ calculated for $C_{94}H_{160}N_4O_{14}$ = 1570.2004, found: 1570.2014.

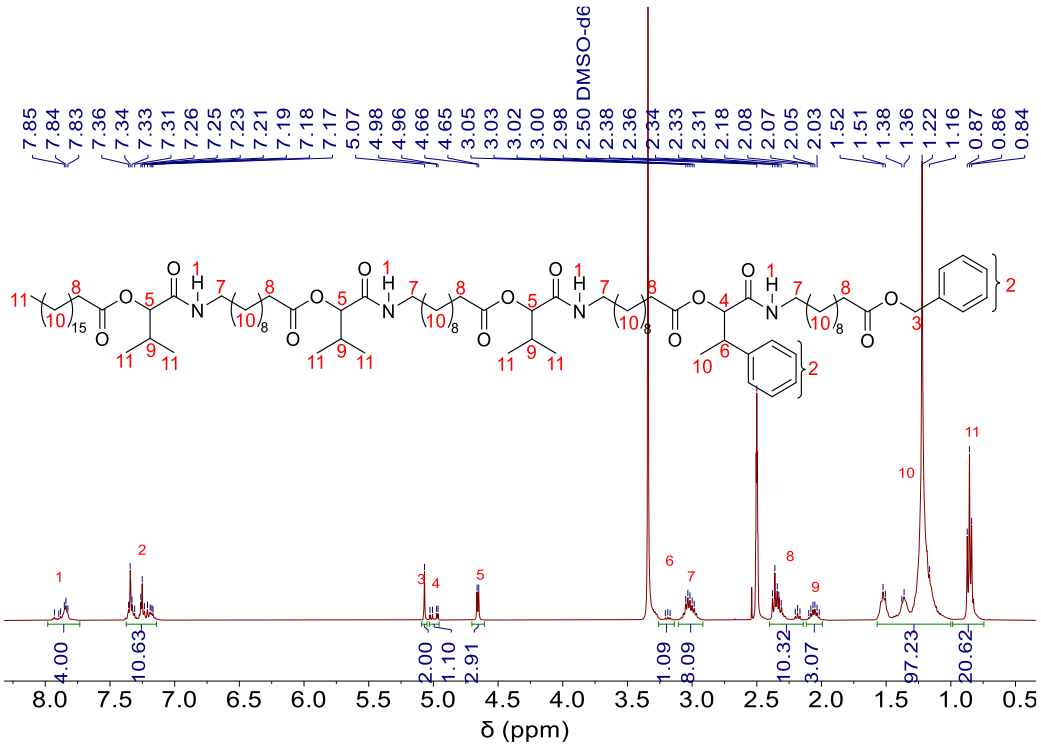

Deprotection (8d of P4)

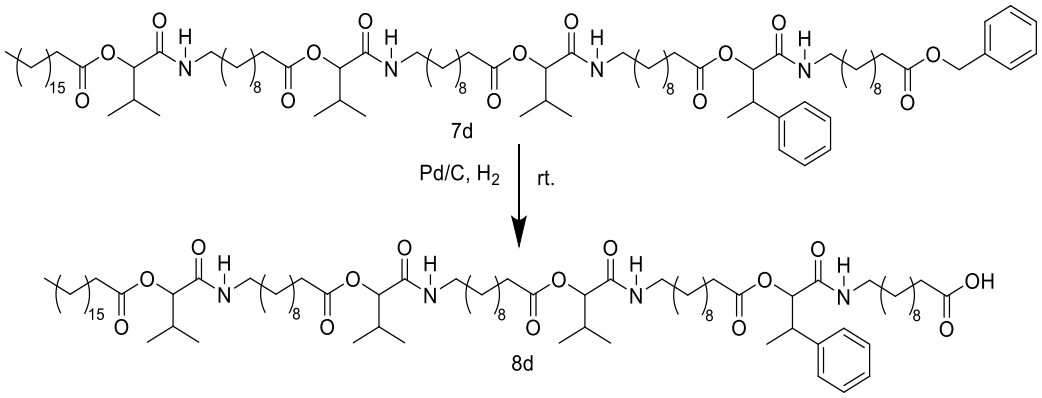

The target product 8d was obtained as a yellow oil in a quantitative yield (4.48g).

^{1}H NMR (400 MHz, DMSO-d_6) δ / ppm: 7.93 – 7.84 (m, 4H, 4 NH, ^{1}), 7.26 – 7.15 (m, 5H, aromatic, ^{2}), 5.03 – 4.96 (2d, J^a = 7.7 Hz, J^b = 4.7 Hz, 1H, 1 CH, ^{3}), 4.66 (d, J = 5.0 Hz, 3H, 3 CH, ^{4}), 3.21 – 3.17 (m, 1H, 1 CH, ^{5}), 3.08 – 2.97 (m, 8H, 4 CH_2, ^{6}), 2.38 – 2.15 (m, 10H, 5 CH_2, ^{7}), 2.08 – 2.02 (m, 3H, 3 CH, ^{8}), 1.53 – 1.17 (m, 97H, 47 CH_2, 1 CH_3, ^{9}), 0.87 – 0.84 (m, 21H, 7 CH_3, ^{10}).

^{13}C NMR (101 MHz, DMSO-d_6) δ / ppm: 174.44, 172.42, 172.14, 172.06, 168.38, 167.98, 167.80, 142.33, 142.21, 128.05, 127.98, 127.72, 127.74, 126.48, 126.40, 77.38, 77.06, 76.81, 40.93, 40.57, 38.27, 38.19, 33.66, 33.41, 31.30, 29.87, 29.03, 28.95, 28.88, 28.83, 28.71, 28.58, 28.44, 28.39, 28.25, 26.25, 24.29, 22.09, 18.57, 17.90, 17.10, 14.74, 13.90.

IR (ATR platinum diamond): ν / cm^{-1} = 3305.5, 3093.6, 2922.9, 2852.9, 1740.1, 1651.7, 1536.5, 1464.5, 1369.9, 1232.1, 1162.2, 1110.7, 1009.9, 923.6, 763.1, 721.9, 699.3, 649.9, 536.8, 411.4.

ESI-MS m/z: $[M+H]^+$ calculated for $C_{87}H_{154}N_4O_{14}$ = 1480.1534, found: 1480.1529.

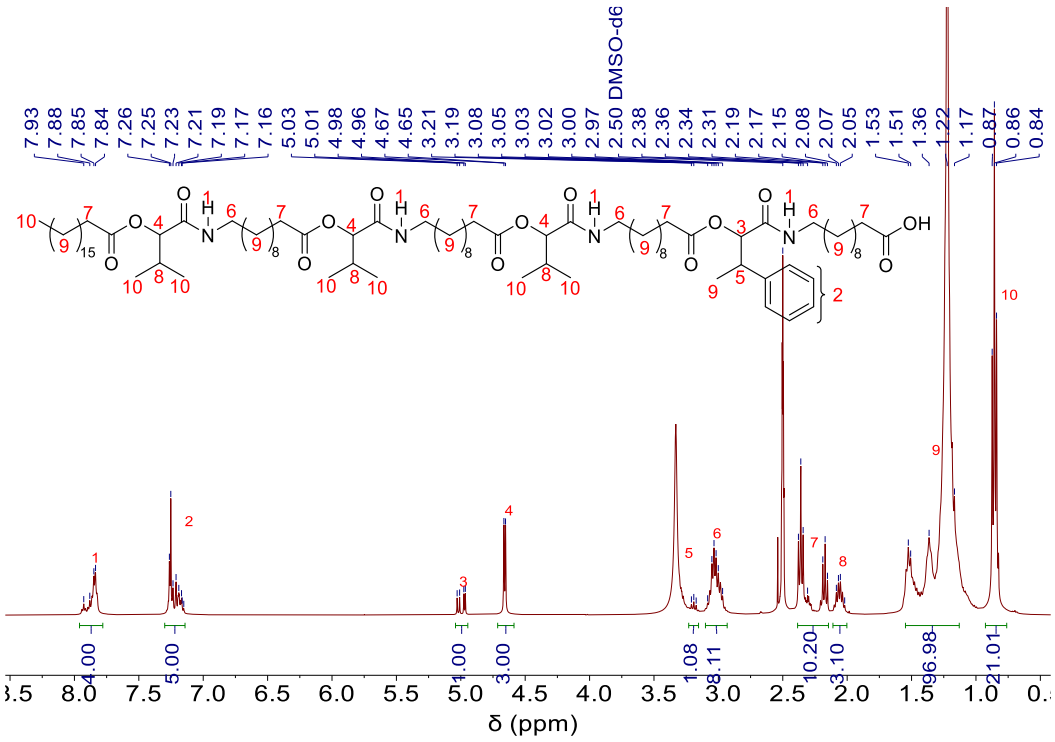

Passerini reaction to synthesize P4

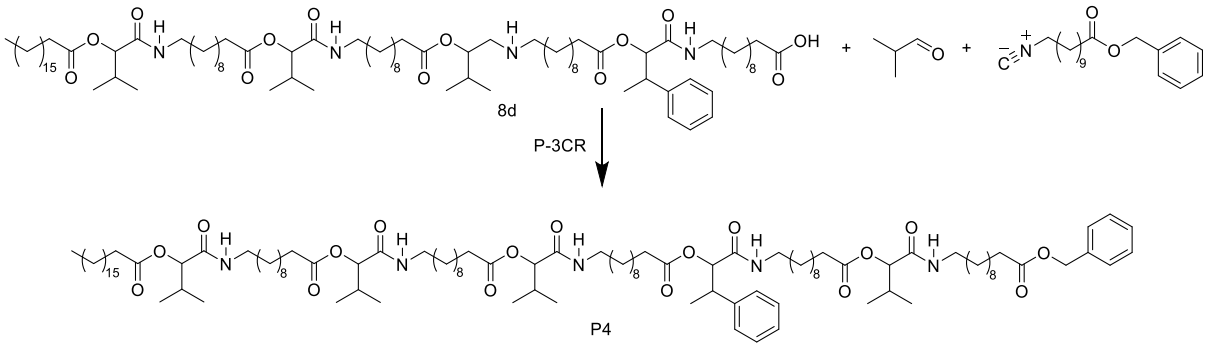

P4 was obtained as a yellow oil in a yield of 90% (4.35g).

^{1}H NMR (400 MHz, DMSO-d_6) δ / ppm: 7.94 – 7.84 (m, 5H, NH, ^{1}), 7.36 – 7.17 (m, 10H, aromatic, ^{2}), 5.07 (s, 2H, CH_2, ^{3}), 5.03 – 4.96 (2d, J^a = 7.7 Hz, J^b = 4.7 Hz, 1H, 1 CH, ^{4}), 4.66 – 4.65 (d, J = 5.1 Hz, 4H, 4 CH, ^{5}), 3.21 – 3.17 (d, J = 7.3 Hz, 1H, 1 CH, ^{6}), 3.07 – 2.98 (m, 10H, 4 CH_2, ^{7}), 2.38 – 2.17 (m, 12H, 6 CH_2, ^{8}), 2.08 – 2.03 (m, 4H, 4 CH, ^{9}), 1.52 – 1.16 (m, 113H, 55 CH_2, 1 CH_3, ^{10}), 0.87 – 0.84 (m, 27H, 9 CH_3, ^{11}).
^{13}C NMR (101 MHz, DMSO-d_6) δ / ppm: 172.73, 172.45, 168.38, 136.29, 128.38, 128.05, 127.89, 127.64, 77.40, 65.25, 38.19, 33.46, 33.41, 31.29, 29.87, 29.01, 28.93, 28.86, 28.81, 28.70, 28.43, 26.24, 24.26, 24.40, 24.48, 22.09, 18.58, 17.10, 14.76, 13.92.
IR (ATR platinum diamond): ν / cm^{-1} = 3305.5, 3089.5, 2922.9, 2852.9, 1738.1, 1651.7, 1534.5, 1462.5, 1369.9, 1232.1, 1160.1, 1110.7, 1005.8, 921.5, 763.1, 721.9, 699.3, 645.9, 536.8, 411.4.
ESI-MS m/z: $[M+H]^+$ calculated for $C_{110}H_{189}N_5O_{17}$ = 1853.4151, found: 1853.4178.

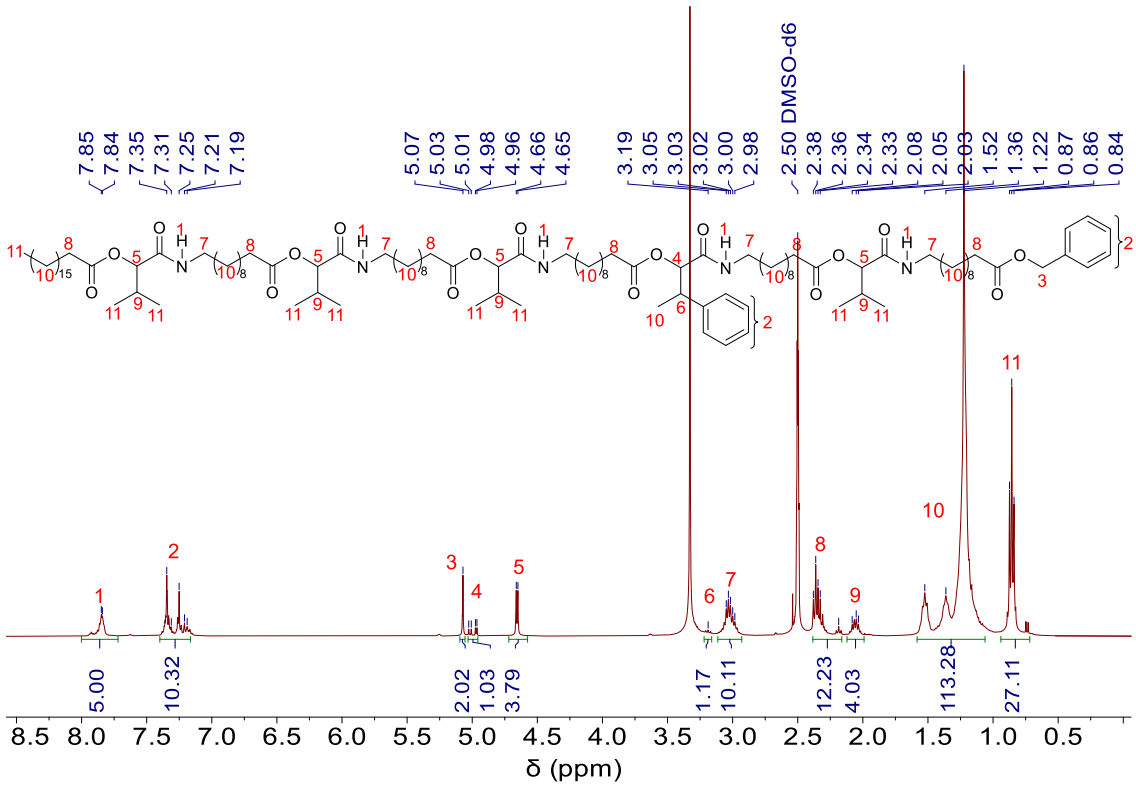

Passerini reaction (7e of P5)

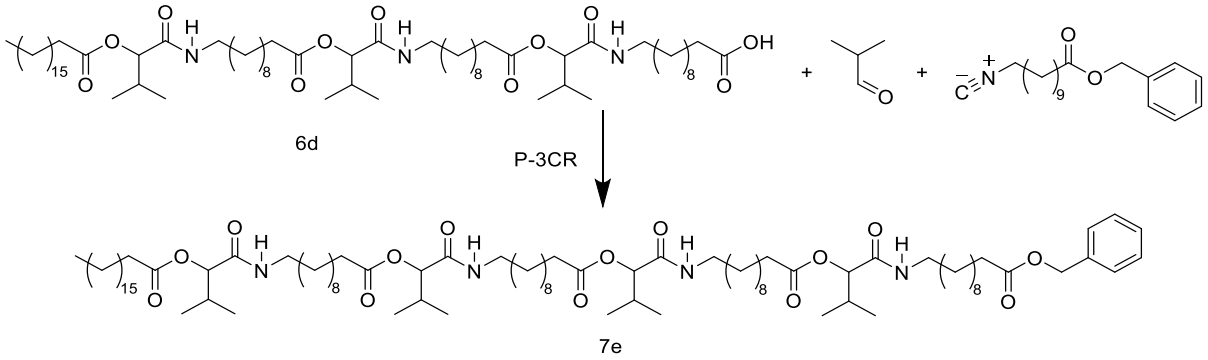

The target product 7e as a white solid in a yield of 85% (5.28g).

^{1}H NMR (400 MHz, $CDCl_3$) δ / ppm: 7.36 – 7.31 (m, 5H, aromatic, ^{1}), 5.97 – 5.94 (t, J = 5.7 Hz, 4 H, NH, ^{2}), 5.11 (s, 2 H, CH_2, ^{3}), 5.06 – 5.04 (m, 4H, 4 CH, ^{4}), 3.32 – 3.20 (m, 8H, 4 CH_2, ^{5}), 2.42 – 2.26 (m, 14H, 5 CH_2, 4 CH, ^{6}), 1.69 – 1.25 (m, 94H, 47 CH_2, ^{7}), 0.95 – 0.86 (m, 27H, 9 CH_3, ^{8}).

^{13}C NMR (101 MHz, $CDCl_3$) δ / ppm: 173.82, 172.70, 169.41, 169.39, 128.68, 128.29, 78.07, 78.04, 66.20, 39.29, 34.46, 34.43, 32.06, 30.65, 29.83, 29.79, 29.74, 29.61, 29.57, 29.48, 29.41, 29.34, 29.31, 29.27, 29.24, 26.97, 25.19, 25.14, 25.08, 22.83, 18.92, 17.11.

IR (ATR platinum diamond): ν / cm^{-1} = 3305.5, 3091.5, 2922.9, 2852.9, 1740.1, 1651.7, 1534.5, 1462.5, 1369.9, 1234.1, 1162.2, 1110.7, 1005.8, 925.6, 721.9, 697.3, 645.9, 409.3.

ESI-MS m/z: $[M+H]^+$ calculated for $C_{89}H_{158}N_4O_{14}$ = 1508.1847, found: 1508.1854.

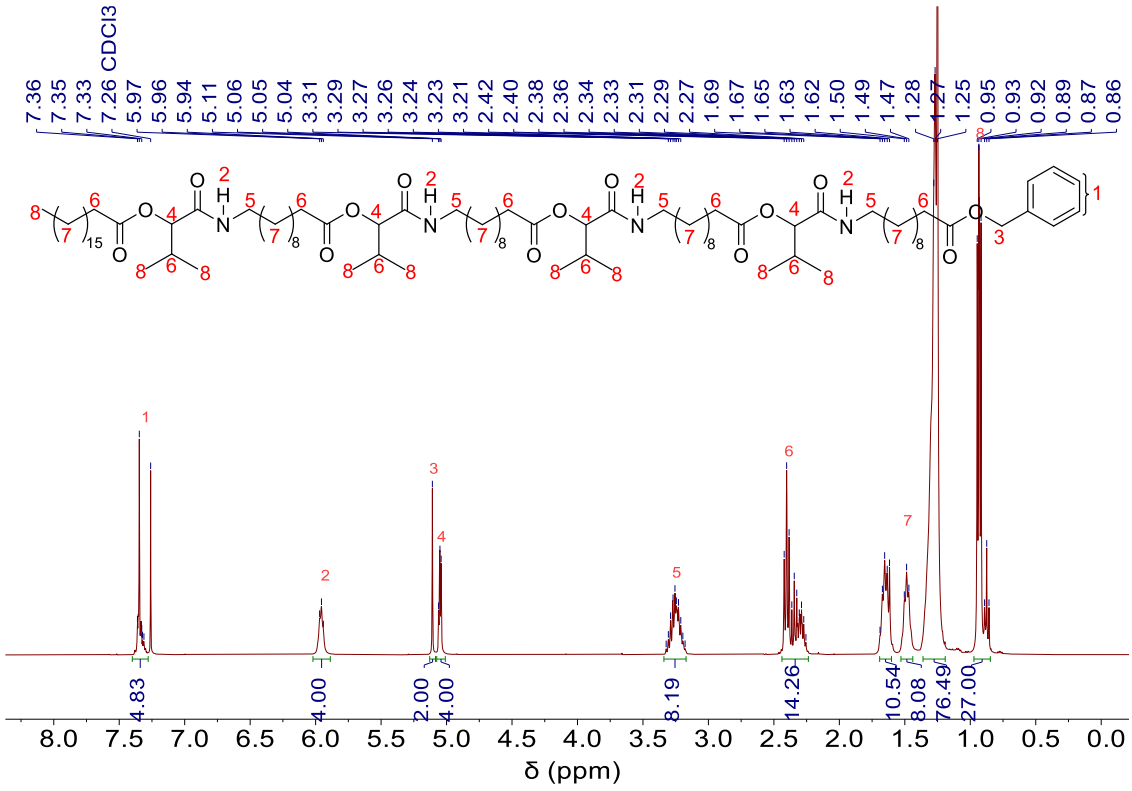

Deprotected reaction (8e of P5)

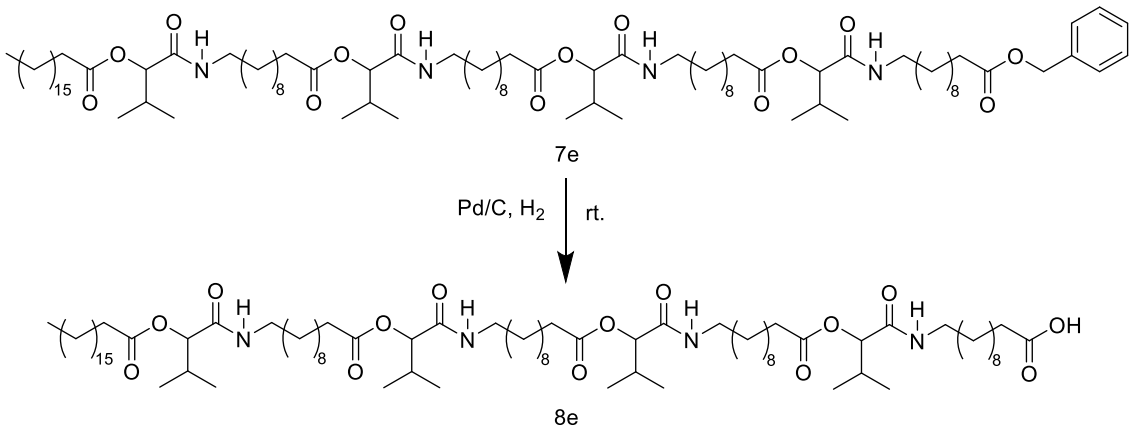

The target product 8e was obtained in quantitative yield as a yellow oil. (3.66g)

^{1}H NMR (400 MHz, $CDCl_3$) δ / ppm: 6.05 – 5.98 (m, 4H, NH, ^{1}), 5.06 - 5.04 (d, J = 3.5 Hz, 4H, 4 CH, ^{2}), 3.32 – 3.18 (m, 8H, 4 CH_2, ^{3}), 2.42 – 2.15 (m, 14H, 4 CH, 5 CH_2, ^{4}), 1.67 – 1.25 (m, 94H, 47 CH_2, ^{5}), 0.94 – 0.85 (m, 27H, 9 CH_3, ^{6}).
^{13}C NMR (101 MHz, $CDCl_3$) δ / ppm: 172.79, 172.72, 169.58, 169.49, 78.07, 78.02, 39.33, 39.30, 39.26, 34.44, 34.41, 33.99, 32.05, 30.63, 29.77, 29.56, 29.33, 29.25, 29.09, 26.89, 25.17, 24.89, 22.81, 18.90, 17.11, 14.24.
IR (ATR platinum diamond): ν / cm^{-1} = 3305.5, 3091.5, 2922.9, 2852.9, 1740.1, 1651.7, 1536.5, 1464.5, 1369.9, 1234.1, 1160.1, 1110.7, 1007.9, 925.6, 721.9, 645.9, 413.4.
ESI-MS m/z: $[M+H]^+$ calculated for $C_{82}H_{152}N_4O_{14}$ = 1418.1378, found: 1418.1382.

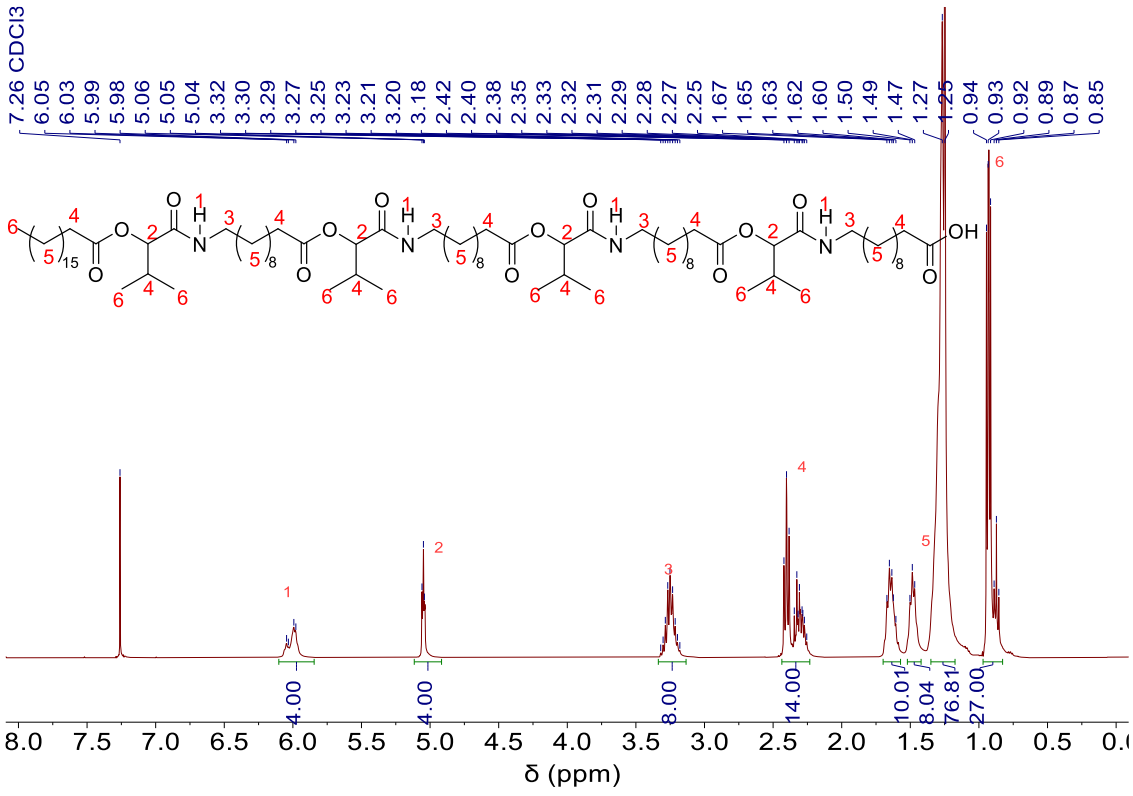

Passerini reaction to synthesize P5

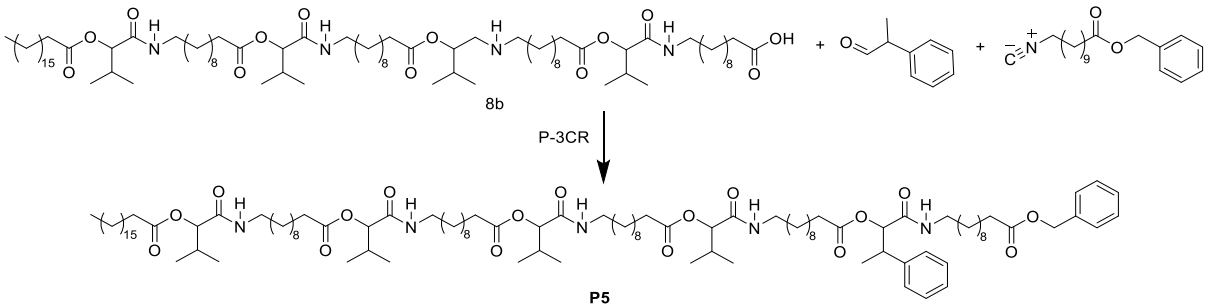

P5 was obtained as a yellow oil in a yield of 92% (3.40g).

^{1}H NMR (400 MHz, DMSO-d_6) δ / ppm: 7.94 – 7.83 (m, 5H, NH, ^{1}), 7.35 – 7.17 (m, 10H, aromatic, ^{2}), 5.07 (s, 2H, CH_2, ^{3}), 5.03 – 4.96 (2d, J^a = 7.6 Hz, J^b = 4.5Hz, 1H, 1CH, ^{4}), 4.66 – 4.65 (d, J = 5.1 Hz, 4H, 4 CH, ^{5}), 3.21 – 3.18 (d, J = 7.3 Hz, 1H, 1 CH, ^{6}), 3.07 – 2.98 (m, 10H, 4 CH_2, ^{7}), 2.38 – 2.17 (m, 12H, 6 CH_2, ^{8}), 2.08 – 2.04 (m, 4H, 4 CH, ^{9}), 1.54 – 1.22 (m, 113H, 55 CH_2, 1 CH_3, ^{10}), 0.87 – 0.84 (m, 27H, 9 CH_3, ^{11}).
^{13}C NMR (101 MHz, DMSO-d_6) δ / ppm: 172.71, 172.43, 170.31, 168.37, 142.34, 136.29, 128.37, 128.05, 127.93, 127.88, 127.71, 127.63, 77.38, 33.40, 31.29, 29.86, 29.01, 28.93, 28.87, 28.82, 28.70, 28.67, 28.43, 28.38, 26.24, 24.39, 22.08, 20.74, 18.57, 17.11, 14.07, 13.91.
IR (ATR platinum diamond): ν / cm^{-1} = 3303.4, 3095.6, 2922.9, 2852.9, 1738.1, 1651.7, 1534.5, 1462.5, 1369.9, 1232.1, 1160.1, 1110.7, 1003.8, 925.6, 734.3, 699.3, 411.4.
ESI-MS m/z: $[M+H]^+$ calculated for $C_{110}H_{189}N_5O_{17}$ = 1853.4151, found: 1853.4163.

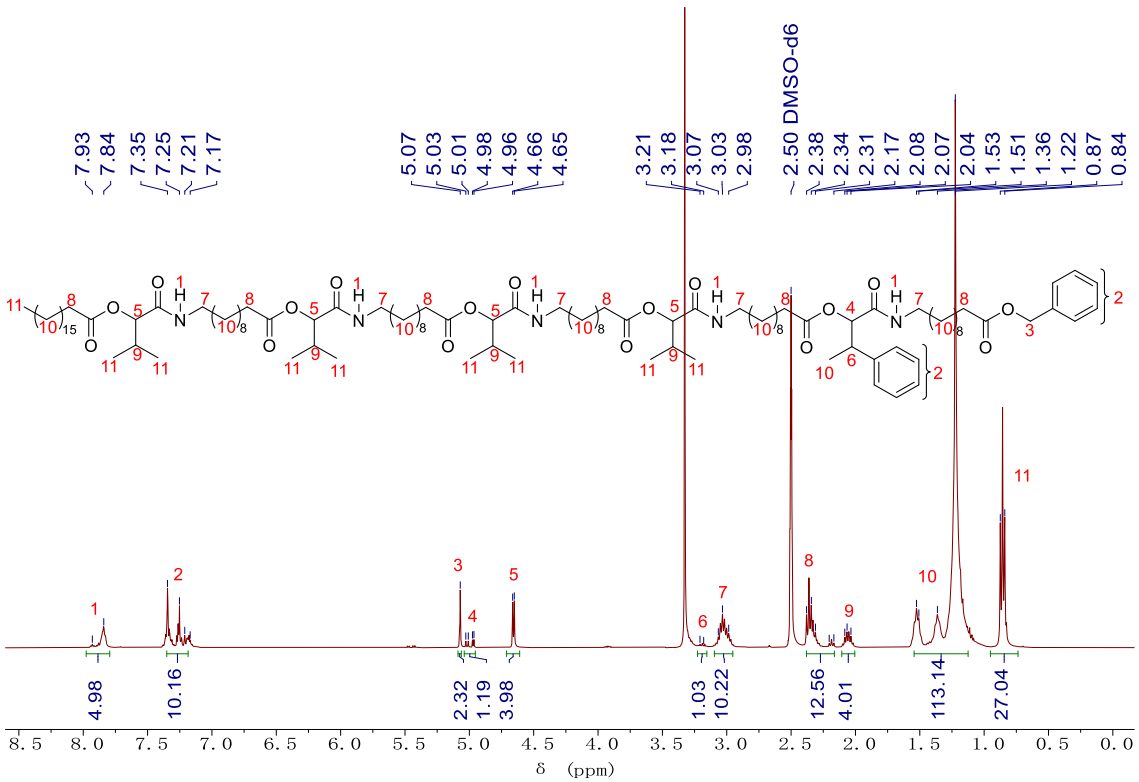

Passerini reaction to synthesize P0

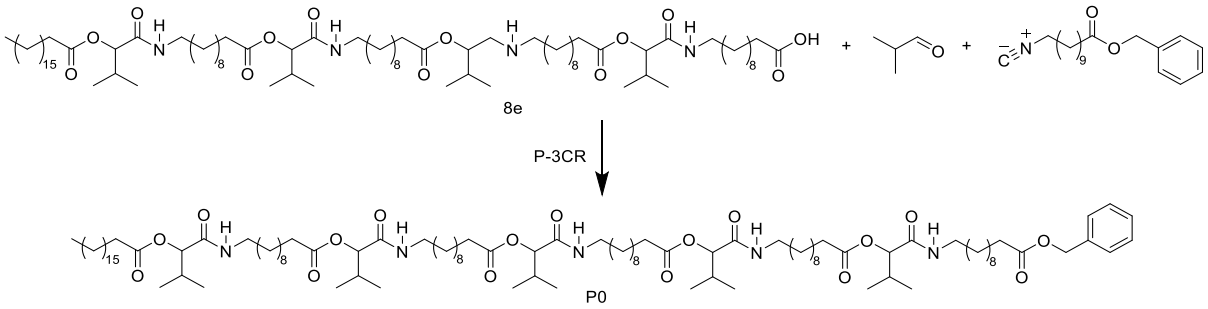

P0 was obtained as a yellow oil in a yield of 87% (1.02g).

^{1}H NMR (400 MHz, DMSO-d_6) δ / ppm: 7.85 (s, 5H, 5 NH, ^{1}), 7.35 (s, 5H, aromatic, ^{2}), 5.08 (s, 2H, 1 CH_2, ^{3}), 4.66 (d, J = 5.1 Hz, 5H, 5 CH, ^{4}), 3.09 – 2.97 (m, 10H, 5 CH_2, ^{5}), 2.36 (m, J = 6.7, 6.1 Hz, 12H, 6 CH_2, ^{6}), 2.10 – 2.02 (m, 5H, 5 CH, ^{7}), 1.54 – 1.18 (m, 115H, 56 CH_2, 1 CH_3, ^{8}), 0.86 (t, J = 7.0 Hz, 33H, 11 CH_3, ^{9}).

^{13}C NMR (101 MHz, DMSO-d_6) δ / ppm: 172.73, 172.45, 168.38, 128.39, 127.95, 77.40, 33.40, 31.29, 29.87, 29.01, 28.93, 28.82, 28.70, 28.67, 28.43, 26.24, 24.40, 22.09, 18.59, 17.71, 13.93.

IR (ATR platinum diamond): ν / cm^{-1} = 3303.4, 2922.9, 2852.9, 1738.1, 1653.7, 1534.5, 1462.5, 1369.9, 1236.2, 1162.2, 1110.7, 1005.8, 923.6, 721.9, 699.3, 644.9, 538.9, 413.4.

ESI-MS m/z: $[M+H]^+$ calculated for $C_{105}H_{187}N_5O_{17}$ = 1791.3995, found: 1791.4003

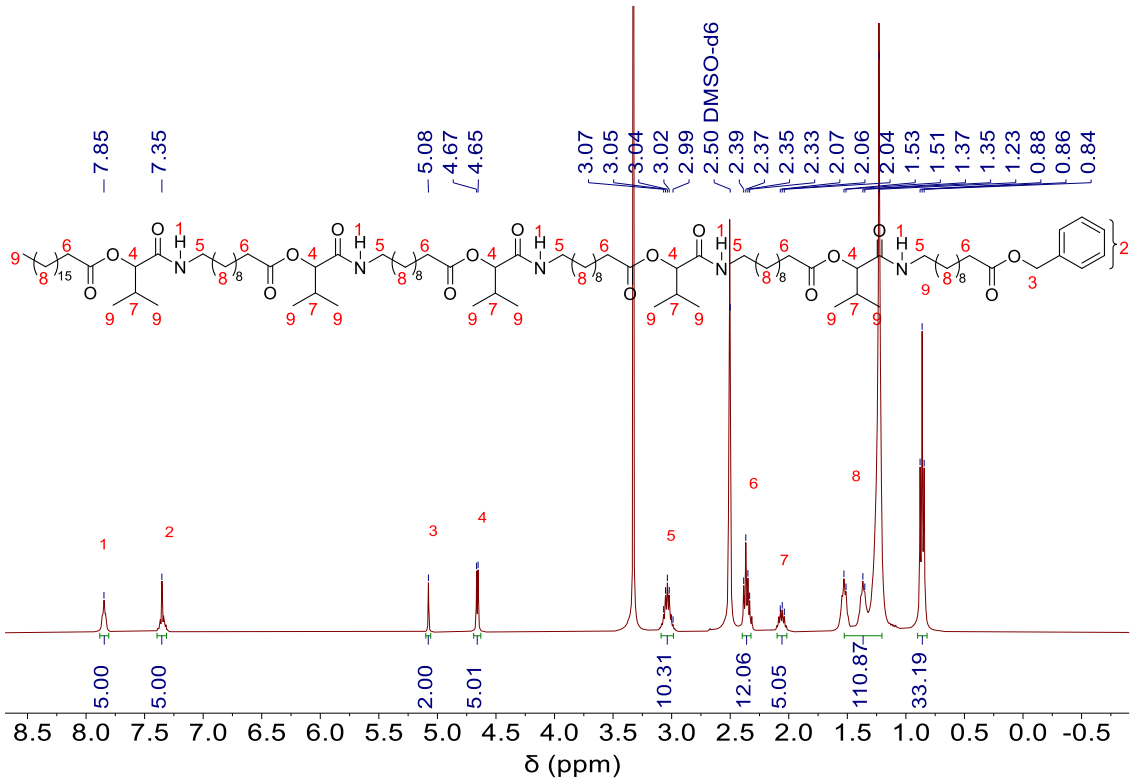

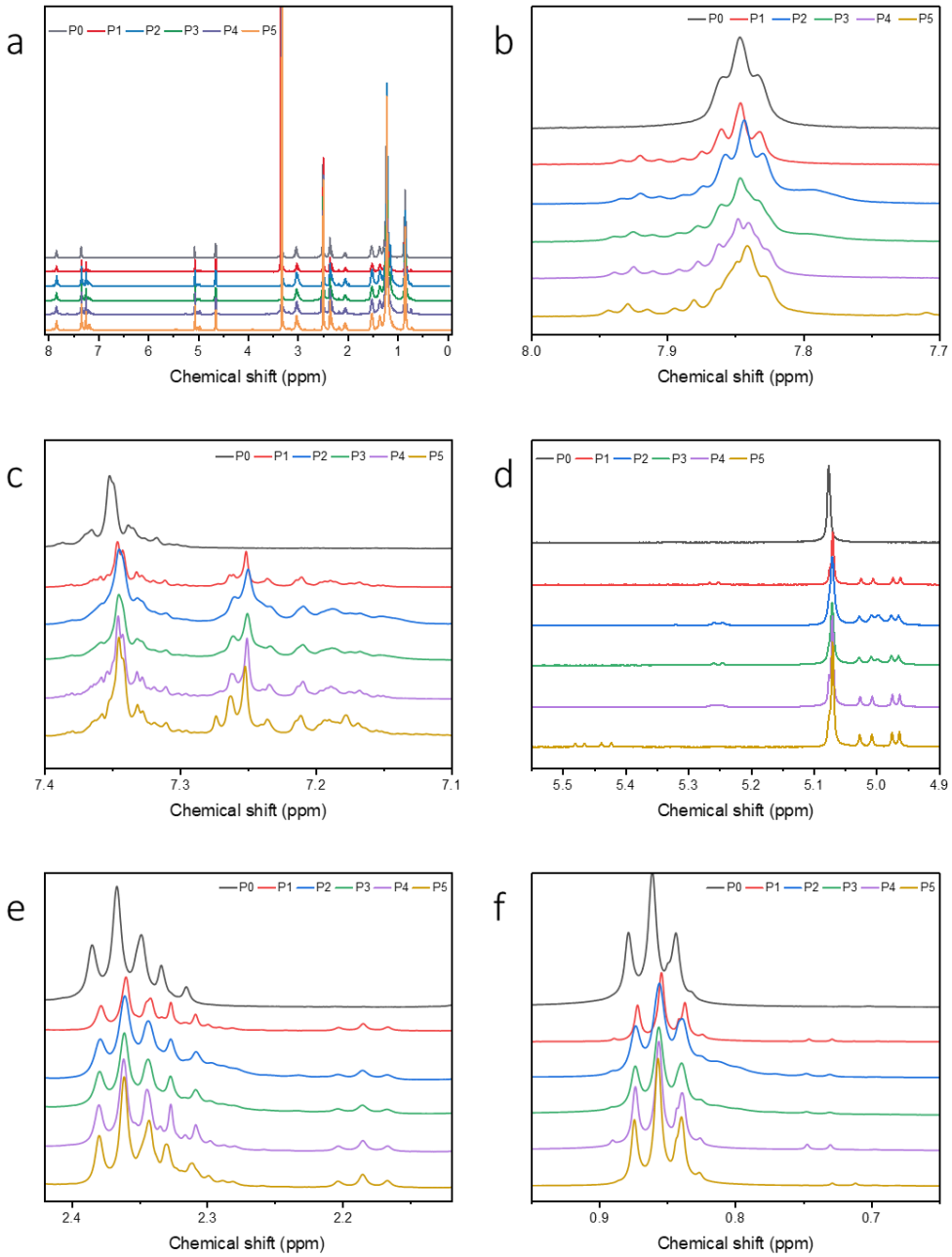

Supplementary Figure 1: a) ^{1}H - NMR spectra of pentamers P0-P5 in the whole range. b) ^{1}H - NMR signals between 8.0 - 7.7 ppm. c) ^{1}H - NMR signals between 7.4 - 7.1 ppm. d) ^{1}H - NMR signals between 5.5 - 4.9 ppm. e) ^{1}H - NMR signals between 2.42 - 2.12 ppm. f) ^{1}H - NMR signals between 1.0 - 0.6 ppm.

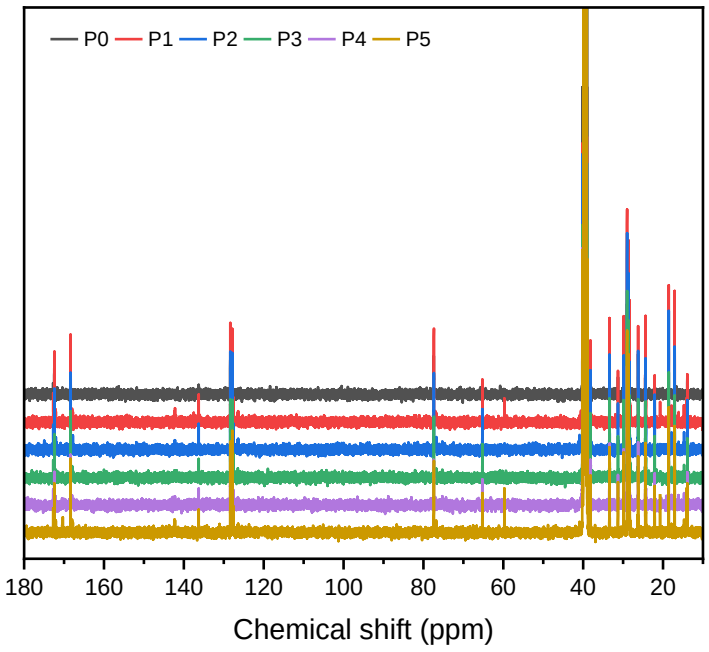

Supplementary Figure 2: ^{13}C-NMR spectra of pentamers **P0-P5**.

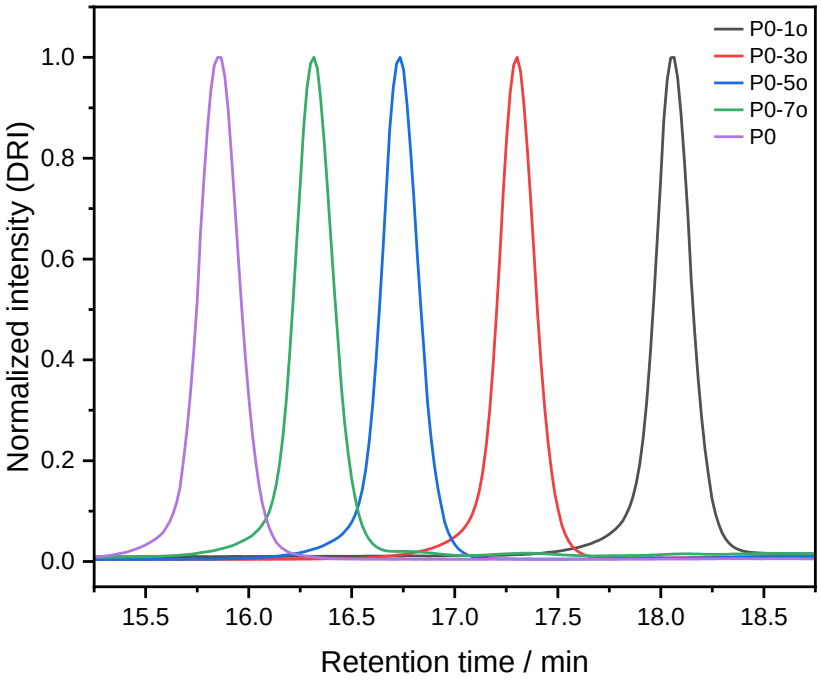

Supplementary Figure 3: Comparison of the SEC curves after each Passerini reaction step for the synthesis of pentamer **P0**.

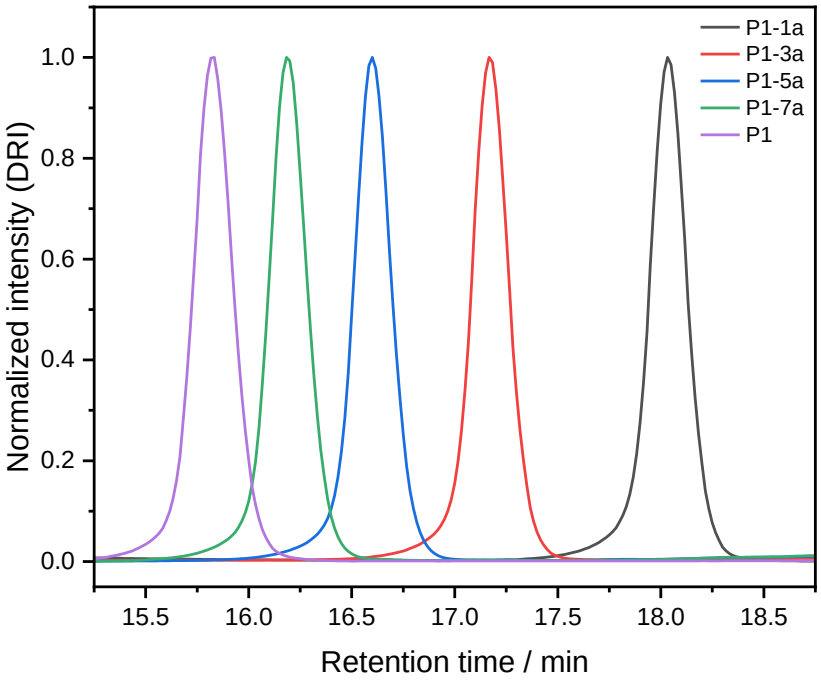

Supplementary Figure 4: Comparison of the SEC curves after each Passerini reaction step for the synthesis of pentamer **P1**.

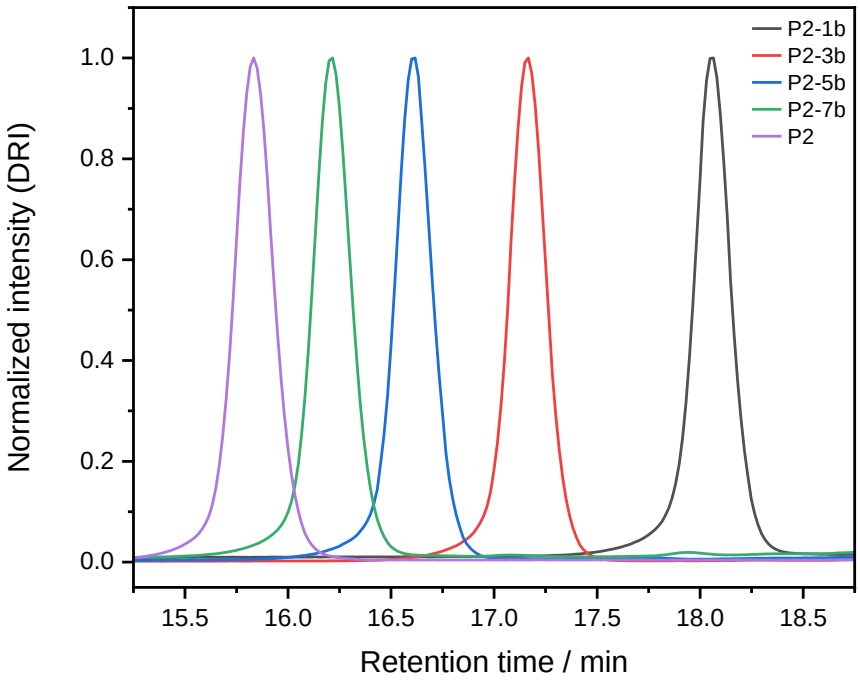

Supplementary Figure 5: Comparison of the SEC curves after each Passerini reaction step for the synthesis of pentamer **P2**.

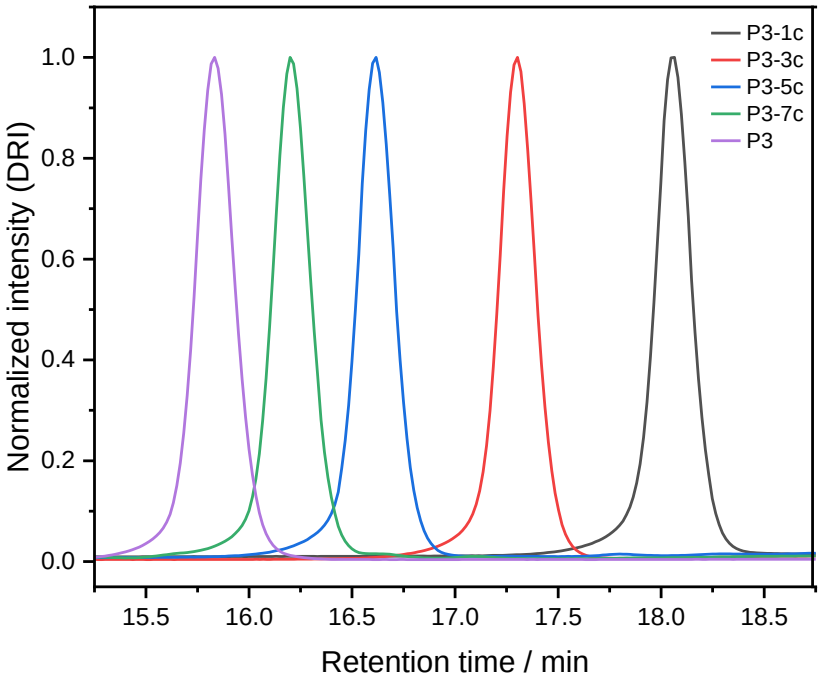

Supplementary Figure 6: Comparison of the SEC curves after each Passerini reaction step for the synthesis of pentamer **P3**.

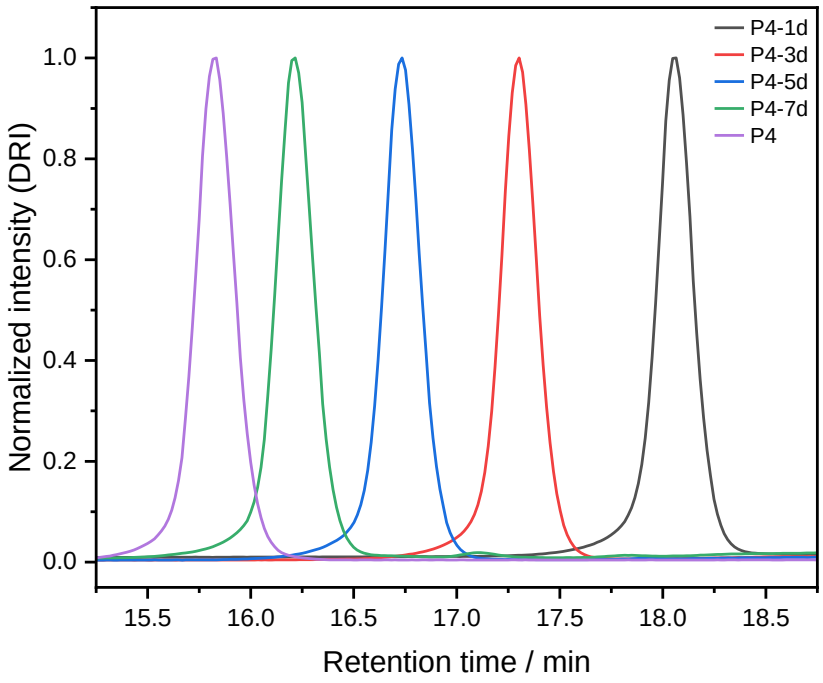

Supplementary Figure 7: Comparison of the SEC curves after each Passerini reaction step for the synthesis of pentamer **P4**.

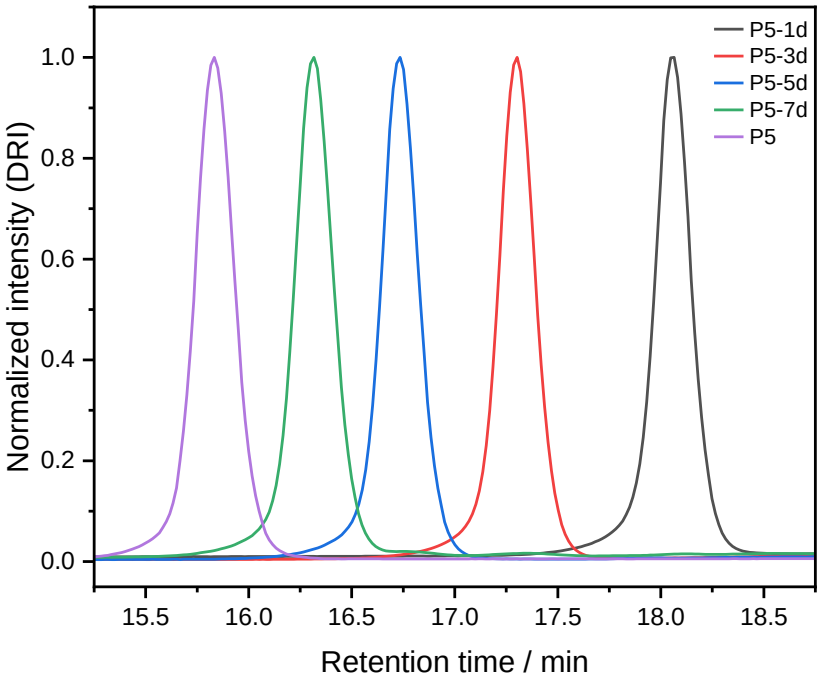

Supplementary Figure 8: Comparison of the SEC curves after each Passerini reaction step for the synthesis of pentamer **P5**.

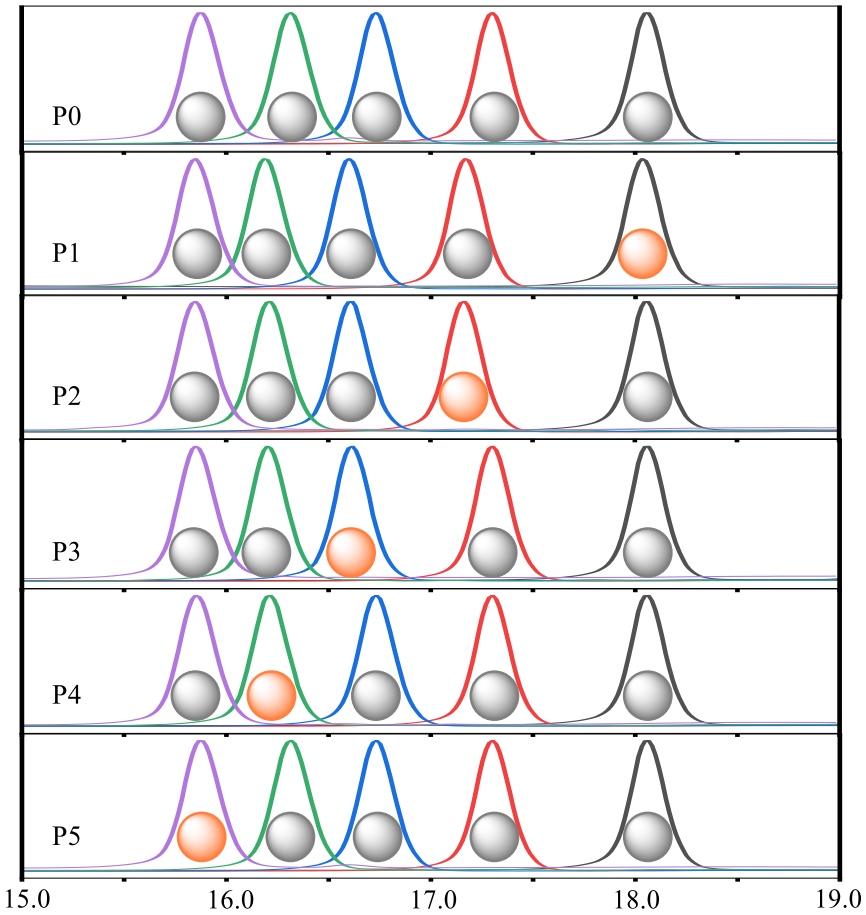

Supplementary Figure 9: SEC traces of the pentamers **P0 – P5** and the corresponding precursor oligomers. The α-methylphenyl side chain could be installed in every possible position of the pentamer, as depicted as orange spheres. The isopropyl moiety is shown in gray and the spheres represent the order of addition of the repeating units.

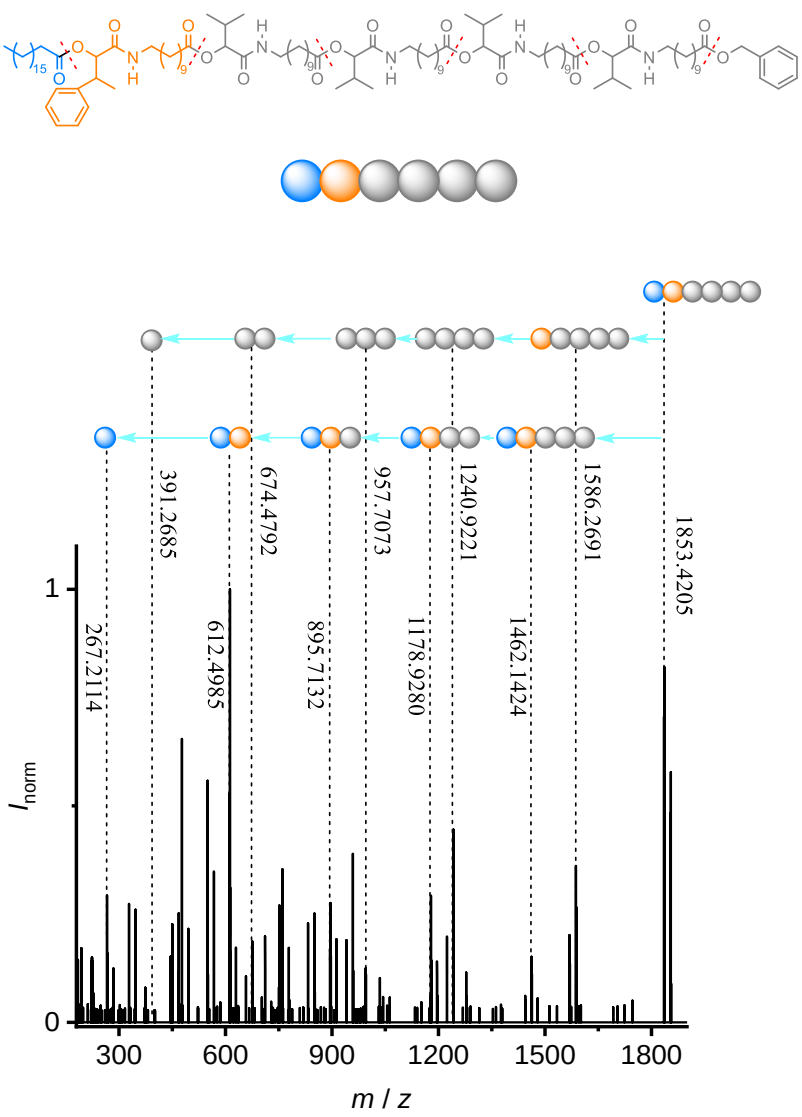

Supplementary Figure 10: ESI-MS/MS fragmentation of **P1** ion from α-cleavage of the (C=O)-O bond at m/z = 1853.4205 Da recorded in positive mode. (with an NCE of 19)

P1	α-cleavage				
	Calc. / Da	Detected / Da		Calc. / Da	Detected / Da
α	267.2282	267.2114	y_5^+	1586.2069	1586.2091
b_1^+	612.4986	612.4985	y_4^+	1240.9165	1240.9221
b_2^+	895.7134	895.7132	y_3^+	957.7017	957.7073
b_3^+	1178.9281	1178.9345	y_2^+	674.4870	674.4861
b_4^+	1462.1429	1462.1474	y_1^+	391.2723	391.2732
b_5^+	1745.3637	/	ω	108.0572	/

Supplementary Table 1: In combination with Supplementary Figure 10, the calculated masses and detected masses of fragments are summarized.

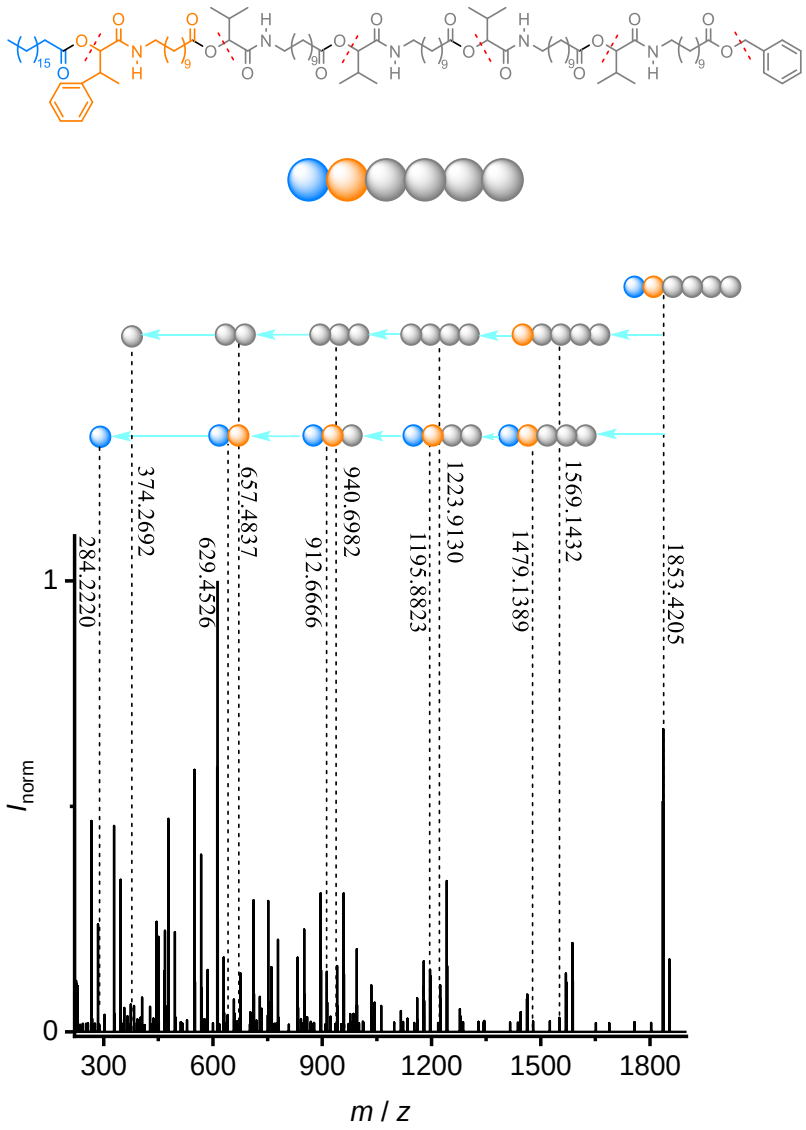

Supplementary Figure 11: ESI-MS/MS fragmentation of **P1** ion from cleavage via McLafferty rearrangement at m/z = 1853.4205 Da recorded in positive mode. (with an NCE of 20)

P1	Cleavage via McLafferty rearrangement				
	Calc. / Da	Detected / Da		Calc. / Da	Detected / Da
α	284.2715	284.2220	y_5^+	1569.1436	1569.1432
b_1^+	629.5019	629.4526	y_4^+	1223.9132	1223.9130
b_2^+	912.7167	912.6666	y_3^+	940.6985	940.6982
b_3^+	1195.9314	1195.8823	y_2^+	657.4837	657.4837
b_4^+	1479.1462	1479.1389	y_1^+	374.2690	374.2692
b_5^+	1762.3609	/	ω	91.0542	/

Supplementary Table 2: In combination with Supplementary Figure 11, the calculated masses and detected masses of fragments are summarized.

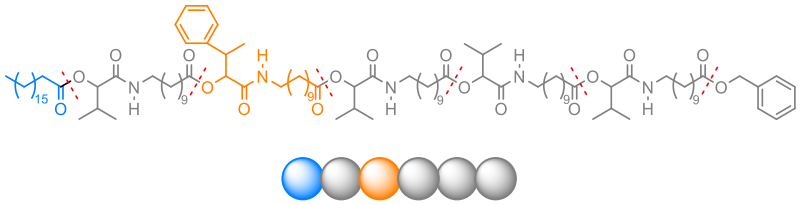

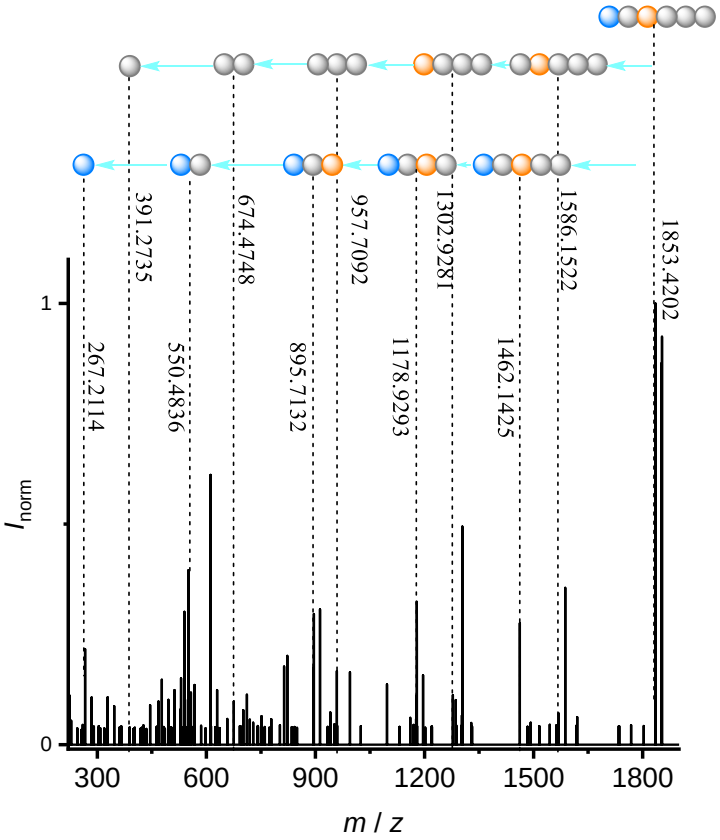

Supplementary Figure 12: ESI-MS/MS fragmentation of **P2** ion from α-cleavage of the (C=O)-O bond at m/z = 1853.4202 Da recorded in positive mode. (with an NCE of 19)

P2	α-cleavage				
	Calc. / Da	Detected / Da		Calc. / Da	Detected / Da
α	267.2282	267.2117	y_5^+	1586.1469	1586.1522
b_1^+	550.4830	550.4836	y_4^+	1302.9321	1302.9281
b_2^+	895.7134	895.7132	y_3^+	957.7017	957.7092
b_3^+	1178.9281	1178.9293	y_2^+	674.4870	674.4948
b_4^+	1462.1429	1462.1425	y_1^+	391.2723	391.2735
b_5^+	1745.3637	/	ω	108.0575	/

Supplementary Table 3: In combination with Supplementary Figure 12, the calculated masses and detected masses of fragments are summarized.

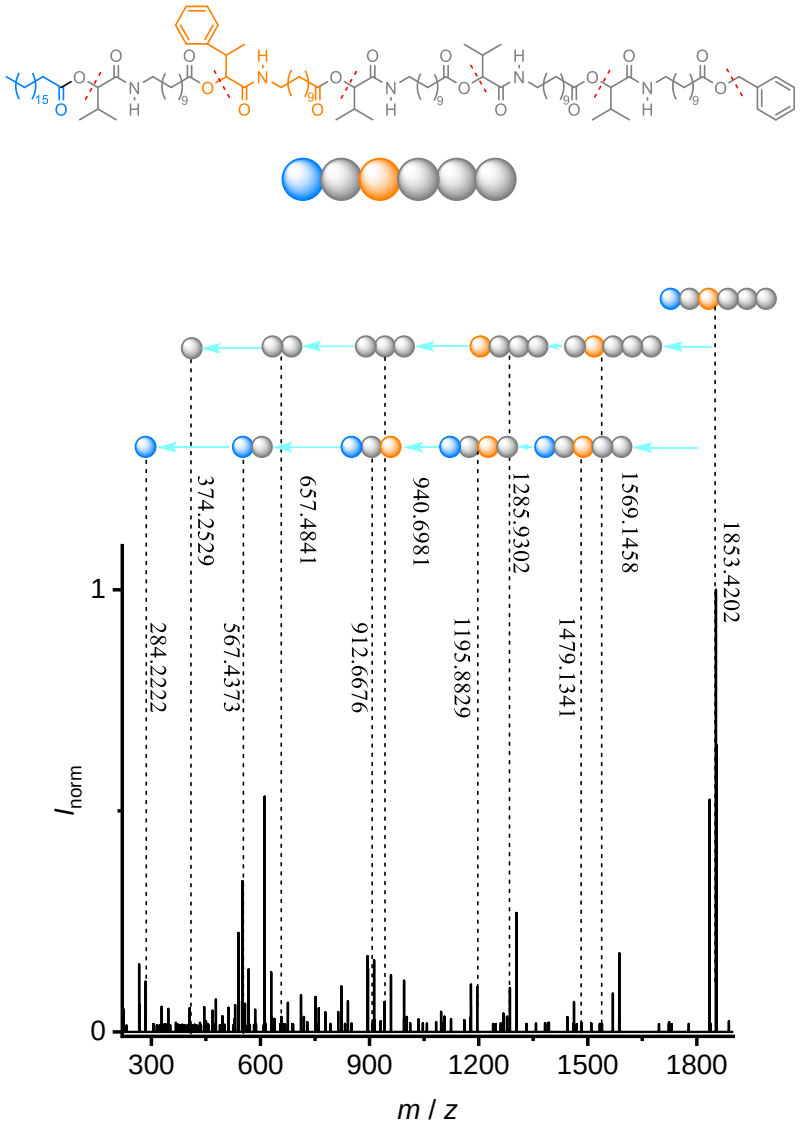

Supplementary Figure 13: ESI-MS/MS fragmentation of **P2** ion from cleavage via McLafferty rearrangement at m/z = 1853.4202 Da recorded in positive mode. (with an NCE of 20)

P2	Cleavage via McLafferty rearrangement				
	Calc. / Da	Detected / Da		Calc. / Da	Detected / Da
α	284.2715	284.2222	y_5^+	1569.1436	1569.1458
b_1^+	567.4863	567.4373	y_4^+	1285.9289	1285.9302
b_2^+	912.7167	912.6676	y_3^+	940.6985	940.6981
b_3^+	1195.9314	1195.8829	y_2^+	657.4837	657.4841
b_4^+	1479.1462	1479.1341	y_1^+	374.2690	374.2529
b_5^+	1762.3609	/	ω	91.0542	/

Supplementary Table 4: In combination with Supplementary Figure 13, the calculated masses and detected masses of fragments are summarized.

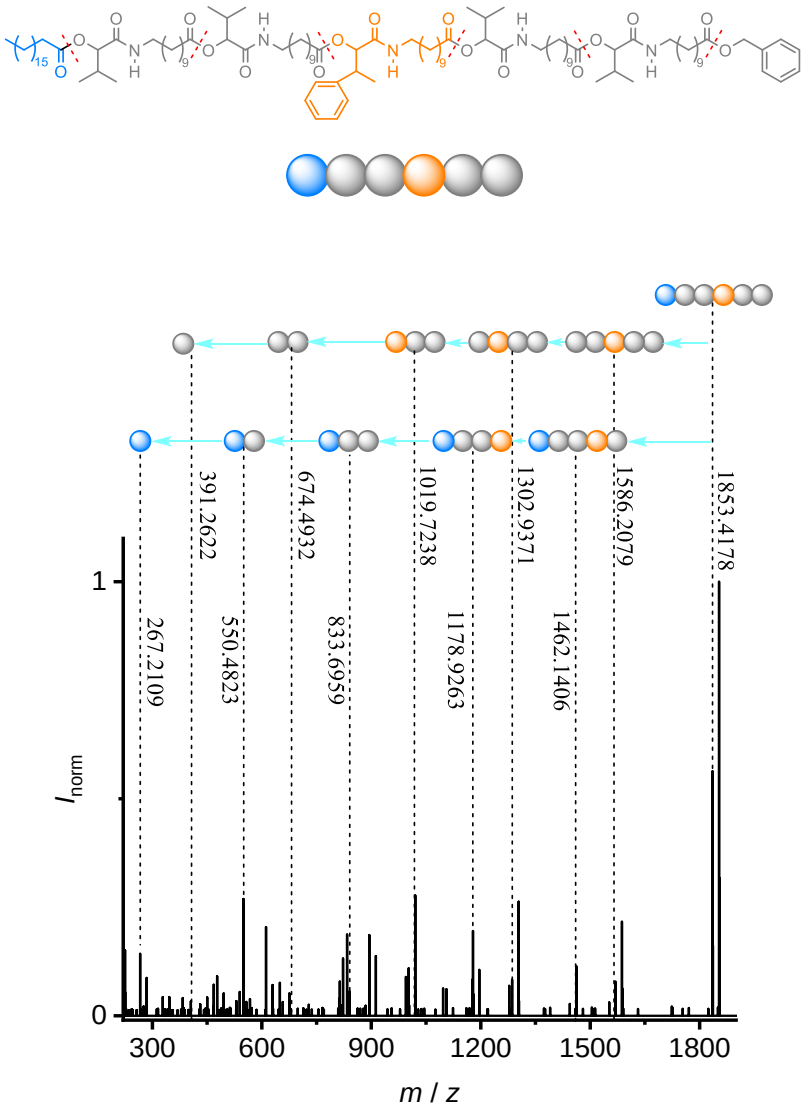

Supplementary Figure 14: ESI-MS/MS fragmentation of **P3** ion from α-cleavage of the (C=O)-O bond at m/z = 1853.4178 Da recorded in positive mode. (with an NCE of 19).

P3	α-cleavage				
	Calc. / Da	Detected / Da		Calc. / Da	Detected / Da
α	267.2282	267.2109	y_5^+	1586.2069	1586.2079
b_1^+	550.4830	550.4823	y_4^+	1302.9321	1302.9371
b_2^+	833.6977	833.6959	y_3^+	1019.7174	1019.7238
b_3^+	1178.9281	1178.9263	y_2^+	674.4870	674.4932
b_4^+	1462.1429	1462.1406	y_1^+	391.2723	391.2622
b_5^+	1745.3637	/	ω	108.0572	/

Supplementary Table 5: In combination with Supplementary Figure 14, the calculated masses and detected masses of fragments are summarized.

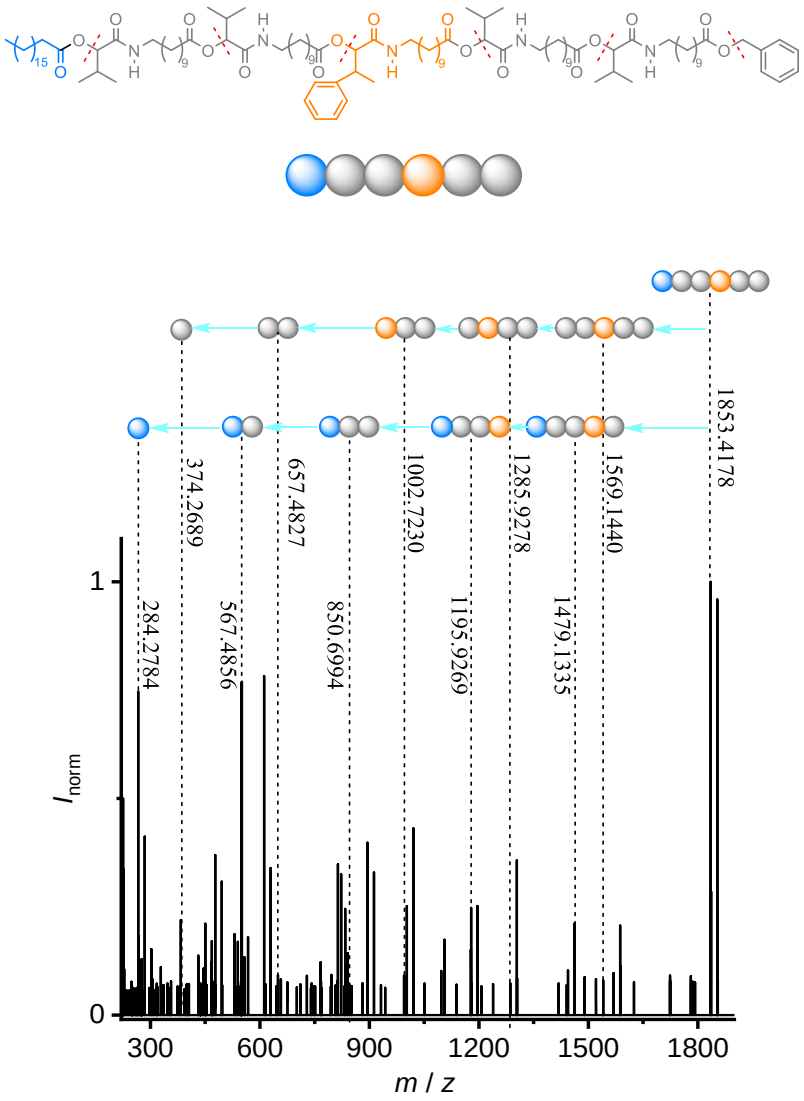

Supplementary Figure 15: ESI-MS/MS fragmentation of **P3** ion from cleavage via McLafferty rearrangement at m/z = 1853.4178 Da recorded in positive mode. (with an NCE of 20)

P3	Cleavage via McLafferty rearrangement				
	Calc. / Da	Detected / Da		Calc. / Da	Detected / Da
α	284.2715	284.2784	y_5^+	1569.1436	1569.1440
b_1^+	567.4863	567.4856	y_4^+	1285.9289	1285.9278
b_2^+	850.7010	850.6994	y_3^+	1002.7141	1002.7230
b_3^+	1195.9314	1195.9269	y_2^+	657.4837	657.4827
b_4^+	1479.1462	1479.1335	y_1^+	374.2690	374.2689
b_5^+	1762.3609	/	ω	91.0542	/

Supplementary Table 6: In combination with Supplementary Figure 15, the calculated masses and detected masses of fragments are summarized.

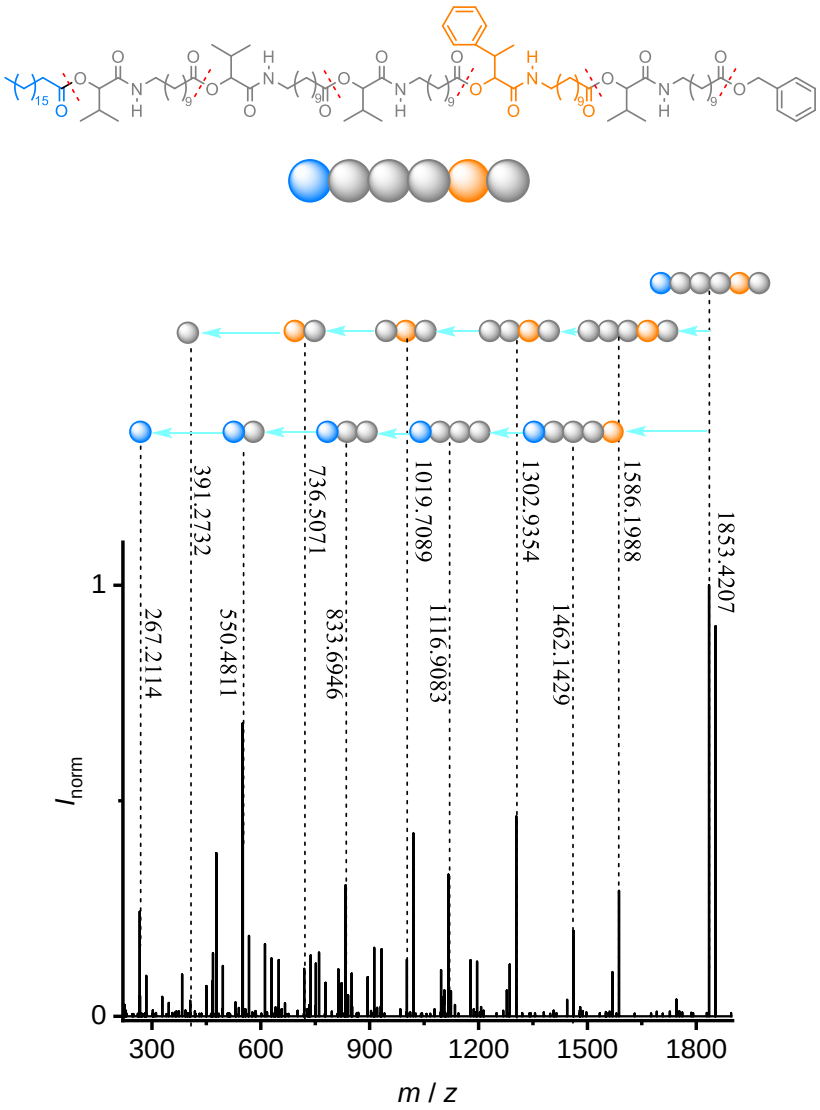

Supplementary Figure 16: ESI-MS/MS fragmentation of **P4** ion from α-cleavage of the (C=O)-O bond at m/z = 1853.4207 Da recorded in positive mode. (with an NCE of 19)

P4	α-cleavage				
	Calc. / Da	Detected / Da		Calc. / Da	Detected / Da
α	267.2282	267.2104	y_5^+	1586.2069	1586.1988
b_1^+	550.4830	550.4811	y_4^+	1302.9321	1302.9354
b_2^+	833.6977	833.6946	y_3^+	1019.7174	1019.7089
b_3^+	1116.9125	1116.9083	y_2^+	736.5027	736.5071
b_4^+	1462.1429	1462.1429	y_1^+	391.2723	391.2732
b_5^+	1745.3576	/	ω	108.0572	/

Supplementary Table 7: In combination with Supplementary Figure 16, the calculated masses and detected masses of fragments are summarized.

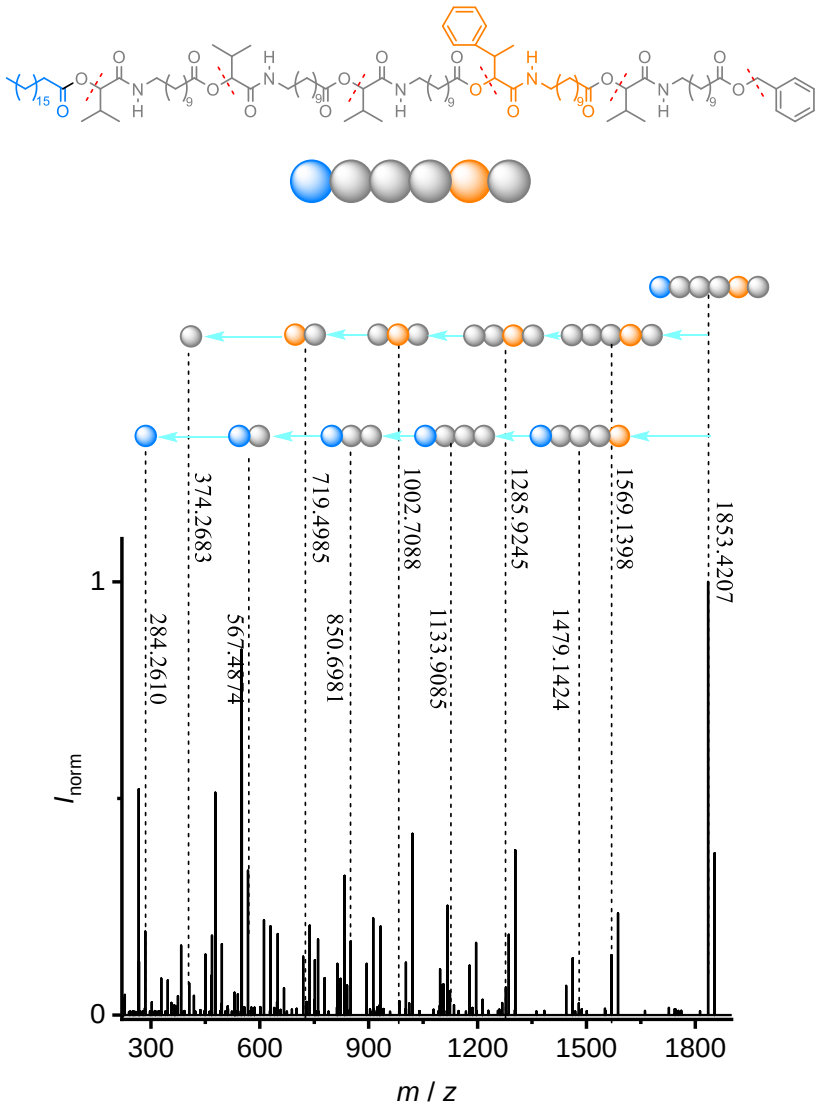

Supplementary Figure 17: ESI-MS/MS fragmentation of **P4** ion from cleavage via McLafferty rearrangement at m/z = 1853.4207 Da recorded in positive mode. (with an NCE of 20)

P4	Cleavage via McLafferty rearrangement				
	Calc. / Da	Detected / Da		Calc. / Da	Detected / Da
α	284.2715	284.2610	y_5^+	1569.1436	1569.1397
b_1^+	567.4863	567.4874	y_4^+	1285.9289	1285.9245
b_2^+	850.7010	850.6981	y_3^+	1002.7141	1002.7088
b_3^+	1133.9158	1133.9085	y_2^+	719.4994	719.4985
b_4^+	1479.1462	1479.1424	y_1^+	374.2690	374.2683
b_5^+	1762.3609	/	ω	91.0542	/

Supplementary Table 8: In combination with Supplementary Figure 17, the calculated masses and detected masses of fragments are summarized.

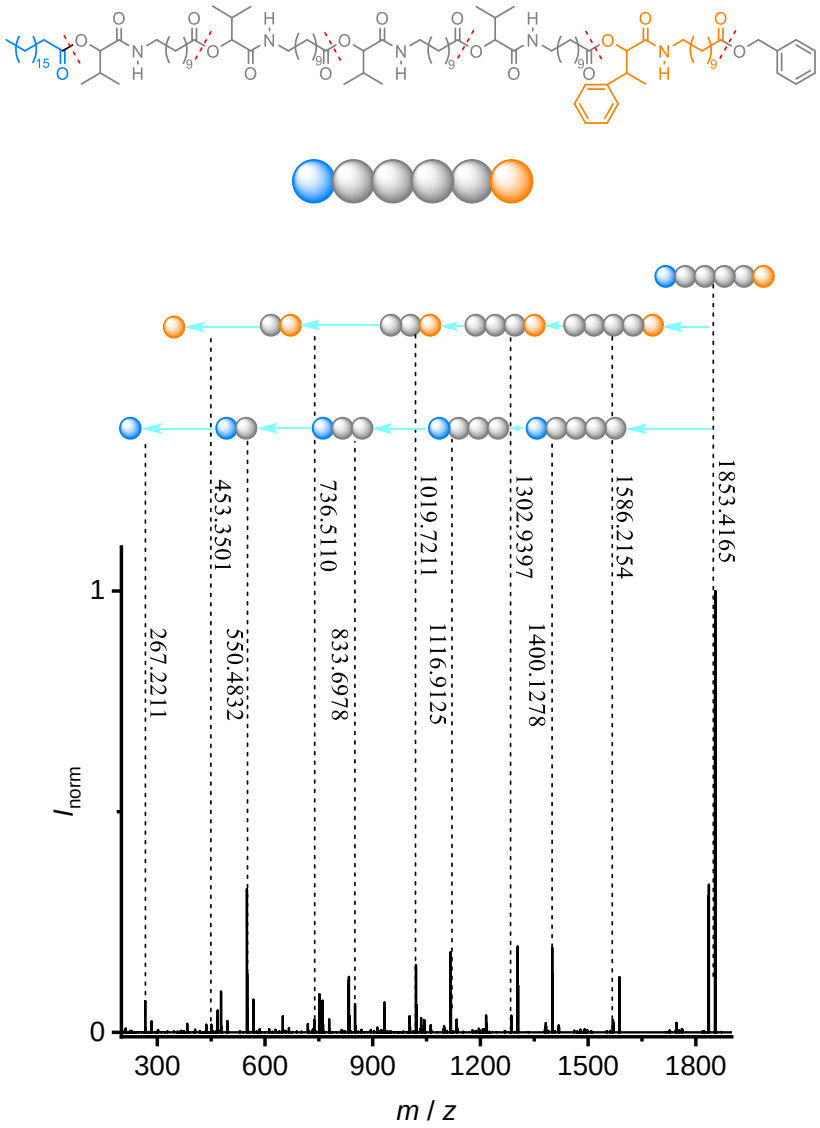

Supplementary Figure 18: ESI-MS/MS fragmentation of **P5** ion from α-cleavage of the (C=O)-O bond at m/z = 1853.4165 Da recorded in positive mode. (with an NCE of 19)

P5	α-cleavage				
	Calc. / Da	Detected / Da		Calc. / Da	Detected / Da
α	267.2282	267.2211	y_5^+	1586.2069	1586.2154
b_1^+	550.4830	550.4832	y_4^+	1302.9321	1302.9397
b_2^+	833.6977	833.6978	y_3^+	1019.7174	1019.7211
b_3^+	1116.9125	1116.9125	y_2^+	736.5027	736.5110
b_4^+	1400.1272	1400.1278	y_1^+	453.2879	453.3501
b_5^+	1745.3576	/	ω	108.0572	/

Supplementary Table 9: In combination with Supplementary Figure 18, the calculated masses and detected masses of fragments are summarized.

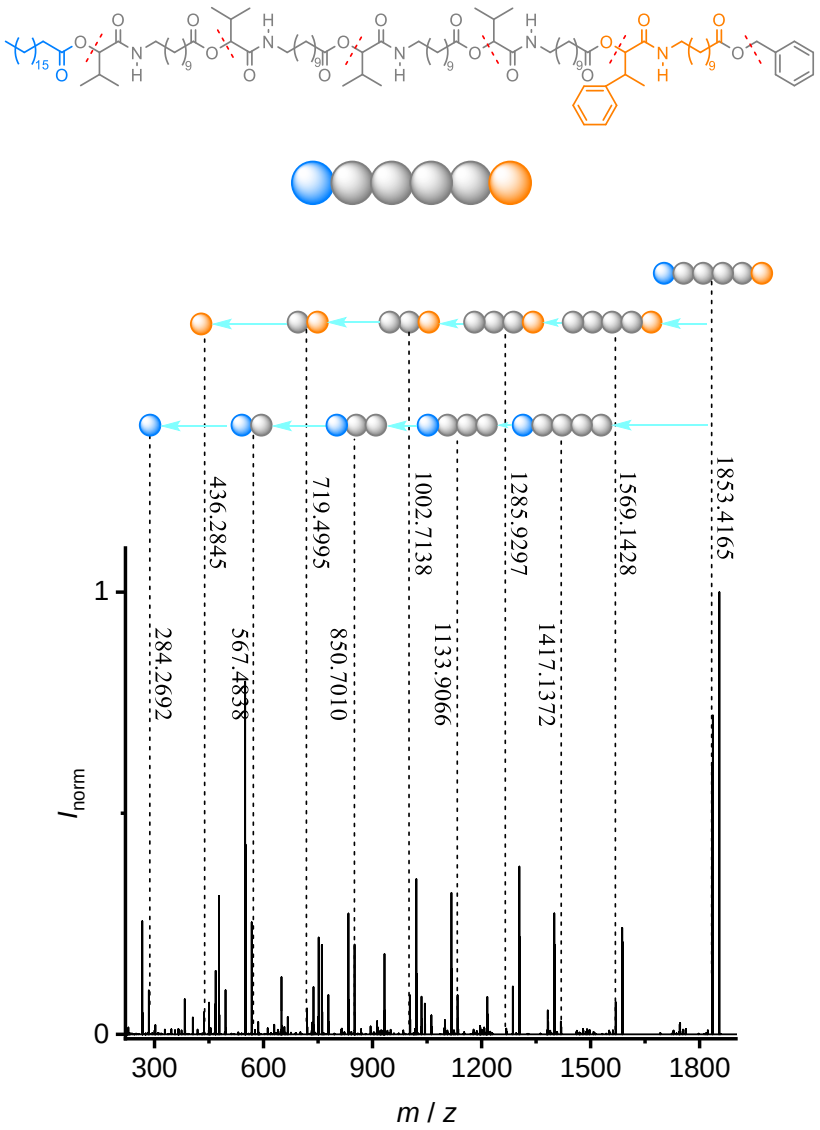

Supplementary Figure 19: ESI-MS/MS fragmentation of **P5** ion from cleavage via McLafferty rearrangement at m/z = 1853.4165 Da recorded in positive mode. (with an NCE of 20)

P5	Cleavage via McLafferty rearrangement				
	Calc. / Da	Detected / Da		Calc. / Da	Detected / Da
α	284.2715	284.2692	y_5^+	1569.1436	1569.1428
b_1^+	567.4863	567.4838	y_4^+	1285.9289	1285.9297
b_2^+	850.7010	850.6994	y_3^+	1002.7141	1002.7138
b_3^+	1133.9158	1133.9066	y_2^+	719.4994	719.4995
b_4^+	1417.1305	1417.1372	y_1^+	436.2846	436.2845
b_5^+	1762.3609	/	ω	91.0542	/

Supplementary Table 10: In combination with Supplementary Figure 19, the calculated masses and detected masses of fragments are summarized.

6.3.2 Effects of component structure on macrocyclization *via* the Passerini reaction

3,6-dinitro-9-N-ethyl-carbazole

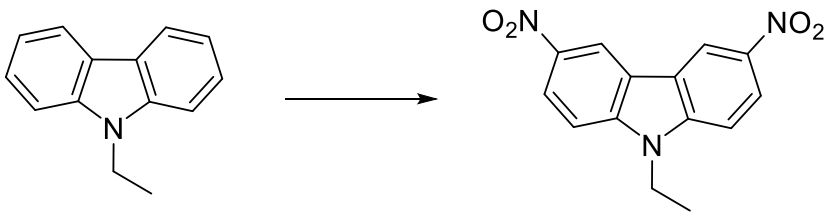

^{1}H-NMR (400 MHz, DMSO-d_6) δ 9.50 (d, J = 2.3 Hz, 2H, ^{1}), 8.45 (dd, J^a = 9.1Hz, J^b = 2.4 Hz, 2H, ^{2}), 7.95 (d, J = 9.1 Hz, 2H, ^{3}), 4.62 (q, J = 7.2 Hz, 2H, ^{4}), 1.37 (t, J = 7.2 Hz, 3H, ^{5}).
^{13}C-NMR (101 MHz, DMSO-d_6) δ 144.20, 141.26, 122.66, 122.12, 118.77, 110.70, 38.29, 13.74.
IR (ATR platinum diamond): v [cm^{-1}] = 3313.6, 3085.4, 2980.6, 2963.7, 1628.7, 1600, 1581.7, 1505.1, 1478.5, 1467.9, 1330.6, 1307.9, 1270.7, 1233.6, 1149.6, 1132.3, 1094.1, 1019.1, 950.4, 908.3, 898.2, 848.1, 825.6, 817.6, 787.1, 752.0, 719.8, 664.6, 640.2, 602.6, 593.3, 561.0, 532.9, 417.0.
ESI-MS m/z: $[M+H]^+$ calculate for $[C_{14}H_{11}N_3O_4]^+$ = 286.0822, found: 286.0818.

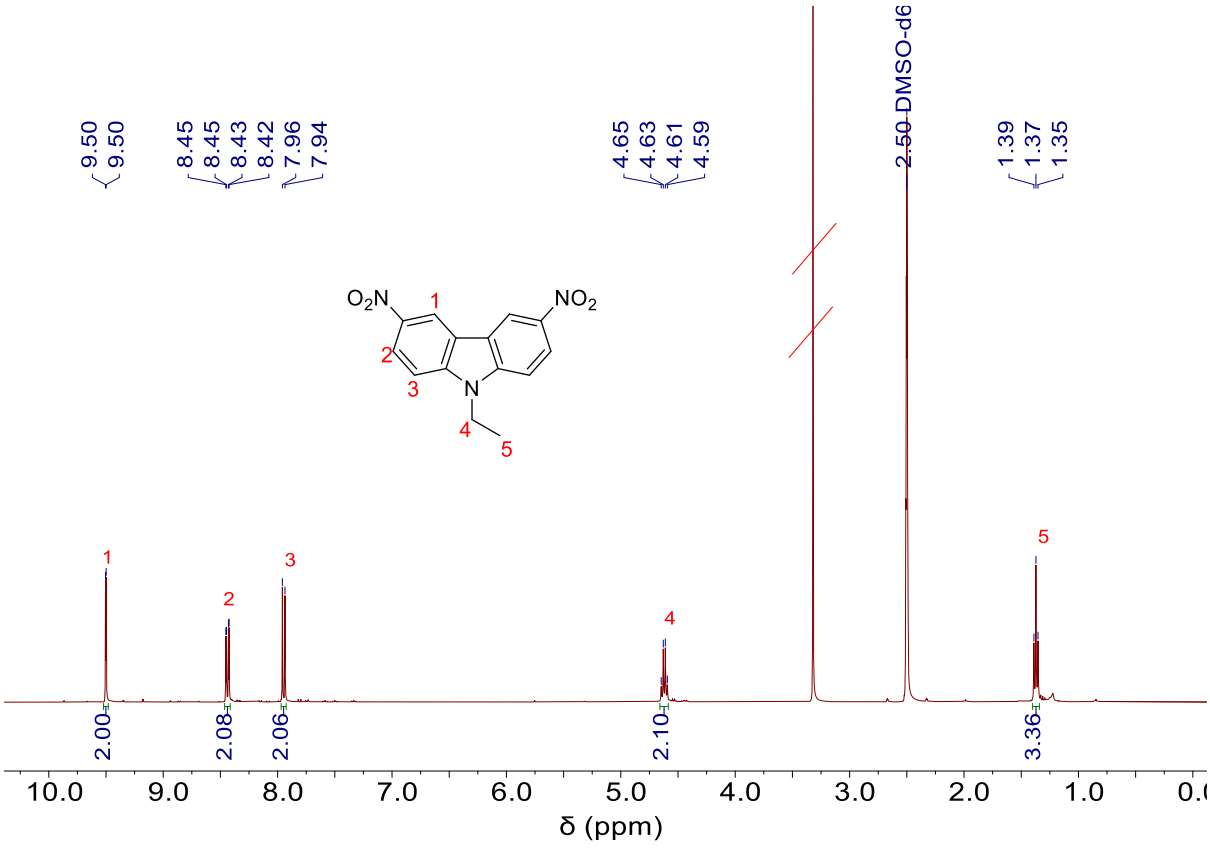

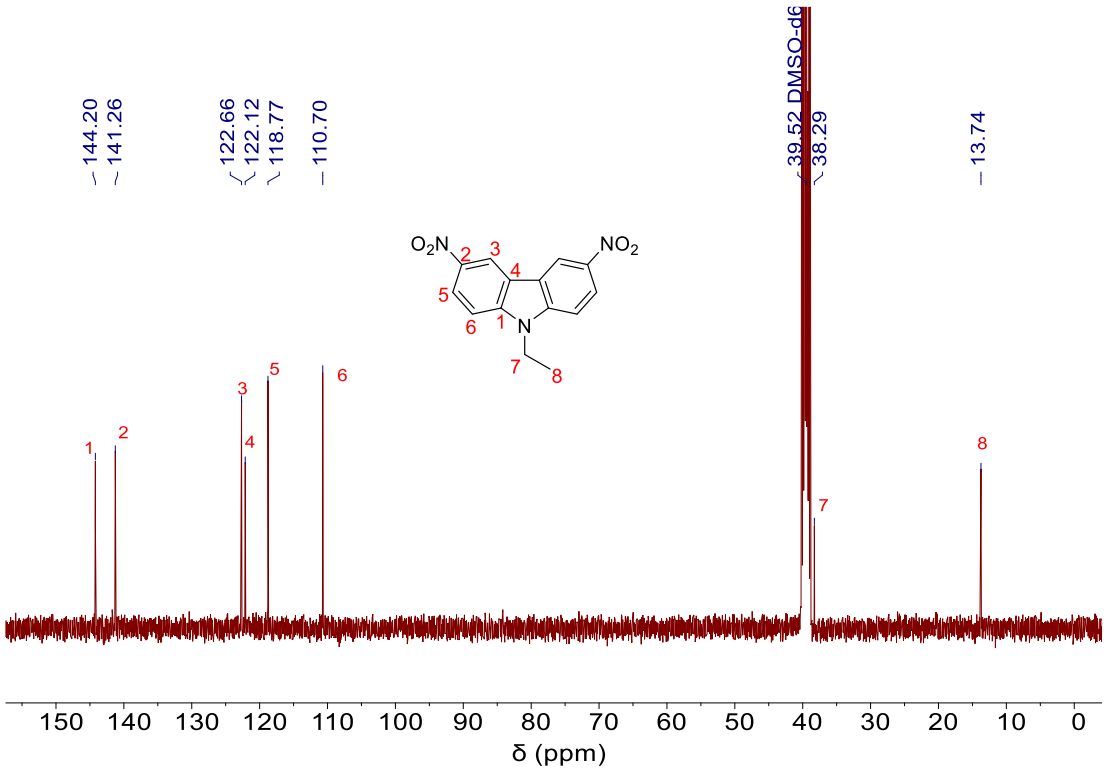
144.20
141.26
122.66
122.12
118.77
110.70
39.52 DMSO-d6
38.29
13.74
O2N
NO2
N
1
2
3
4
5
6
7
8
150 140 130 120 110 100 90 80 70 60 50 40 30 20 10 0
δ (ppm)

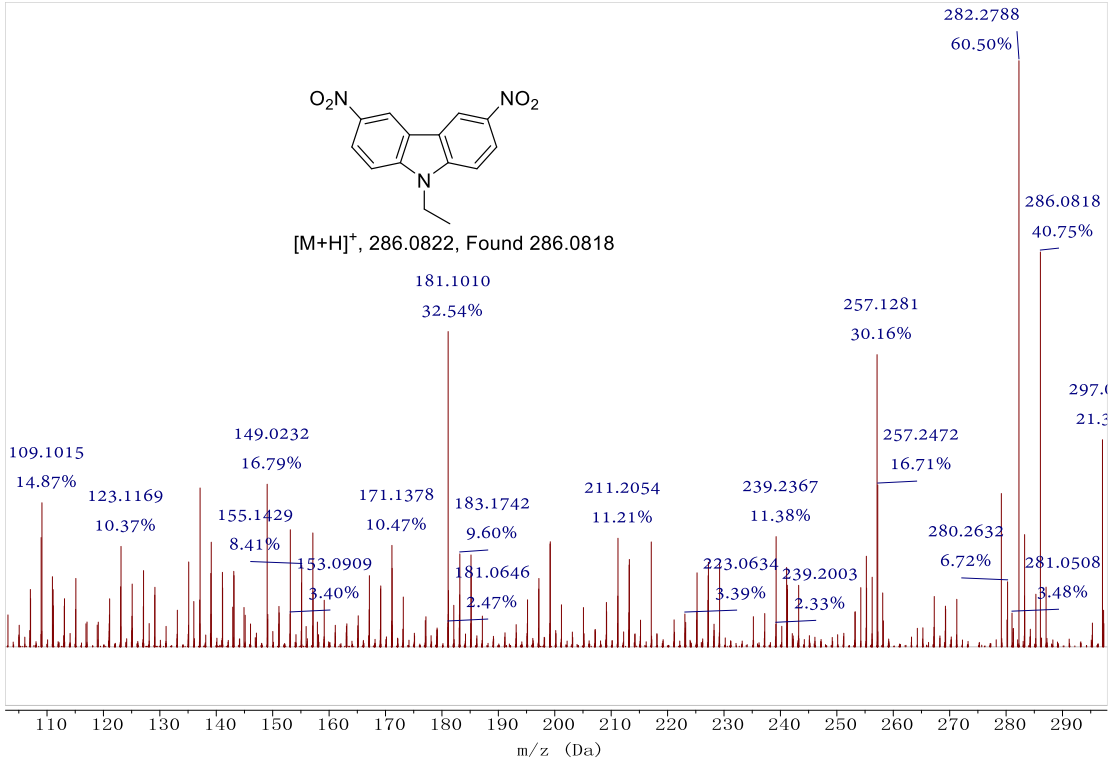
O2N
NO2
N
[M+H]+, 286.0822, Found 286.0818
282.2788
60.50%
286.0818
40.75%
181.1010
32.54%
257.1281
30.16%
257.2472
16.71%
149.0232
16.79%
109.1015
14.87%
123.1169
10.37%
155.1429
8.41%
153.0909
3.40%
171.1378
10.47%
183.1742
9.60%
181.0646
2.47%
211.2054
11.21%
239.2367
11.38%
223.0634
3.39%
239.2003
2.33%
280.2632
6.72%
281.0508
3.48%
110 120 130 140 150 160 170 180 190 200 210 220 230 240 250 260 270 280 290
m/z (Da)

3,6-diamino-9- N-methyl-carbazole

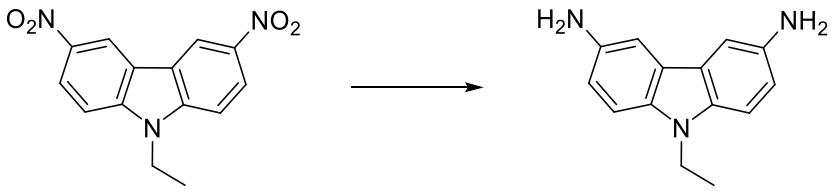

^{1}H-NMR (400 MHz, DMSO-d_6) δ 7.19 – 7.07 (m, 4H, ^{1}), 6.75 (dd, J = 8.5, 2.2 Hz, 2H, ^{2}), 4.68 (s, 4H, ^{3}), 4.19 (q, J = 7.0 Hz, 2H, ^{4}), 1.19 (t, J = 7.1 Hz, 3H, ^{5}).
^{13}C-NMR (101 MHz, DMSO-d_6) δ 140.52, 133.46, 122.53, 114.71, 108.95, 104.10, 36.77, 13.69.
IR (ATR platinum diamond): ν [cm^{-1}] = 3401.7, 3383.3, 3297.5, 3182.3, 3016.2, 2961.9, 1636.8, 1577.7, 1494.0, 1475.5, 1454.2, 1327.0, 1314.4, 1215.9, 1177.5, 1144.7, 1084.1, 871.1, 799.7, 779.7, 619.5, 587.7, 566.7, 493.9, 456.6, 421.8, 406.8.
ESI-MS m/z: $[M+H]^+$ calculate for $[C_{14}H_{15}N_3]^+$ = 226.1339, found: 226.1337.

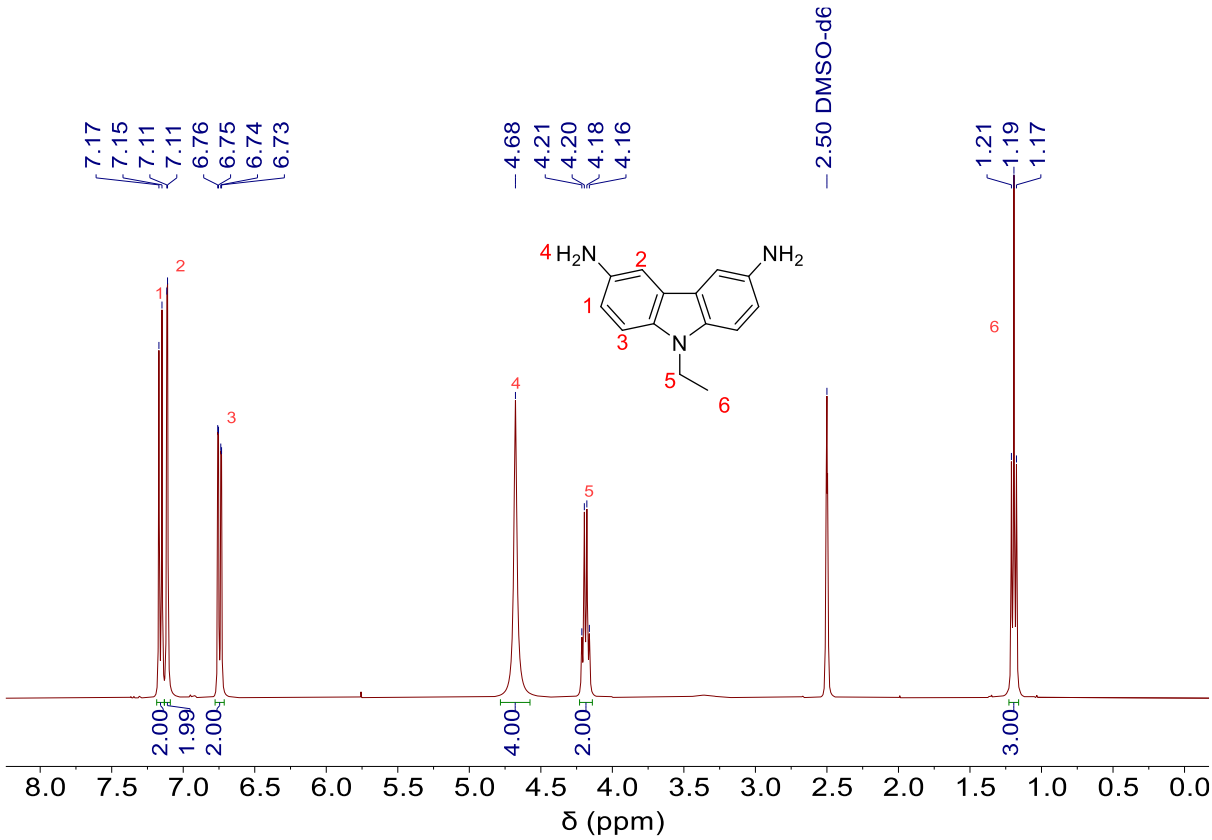

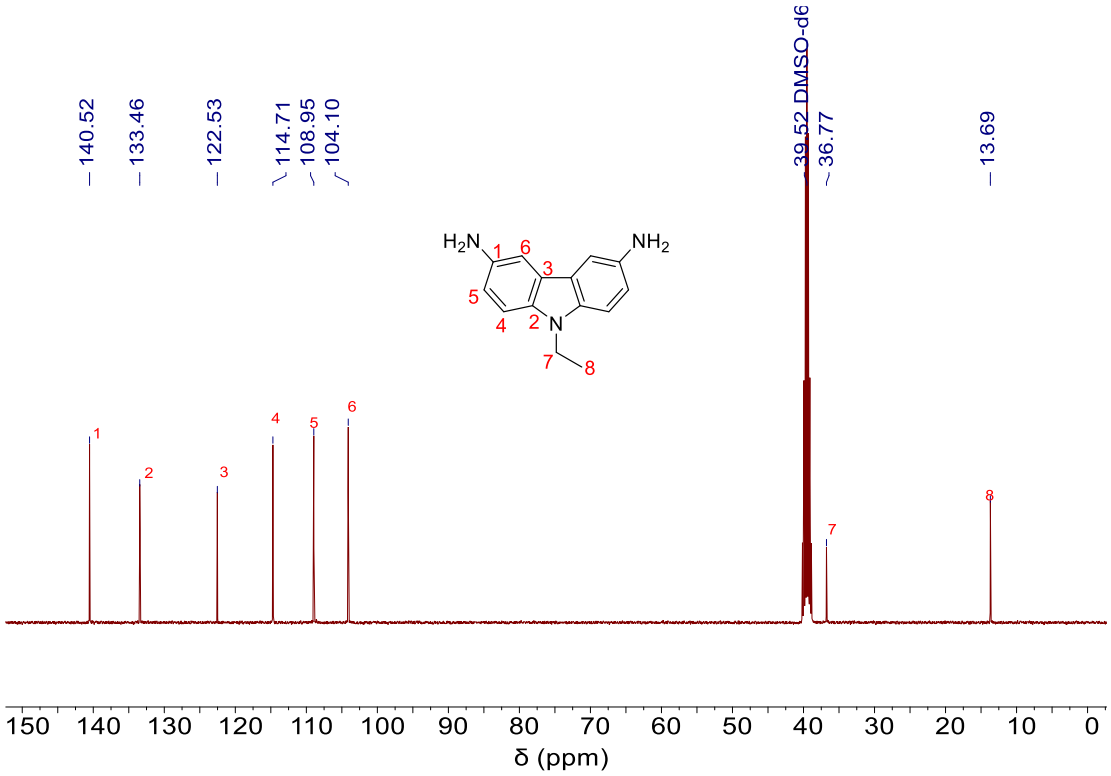
140.52
133.46
122.53
114.71
108.95
104.10
39.52 DMSO-d6
36.77
13.69
H2N
NH2
1
2
3
4
5
6
7
8
150 140 130 120 110 100 90 80 70 60 50 40 30 20 10 0
δ (ppm)

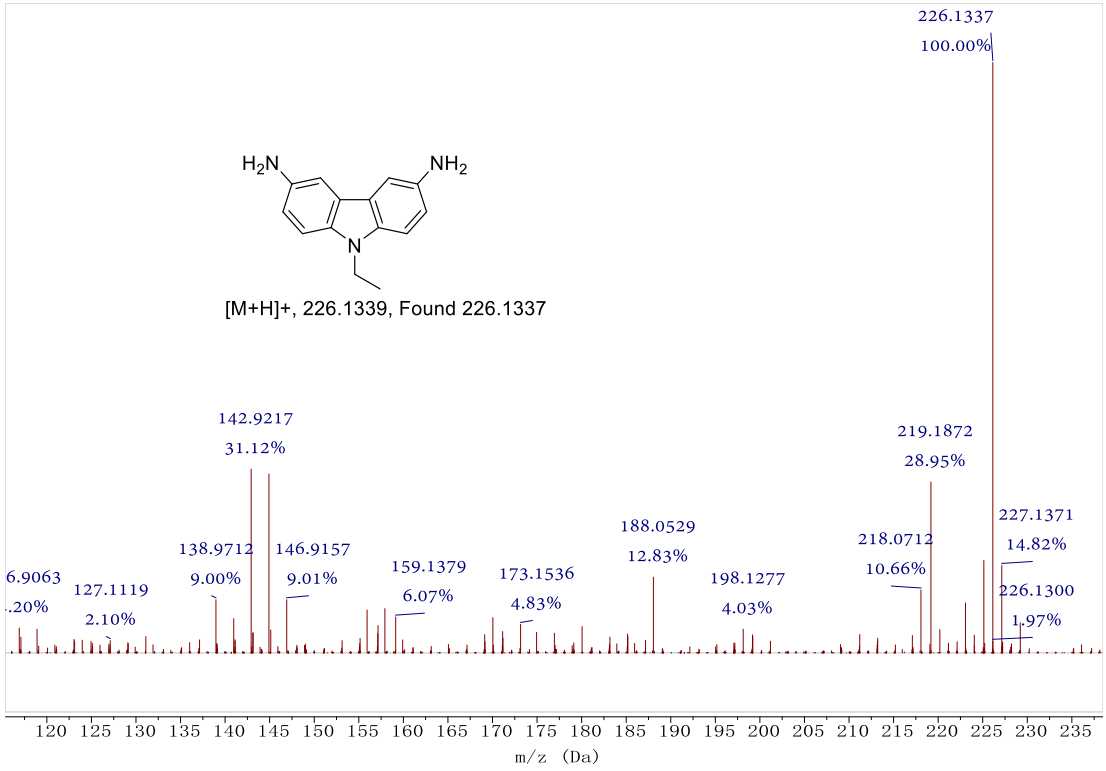
H2N
NH2
[M+H]+, 226.1339, Found 226.1337
226.1337
100.00%
142.9217
31.12%
219.1872
28.95%
227.1371
14.82%
188.0529
12.83%
138.9712
9.00%
146.9157
9.01%
159.1379
6.07%
173.1536
4.83%
218.0712
10.66%
198.1277
4.03%
226.1300
1.97%
127.1119
2.10%
6.9063
.20%
120 125 130 135 140 145 150 155 160 165 170 175 180 185 190 195 200 205 210 215 220 225 230 235
m/z (Da)

3,6-diisocyano-9-ethyl-carbazole

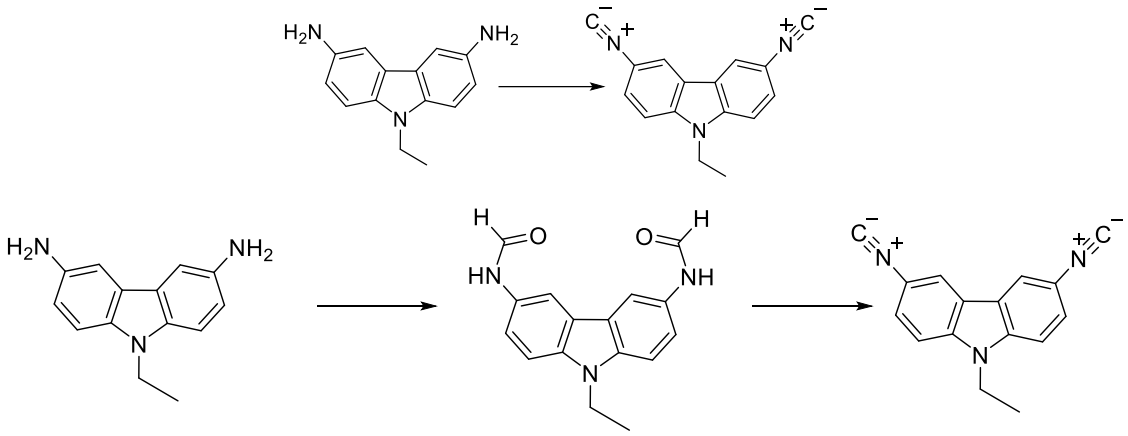

^{1}H-NMR (400 MHz, DMSO-*d*$_6$) δ 8.46 (d, *J* = 1.9 Hz, 2H), 7.74 (d, J = 8.7 Hz, 2H), 7.65 (dd, J = 8.7, 2.0 Hz, 2H), 4.47 (q, J = 7.1 Hz, 2H), 1.29 (t, J = 7.1 Hz, 3H).
^{13}C-NMR (101 MHz, DMSO-*d*$_6$) δ 162.51, 139.85, 124.79, 121.51, 119.52, 117.77, 110.86, 37.59, 13.68.
IR (ATR platinum diamond): *ν*[cm^{-1}] = 2982.7, 2933.4, 2121.6, 1631.0, 1594.1, 1486.1, 1458.0, 1384.9, 1350.1, 1330.1, 1304.0, 1239.5, 1148.1, 1085.1, 1056.9, 1020.4, 946.4, 879.8, 865.2, 802.3, 747.1, 733.2, 653.4, 584.3, 562.0, 482.4, 423.5.
ESI-MS m/z: $[M+H]^+$ calculate for $[C_{16}H_{11}N_3]^+$ = 246.1026, found: 246.1025.

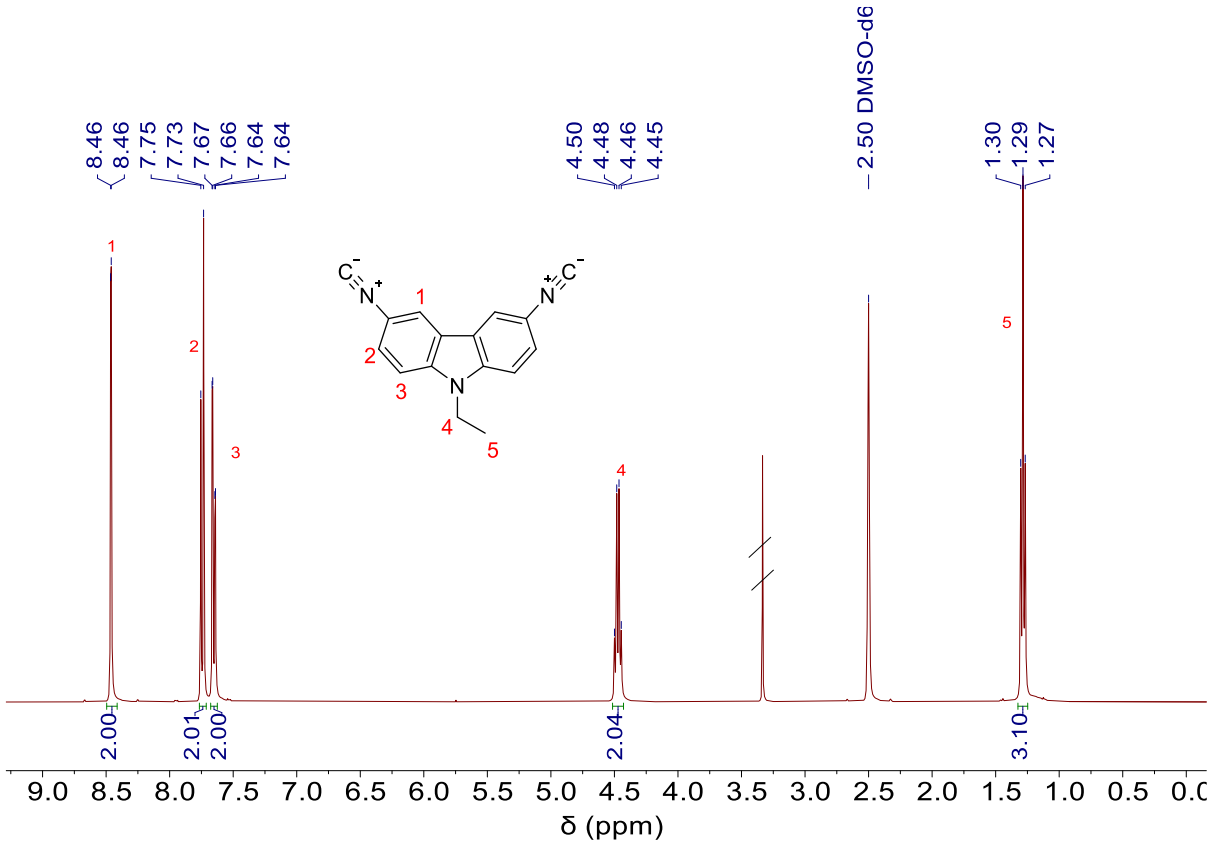

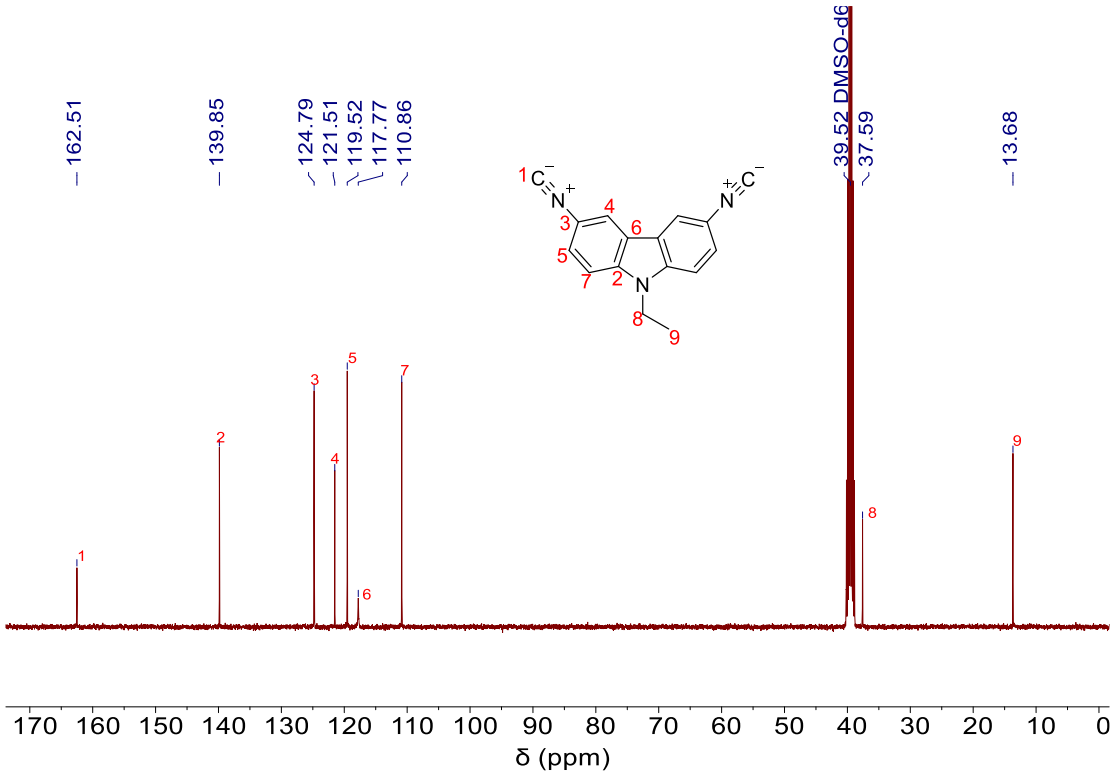
162.51
139.85
124.79
121.51
119.52
117.77
110.86
39.52 DMSO-d6
37.59
13.68
170 160 150 140 130 120 110 100 90 80 70 60 50 40 30 20 10 0
δ (ppm)

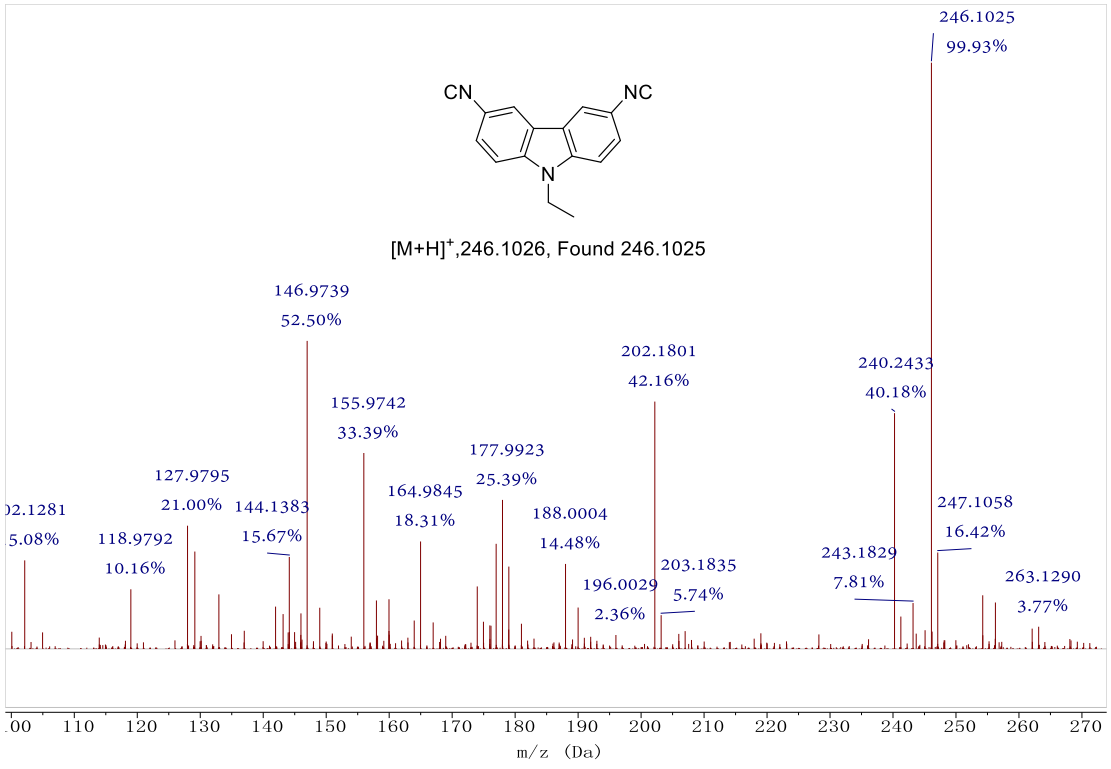
CN
NC
N
[M+H]+,246.1026, Found 246.1025
246.1025
99.93%
146.9739
52.50%
202.1801
42.16%
240.2433
40.18%
155.9742
33.39%
177.9923
25.39%
127.9795
21.00%
164.9845
18.31%
144.1383
15.67%
188.0004
14.48%
247.1058
16.42%
118.9792
10.16%
203.1835
5.74%
243.1829
7.81%
196.0029
2.36%
263.1290
3.77%
m/z (Da)

9-ethyl-3,6-diisocyano-9H-carbazole, isobutyraldehyde reacted with suberic acid (C3)

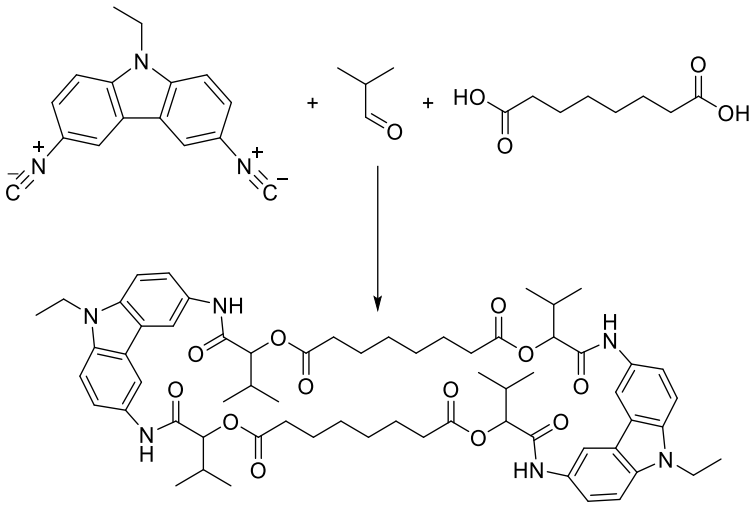

^{1}H-NMR (400 MHz, DMSO) δ 9.86 (d, *J* = 16.5 Hz, 4H, ^{1}), 8.15 – 7.27 (m, 12H, ^{2}), 4.68 – 4.61 (m, 4H, ^{3}), 4.47 – 4.36 (m, 4H, ^{4}), 2.20 – 2.15(m, 12H, ^{5}), 1.52 – 1.43 (m, 6H, ^{6}), 1.34 – 1.11 (m, 16H, ^{7}), 1.08 – 1.01 (m, 24H, ^{8}).

^{13}C-NMR (101 MHz, DMSO) δ 173.40, 168.13, 159.16, 129.51, 121.63, 120.39, 113.57, 110.71, 109.36, 108.99, 79.58, 37.25, 33.81, 29.32, 25.52, 18.53, 18.44, 18.07, 17.93, 13.72.

IR: 3408.9, 3258.3, 3077.5, 2964.3, 2926.1, 2854.8, 1736.8, 1658.4, 1590.8, 1517.4, 1482.8, 1422.2, 1375.3, 1309.8, 1220.4, 1148.5, 1121.9, 1089.7, 991.6, 873.3, 859.5, 802.5, 730.9, 690.3, 645.6, 618.1, 587.2, 542.4, 507.7, 468.6, 422.9.

ESI-MS m/z: $[M+H]^+$ calculate for $[C_{64}H_{82}N_6O_{12}]^+$ = 1127.6063, found: 1127.6036.

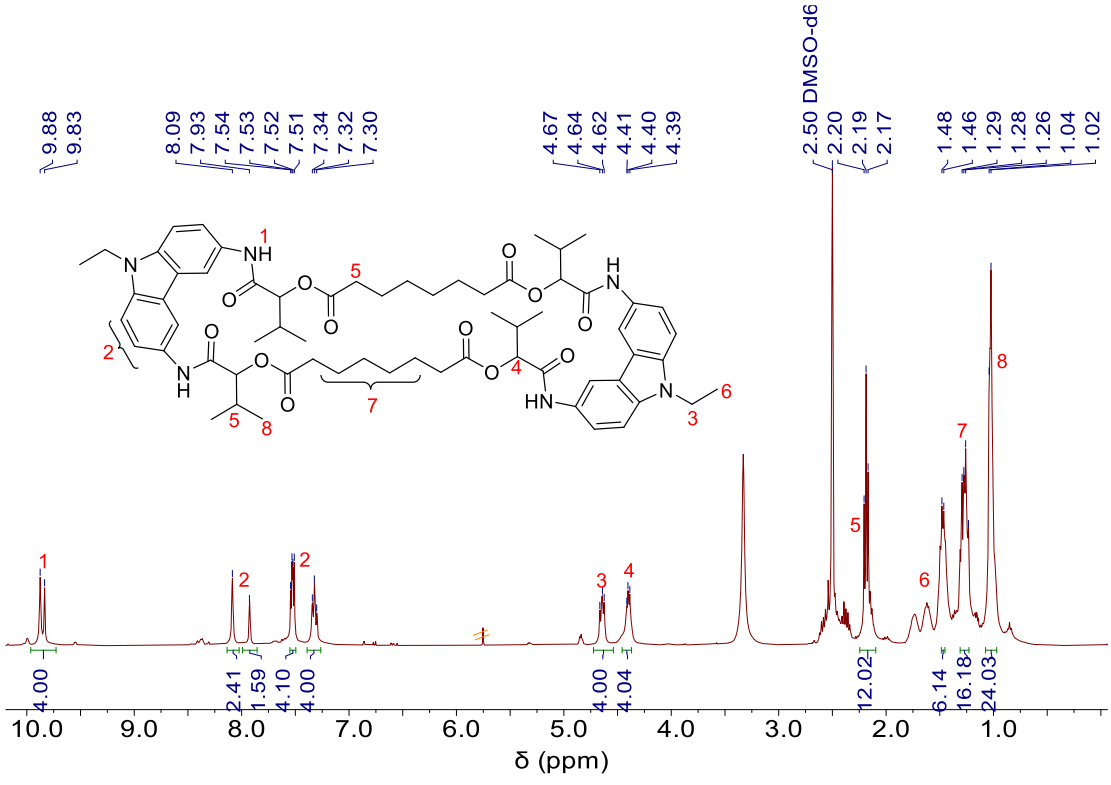

9-ethyl-3,6-diisocyano-9H-carbazole, isobutyraldehyde reacted with azelaic acid (**C4**)

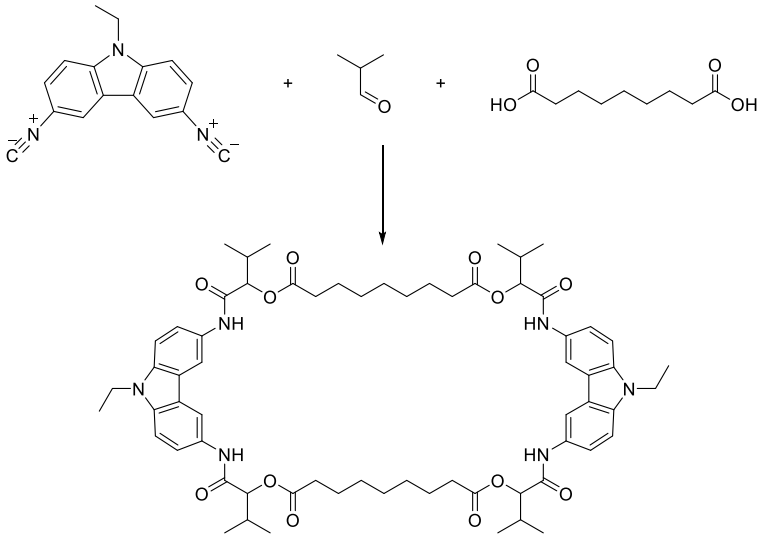

^{1}H-NMR (400 MHz, DMSO) δ 10.03 – 9.98 (m, 4H, ^{1}), 8.49 – 7.14 (m, 12H, ^{2}), 4.78 – 4.58 (m, 4H, ^{3}), 4.41 – 4.32 (m, 4H, ^{4}), 2.43 – 2.11 (m, 12H, ^{5}), 1.68 – 1.50 (m, 6H, ^{6}), 1.46 – 1.20 (m, 20H, ^{7}), 1.06 – 0.97 (m, 24H, ^{8}).

^{13}C-NMR (101 MHz, DMSO) δ 173.51, 168.10, 158.96, 137.59, 130.01, 122.13, 120.58, 116.92, 114.06, 111.00, 109.62, 78.91, 34.09, 30.00, 29.73, 25.96, 19.24, 17.88, 14.26.

IR: 3387.1, 3324.3, 2962.5, 2924.5, 2872.9, 2854.9, 1743.1, 1664.1, 1524.1, 1483.8, 1463.8, 1415.6, 1373.3, 1347.3, 1311.7, 1235.4, 1160.7, 1139.8, 1100.9, 1010.2, 911.8, 880.3, 863.8, 802.9, 787.2, 719.7, 622.5, 580.8, 506.1, 472.7, 448.9, 422.5.

ESI-MS m/z: $[M+H]^+$ calculate for $[C_{66}H_{86}N_6O_{12}]^+$ = 1155.6376, found: 1155.6357.

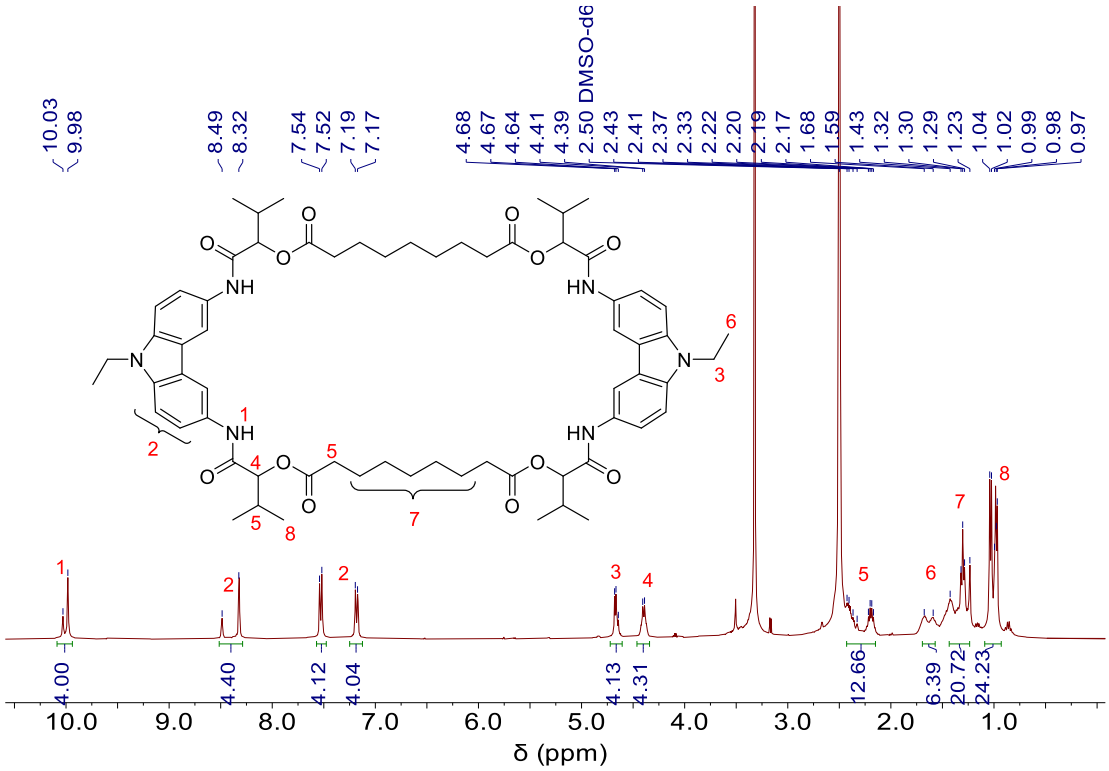

9-ethyl-3,6-diisocyano-9H-carbazole, isobutyraldehyde reacted with sebacic acid (**C5**)

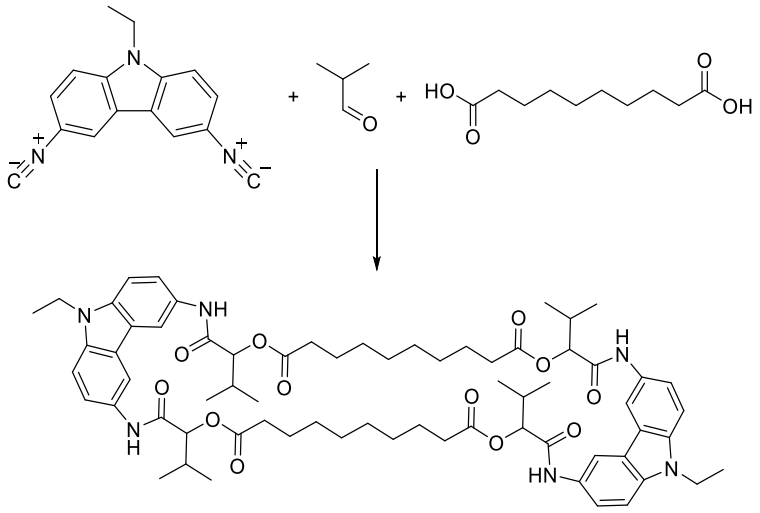

^{1}H-NMR (400 MHz, DMSO) δ 9.92 (d, *J* = 24.5 Hz, 4H, ^{1}), 8.47 – 7.35 (m, 12H, ^{2}), 4.76 (d, *J* = 5.8 Hz, 4H, ^{3}), 4.39 (d, *J* = 7.4 Hz, 4H, ^{4}), 2.38 – 2.16 (m, 12H, ^{5}), 1.77 – 1.54 (m, 6H, ^{6}), 1.50 – 1.19 (m, 24H, ^{7}), 1.02 – 0.79 (m, 24H, ^{8}).
^{13}C-NMR (101 MHz, DMSO) δ 173.63, 167.73, 158.96, 137.24, 130.75, 122.19, 119.35, 112.25, 111.92, 109.62, 78.91, 34.15, 30.17, 29.87, 29.18, 25.84, 19.10, 18.10, 14.17.
IR: 3338.4, 3260.4, 3089.7, 2958.4, 2923.9, 2853.3, 1728.0, 1673.8, 1656.6, 1595.9, 1520.8, 1493.8, 1481.7, 1445.1, 1421.8, 1404.2, 1374.7, 1312.7, 1291.0, 1222.4, 1181.2, 1138.1, 1122.0, 1083.2, 1027.4, 880.3, 864.5, 798.0, 785.8, 730.3, 688.0, 635.8, 620.8, 602.6, 582.3, 542.6, 459.1, 414.2.
ESI-MS m/z: $[M+H]^+$ calculate for $[C_{68}H_{90}N_6O_{12}]^+$ = 1183.6689, found: 1183.6657.

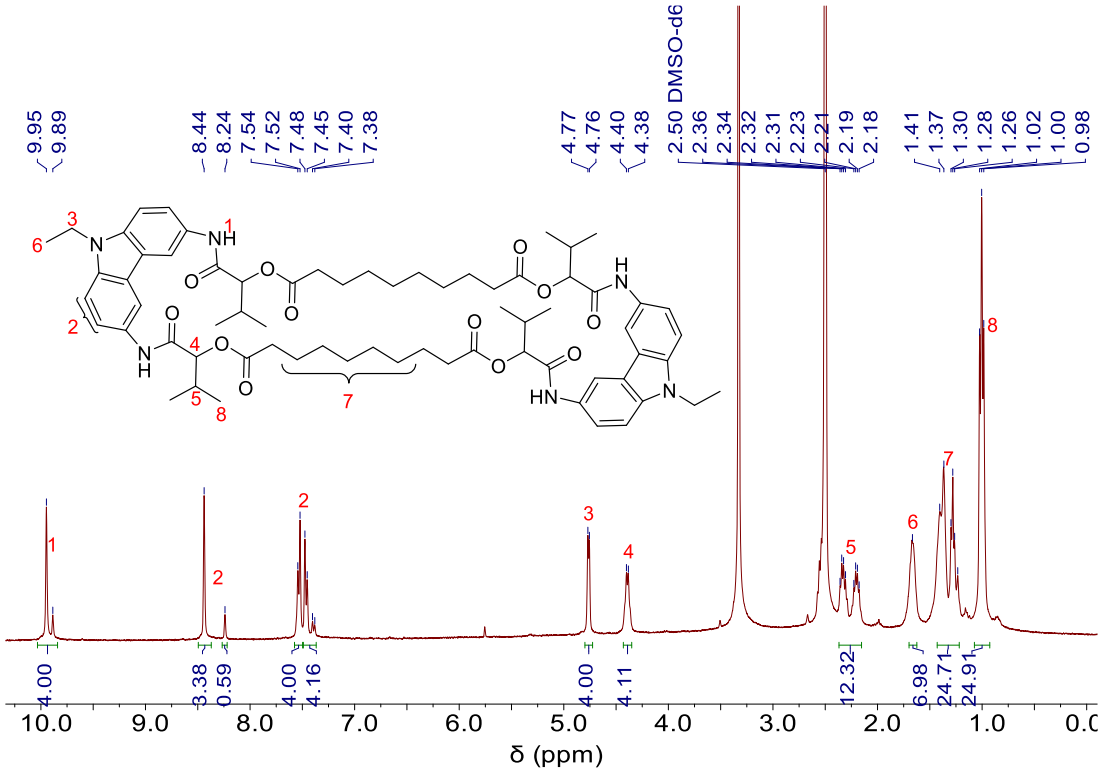

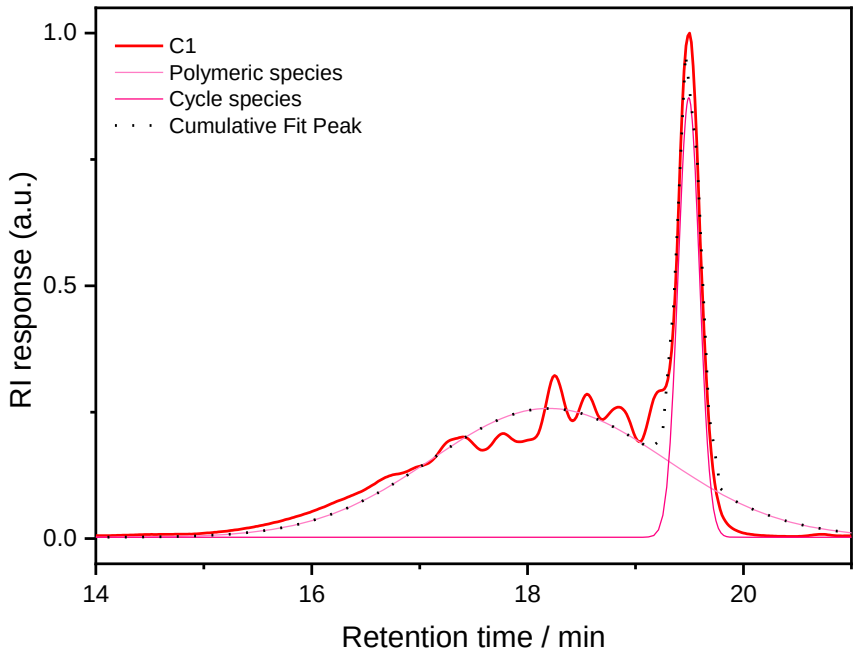

Supplementary Figure 20: Peak deconvolution of SEC diagrams from crude products **C1**.

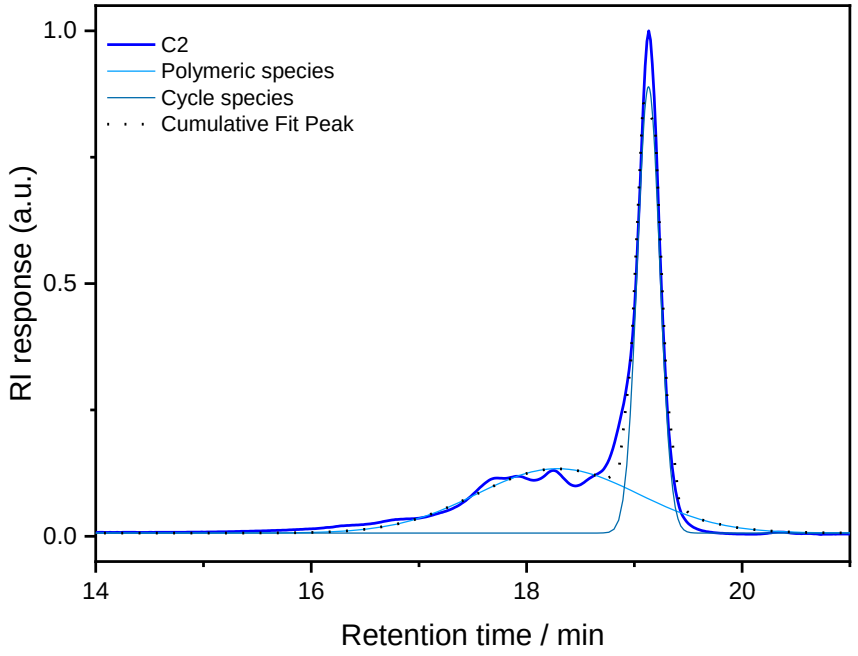

Supplementary Figure 21: Peak deconvolution of SEC diagrams from crude products **C2**.

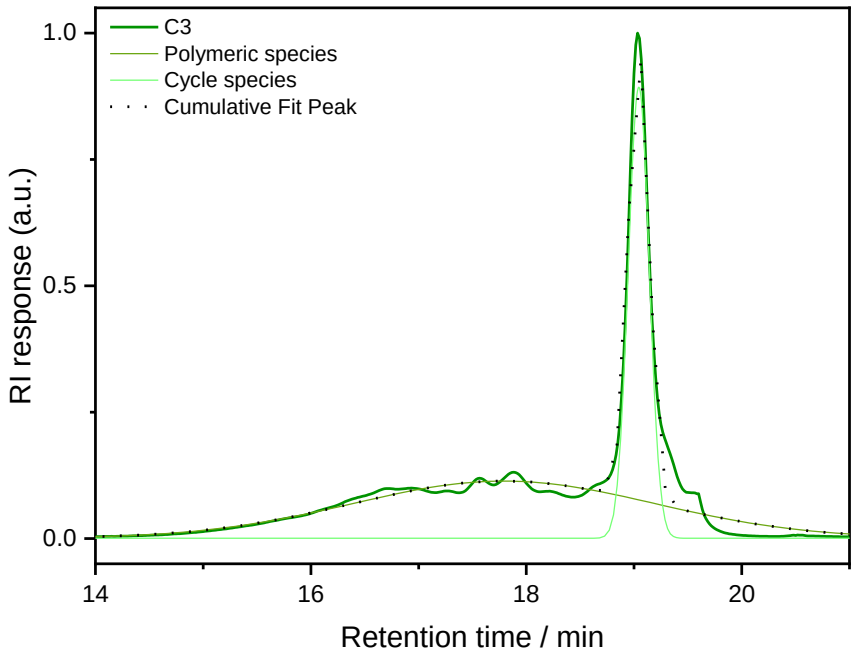

Supplementary Figure 22: Peak deconvolution of SEC diagrams from crude products **C3**.

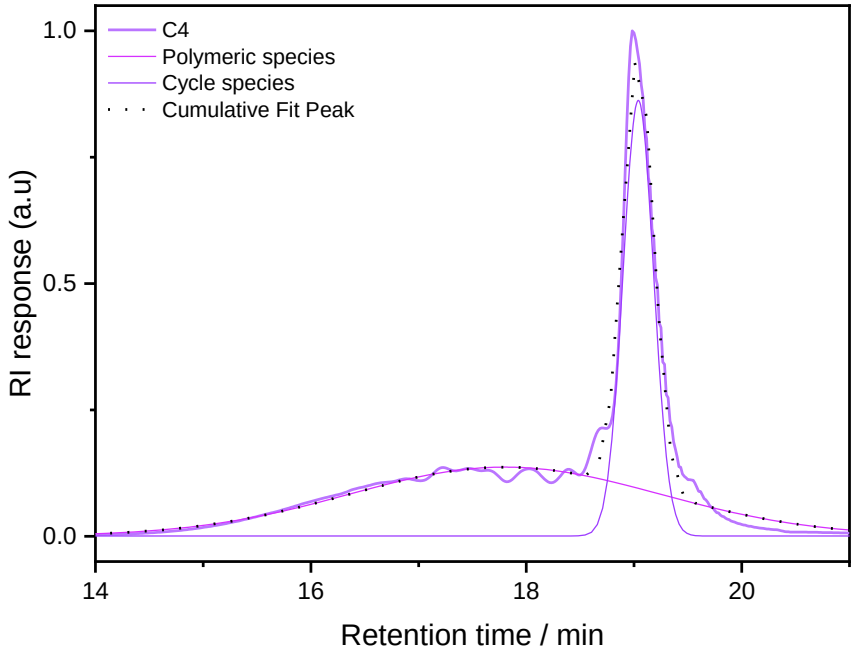

Supplementary Figure 23: Peak deconvolution of SEC diagrams from crude products **C4.**

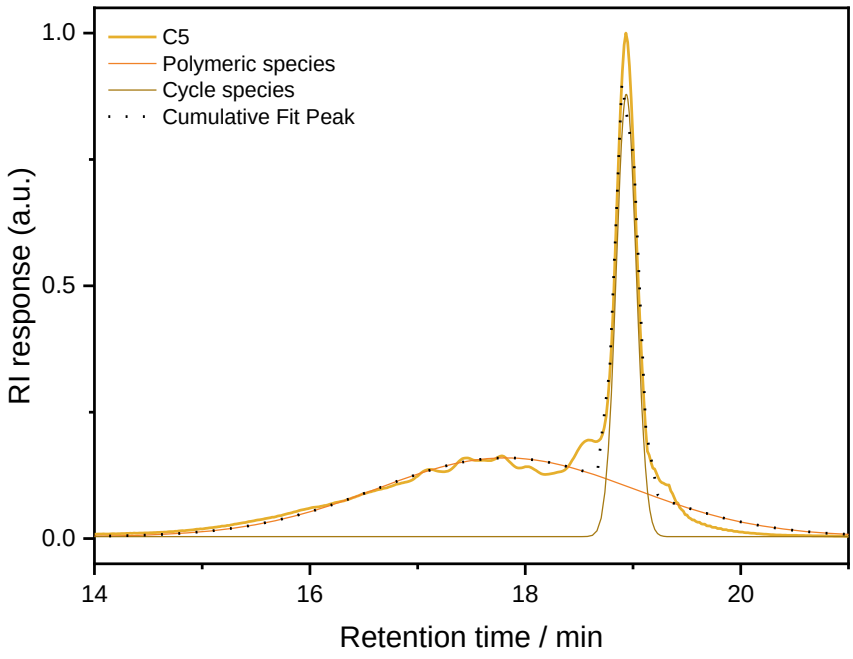

Supplementary Figure 24: Peak deconvolution of SEC diagrams from crude products **C5**.

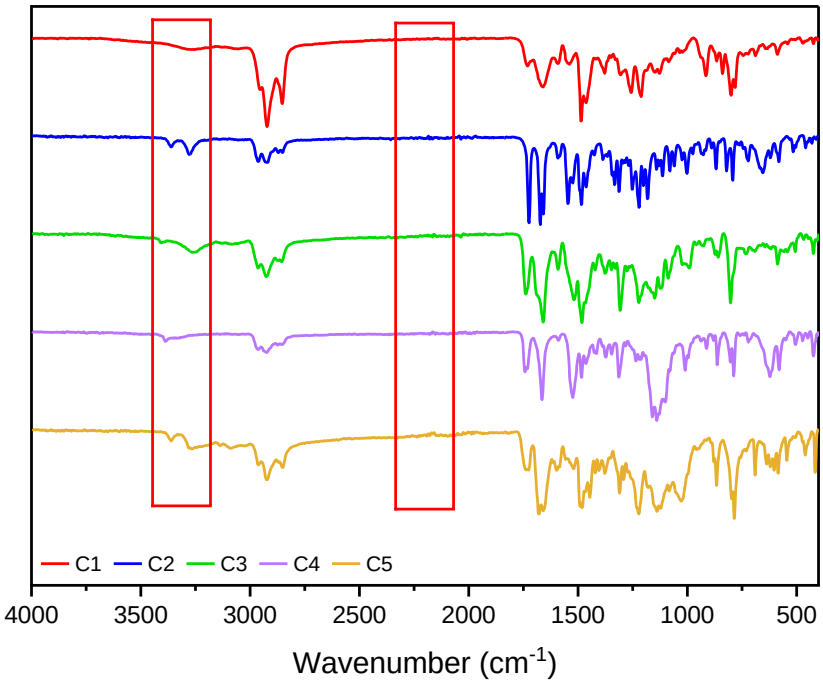

Supplementary Figure 25: IR spectra of purified products **C1-C5**

2,13-diisopropyl-1,14-dioxa-4,11-diazacycloicosane-3,12,15,20-tetraone (1,6-diisocyanohexan, isobutyraldehyde reacted with adipic acid) (**C6**)

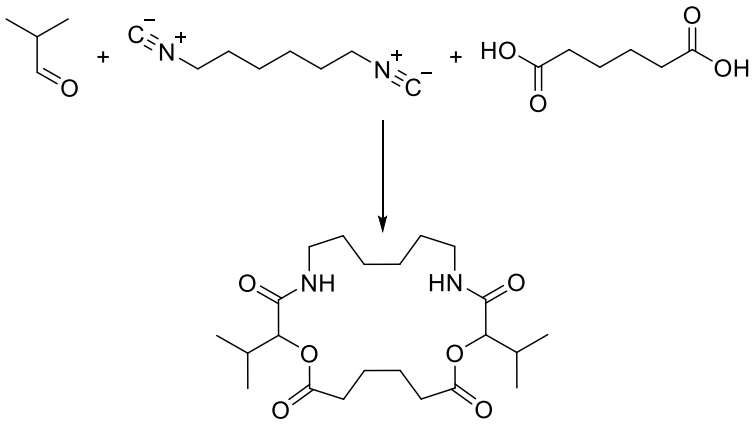

^{1}H-NMR (400 MHz, Chloroform-*d*) δ 6.04 (dt, *J* = 52.4, 6.0 Hz, 2H, ^{1}), 4.87 – 4.84 (m, 2H, ^{2}), 3.45 – 3.10 (m, 4H, ^{3}), 2.57 – 2.36 (m, 4H, ^{4}), 2.30 – 2.20 (m, 2H, ^{5}), 1.83 – 1.21 (m, 12H, ^{6}), 0.98 – 0.81 (m, 12H, ^{7}).

^{13}C-NMR (101 MHz, $CDCl_3$) δ 172.84, 172.55, 169.62, 169.47, 79.11, 78.95, 38.39, 38.22, 33.86, 33.74, 30.39, 30.26, 29.31, 28.99, 25.26, 25.14, 24.49, 24.25, 18.96, 18.89, 17.42, 17.38.

IR: 3307.1, 3082.4, 2959.1, 2928.5, 2871.3, 2854.7, 1728.4, 1656.3, 1542.7, 1461.1, 1406.9, 1372.1, 1274.5, 1165.1, 1137.3, 1082.4, 1003.3, 925.1, 735.1, 686.2, 512.2,

ESI-MS m/z: $[M+H]^+$ calculate for $[C_{22}H_{38}N_2O_6]^+$ = 427.2803, found: 427.2800.

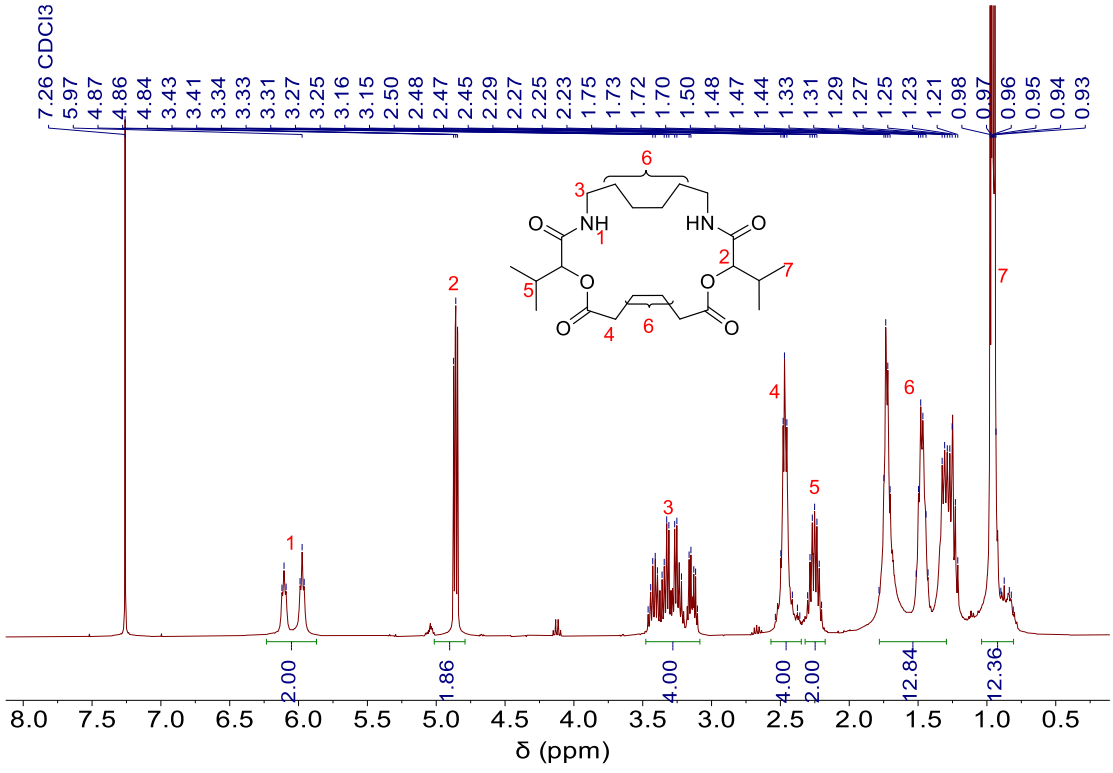

2,13-diisopropyl-1,14-dioxa-4,11-diazacyclohenicosane-3,12,15,21-tetraon (1,6-diisocyanohexan, isobutyraldehyde reacted with pimelic acid) **(C7)**

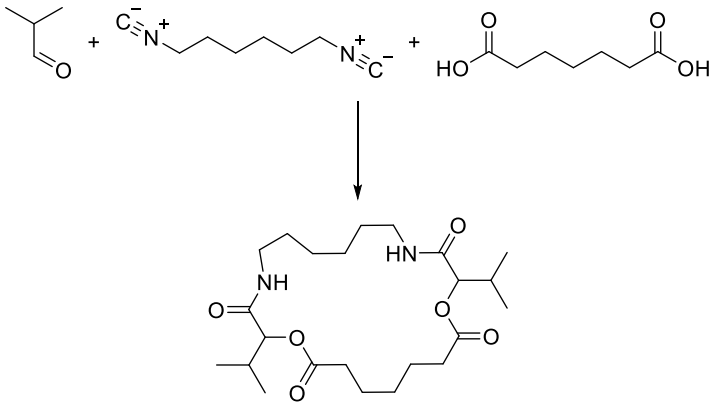

^{1}H-NMR (400 MHz, Chloroform-*d*) δ 5.98 (dt, *J* = 26.8, 6.1 Hz, 2H, ^{1}), 4.97 (dd, *J* = 32.3, 4.9 Hz, 2H, ^{2}), 3.52 – 3.02 (m, 4H, ^{3}), 2.51 – 2.33 (m, 3H, ^{4}), 2.30 – 2.20(m, 2H, ^{5}), 1.83 – 1.21 (m, 14H, ^{6}), 0.94 – 0.91 (m, 12H, ^{7}).

^{13}C-NMR (101 MHz, $CDCl_3$) δ 172.45, 172.36, 169.52, 169.47, 78.57, 78.53, 38.56, 34.04, 33.76, 30.35, 30.22, 29.30, 29.13, 28.33, 28.12, 26.01, 25.84, 24.87, 24.70, 24.49, 18.85, 18.82, 17.31, 17.18.

IR: 3278.3, 3077.2, 2962.2, 2933.3, 2874.9, 2857.8, 1741.6, 1648.6, 1539.8, 1460.7, 1438.5, 1412.9, 1371.1, 1286.6, 1232.7, 1162.5, 1126.4, 1094.1, 1003.9, 897.7, 705.8, 649.8, 453.5.

ESI-MS m/z: $[M+H]^+$ calculate for $[C_{23}H_{40}N_2O_6]^+$ = 441.2959, found: 441.2957.

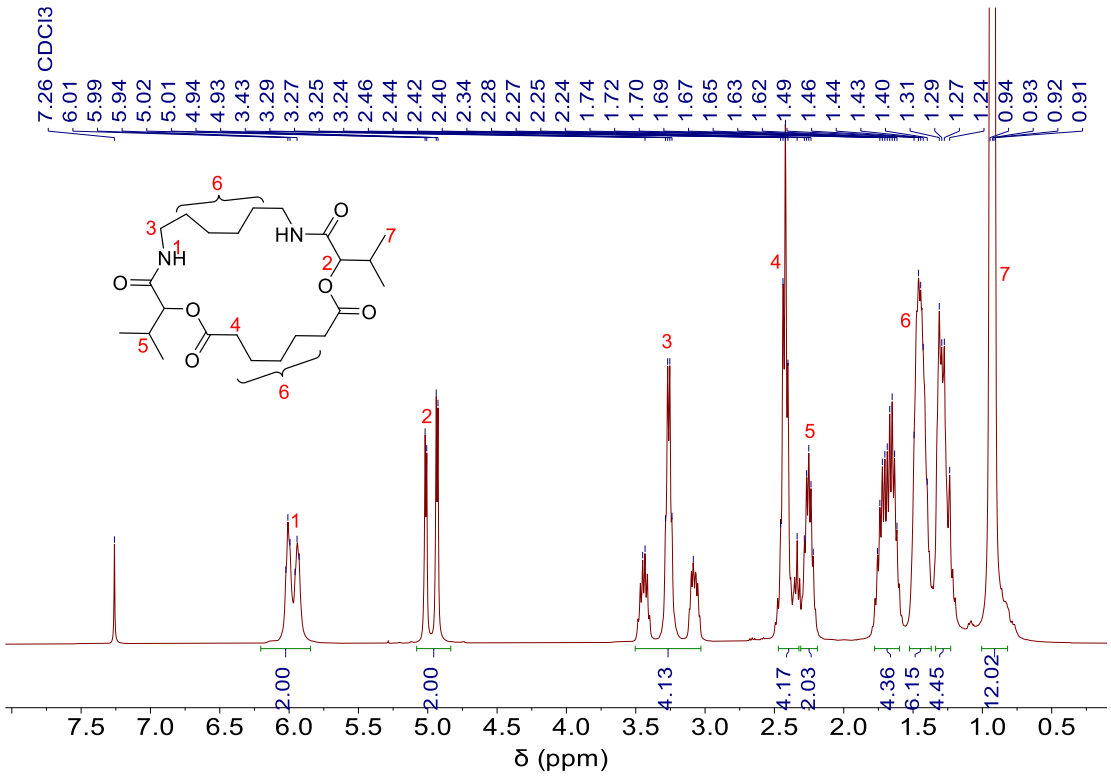

2,13-diisopropyl-1,14-dioxa-4,11-diazacyclodocosane-3,12,15,22-tetraone (1,6-diisocyanohexan, isobutyraldehyde reacted with suberic acid) **(C8)**

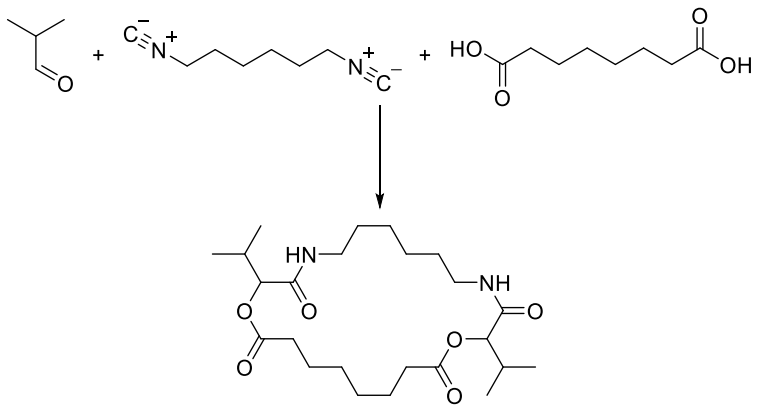

^{1}H-NMR (400 MHz, Chloroform-*d*) δ 5.92 (q, *J* = 6.0 Hz, 2H, ^{1}), 4.96 (dd, *J* = 14.3, 4.9 Hz, 2H, ^{2}), 3.47 – 3.05 (m, 4H, ^{3}), 2.43 – 2.39 (m, 4H, ^{4}), 2.30 – 2.08 (m, 2H, ^{5}), 1.73– 1.20 (m, 16H, ^{6}), 0.97 – 0.89 (m, 12H, ^{7}).

^{13}C-NMR (101 MHz, $CDCl_3$) δ 172.61, 172.57, 169.40, 169.36, 78.61, 78.55, 38.75, 34.28, 30.29, 30.15, 29.45, 29.37, 29.05, 29.02, 26.33, 26.23, 25.19, 25.17, 18.87, 18.83, 17.27, 17.18.

IR: 3267.3, 3087.5, 2959.9, 2930.6, 2872.8, 2858.1, 1739.2, 1649.5, 1538.8, 1465.7, 1370.8, 1300.2, 1254.8, 1225.7, 1156.2, 1125.6, 1092.5, 997.9, 927.4, 725.2, 665.4, 406.3,

ESI-MS m/z: $[M+H]^+$ calculate for $[C_{24}H_{42}N_2O_6]^+$ = 455.3116, found: 455.3113.

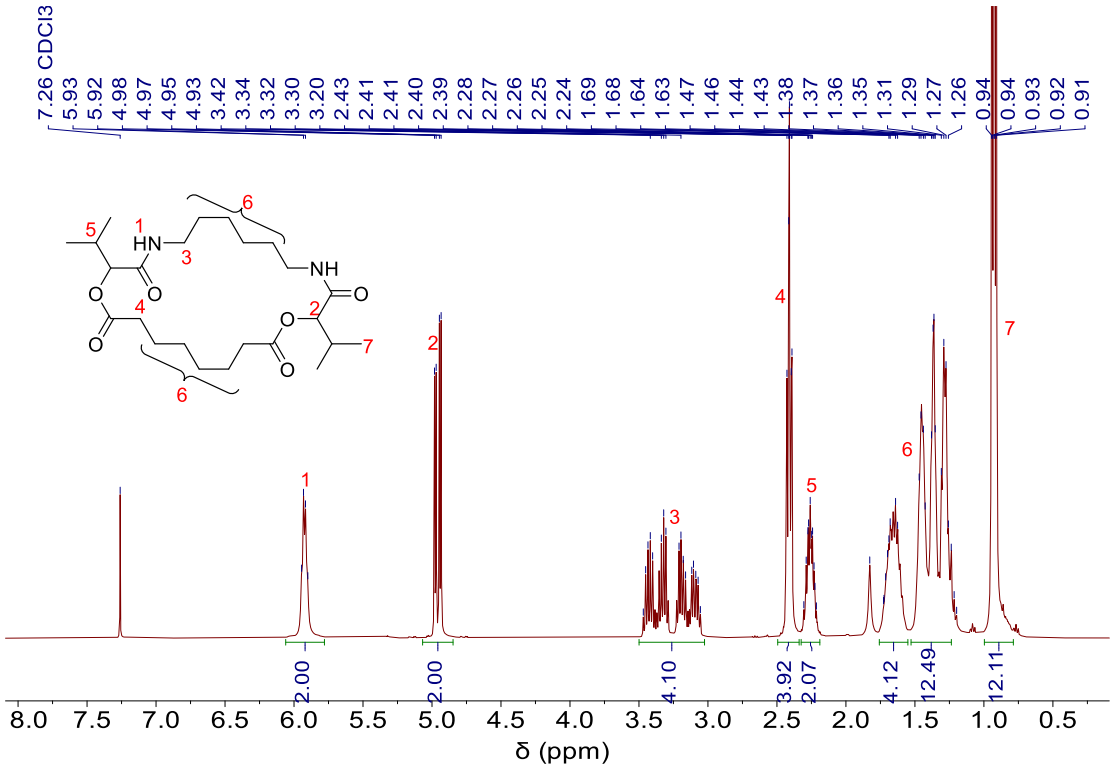

2,13-diisopropyl-1,14-dioxa-4,11-diazacyclotricosane-3,12,15,23-tetraone (1,6-diisocyanohexan, isobutyraldehyde reacted with azelaic acid) **(C9)**

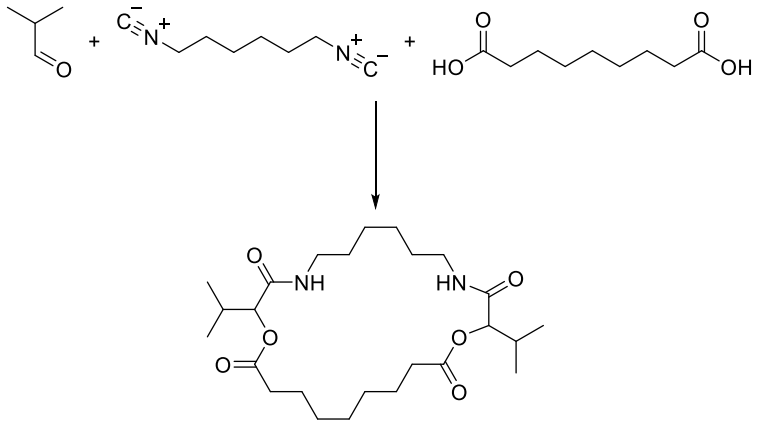

^{1}H-NMR (400 MHz, Chloroform-*d*) δ 5.93 (m, 2H, ^{1}), 5.04 (dd, *J* = 27.7, 4.6 Hz, 2H, ^{2}), 3.54 – 3.00 (m, 4H, ^{3}), 2.54 – 2.24 (m, 4H, ^{4}), 2.34 – 2.20 (m, 2H, ^{5}), 1.79 – 1.19 (m, 18H, ^{6}), 1.00 – 0.87 (m, 12H, ^{7}).
^{13}C-NMR (101 MHz, $CDCl_3$) δ 172.55, 169.52, 169.40, 78.37, 78.30, 38.89, 34.07, 30.43, 30.24, 29.34, 28.92, 26.58, 26.41, 25.00, 18.88, 17.17, 17.05.
IR: 3278.1, 3068.6, 2963.3, 2932.7, 2874.6, 2856.6, 1741.8, 1645.6, 1537.5, 1466.7, 1372.5, 1164.4, 1125.9, 1001.1, 725.1, 642.7, 404.5,
ESI-MS m/z: $[M+H]^+$ calculate for $[C_{25}H_{44}N_2O_6]^+$ = 469.3272, found: 469.3270.

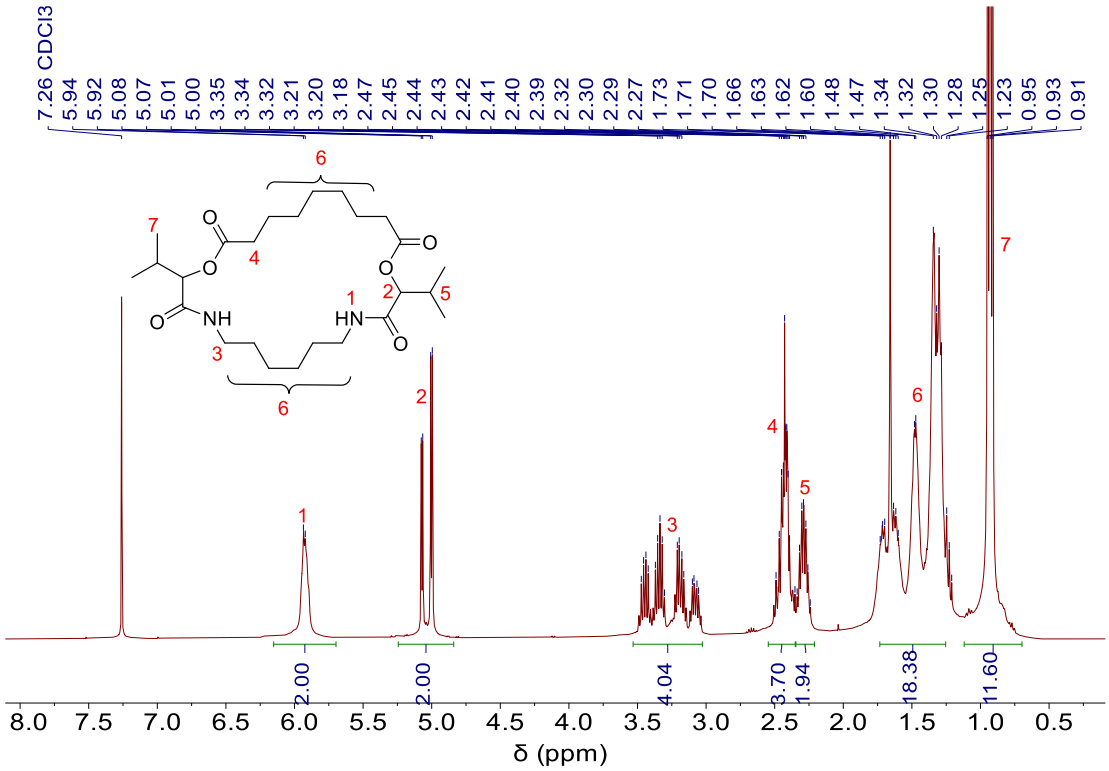

2,13-diisopropyl-1,14-dioxa-4,11-diazacyclotetracosane-3,12,15,24-tetraone (1,6-diisocyanohexan, isobutyraldehyde reacted with sebacic acid) **(C10)**

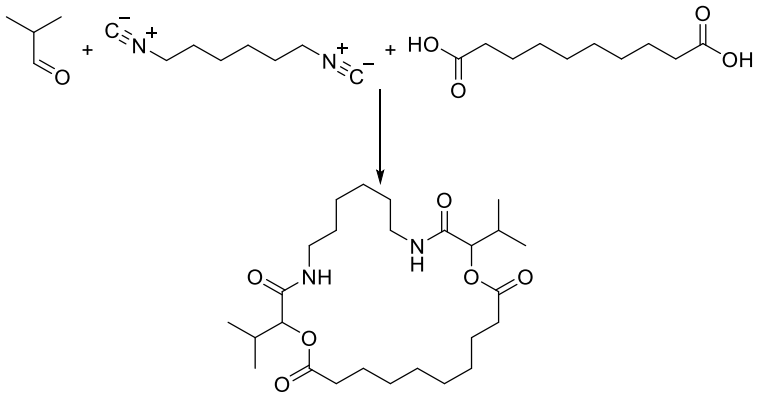

^{1}H-NMR (400 MHz, Chloroform-*d*) δ 5.96 (q, *J* = 5.4 Hz, 2H, ^{1}), 5.08 (dd, *J* = 12.3, 4.3 Hz, 2H, ^{2}), 3.56 – 3.05 (m, 4H, ^{3}), 2.49 – 2.35 (m, 4H, ^{4}), 2.33 – 2.25 (m, 2H, ^{5}), 1.81 – 1.13 (m, 20H, ^{6}), 1.04 – 0.77 (m, 12H, ^{7}).

^{13}C-NMR (101 MHz, $CDCl_3$) δ 172.41, 169.43, 169.36, 78.11, 39.00, 38.98, 34.38, 30.54, 30.43, 29.54, 29.52, 29.06, 29.04, 29.02, 26.84, 26.81, 25.27, 25.25, 18.87, 18.86, 17.04, 16.98.

IR: 3288.1, 3077.3, 2962.2, 2929.3, 2872.5, 2856.1, 1740.9, 1646.4, 1531.3, 1463.6, 1370.7, 1161.9, 1125.4, 1089.3, 1005.3, 721.6, 639.3, 489.1, 409.2

ESI-MS m/z: $[M+H]^+$ calculate for $[C_{26}H_{46}N_2O_6]^+$ = 483.3429, found: 483.3425.

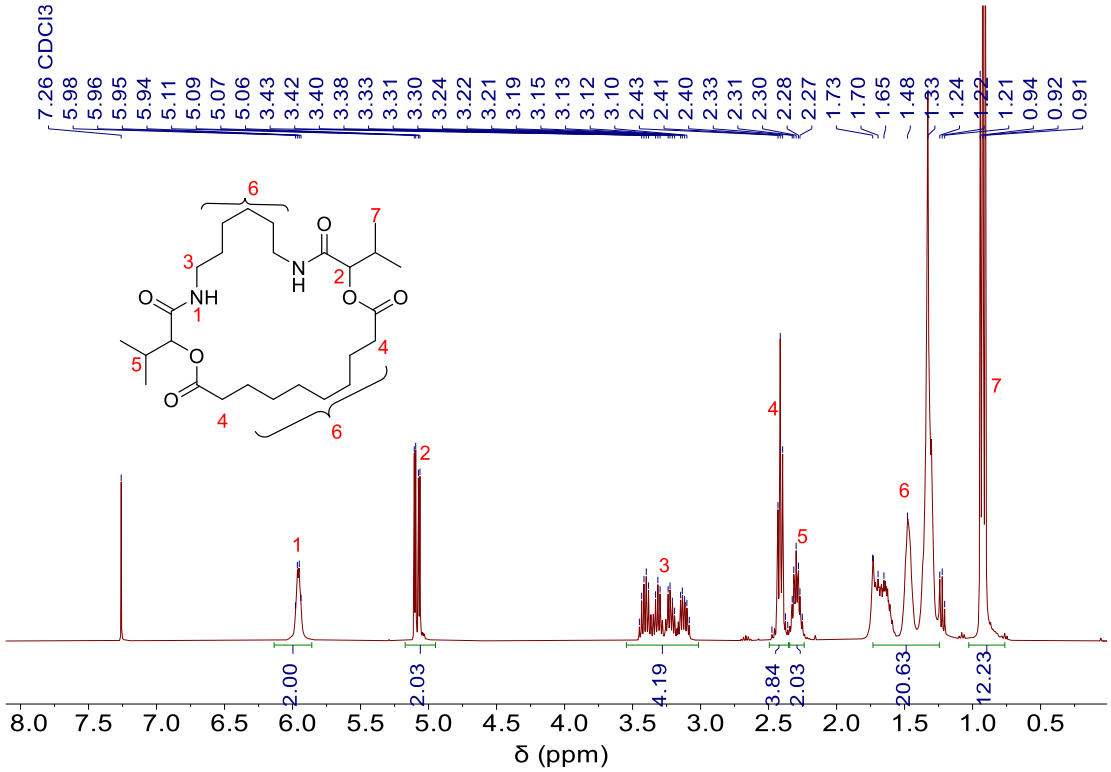

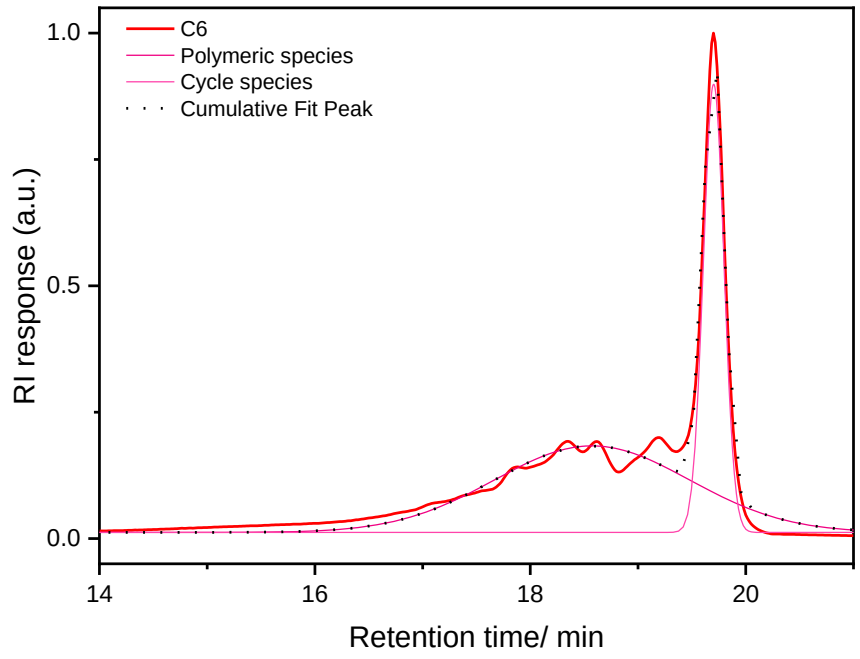

Supplementary Figure 26: Peak deconvolution of SEC diagrams from crude products **C6**.

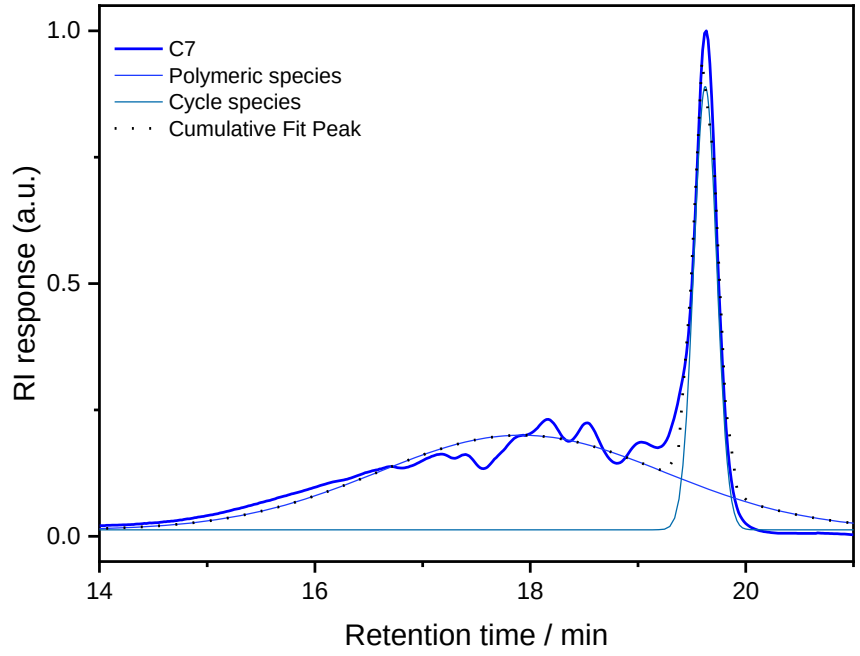

Supplementary Figure 27: Peak deconvolution of SEC diagrams from crude products **C7.**

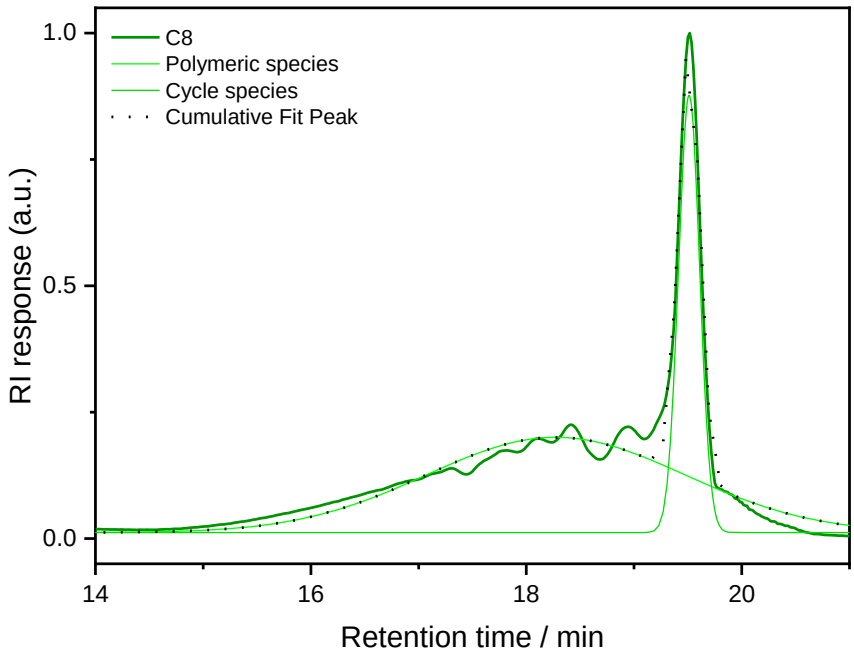

Supplementary Figure 28: Peak deconvolution of SEC diagrams from crude products **C8.**

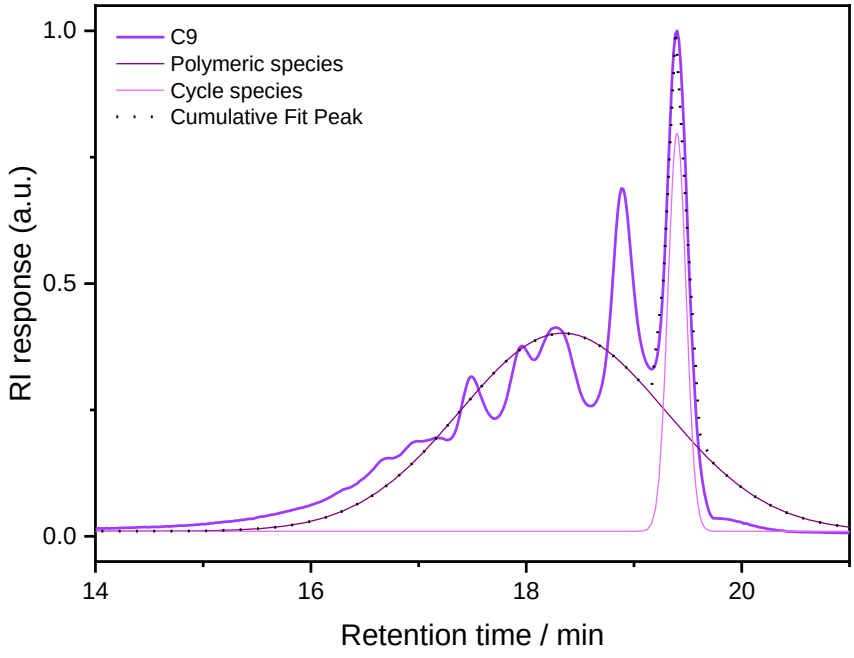

Supplementary Figure 29: Peak deconvolution of SEC diagrams from crude products **C9.**

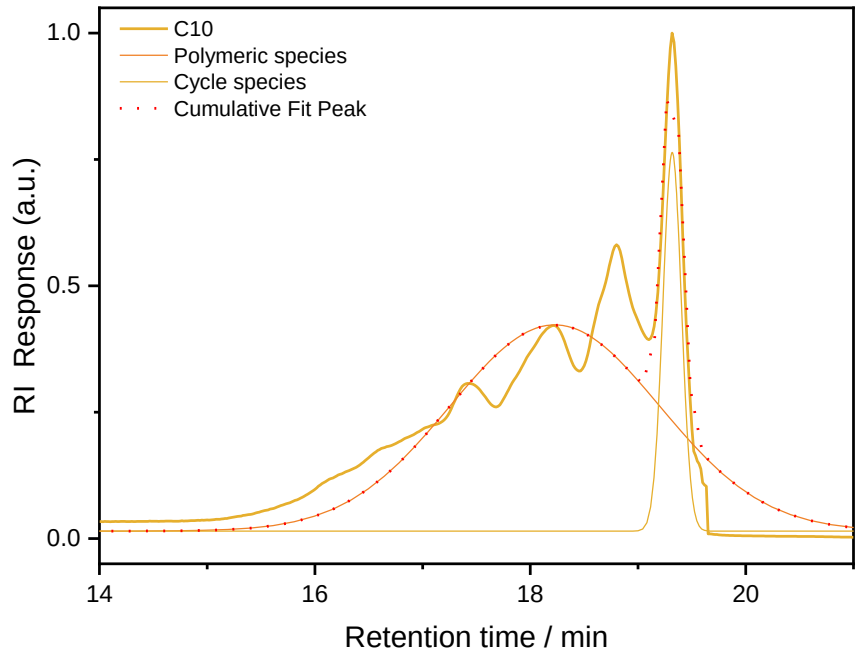

Supplementary Figure 30: Peak deconvolution of SEC diagrams from crude products **C10.**

1,6-Diisocyanohexane **8** reacted in P-3CR

Diacid / Product	Theoretical value(H^+)	Experimental value(H^+)	yield
Adipic acid (**C6**)	427.2803	427.2801	27%
Pimelic acid (**C7**)	441.2959	441.2957	30%
Suberic acid (**C8**)	455.3116	455.3127	34%
Azelaic acid (**C9**)	469.3272	469.3271	24%
Sebacic acid (**C10**)	483.3429	483.3425	21%

Supplementary Table 11: Theoretical values for the molecular weights of the cyclic macromolecules and the values found in ESI-MS, as well as the final yield.

Peak deconvolution.

Product	Polymer species	Cycle species
C6	69%	31%
C7	65%	35%
C8	61%	39%
C9	63%	27%
C10	76%	24%

Supplementary Table 12: Determination of signal areas of polymeric products and macrocycles for products **C6-C10** using a peak deconvolution.

7 Appendix

7.1 List of Abbreviation

ADMET	Acyclic diene metathesis
ASCII	American Standard Coder for Information Interchange
COSY	Correlation spectroscopy
CuAAC	Copper-catalyzed azide/alkyne cycloaddition
Cy	Cyclohexane
DCM	Dichloromethane
DMSO	Dimethyl sulfoxide
DMSO-d_6	Deuturated dimethyl sulfoxide
DNA	Deoxyribonucleic acid
DOSY	Diffusion ordered spectroscopy
DSC	Differential scanning calorimetry
EA	Ethyl acetate
ESI	Electrospray ionization
ESI-MS	Electrospray ionization - mass spectrometry
ESI-MS/MS	Electrospray ionization tandem mass spectrometry
EWG	Electron withdrawing group
GPC	Gel permeation chromatography
HBTU	Hexafluorophosphate benzotriazole tetramethyl uronium
HMBC	Heteronuclear multiple bond correlation
HSQC	Heteronuclear single quantum coherence spectroscopy
IEG	Iterative exponential growth
IMCR	Isocyanide-based multicomponent reaction
Inorm	Normalized intensity
IR	Infrared
IUPAC	International Union of Pure and Applied Chemistry
LC-MS	Liquid chromatography – mass spectrometry

LC-MS/MS	Liquid chromatography – tandem mass spectrometry
m	Mass
M	Molar mass
m/z	Mass-to-charge ratio
MALDI-MS	matrix assisted laser desorption ionization – mass spectrometry
MALDI-MS/MS	matrix assisted laser desorption ionization – tandem mass spectrometry
MCR	Multicomponent reaction
Mg	Milligram
Min	Minute
Mn	Number of average molar mass
MS	Mass spectrometry
Mw	Mass average molar mass
NCE	Normalized collision energy
nm	Nanometer
NMR	Nuclear magnetic resonance
OEG	Oligo(ethylene glycol)
OPE	oligo(phenylene ethynylene)
P-3CR	Passerini-three-component reaction
PEG	Poly(ethylene glycol)
ppm	Parts per million
rt	Room temperature
SEC	Size exclusion chromatography
SPPS	Solid phase peptide synthesis
TAD	1,2,4-Triazoline-3,5-diones
TBAF	N,N,N-Tributylbutan-1-aminium fluoride
TEA	Triethylamine
TFA	Trifluoroacetic acid
TGA	Thermogravimetric analysis
THF	Tetrahydrofuran

THP	Tetrahydropyran
TLC	Thin-layer chromatography
p-TsCl	para-toluenesulfonylchloride
U-4CR	Ugi-four-component reaction
µL	Mikroliter
wt%	Weight percent

7.2 List of Schemes

7.3 List of Figures

7.4 List of Tables

8 Refence

(1) Domling, A.; Ugi, I. I. Multicomponent Reactions with Isocyanides. *Angew Chem Int Ed Engl* **2000**, *39* (18), 3168-3210. DOI: 10.1002/1521-377

(2) Domling, A. Recent developments in isocyanide based multicomponent reactions in applied chemistry. *Chem Rev* **2006**, *106* (1), 17-89. DOI: 10.1021/cr0505728

(3) Cioc, R. C.; Ruijter, E.; Orru, R. V. A. Multicomponent reactions: advanced tools for sustainable organic synthesis. *Green Chem.* **2014**, *16* (6), 2958-2975. DOI: 10.1039/c4gc00013g.

(4) Ugi, I.; Dömling, A.; Hörl, W. Multicomponent reactions in organic chemistry. *Endeavour* **1994**, *18* (3), 115-122. DOI: 10.1016/S0160-9327(05)80086-9.

(5) Slobbe, P.; Ruijter, E.; Orru, R. V. A. Recent applications of multicomponent reactions in medicinal chemistry. *MedChemComm* **2012**, *3* (10). DOI: 10.1039/c2md20089a.

(6) Akritopoulou-Zanze, I. Isocyanide-based multicomponent reactions in drug discovery. *Curr Opin Chem Biol* **2008**, *12* (3), 324-331. DOI: 10.1016/j.cbpa.2008.02.004

(7) Wang, S.; Fu, C.; Wei, Y.; Tao, L. Facile One-Pot Synthesis of New Functional Polymers through Multicomponent Systems. *Macromolecular Chemistry and Physics* **2014**, *215* (6), 486-492.

(8) Kreye, O.; Toth, T.; Meier, M. A. Introducing multicomponent reactions to polymer science: Passerini reactions of renewable monomers. *J Am Chem Soc* **2011**, *133* (6), 1790-1792. DOI: 10.1021/ja1113003

(9) Dömling, A. Isocyanide based multi component reactions in combinatorial chemistry. *Combinatorial Chemistry & High Throughput Screening* **1998**, *1* (1), 1-22.

(10) Oertel, K.; Zech, G.; Kunz, H. Stereoselective Combinatorial Ugi-Multicomponent Synthesis on Solid Phase. *Angewandte Chemie International Edition* **2000**, *39* (8), 1431-1433. DOI: 10.1002/(sici)1521-3773(20000417).

(11) Yang, B.; Zhao, Y.; Wei, Y.; Fu, C.; Tao, L. The Ugi reaction in polymer chemistry: syntheses, applications and perspectives. *Polymer Chemistry* **2015**, *6* (48), 8233-8239. DOI: 10.1039/c5py01398d.

(12) Strecker, A. Ueber die künstliche Bildung der Milchsäure und einen neuen, dem Glycocoll homologen Körper. *Justus Liebigs Annalen der Chemie* **1850**, *75* (1), 27-45. DOI: 10.1002/jlac.18500750103.

(13) Hantzsch, A. Ueber die Synthese pyridinartiger Verbindungen aus Acetessigäther und Aldehydammoniak. *Justus Liebigs Annalen der Chemie* **1882**, *215* (1), 1-82. DOI: 10.1002/jlac.18822150102.

(14) Hantzsch, A.; Werner, A. Ueber räumliche Anordnung der Atome in stickstoffhaltigen Molekülen. *Berichte der deutschen chemischen Gesellschaft* **1890**, *23* (1), 11-30. DOI: 10.1002/cber.18900230104.

(15) Biginelli, P. Ueber aldehyduramide des acetessigäthers. *Berichte der deutschen chemischen Gesellschaft* **1891**, *24* (1), 1317-1319.

(16) Mannich, C.; Krösche, W. Ueber ein Kondensationsprodukt aus Formaldehyd, Ammoniak und Antipyrin. *Archiv der Pharmazie* **1912**, *250* (1), 647-667. DOI: 10.1002/ardp.19122500151

(17) Passerini, M.; Simone, L. Sopra gli isonitrili (I). Composto del p-isonitril-azobenzolo con acetone ed acido acetico. *Gazz. Chim. Ital* **1921**, *51* (2), 126-129.

(18) Fields, E. K. The Synthesis of Esters of Substituted Amino Phosphonic Acids1a. *Journal of the American Chemical Society* **1952**, *74* (6), 1528-1531. DOI: 10.1021/ja01126a054.

(19) Asinger, F. Über die gemeinsame Einwirkung von Schwefel und Ammoniak auf Ketone. *Angewandte Chemie* **1956**, *68* (12), 413-413.
(20) Ugi, I. K. Versammlungsberichte. *Angewandte Chemie* **1959**, *71* (11), 373-388. DOI: 10.1002/ange.19590711110.
(21) Naithani, K.; Bhowmik, S. Trends in the Synthesis of Antimicrobial Derivatives by using the Gewald, Strecker, and Groebke-Blackburn-Bienaymé (GBB) Reactions. *Medicinal Chemistry* **2024**, *20* (7), 663-688. DOI: 10.2174/0115734064282699240315042428.
(22) Xu, J.; Fan, W. G.; Popowycz, F.; Queneau, Y.; Gu, Y. L. Multicomponent Reactions: A New Strategy for Enriching the Routes of Value-Added Conversions of Bio-platform Molecules. *Chinese Journal of Organic Chemistry* **2019**, *39* (8), 2131-2138. DOI: 10.6023/cjoc201904065.
(23) Manchado, A.; Ramos, V. E.; Díez, D.; Garrido, N. M. Multicomponent Domino Reaction in the Asymmetric Synthesis of Cyclopentan c pyran Core of Iridoid Natural Products. *Molecules* **2020**, *25* (6). DOI: 10.3390/molecules25061308.
(24) Agarwal, M.; Verma, K.; Pathak, G.; Pathak, S.; Mathur, J.; Kumar, M. Advances in Isocyanide-Based Multicomponent Synthesis of Quinoxaline Scaffolds. *Chemistryselect* **2023**, *8* (34). DOI: 10.1002/slct.202301448.
(25) Fragkiadakis, M.; Zingiridis, M.; Loukopoulos, E.; Neochoritis, C. G. New oxacycles on the block: benzodioxepinones via a Passerini reaction. *Molecular Diversity* **2024**, *28* (1), 29-35. DOI: 10.1007/s11030-022-10502-9.
(26) Cores, A.; Carbajales, C.; Coelho, A. Multicomponent Reactions in Antimitotic Drug Discovery. *Current Topics in Medicinal Chemistry* **2014**, *14* (20), 2209-2230. DOI: 10.2174/1568026614666141127115130.
(27) Maddila, S.; Jonnalagadda, S. B.; Gangu, K. K.; Maddila, S. N. Recent Advances in the Synthesis of Pyrazole Derivatives Using Multicomponent Reactions. *Current Organic Synthesis* **2017**, *14* (5), 634-653. DOI: 10.2174/1570179414666161104162038.
(28) de Marigorta, E. M.; de Los Santos, J. M.; de Retana, A. M. O.; Vicario, J.; Palacios, F. Multicomponent reactions (MCRs): a useful access to the synthesis of benzo-fused γ-lactams. *Beilstein Journal of Organic Chemistry* **2019**, *15*, 1065-1085. DOI: 10.3762/bjoc.15.104.
(29) Gazzotti, S.; Rainoldi, G.; Silvani, A. Exploitation of the Ugi-Joullie reaction in drug discovery and development. *Expert Opinion on Drug Discovery* **2019**, *14* (7), 639-652. DOI: 10.1080/17460441.2019.1604676.
(30) Younus, H. A.; Al-Rashida, M.; Hameed, A.; Uroos, M.; Salar, U.; Rana, S.; Khan, K. M. Multicomponent reactions (MCR) in medicinal chemistry: a patent review (2010-2020). *Expert Opinion on Therapeutic Patents* **2021**, *31* (3), 267-289. DOI: 10.1080/13543776.2021.1858797.
(31) Botta, L.; Cesarini, S.; Zippilli, C.; Bizzarri, B. M.; Fanelli, A.; Saladino, R. Multicomponent Reactions in the Synthesis of Antiviral Compounds. *Current Medicinal Chemistry* **2022**, *29* (12), 2013-2050. DOI: 10.2174/0929867328666211007121837.
(32) Quazi, S.; Rashid, M. T.; Malik, J. A.; Gavas, S. The Discovery of Novel Antimicrobial Agents through the Application of Isocyanide-Based Multicomponent Reactions. *Antibiotics-Basel* **2023**, *12* (5). DOI: 10.3390/antibiotics12050849.
(33) Zhang, J.; Kang, S. S.; Zhang, Z.; Li, M. Multiscale and multicomponent layer by layer assembly of optical thin films triggered by electrochemical coupling reactions of N-alkylcarbazoles. *Chinese Chemical Letters* **2016**, *27* (4), 487-491. DOI: 10.1016/j.cclet.2016.01.035.
(34) Tan, J. N.; Ahmar, M.; Queneau, Y. Glycosyloxymethylfurfural (GMF) in Multicomponent

Aza-Morita-Baylis-Hillman Reaction: Rapid Access to Highly Functionalized Carbohydrate Scaffolds. *Current Organic Synthesis* **2018**, *15* (3), 430-435. DOI: 10.2174/1570179415666180103155212.

(35) Sharma, U. K.; Ranjan, P.; Van der Eycken, E. V.; You, S. L. Sequential and direct multicomponent reaction (MCR)-based dearomatization strategies. *Chemical Society Reviews* **2020**, *49* (23), 8721-8748. DOI: 10.1039/d0cs00128g.

(36) Chaudhary, A. Recent development in the synthesis of heterocycles by 2-naphthol-based multicomponent reactions. *Molecular Diversity* **2021**, *25* (2), 1211-1245. DOI: 10.1007/s11030-020-10076-4.

(37) Pinto, L. M. A.; Adeoye, O.; Thomasi, S. S.; Francisco, A. P.; Cabral-Marques, H. A single-step multicomponent synthesis of a quinoline derivative and the characterization of its cyclodextrin inclusion complex. *Journal of Molecular Structure* **2021**, *1237*. DOI: 10.1016/j.molstruc.2021.130391.

(38) Fu, J.; He, Z. Y.; Hu, X.; Guo, T.; Liang, Y.; Deng, F. J.; Liu, M. Y.; Wen, Y. Q.; Zhang, X. Y.; Wei, Y. Synthesis of amphiphilic AIE fluorescent nanoparticles via CO2 involved multicomponent reaction and its biological imaging potential. *Dyes and Pigments* **2023**, *210*. DOI: 10.1016/j.dyepig.2022.110990.

(39) Saini, K. K.; Rani, R.; Muskan; Khanna, N.; Mehta, B.; Kumar, R. An Overview of Recent Advances in Hantzsch's Multicomponent Synthesis of 1,4-Dihydropyridines: A Class of Prominent Calcium Channel Blockers. *Current Organic Chemistry* **2023**, *27* (2), 119-129. DOI: 10.2174/1385272827666230403112419.

(40) Tang, M.; Xing, D.; Cai, M. Q.; Hu, W. H. Diazo Compounds-Involved Catalytic Asymmetric Multicomponent Reactions. *Chinese Journal of Organic Chemistry* **2014**, *34* (7), 1268-1276. DOI: 10.6023/cjoc201404010.

(41) Yang, L.; Zhang, Z.; Cheng, B. F.; You, Y. Z.; Wu, D. C.; Hong, C. Y. Two tandem multicomponent reactions for the synthesis of sequence-defined polymers. *Science China-Chemistry* **2015**, *58* (11), 1734-1740. DOI: 10.1007/s11426-015-5448-0.

(42) Bhat, S. I. One-Pot Construction of Bis-Heterocycles through Isocyanide Based Multicomponent Reactions. *Chemistryselect* **2020**, *5* (27), 8040-8061. DOI: 10.1002/slct.202002154.

(43) Longo, L. S.; Siqueira, F. A.; Anjos, N. S.; Santos, G. F. D. Scandium(III)-Triflate-Catalyzed Multicomponent Reactions for the Synthesis of Nitrogen Heterocycles. *Chemistryselect* **2021**, *6* (20), 5097-5109. DOI: 10.1002/slct.202101032.

(44) Thopate, Y.; Singh, R.; Rastogi, S. K.; Sinha, A. K. Cascade Multicomponent Reaction Involving Unprecedented Gould Jacobs-Heck/Suzuki Coupling-Hydrolysis-Decarboxylation Reactions in One Pot: Rapid Synthesis of Hybrid Heterocyclic Molecules. *Asian Journal of Organic Chemistry* **2022**, *11* (8). DOI: 10.1002/ajoc.202200343.

(45) Yadav, P.; Varma, A. A.; Punnya, A. J.; Gopinath, P. Photoredox-mediated Multicomponent Reactions. *Asian Journal of Organic Chemistry* **2022**, *11* (10). DOI: 10.1002/ajoc.202200390.

(46) Llevot, A.; Boukis, A. C.; Oelmann, S.; Wetzel, K.; Meier, M. A. R. An Update on Isocyanide-Based Multicomponent Reactions in Polymer Science. *Top Curr Chem (Cham)* **2017**, *375* (4), 66. DOI: 10.1007/s41061-017-0153-4

(47) Ugi, I.; Werner, B.; Dömling, A. The chemistry of isocyanides, their multicomponent reactions and their libraries. *Molecules* **2003**, *8* (1), 53-66.

(48) Ugi, I.; Fetzer, U.; Eholzer, U.; Knupfer, H.; Offermann, K. Isonitrile Syntheses. *Angewandte Chemie International Edition in English* **1965**, *4* (6), 472-484. DOI: 10.1002/anie.196504721.
(49) Lieke, W. Ueber das cyanallyl. *Justus Liebigs Annalen der Chemie* **1859**, *112* (3), 316-321.
(50) Gautier, A.; Chern, J. L. A. 142, 289. e) Gauteir, A. *Justus Liebigs Ann. Chern* **1869**, *146*, 119.
(51) Hofmann, A. W. Ueber eine neue Reihe von Homologen der Cyanwasserstoffsäure. *Justus Liebigs Annalen der Chemie* **1867**, *144* (1), 114-120. DOI: 10.1002/jlac.18671440116.
(52) Si, Y. X.; Zhu, P. F.; Zhang, S. L. Synthesis of Isocyanides by Reacting Primary Amines with Difluorocarbene. *Org Lett* **2020**, *22* (22), 9086-9090. DOI: 10.1021/acs.orglett.0c03472
(53) Kitano, Y.; Chiba, K.; Tada, M. A direct conversion of alcohols to isocyanides. *Tetrahedron Lett* **1998**, *39* (14), 1911-1912. DOI: Doi 10.1016/S0040-4039(98)00045-8.
(54) Gassman, P. G.; Guggenheim, T. L. Opening of Epoxides with Trimethylsilyl Cyanide to Produce Beta-Hydroxy Isonitriles - a General-Synthesis of Oxazolines and Beta-Amino Alcohols. *Journal of the American Chemical Society* **1982**, *104* (21), 5849-5850. DOI: DOI 10.1021/ja00385a078.
(55) Ugi, I.; Meyr, R. Neue darstellungsmethode für isonitrile. *Angewandte Chemie* **1958**, *70* (22-23), 702-703.
(56) Waibel, K. A.; Nickisch, R.; Möhl, N.; Seim, R.; Meier, M. A. R. A more sustainable and highly practicable synthesis of aliphatic isocyanides. *Green Chemistry* **2020**, *22* (3), 933-941. DOI: 10.1039/c9gc04070f.
(57) Efraty, A.; Feinstein, I.; Wackerle, L.; Goldman, A. Synthesis of some aromatic diisocyanides with trichloromethyl chloroformate. *The Journal of Organic Chemistry* **1980**, *45* (20), 4059-4061. DOI: 10.1021/jo01308a027.
(58) Skorna, G.; Ugi, I. Isocyanide Synthesis with Diphosgene. *Angewandte Chemie International Edition in English* **1977**, *16* (4), 259-260. DOI: 10.1002/anie.197702591.
(59) Keating, T. A.; Armstrong, R. W. Postcondensation modifications of Ugi four-component condensation products: 1-Isocyanocyclohexene as a convertible isocyanide. Mechanism of conversion, synthesis of diverse structures, and demonstration of resin capture. *Journal of the American Chemical Society* **1996**, *118* (11), 2574-2583. DOI: DOI 10.1021/ja953868b.
(60) Ugi, I.; Meyr, R. Isonitrile, I. Darstellung von Isonitrilen aus monosubstituierten Formamiden durch Wasserabspaltung. *Chemische Berichte* **1960**, *93* (1), 239-248.
(61) Neochoritis, C. G.; Zarganes-Tzitzikas, T.; Stotani, S.; Dömling, A.; Herdtweck, E.; Khoury, K.; Dömling, A. Leuckart–Wallach route toward isocyanides and some applications. *ACS combinatorial science* **2015**, *17* (9), 493-499.
(62) Guirado, A.; Zapata, A.; Fenor, M. Electrochemical Reduction of Carbonimidoyl Dichlorides - a New Method for the Preparation of Isocyanides. *Tetrahedron Lett* **1992**, *33* (33), 4779-4782. DOI: Doi 10.1016/S0040-4039(00)61284-4.
(63) Leech, M. C.; Petti, A.; Tanbouza, N.; Mastrodonato, A.; Goodall, I. C. A.; Ollevier, T.; Dobbs, A. P.; Lam, K. Anodic Oxidation of Aminotetrazoles: A Mild and Safe Route to Isocyanides. *Org Lett* **2021**, *23* (24), 9371-9375. DOI: 10.1021/acs.orglett.1c03475
(64) Massarotti, A.; Brunelli, F.; Aprile, S.; Giustiniano, M.; Tron, G. C. Medicinal Chemistry of Isocyanides. *Chemical Reviews* **2021**, *121* (17), 10742-10788. DOI: 10.1021/acs.chemrev.1c00143.
(65) Inoue, Y.; Takashima, S.; Nogata, Y.; Yoshimura, E.; Chiba, K.; Kitano, Y. Isocyanides Derived from α,α-Disubstituted Amino Acids: Synthesis and Antifouling Activity Assessment. *Chemistry & Biodiversity* **2018**, *15* (3), e1700571. DOI: 10.1002/cbdv.201700571.

(66) Kitano, Y.; Yokoyama, A.; Nogata, Y.; Shinshima, K.; Yoshimura, E.; Chiba, K.; Tada, M.; Sakaguchi, I. Synthesis and anti-barnacle activities of novel 3-isocyanotheonellin analogues. *Biofouling* **2003**, *19*, 187-192. DOI: 10.1080/0892701021000053390.
(67) Barreto, A. D. S.; Andrade, C. K. Z. Synthesis of (macro) heterocycles by consecutive/repetitive isocyanide-based multicomponent reactions. *Beilstein Journal of Organic Chemistry* **2019**, *15*, 906-930. DOI: 10.3762/bjoc.15.88.
(68) Manenti, M.; Gusmini, S.; Lo Presti, L.; Silvani, A. Exploiting Enantiopure β-Amino Boronic Acids in Isocyanide-Based Multicomponent Reactions. *European Journal of Organic Chemistry* **2022**, *2022* (25). DOI: 10.1002/ejoc.202200435.
(69) Nazeri, M. T.; Nasiriani, T.; Farhid, H.; Javanbakht, S.; Bahri, F.; Shadi, M.; Shaabani, A. Sustainable Synthesis of Pseudopeptides via Isocyanide-Based Multicomponent Reactions in Water. *Acs Sustainable Chemistry & Engineering* **2022**, *10* (25), 8115-8134. DOI: 10.1021/acssuschemeng.2c01030.
(70) Hulme, C.; Gore, V. "Multi-component reactions : Emerging chemistry in drug discovery" 'From xylocain to crixivan'. *Current Medicinal Chemistry* **2003**, *10* (1), 51-80. DOI: 10.2174/0929867033368600.
(71) Akritopoulou-Zanze, I. Isocyanide-based multicomponent reactions in drug discovery. *Current Opinion in Chemical Biology* **2008**, *12* (3), 324-331. DOI: 10.1016/j.cbpa.2008.02.004.
(72) Wiemann, J.; Heller, L.; Csuk, R. An access to a library of novel triterpene derivatives with a promising pharmacological potential by Ugi and Passerini multicomponent reactions. *European Journal of Medicinal Chemistry* **2018**, *150*, 176-194. DOI: 10.1016/j.ejmech.2018.02.060.
(73) Lei, X. F.; Thomaidi, M.; Angeli, G. K.; Dömling, A.; Neochoritis, C. G. Fluorene-Based Multicomponent Reactions. *Synlett* **2022**, *33* (02), 155-160. DOI: 10.1055/a-1471-9080.
(74) Llevot, A.; Boukis, A. C.; Oelmann, S.; Wetzel, K.; Meier, M. A. R. An Update on Isocyanide-Based Multicomponent Reactions in Polymer Science. *Topics in Current Chemistry* **2017**, *375* (4). DOI: 10.1007/s41061-017-0153-4.
(75) Cai, Z. X.; Ren, Y.; Li, X. F.; Shi, J. B.; Tong, B.; Dong, Y. P. Functional Isocyanide-Based Polymers. *Accounts of Chemical Research* **2020**, *53* (12), 2879-2891. DOI: 10.1021/acs.accounts.0c00514.
(76) Cheng, T. Y.; Chen, Y. Z.; Ding, J.; Qin, A. J.; Tang, B. Z. Isocyanoacetate-Aldehyde Polymerization: A Facile Tool toward Functional Oxazoline-Containing Polymers. *Macromolecular Rapid Communications* **2020**, *41* (12). DOI: 10.1002/marc.202000179.
(77) Wang, X. H.; Li, B. X.; Peng, J. W.; Wang, B. N.; Qin, A. J.; Tang, B. Z. Multicomponent Polymerization of Alkynes, Isocyanides, and Isocyanates toward Heterocyclic Polymers. *Macromolecules* **2021**, *54* (14), 6753-6761. DOI: 10.1021/acs.macromol.1c00556.
(78) Li, M. Z.; Fu, X. Y.; Wang, J.; Qin, A. J.; Tang, B. Z. Progress in Isocyanide-Based Step-Growth Polymerization. *Macromolecular Chemistry and Physics* **2023**, *224* (3). DOI: 10.1002/macp.202200352.
(79) Van Leusen, A. M.; Wildeman, J.; Oldenziel, O. H. Chemistry of sulfonylmethyl isocyanides. 12. Base-induced cycloaddition of sulfonylmethyl isocyanides to carbon,nitrogen double bonds. Synthesis of 1,5-disubstituted and 1,4,5-trisubstituted imidazoles from aldimines and imidoyl chlorides. *The Journal of Organic Chemistry* **1977**, *42* (7), 1153-1159. DOI: 10.1021/jo00427a012.
(80) Bon, R. S.; Hong, C.; Bouma, M. J.; Schmitz, R. F.; de Kanter, F. J.; Lutz, M.; Spek, A. L.; Orru, R. V. Novel Multicomponent Reaction for the Combinatorial Synthesis of 2-Imidazolines.

Org Lett **2003**, *5* (20), 3759-3762. DOI: 10.1021/ol035521g

(81) Lipp, M.; Dallacker, F.; Köcker, I. M. z. Über die Addition von Schwefel und Selen an Isonitrile. *Monatshefte für Chemie und verwandte Teile anderer Wissenschaften* **1959**, *90* (1), 41-48. DOI: 10.1007/BF00901130.

(82) Németh, A. G.; Keserű, G. M.; Ábrányi-Balogh, P. A novel three-component reaction between isocyanides, alcohols or thiols and elemental sulfur: a mild, catalyst-free approach towards O-thiocarbamates and dithiocarbamates. *Beilstein Journal of Organic Chemistry* **2019**, *15*, 1523-1533. DOI: 10.3762/bjoc.15.155.

(83) Ugi, I.; Steinbruckner, C. Concerning a new condensation principle. *Angew. Chem* **1960**, *72* (267), 1701-1705.

(84) Ugi, I. The α-Addition of Immonium Ions and Anions to Isonitriles Accompanied by Secondary Reactions. *Angewandte Chemie International Edition in English* **1962**, *1* (1), 8-21. DOI: 10.1002/anie.196200081.

(85) Ugi, I. Neuere Methoden der präparativen organischen Chemie IV Mit Sekundär-Reaktionen gekoppelte α-Additionen von Immonium-Ionen und Anionen an Isonitrile. *Angewandte Chemie* **1962**, *74* (1), 9-22.

(86) Ugi, I.; Rosendahl, F. K.; Bodesheim, F. Isonitrile, XIII. Kondensation von primären Aminen und Ketonen mit Isonitrilen und Rhodanwasserstoffsäure. *Justus Liebigs Annalen der Chemie* **1963**, *666* (1), 54-61.

(87) Ugi, I.; Steinbrückner, C. Isonitrile, II. Reaktion von isonitrilen mit carbonylverbindungen, aminen und stickstoffwasserstoffsäure. *Chemische Berichte* **1961**, *94* (3), 734-742.

(88) Ugi, I.; Steinbrückner, C. Isonitrile, IX. α-Addition von Immonium-Ionen und Carbonsäure-Anionen an Isonitrile. *Chemische Berichte* **1961**, *94* (10), 2802-2814. DOI: 10.1002/cber.19610941032.

(89) Keating, T. A.; Armstrong, R. W. The Ugi five-component condensation using CO, CS, and COS as oxidized carbon sources. *Journal of Organic Chemistry* **1998**, *63* (3), 867-871. DOI: DOI 10.1021/jo971463z.

(90) Sehlinger, A.; Schneider, R.; Meier, M. A. Ugi reactions with CO2 : access to functionalized polyurethanes, polycarbonates, polyamides, and polyhydantoins. *Macromol Rapid Commun* **2014**, *35* (21), 1866-1871. DOI: 10.1002/marc.201400385

(91) Borthwick, A. D.; Liddle, J.; Davies, D. E.; Exall, A. M.; Hamlett, C.; Hickey, D. M.; Mason, A. M.; Smith, I. E.; Nerozzi, F.; Peace, S. Pyridyl-2, 5-diketopiperazines as potent, selective, and orally bioavailable oxytocin antagonists: synthesis, pharmacokinetics, and in vivo potency. *Journal of Medicinal Chemistry* **2012**, *55* (2), 783-796.

(92) Demharter, A.; Hörl, W.; Herdtweck, E.; Ugi, I. Synthesis of Chiral 1,1′-Iminodicarboxylic Acid Derivatives from α-Amino Acids, Aldehydes, Isocyanides, and Alcohols by the Diastereoselective Five-Center–Four-Component Reaction. *Angewandte Chemie International Edition in English* **1996**, *35* (2), 173-175. DOI: 10.1002/anie.199601731.

(93) El Kaim, L.; Grimaud, L.; Oble, J. Phenol Ugi-smiles systems: strategies for the multicomponent N-arylation of primary amines with isocyanides, aldehydes, and phenols. *Angew Chem Int Ed Engl* **2005**, *44* (48), 7961-7964. DOI: 10.1002/anie.200502636

(94) Kaim, L. E.; Gizolme, M.; Grimaud, L.; Oble, J. Smiles Rearrangements in Ugi- and Passerini-Type Couplings New Multicomponent Access to O- and N-Arylamides. *J Org Chem* **2007**, *72* (11), 4169-4180. DOI: 10.1021/jo070202e

(95) Levy, A. A.; Rains, H. C.; Smiles, S. CCCCLII.—The rearrangement of hydroxy-sulphones. Part I. *Journal of the Chemical Society (Resumed)* **1931**, 3264-3269.
(96) Nutt, R. F.; Joullie, M. M. Four-component condensation: a new versatile method for the synthesis of substituted prolyl peptides. *Journal of the American Chemical Society* **1982**, *104* (21), 5852-5853. DOI: 10.1021/ja00385a080.
(97) Katsuyama, A.; Matsuda, A.; Ichikawa, S. Revisited Mechanistic Implications of the Joullie-Ugi Three-Component Reaction. *Org Lett* **2016**, *18* (11), 2552-2555. DOI: 10.1021/acs.orglett.6b00827
(98) Nazeri, M. T.; Farhid, H.; Mohammadian, R.; Shaabani, A. Cyclic Imines in Ugi and Ugi-Type Reactions. *ACS Comb Sci* **2020**, *22* (8), 361-400. DOI: 10.1021/acscombsci.0c00046
(99) Bienaymé, H.; Bouzid, K. A New Heterocyclic Multicomponent Reaction For the Combinatorial Synthesis of Fused 3-Aminoimidazoles. *Angewandte Chemie International Edition* **1998**, *37* (16), 2234-2237. DOI: 10.1002/(sici)1521-3773(19980904)
(100) Blackburn, C.; Guan, B.; Fleming, P.; Shiosaki, K.; Tsai, S. Parallel synthesis of 3-aminoimidazo[1,2-a]pyridines and pyrazines by a new three-component condensation. *Tetrahedron Lett* **1998**, *39* (22), 3635-3638. DOI: 10.1016/S0040-4039(98)00653-4.
(101) Groebke, K.; Weber, L.; Mehlin, F. Synthesis of imidazo [1, 2-a] annulated pyridines, pyrazines and pyrimidines by a novel three-component condensation. *Synlett* **1998**, *1998* (06), 661-663.
(102) Boltjes, A.; Domling, A. The Groebke-Blackburn-Bienayme Reaction. *Eur J Chem* **2019**, *2019* (42), 7007-7049. DOI: 10.1002/ejoc.201901124
(103) Baviskar, A. T.; Madaan, C.; Preet, R.; Mohapatra, P.; Jain, V.; Agarwal, A.; Guchhait, S. K.; Kundu, C. N.; Banerjee, U. C.; Bharatam, P. V. N-fused imidazoles as novel anticancer agents that inhibit catalytic activity of topoisomerase IIalpha and induce apoptosis in G1/S phase. *J Med Chem* **2011**, *54* (14), 5013-5030. DOI: 10.1021/jm200235u
(104) Bode, M. L.; Gravestock, D.; Moleele, S. S.; van der Westhuyzen, C. W.; Pelly, S. C.; Steenkamp, P. A.; Hoppe, H. C.; Khan, T.; Nkabinde, L. A. Imidazo[1,2-a]pyridin-3-amines as potential HIV-1 non-nucleoside reverse transcriptase inhibitors. *Bioorganic & Medicinal Chemistry* **2011**, *19* (14), 4227-4237. DOI: 10.1016/j.bmc.2011.05.062.
(105) Heck, S.; Doemling, A. A versatile multi-component one-pot thiazole synthesis. *Synlett* **2000**, *2000* (03), 424-426.
(106) Elders, N.; Ruijter, E.; de Kanter, F. J.; Groen, M. B.; Orru, R. V. Selective formation of 2-imidazolines and 2-substituted oxazoles by using a three-component reaction. *Chemistry* **2008**, *14* (16), 4961-4973. DOI: 10.1002/chem.200800271
(107) Nguyen, T. B.; Ermolenko, L.; Al-Mourabit, A. Three-component reaction between isocyanides, aliphatic amines and elemental sulfur: Preparation of thioureas under mild conditions with complete atom economy. *Synthesis* **2014**, *46* (23), 3172-3179.
(108) Tian, T.; Hu, R.; Tang, B. Z. Room temperature one-step conversion from elemental sulfur to functional polythioureas through catalyst-free multicomponent polymerizations. *Journal of the American Chemical Society* **2018**, *140* (19), 6156-6163.
(109) Baker, R. H.; Stanonis, D. The Passerini Reaction. III. Stereochemistry and Mechanism1,2. *Journal of the American Chemical Society* **1951**, *73* (2), 699-702. DOI: 10.1021/ja01146a060.
(110) Ugi, I.; Bodesheim, F. Isonitrile, VIII. umsetzung von isonitrilen mit hydrazonen und stickstoffwasserstoffsäure. *Chemische Berichte* **1961**, *94* (10), 2797-2801.

(111) Hagedorn, I.; Eholzer, U. Isonitrile, VII. Einstufige Synthese von α-Hydroxysäure-amiden durch Abwandlung der Passerini-Reaktion. *Chemische Berichte* **1965**, *98* (3), 936-940. DOI: 10.1002/cber.19650980337.
(112) Pirrung, M. C.; Sarma, K. D. Multicomponent Reactions Are Accelerated in Water. *J Am Chem Soc* **2004**, *126* (2), 444-445. DOI: 10.1021/ja038583a
(113) Ramozzi, R.; Morokuma, K. Revisiting the Passerini reaction mechanism: existence of the nitrilium, organocatalysis of its formation, and solvent effect. *J Org Chem* **2015**, *80* (11), 5652-5657. DOI: 10.1021/acs.joc.5b00594
(114) Ngouansavanh, T.; Zhu, J. Alcohols in Isonitrile-Based Multicomponent Reaction: Passerini Reaction of Alcohols in the Presence of O-Iodoxybenzoic Acid. *Angewandte Chemie* **2006**, *118* (21), 3575-3577. DOI: 10.1002/ange.200600588.
(115) Maeda, S.; Komagawa, S.; Uchiyama, M.; Morokuma, K. Finding reaction pathways for multicomponent reactions: the Passerini reaction is a four-component reaction. *Angew Chem Int Ed Engl* **2011**, *50* (3), 644-649. DOI: 10.1002/anie.201005336
(116) Onwukamike, K. N.; Grelier, S.; Grau, E.; Cramail, H.; Meier, M. A. R. On the direct use of CO(2) in multicomponent reactions: introducing the Passerini four component reaction. *RSC Adv* **2018**, *8* (55), 31490-31495. DOI: 10.1039/c8ra07150k
(117) Nixey, T.; Hulme, C. Rapid generation of cis-constrained norstatine analogs using a TMSN3-modified Passerini MCC/N-capping strategy. *Tetrahedron Lett* **2002**, *43* (38), 6833-6835.
(118) El Kaim, L.; Gizolme, M.; Grimaud, L. O-Arylative Passerini Reactions. *Org Lett* **2006**, *8* (22), 5021-5023. DOI: 10.1021/ol0617502
(119) Ugi, I.; Rosendahl, K. Isonitrile, VI. Umsetzungen von isonitrilen mit ketenen. *Chemische Berichte* **1961**, *94* (8), 2233-2238.
(120) Neidlein, R. Notizen: Reaktionen mit Acyl-isocyanaten. *Zeitschrift für Naturforschung B* **1964**, *19* (12), 1159-1160. DOI: doi:10.1515/znb-1964-1217
(121) Soeta, T.; Kojima, Y.; Ukaji, Y.; Inomata, K. O-silylative Passerini reaction: a new one-pot synthesis of alpha-siloxyamides. *Org Lett* **2010**, *12* (19), 4341-4343. DOI: 10.1021/ol101763w
(122) Soeta, T.; Matsuzaki, S.; Ukaji, Y. A One-Pot O-Sulfinative Passerini/Oxidation Reaction: Synthesis of α-(Sulfonyloxy)amide Derivatives. *The Journal of Organic Chemistry* **2015**, *80* (7), 3688-3694. DOI: 10.1021/acs.joc.5b00131.
(123) Soeta, T.; Matsuzaki, S.; Ukaji, Y. A one-pot O-phosphinative Passerini/Pudovik reaction: efficient synthesis of highly functionalized alpha-(phosphinyloxy)amide derivatives. *Chemistry* **2014**, *20* (17), 5007-5012. DOI: 10.1002/chem.201304618
(124) Neochoritis, C. G.; Zhao, T.; Dömling, A. Tetrazoles via Multicomponent Reactions. *Chem Rev* **2019**, *119* (3), 1970-2042. DOI: 10.1021/acs.chemrev.8b00564
(125) Kaim, L. E.; Gizolme, M.; Grimaud, L.; Oble, J. Smiles Rearrangements in Ugi- and Passerini-Type Couplings New Multicomponent Access to O- and N-Arylamides. *J Org Chem* **2007**, *72* (11), 4169-4180. DOI: 10.1021/jo070202e
(126) Wahby, Y.; Abdel-Hamid, H.; Ayoup, M. S. Two decades of recent advances of Passerini reactions: synthetic and potential pharmaceutical applications. *New Journal of Chemistry* **2022**, *46* (4), 1445-1468. DOI: 10.1039/d1nj03832j.
(127) Deng, X. X.; Li, L.; Li, Z. L.; Lv, A.; Du, F. S.; Li, Z. C. Sequence Regulated Poly(ester-amide)s Based on Passerini Reaction. *ACS Macro Lett* **2012**, *1* (11), 1300-1303. DOI: 10.1021/mz300456p

(128) Wang, Y.-Z.; Deng, X.-X.; Li, L.; Li, Z.-L.; Du, F.-S.; Li, Z.-C. One-pot synthesis of polyamides with various functional side groups via Passerini reaction. *Polym. Chem.* **2013**, *4* (3), 444-448. DOI: 10.1039/c2py20927f.
(129) Kakuchi, R. Multicomponent reactions in polymer synthesis. *Angewandte Chemie International Edition* **2014**, *53* (1).
(130) Tao, L.; Zhu, C.; Wei, Y.; Zhao, Y. Biginelli multicomponent reactions in polymer science. *Adv Polym Sci* **2015**, 43-59.
(131) Zhang, J.; Lin, S. X.; Cheng, D. J.; Liu, X. Y.; Tan, B. Phosphoric acid-catalyzed asymmetric classic Passerini reaction. *J Am Chem Soc* **2015**, *137* (44), 14039-14042. DOI: 10.1021/jacs.5b09117
(132) Lambruschini, C.; Moni, L.; Banfi, L. Diastereoselectivity in Passerini Reactions of Chiral Aldehydes and in Ugi Reactions of Chiral Cyclic Imines. *European Journal of Organic Chemistry* **2020**, *2020* (25), 3766-3778. DOI: 10.1002/ejoc.202000016.
(133) Yue, T.; Wang, M. X.; Wang, D. X.; Masson, G.; Zhu, J. Catalytic asymmetric Passerini-type reaction: chiral aluminum-organophosphate-catalyzed enantioselective alpha-addition of isocyanides to aldehydes. *J Org Chem* **2009**, *74* (21), 8396-8399. DOI: 10.1021/jo901776
(134) Wang, S. X.; Wang, M. X.; Wang, D. X.; Zhu, J. Catalytic enantioselective Passerini three-component reaction. *Angew Chem Int Ed Engl* **2008**, *47* (2), 388-391. DOI: 10.1002/anie.200704315
(135) Kumar, B.; Maity, J.; Shankar, B.; Kumar, S.; Kavita; Prasad, A. K. Synthesis of d-glycopyranosyl depsipeptides using Passerini reaction. *Carbohydr Res* **2021**, *500*, 108236. DOI: 10.1016/j.carres.2021.108236
(136) Liu, Y.; Olsen, P.; Qi, H. Passerini three-component reaction for the synthesis of saccharide branched cellulose. *Int J Biol Macromol* **2023**, *253* (Pt 8), 127367. DOI: 10.1016/j.ijbiomac.2023.127367
(137) Meier, M. A. R.; Barner-Kowollik, C. A New Class of Materials: Sequence-Defined Macromolecules and Their Emerging Applications. *Adv Mater* **2019**, *31* (26), e1806027. DOI: 10.1002/adma.201806027
(138) Watson, J. D.; Crick, F. H. The structure of DNA. *Cold Spring Harb Symp Quant Biol* **1953**, *18*, 123-131. DOI: 10.1101/sqb.1953.018.01.020
(139) Crick, F. H. The origin of the genetic code. *J Mol Biol* **1968**, *38* (3), 367-379. DOI: 10.1016/0022-2836(68)90392-6
(140) Ambrogelly, A.; Palioura, S.; Söll, D. Natural expansion of the genetic code. *Nat Chem Biol* **2007**, *3* (1), 29-35. DOI: 10.1038/nchembio847
(141) Nurk, S.; Koren, S.; Rhie, A.; Rautiainen, M.; Bzikadze, A. V.; Mikheenko, A.; Vollger, M. R.; Altemose, N.; Uralsky, L.; Gershman, A.; et al. The complete sequence of a human genome. *Science* **2022**, *376* (6588), 44-53. DOI: 10.1126/science.abj6987
(142) Jenkins, A. D.; Kratochvil, P.; Stepto, R. F. T.; Suter, U. W. Glossary of basic terms in polymer science. *Pure Appl Chem* **1996**, *68* (12), 2287-2311. DOI: DOI 10.1351/pac199668122287.
(143) Lutz, J.-F. Aperiodic copolymers. ACS Publications: 2014.
(144) Lutz, J. F.; Ouchi, M.; Liu, D. R.; Sawamoto, M. Sequence-controlled polymers. *Science* **2013**, *341* (6146), 1238149. DOI: 10.1126/science.1238149
(145) Solleder, S. C.; Schneider, R. V.; Wetzel, K. S.; Boukis, A. C.; Meier, M. A. R. Recent Progress in the Design of Monodisperse, Sequence-Defined Macromolecules. *Macromol Rapid Commun*

2017, *38* (9). DOI: 10.1002/marc.201600711
(146) Merrifield, R. B. Solid phase peptide synthesis. I. The synthesis of a tetrapeptide. *Journal of the American Chemical Society* **1963**, *85* (14), 2149-2154.
(147) Merrifield, R. B. Solid phase synthesis (Nobel lecture). *Angewandte Chemie International Edition in English* **1985**, *24* (10), 799-810.
(148) Merrifield, R. B.; Stewart, J. M.; Jernberg, N. Instrument for automated synthesis of peptides. *Anal Chem* **1966**, *38* (13), 1905-1914. DOI: 10.1021/ac50155a057
(149) Espeel, P.; Carrette, L. L. G.; Bury, K.; Capenberghs, S.; Martins, J. C.; Du Prez, F. E.; Madder, A. Multifunctionalized Sequence-Defined Oligomers from a Single Building Block. *Angewandte Chemie International Edition* **2013**, *52* (50), 13261-13264. DOI: 10.1002/anie.201307439.
(150) Martens, S.; Van den Begin, J.; Madder, A.; Du Prez, F. E.; Espeel, P. Automated synthesis of monodisperse oligomers, featuring sequence control and tailored functionalization. *Journal of the American Chemical Society* **2016**, *138* (43), 14182-14185.
(151) Holloway, J. O.; Aksakal, S.; Du Prez, F. E.; Becer, C. R. Tailored modification of thioacrylates in a versatile, sequence-defined procedure. *Macromolecular Rapid Communications* **2017**, *38* (24), 1700500.
(152) Martens, S.; Landuyt, A.; Espeel, P.; Devreese, B.; Dawyndt, P.; Du Prez, F. Multifunctional sequence-defined macromolecules for chemical data storage. *Nature Communications* **2018**, *9* (1), 4451.
(153) Mertens, C.; Soete, M.; Ślęczkowski, M. L.; Palmans, A. R.; Meijer, E.; Badi, N.; Du Prez, F. E. Stereocontrolled, multi-functional sequence-defined oligomers through automated synthesis. *Polymer Chemistry* **2020**, *11* (26), 4271-4280.
(154) Mertens, C.; Aksakal, R.; Badi, N.; Du Prez, F. E. Sequence-defined oligoampholytes using hydrolytically stable vinyl sulfonamides: design and UCST behaviour. *Polymer Chemistry* **2021**, *12* (29), 4193-4204.
(155) Holloway, J. O.; Mertens, C.; Du Prez, F. E.; Badi, N. Automated Synthesis Protocol of Sequence-Defined Oligo-Urethane-Amides Using Thiolactone Chemistry. *Macromolecular Rapid Communications* **2019**, *40* (1), 1800685.
(156) Soete, M.; Mertens, C.; Aksakal, R.; Badi, N.; Du Prez, F. Sequence-encoded macromolecules with increased data storage capacity through a thiol-epoxy reaction. *ACS Macro Letters* **2021**, *10* (5), 616-622.
(157) Székely, G.; Schaepertoens, M.; Gaffney, P. R.; Livingston, A. G. Iterative synthesis of monodisperse PEG homostars and linear heterobifunctional PEG. *Polymer Chemistry* **2014**, *5* (3), 694-697.
(158) Dong, R.; Liu, R.; Gaffney, P. R. J.; Schaepertoens, M.; Marchetti, P.; Williams, C. M.; Chen, R.; Livingston, A. G. Sequence-defined multifunctional polyethers via liquid-phase synthesis with molecular sieving. *Nat Chem* **2019**, *11* (2), 136-145. DOI: 10.1038/s41557-018-0169-6
(159) Trinh, T. T.; Oswald, L.; Chan-Seng, D.; Lutz, J. F. Synthesis of molecularly encoded oligomers using a chemoselective "AB + CD" iterative approach. *Macromol Rapid Commun* **2014**, *35* (2), 141-145. DOI: 10.1002/marc.201300774
(160) Trinh, T. T.; Laure, C.; Lutz, J.-F. Synthesis of Monodisperse Sequence-Defined Polymers Using Protecting-Group-Free Iterative Strategies. *Macromolecular Chemistry and Physics* **2015**, *216* (14), 1498-1506. DOI: 10.1002/macp.201500072.
(161) Fiers, G.; Chouikhi, D.; Oswald, L.; Al Ouahabi, A.; Chan-Seng, D.; Charles, L.; Lutz, J.-F.

Orthogonal Synthesis of Xeno Nucleic Acids. *Chemistry – A European Journal* **2016**, *22* (50), 17945-17948. DOI: 10.1002/chem.201604386.

(162) Gunay, Ufuk S.; Petit, Benoît E.; Karamessini, D.; Al Ouahabi, A.; Amalian, J.-A.; Chendo, C.; Bouquey, M.; Gigmes, D.; Charles, L.; Lutz, J.-F. Chemoselective Synthesis of Uniform Sequence-Coded Polyurethanes and Their Use as Molecular Tags. *Chem* **2016**, *1* (1), 114-126. DOI: 10.1016/j.chempr.2016.06.006.

(163) Mondal, T.; Greff, V.; Petit, B. É.; Charles, L.; Lutz, J.-F. Efficient Protocol for the Synthesis of "N-Coded" Oligo- and Poly(N-Substituted Urethanes). *ACS Macro Letters* **2019**, *8* (8), 1002-1005. DOI: 10.1021/acsmacrolett.9b00446.

(164) Cavallo, G.; Clément, J.-L.; Gigmes, D.; Charles, L.; Lutz, J.-F. Selective Bond Cleavage in Informational Poly(Alkoxyamine Phosphodiester)s. *Macromolecular Rapid Communications* **2020**, *41* (12), 2000215. DOI: 10.1002/marc.202000215.

(165) Lutz, J.-F. Defining the Field of Sequence-Controlled Polymers. *Macromolecular Rapid Communications* **2017**, *38* (24), 1700582. DOI: 10.1002/marc.201700582.

(166) Amalian, J.-A.; Mondal, T.; Konishcheva, E.; Cavallo, G.; Petit, B. E.; Lutz, J.-F.; Charles, L. Desorption Electrospray Ionization (DESI) of Digital Polymers: Direct Tandem Mass Spectrometry Decoding and Imaging from Materials Surfaces. *Advanced Materials Technologies* **2021**, *6* (4), 2001088. DOI: 10.1002/admt.202001088.

(167) Charles, L.; Cavallo, G.; Monnier, V.; Oswald, L.; Szweda, R.; Lutz, J.-F. MS/MS-Assisted Design of Sequence-Controlled Synthetic Polymers for Improved Reading of Encoded Information. *Journal of The American Society for Mass Spectrometry* **2017**, *28* (6), 1149-1159. DOI: 10.1007/s13361-016-1543-5.

(168) Charles, L.; Lutz, J.-F. Design of Abiological Digital Poly(phosphodiester)s. *Accounts of Chemical Research* **2021**, *54* (7), 1791-1800. DOI: 10.1021/acs.accounts.1c00038.

(169) Poyer, S.; Fouquet, T.; Sato, H.; Lutz, J.-F.; Charles, L. Convenient Graphical Visualization of Messages Encoded in Sequence-Defined Synthetic Polymers Using Kendrick Mass Defect Analysis of their MS/MS Data. *Macromolecular Chemistry and Physics* **2018**, *219* (16), 1800173. DOI: 10.1002/macp.201800173.

(170) Al Ouahabi, A.; Amalian, J.-A.; Charles, L.; Lutz, J.-F. Mass spectrometry sequencing of long digital polymers facilitated by programmed inter-byte fragmentation. *Nature Communications* **2017**, *8* (1), 967. DOI: 10.1038/s41467-017-01104-3.

(171) Schutz, T.; Sergent, I.; Obeid, G.; Oswald, L.; Al Ouahabi, A.; Baxter, P. N. W.; Clement, J. L.; Gigmes, D.; Charles, L.; Lutz, J. F. Conception and Evaluation of a Library of Cleavable Mass Tags for Digital Polymers Sequencing. *Angew Chem Int Ed Engl* **2023**, *62* (45), e202310801. DOI: 10.1002/anie.202310801

(172) Grate, J. W.; Mo, K.-F.; Daily, M. D. Triazine-Based Sequence-Defined Polymers with Side-Chain Diversity and Backbone–Backbone Interaction Motifs. *Angewandte Chemie International Edition* **2016**, *55* (12), 3925-3930. DOI: 10.1002/anie.201509864.

(173) Khanal, A.; Fang, S. Solid phase stepwise synthesis of polyethylene glycols. *Chemistry–A European Journal* **2017**, *23* (60), 15133-15142.

(174) Keegstra, E. M. D.; Zwikker, J. W.; Roest, M. R.; Jenneskens, L. W. A highly selective synthesis of monodisperse oligo(ethylene glycols). *The Journal of Organic Chemistry* **1992**, *57* (24), 6678-6680. DOI: 10.1021/jo00050a065.

(175) Chen, Y.; Baker, G. L. Synthesis and Properties of ABA Amphiphiles. *J Org Chem* **1999**, *64*

(18), 6870-6873. DOI: 10.1021/jo990620m
(176) Ahmed, S. A. Photochromism of dihydroindolizines Part VI: synthesis and photochromic behavior of a novel type of IR-absorbing photochromic compounds based on highly conjugated dihydroindolizines. *Journal of physical organic chemistry* **2006**, *19* (7), 402-414.
(177) Niculescu-Duvaz, D.; Getaz, J.; Springer, C. J. Long Functionalized Poly(ethylene glycol)s of Defined Molecular Weight: Synthesis and Application in Solid-Phase Synthesis of Conjugates. *Bioconjug Chem* **2008**, *19* (4), 973-981. DOI: 10.1021/bc060242
(178) Maranski, K.; Andreev, Y. G.; Bruce, P. G. Synthesis of poly(ethylene oxide) approaching monodispersity. *Angew Chem Int Ed Engl* **2014**, *53* (25), 6411-6413. DOI: 10.1002/anie.20140343.
(179) Zhang, H.; Li, X.; Shi, Q.; Li, Y.; Xia, G.; Chen, L.; Yang, Z.; Jiang, Z. X. Highly efficient synthesis of monodisperse poly(ethylene glycols) and derivatives through macrocyclization of oligo(ethylene glycols). *Angew Chem Int Ed Engl* **2015**, *54* (12), 3763-3767. DOI: 10.1002/anie.201410309
(180) Zydziak, N.; Feist, F.; Huber, B.; Mueller, J. O.; Barner-Kowollik, C. Photo-induced sequence defined macromolecules via hetero bifunctional synthons. *Chemical Communications* **2015**, *51* (10), 1799-1802, 10.1039/C4CC08756A. DOI: 10.1039/C4CC08756A.
(181) Gruendling, T.; Oehlenschlaeger, K. K.; Frick, E.; Glassner, M.; Schmid, C.; Barner-Kowollik, C. Rapid UV Light-Triggered Macromolecular Click Conjugations via the Use of o-Quinodimethanes. *Macromolecular rapid communications* **2011**, *32* (11), 807-812.
(182) Zydziak, N.; Konrad, W.; Feist, F.; Afonin, S.; Weidner, S.; Barner-Kowollik, C. Coding and decoding libraries of sequence-defined functional copolymers synthesized via photoligation. *Nature Communications* **2016**, *7* (1), 13672.
(183) Konrad, W.; Fengler, C.; Putwa, S.; Barner-Kowollik, C. Protection-Group-Free Synthesis of Sequence-Defined Macromolecules via Precision λ-Orthogonal Photochemistry. *Angewandte Chemie International Edition* **2019**, *58* (21), 7133-7137. DOI: 10.1002/anie.201901933.
(184) Paynter, O. I.; Simmonds, D. J.; Whiting, M. C. The synthesis of long-chain unbranched aliphatic compounds by molecular doubling. *Journal of the Chemical Society, Chemical Communications* **1982**, (20), 1165-1166.
(185) Bidd, I.; Whiting, M. C. The synthesis of pure n-paraffins with chain-lengths between one and four hundred. *Journal of the Chemical Society, Chemical Communications* **1985**, (9), 543-544.
(186) Brooke, G. M.; Burnett, S.; Mohammed, S.; Proctor, D.; Whiting, M. C. A versatile process for the syntheses of very long chain alkanes, functionalised derivatives and some branched chain hydrocarbons. *Journal of the Chemical Society, Perkin Transactions 1* **1996**, (13), 1635-1645.
(187) Takizawa, K.; Tang, C.; Hawker, C. J. Molecularly defined caprolactone oligomers and polymers: synthesis and characterization. *J Am Chem Soc* **2008**, *130* (5), 1718-1726. DOI: 10.1021/ja077149w
(188) Takizawa, K.; Nulwala, H.; Hu, J.; Yoshinaga, K.; Hawker, C. J. Molecularly defined (L)-lactic acid oligomers and polymers: Synthesis and characterization. *Journal of Polymer Science Part A: Polymer Chemistry* **2008**, *46* (18), 5977-5990. DOI: 10.1002/pola.22944.
(189) Huang, B.; Hermes, M. E. Homogeneous polyesters of predetermined length, composition, and sequence: Model synthesis of alternating glycolic-acid-co-(L)-lactic-acid oligomers. *Journal of Polymer Science Part A: Polymer Chemistry* **1995**, *33* (9), 1419-1429. DOI: 10.1002/pola.1995.080330902.
(190) Burns, C. J.; Field, L. D.; Hashimoto, K.; Petteys, B. J.; Ridley, D. D.; Sandanayake, K. R. A.

S. A Convenient Synthetic Route to Differentially Functionalized Long Chain Polyethylene Glycols. *Synthetic Communications* **1999**, *29* (13), 2337-2347. DOI: 10.1080/00397919908086236.

(191) Loiseau, F. A.; Hii, K. K.; Hill, A. M. Multigram Synthesis of Well-Defined Extended Bifunctional Polyethylene Glycol (PEG) Chains. *The Journal of Organic Chemistry* **2004**, *69* (3), 639-647. DOI: 10.1021/jo035042v.

(192) French, A. C.; Thompson, A. L.; Davis, B. G. High-Purity Discrete PEG-Oligomer Crystals Allow Structural Insight. *Angewandte Chemie International Edition* **2009**, *48* (7), 1248-1252. DOI: 10.1002/anie.200804623.

(193) Zhang, J.; Moore, J. S.; Xu, Z.; Aguirre, R. A. Nanoarchitectures. 1. Controlled synthesis of phenylacetylene sequences. *Journal of the American Chemical Society* **1992**, *114* (6), 2273-2274. DOI: 10.1021/ja00032a060.

(194) Xu, Z.; Kahr, M.; Walker, K. L.; Wilkins, C. L.; Moore, J. S. Phenylacetylene dendrimers by the divergent, convergent, and double-stage convergent methods. *Journal of the American Chemical Society* **1994**, *116* (11), 4537-4550.

(195) Xu, Z.; Moore, J. S. Rapid construction of large-size phenylacetylene dendrimers up to 12.5 nanometers in molecular diameter. *Angewandte Chemie International Edition in English* **1993**, *32* (9), 1354-1357.

(196) Zhang, J.; Pesak, D. J.; Ludwick, J. L.; Moore, J. S. Geometrically-controlled and site-specifically-functionalized phenylacetylene macrocycles. *Journal of the American Chemical Society* **1994**, *116* (10), 4227-4239.

(197) Venkataraman, D.; Lee, S.; Zhang, J.; Moore, J. S. An organic solid with wide channels based on hydrogen bonding between macrocycles. *Nature* **1994**, *371* (6498), 591-593. DOI: 10.1038/371591a0.

(198) Liess, P.; Hensel, V.; Schlüter, A. D. Oligophenylene rods: a repetitive approach. *Liebigs Annalen* **1996**, *1996* (7), 1037-1040.

(199) Geng, Y.; Trajkovska, A.; Katsis, D.; Ou, J. J.; Culligan, S. W.; Chen, S. H. Synthesis, Characterization, and Optical Properties of Monodisperse Chiral Oligofluorenes. *Journal of the American Chemical Society* **2002**, *124* (28), 8337-8347. DOI: 10.1021/ja026165k.

(200) Pearson, D. L.; Schumm, J. S.; Tour, J. M. Iterative divergent/convergent approach to conjugated oligomers by a doubling of molecular length at each iteration. A rapid route to potential molecular wires. *Macromolecules* **1994**, *27* (8), 2348-2350.

(201) Schumm, J. S.; Pearson, D. L.; Tour, J. M. Iterative Divergent/Convergent Approach to Linear Conjugated Oligomers by Successive Doubling of the Molecular Length: A Rapid Route to a 128Å-Long Potential Molecular Wire. *Angewandte Chemie International Edition in English* **1994**, *33* (13), 1360-1363.

(202) Pearson, D. L.; Tour, J. M. Rapid Syntheses of Oligo(2,5-thiophene ethynylene)s with Thioester Termini: Potential Molecular Scale Wires with Alligator Clips. *The Journal of Organic Chemistry* **1997**, *62* (5), 1376-1387. DOI: 10.1021/jo962335y.

(203) Hwang, J.-J.; Tour, J. M. Combinatorial synthesis of oligo(phenylene ethynylene)s. *Tetrahedron* **2002**, *58* (52), 10387-10405. DOI: 10.1016/S0040-4020(02)01409-6.

(204) Li, G.; Wang, X.; Wang, F. A novel in situ deprotection/coupling and iterative divergent/convergent strategy for the synthesis of oligo (1, 4-phenyleneethynylene) s. *Tetrahedron Lett* **2005**, *46* (52), 8971-8973.

(205) Huang, S.; Tour, J. M. Rapid bi-directional synthesis of oligo (1, 4-phenylene ethynylene) s.

Tetrahedron Lett **1999**, *40* (17), 3447-3450.
(206) Leibfarth, F. A.; Johnson, J. A.; Jamison, T. F. Scalable synthesis of sequence-defined, unimolecular macromolecules by Flow-IEG. *Proc Natl Acad Sci U S A* **2015**, *112* (34), 10617-10622. DOI: 10.1073/pnas.1508599112
(207) Barnes, J. C.; Ehrlich, D. J.; Gao, A. X.; Leibfarth, F. A.; Jiang, Y.; Zhou, E.; Jamison, T. F.; Johnson, J. A. Iterative exponential growth of stereo- and sequence-controlled polymers. *Nat Chem* **2015**, *7* (10), 810-815. DOI: 10.1038/nchem.2346
(208) Jiang, Y.; Golder, M. R.; Nguyen, H. V.; Wang, Y.; Zhong, M.; Barnes, J. C.; Ehrlich, D. J.; Johnson, J. A. Iterative Exponential Growth Synthesis and Assembly of Uniform Diblock Copolymers. *J Am Chem Soc* **2016**, *138* (30), 9369-9372. DOI: 10.1021/jacs.6b04964
(209) Zhang, W.; Dong, X.; Cheng, S. Z. D. Reaction: Precision Macromolecules for Self-Assembly. *Chem* **2019**, *5* (3), 492-493. DOI: 10.1016/j.chempr.2019.02.019.
(210) Li, J.; Leclercq, M.; Fossepré, M.; Surin, M.; Glinel, K.; Jonas, A. M.; Fernandes, A. E. Discrete multifunctional sequence-defined oligomers with controlled chirality. *Polymer Chemistry* **2020**, *11* (24), 4040-4046.
(211) Ślęczkowski, M. L.; Segers, I.; Liu, Y.; Palmans, A. R. Sequence-defined l-glutamamide oligomers with pendant supramolecular motifs via iterative synthesis and orthogonal post-functionalization. *Polymer Chemistry* **2020**, *11* (46), 7393-7401.
(212) Murphy, E. A.; Zhang, C.; Bates, C. M.; Hawker, C. J. Chromatographic Separation: A Versatile Strategy to Prepare Discrete and Well-Defined Polymer Libraries. *Accounts of Chemical Research* **2024**, *57* (8), 1202-1213. DOI: 10.1021/acs.accounts.4c00059.
(213) Kamon, Y.; Miura, J.; Okuno, K.; Yamasaki, S.; Nakahata, M.; Hashidzume, A. Synthesis of Stereoregular Uniform Oligomers Possessing a Dense 1,2,3-Triazole Backbone. *Macromolecules* **2023**, *56* (1), 292-304. DOI: 10.1021/acs.macromol.2c01905.
(214) Yin, J.; Choi, S.; Pyle, D.; Guest, J. R.; Dong, G. Backbone Engineering of Monodisperse Conjugated Polymers via Integrated Iterative Binomial Synthesis. *Journal of the American Chemical Society* **2023**, *145* (34), 19120-19128. DOI: 10.1021/jacs.3c08143.
(215) Wicker, A. C.; Leibfarth, F. A.; Jamison, T. F. Flow-IEG enables programmable thermodynamic properties in sequence-defined unimolecular macromolecules. *Polymer Chemistry* **2017**, *8*, 5786-5794.
(216) Huang, Z.; Zhao, J.; Wang, Z.; Meng, F.; Ding, K.; Pan, X.; Zhou, N.; Li, X.; Zhang, Z.; Zhu, X.-l. Combining Orthogonal Chain-End Deprotections and Thiol-Maleimide Michael Coupling: Engineering Discrete Oligomers by an Iterative Growth Strategy. *Angewandte Chemie* **2017**, *56 44*, 13612-13617.
(217) Amir, F.; Jia, Z.; Monteiro, M. J. Sequence Control of Macromers via Iterative Sequential and Exponential Growth. *Journal of the American Chemical Society* **2016**, *138 51*, 16600-16603.
(218) Solleder, S. C.; Meier, M. A. Sequence control in polymer chemistry through the Passerini three-component reaction. *Angewandte Chemie International Edition* **2014**, *53* (3), 711-714.
(219) Solleder, S. C.; Wetzel, K. S.; Meier, M. A. Dual side chain control in the synthesis of novel sequence-defined oligomers through the Ugi four-component reaction. *Polymer Chemistry* **2015**, *6* (17), 3201-3204.
(220) Yang, L.; Zhang, Z.; Cheng, B.; You, Y.; Wu, D.; Hong, C. Two tandem multicomponent reactions for the synthesis of sequence-defined polymers. *Science China Chemistry* **2015**, *58* (11), 1734-1740. DOI: 10.1007/s11426-015-5448-0.

(221) Solleder, S. C.; Zengel, D.; Wetzel, K. S.; Meier, M. A. A Scalable and High-Yield Strategy for the Synthesis of Sequence-Defined Macromolecules. *Angew Chem Int Ed Engl* **2016**, *55* (3), 1204-1207. DOI: 10.1002/anie.201509398
(222) Porel, M.; Alabi, C. A. Sequence-defined polymers via orthogonal allyl acrylamide building blocks. *Journal of the American Chemical Society* **2014**, *136* (38), 13162-13165.
(223) Solleder, S. C.; Martens, S.; Espeel, P.; Du Prez, F.; Meier, M. A. R. Combining Two Methods of Sequence Definition in a Convergent Approach: Scalable Synthesis of Highly Defined and Multifunctionalized Macromolecules. *Chemistry* **2017**, *23* (56), 13906-13909. DOI: 10.1002/chem.201703877
(224) Boukis, A. C.; Meier, M. A. Data storage in sequence-defined macromolecules via multicomponent reactions. *European Polymer Journal* **2018**, *104*, 32-38.
(225) Holloway, J. O.; Wetzel, K. S.; Martens, S.; Du Prez, F. E.; Meier, M. A. Direct comparison of solution and solid phase synthesis of sequence-defined macromolecules. *Polymer Chemistry* **2019**, *10* (28), 3859-3867.
(226) Wang, S.; Tao, Y.; Wang, J.; Tao, Y.; Wang, X. A versatile strategy for the synthesis of sequence-defined peptoids with side-chain and backbone diversity via amino acid building blocks. *Chemical science* **2019**, *10* (5), 1531-1538.
(227) Tuten, B. T.; De Keer, L.; Wiedbrauk, S.; Van Steenberge, P. H.; D'hooge, D. R.; Barner-Kowollik, C. Visible-Light-Induced Passerini Multicomponent Polymerization. *Angewandte Chemie International Edition* **2019**, *58* (17), 5672-5676.
(228) Frölich, M.; Hofheinz, D.; Meier, M. A. R. Reading mixtures of uniform sequence-defined macromolecules to increase data storage capacity. *Communications Chemistry* **2020**, *3* (1), 184. DOI: 10.1038/s42004-020-00431-9.
(229) Arcadia, C. E.; Kennedy, E.; Geiser, J.; Dombroski, A.; Oakley, K.; Chen, S.-L.; Sprague, L.; Ozmen, M.; Sello, J.; Weber, P. M. Multicomponent molecular memory. *Nature communications* **2020**, *11* (1), 691.
(230) Holloway, J. O.; Van Lijsebetten, F.; Badi, N.; Houck, H. A.; Du Prez, F. E. From Sequence-Defined Macromolecules to Macromolecular Pin Codes. *Adv Sci (Weinh)* **2020**, *7* (8), 1903698. DOI: 10.1002/advs.201903698
(231) Wetzel, K. S.; Frölich, M.; Solleder, S. C.; Nickisch, R.; Treu, P.; Meier, M. A. Dual sequence definition increases the data storage capacity of sequence-defined macromolecules. *Communications chemistry* **2020**, *3* (1), 63.
(232) Lee, J. M.; Kwon, J.; Lee, S. J.; Jang, H.; Kim, D.; Song, J.; Kim, K. T. Semiautomated synthesis of sequence-defined polymers for information storage. *Science Advances* **2022**, *8* (10), eabl8614.
(233) Lee, J. M.; Koo, M. B.; Lee, S. W.; Lee, H.; Kwon, J.; Shim, Y. H.; Kim, S. Y.; Kim, K. T. High-density information storage in an absolutely defined aperiodic sequence of monodisperse copolyester. *Nature Communications* **2020**, *11* (1), 56.
(234) Bohn, P.; Weisel, M. P.; Wolfs, J.; Meier, M. A. R. Molecular data storage with zero synthetic effort and simple read-out. *Scientific Reports* **2022**, *12* (1), 13878. DOI: 10.1038/s41598-022-18108-9.
(235) Ng, C. C. A.; Tam, W. M.; Yin, H.; Wu, Q.; So, P.-K.; Wong, M. Y.-M.; Lau, F. C.; Yao, Z.-P. Data storage using peptide sequences. *Nature communications* **2021**, *12* (1), 4242.
(236) Wegelin, S.; Meier, M. A. Solution Self-Assembly of Branched Macromolecules Obtained via

Iterative OPE Synthesis and the Passerini Three-Component Reaction. *Macromolecular Chemistry and Physics* **2024**, *225* (4), 2300337.

(237) Boukis, A. C.; Reiter, K.; Frolich, M.; Hofheinz, D.; Meier, M. A. R. Multicomponent reactions provide key molecules for secret communication. *Nat Commun* **2018**, *9* (1), 1439. DOI: 10.1038/s41467-018-03784-x

(238) Boukis, A. C.; Meier, M. A. R. Data storage in sequence-defined macromolecules via multicomponent reactions. *European Polymer Journal* **2018**, *104*, 32-38. DOI: 10.1016/j.eurpolymj.2018.04.038.

(239) Frolich, M.; Hofheinz, D.; Meier, M. A. R. Reading mixtures of uniform sequence-defined macromolecules to increase data storage capacity. *Commun Chem* **2020**, *3* (1), 184. DOI: 10.1038/s42004-020-00431-9

(240) Wetzel, K. S.; Frolich, M.; Solleder, S. C.; Nickisch, R.; Treu, P.; Meier, M. A. R. Dual sequence definition increases the data storage capacity of sequence-defined macromolecules. *Commun Chem* **2020**, *3* (1), 63. DOI: 10.1038/s42004-020-0308-z

(241) Wesdemiotis, C.; Solak, N.; Polce, M. J.; Dabney, D. E.; Chaicharoen, K.; Katzenmeyer, B. C. Fragmentation pathways of polymer ions. *Mass Spectrometry Reviews* **2011**, *30* (4), 523-559. DOI: 10.1002/mas.20282.